THE GEOLOGY, PETROLOGY, GEOCHEMISTRY,

SULPHIDE AND PLATINUM-GROUP ELEMENT MINERALIZATION OF THE

QUETICO INTRUSIONS, NORTHWESTERN ONTARIO

BY

ALLAN DOUGLAS MACTAVISH ©

A THESIS SUBMITTED IN PARTIAL FULFILLMENT OF THE

REQUIREMENTS FOR THE DEGREE OF

MASTER OF SCIENCE

LAKEHEAD UNIVERSITY

THUNDER BAY, ONTARIO

CANADA

APRIL, 1992

ProQuest Number: 10611845

![ProQuest](ProQuest logo)

ProQuest 10611845

Canada

To my wife, Toni-Lynn, for her love, support, understanding, and never-ending patience; and to my infant daughter, Carli, just for being there.

The Geology, Petrology, Geochemistry, Sulphide and Platinum-group Element Mineralization of the Quetico Intrusions, Northwestern Ontario

Abstract

The Quetico Intrusions are a group of small, geochemically primitive, locally Cu-Ni-PGE-rich, mafic to ultramafic intrusions closely associated with the margins of the Quetico Batholithic Complex. They are composed of distinctively textured, sometimes layered, hornblende-rich, cumulate rocks that range from hornblende wehrlite to quartz diorite. The ultramafic rocks characteristically contain numerous large, interstitial, poikilitic hornblendes up to 3 cm in diameter. The mafic lithologies are often coarsely hornblende-phyric. All rock types contain texturally distinct intermediate to mafic patches and veins that exhibit large, ragged, cored, prismatic to acicular hornblendes referred to as appinites. This study examined fifteen of the Quetico Intrusions, concentrating on those containing mineralized zones. Three intrusions were mapped in detail.

Petrographic examination suggests a crystallization order of: olivine, olivine + clinopyroxene, clinopyroxene (locally orthopyroxene), clinopyroxene + hornblende, hornblende, hornblende + plagioclase. Biotite, apatite and titanite are present within most rock types.

Alteration and the cumulus nature of the rocks precludes the use of whole rock data to show definitive fractionation trends. Instead, emphasis was placed on the quantitative mineral chemistry of olivine and clinopyroxene. Olivine is rich in MgO and exhibits a narrow forsterite range of $Fo_{77.55-80.89}$. Clinopyroxene is generally diopsidic with a compositional range of $Wo_{44.60-50.53}$, $En_{39.03-49.02}$, $Fs_{5.35-11.31}$. Mineral chemistry data, plus the presence of myrmekitic intergrowths of magnetite with clinopyroxene, suggests that the Quetico clinopyroxenes crystallized from a magma of sub-alkaline, possibly calc-alkaline, affinity.

Nine intrusions host mineralized zones containing copper, nickel and platinum-group element mineralization. This mineralization consists of chalcopyrite, pyrrhotite, pentlandite, and magnetite with accessory pyrite and nickeliferous cobaltite, minor cubanite, altaite, empressite, breithauptite, and rare bismuthinite. Violarite and covellite occur as minor alteration products of pentlandite and chalcopyrite, respectively. The major sulphide and accessory phases probably crystallized from a PGM-bearing Ni- and Cu-rich monosulphide phase trapped interstitially to surrounding silicates. The presently observed textures are mainly due to subsolidus reequilibration and to the formation of lower temparature phases as the intrusions slowly cooled.
The platinum-group minerals (PGM) were identified using semi-quantitative EDS techniques and are generally less than

$5\mu m$ in diameter. They include michenerite, hollingworthite, froodite, sobolevskite, and sperrylite. Complex PGM intergrowths are common. Palladian gold is the only PGE-bearing alloy observed. A few PGM are interstitial to, or contained within, silicate minerals, suggesting some form of late-stage remobilization.

A comparison of the Quetico lithologic, textural, petrographic, whole rock, and mineral chemistry data with that of the appinite suite and the Alaskan-type Complexes suggests that the Quetico Intrusions are Archean equivalents of the Caledonian-age appinite suite of Great Britain, Ireland, and elsewhere. They may have crystallized from a water-rich sub-alkaline olivine basalt liquid, possibly of calc-alkaline affinity, at a relatively high P_{H2O} and P_{O2}. They must have crystallized under a relatively high P_{H2O} in order for hornblende to remain stable over such a wide range of magmatic conditions. Assimilation of metasedimentary wall-rock may have resulted in the hybridization of some of the magma.

Acknowledgements

Without the efforts and support of the following this thesis, a daunting task on its own, would never have been written:

Dr. Steven Kissin for his supervision, editing skills, critical comments, and patience over the last 6.5 years.

Ken Fenwick, Northwestern Regional Manager of the Mines and Minerals Branch of the Ontario Ministry of Northern Development and Mines, who initiated this thesis as part of the Atikokan Cobalt-Base Metals-PGE Program under which much of the field work and analytical work was completed.

St. Joe Canada Inc./Bond Gold Canada Inc./LAC Minerals Ltd. present owners of the mining claims surrounding the Kawene and Abiwin Intrusions, and the author's employers since 1987, who allowed the time to work on this thesis.

Fleck Resources Ltd. Joint Venture partner with St. Joe Canada Inc. on the Kawene Project exploration program, who allowed this writer the use of drill logs, diamond drill core, sections, trench maps, and assay results.

The writer would also like to thank the following individuals, in addition to Dr. Kissin, who helped in the preparation of this thesis:

Rick Dutka, now with the geological staff of Placer-Dome's Campbell-Red Lake Gold Mine, for his assistance in the field during our tenure with the Thunder Bay Resident Geologist's Office.

TABLE OF CONTENTS

CHAPTER 1   INTRODUCTION

CHAPTER 2   THE GEOLOGY OF THE QUETICO INTRUSIONS

LIST OF FIGURES

LIST OF TABLES

CHAPTER 1

INTRODUCTION

1.1: General Statement

The Quetico Intrusions are syntectonic, mafic to ultramafic dykes, sills, plugs and small stocks that intrude the metaturbidites of the Quetico Subprovince in close proximity to the granitoid and migmatitic rocks of the Quetico Batholith and its associated satellite intrusions. The fifteen locally Cu-Ni-PGE-rich intrusions examined during this study all occur within or near a narrow metasedimentary belt adjacent to the Quetico Fault Zone that defines the northern boundary of the Quetico Subprovince in the Atikokan area (Pirie, 1978; Kennedy, 1984). The southern boundary of this belt is defined by the migmatized northern contact zone of the Quetico Batholithic Complex (Pirie, 1978; Figure 1.1).

Past studies have shown that the Quetico Intrusions are composed of a variety of hornblende-rich lithologies, ranging from diorite to peridotite. Many of the intrusions host disseminated sulphide zones containing significant values of copper, nickel, platinum, palladium and silver, with lesser gold, cobalt and rhodium. The presence of base and precious metals sparked the interest of numerous mineral exploration companies and the Ontario Geological Survey during the mid-1980's.

Regional Geology of Study Area

Wabigoon   Subprovince

Marmion   Batholith

Steeprock   Succession

ATIKOKAN

Quetico
Fault

9

●3

1

2

Quetico   Batholithic   Complex

Quetico   Subprovince

4 10   11
12   8
6
7
5

N

0   5   10
Km

Figure 1.1
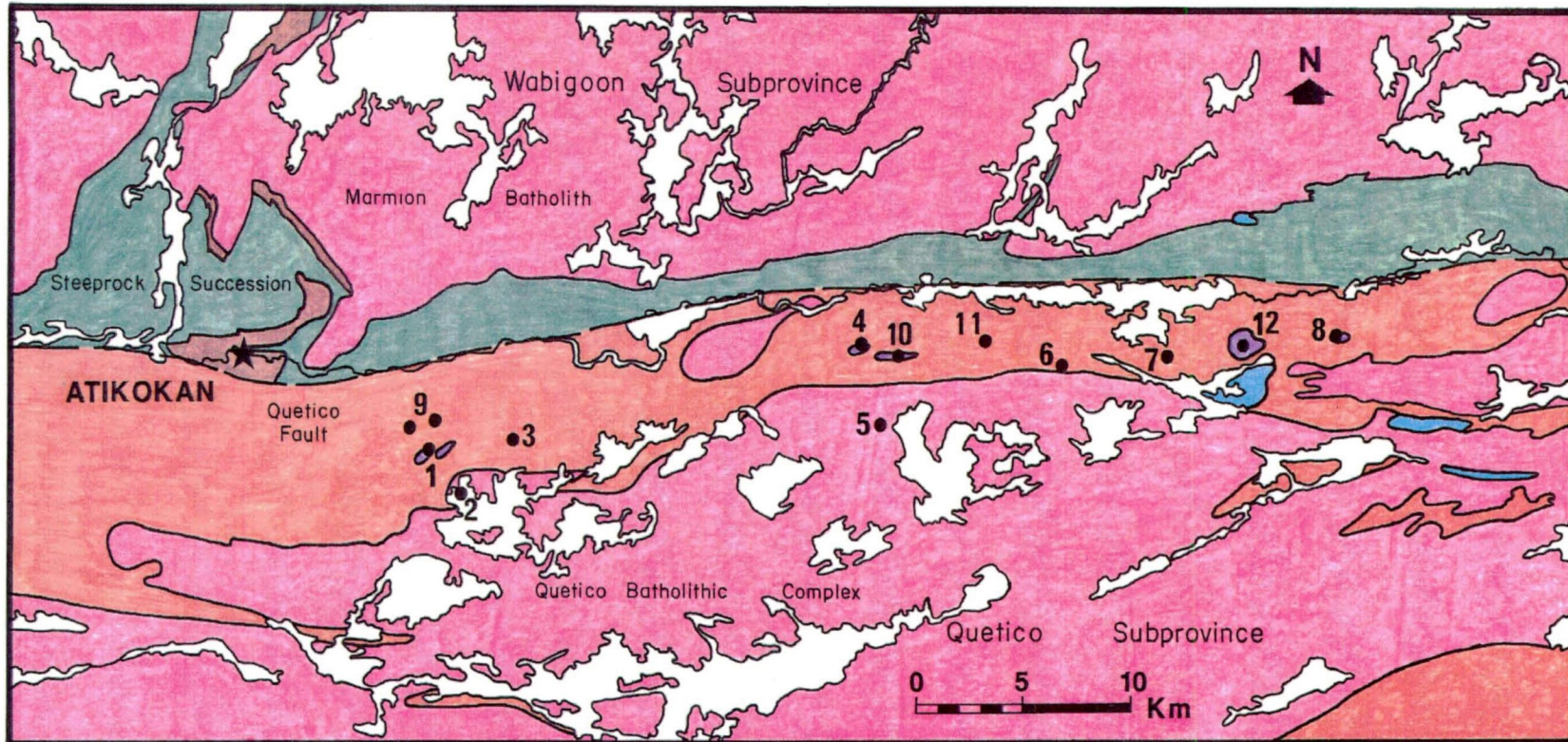
Legend

Felsic to Intermediate Intrusive Rocks (Quetico)
Quetico Intrusions
Clastic Metasedimentary Rocks
Mafic Metavolcanic Rocks
Steeprock Group
Felsic to Intermediate Intrusive Rocks (Marmion)

Quetico Intrusions

1) Plateau Lake
2) Bergman
3) Fire Lake Dykes
4) Kawene
5) Eva Lake
6) Abiwin

7) Mud Lake
8) Chief Peter Lake
9) Plateau Lake Dykes
10) Kawene Lake
11) Heward Lake
12) North Elbow Lake

2

This thesis is an attempt at a combined field, petrological, and geochemical examination of the intrusions and their associated sulphide mineralization. The term, 'Quetico Intrusions', was first used by Watkinson and Irvine (1964) during an examination of the group east of the present study area and will be continued within this work.

1.2: The Quetico Intrusions

1.2.1 - The Regional Geological Setting:

The thesis area (Figure 1.1) lies within the southern Superior Province of the Canadian Precambrian Shield. The northern part of the area is underlain by the granite-greenstone terrain of the Wabigoon Subprovince (Blackburn et al., 1985), whereas the southern portion is composed of the dominantly granite-granodiorite and migmatite terrain of the metasedimentary-derived Quetico Subprovince (Stockwell et al., 1970; Percival and Stern, 1984). The contact between the two subprovinces, at least in this area, is defined by the steeply dipping, transcurrent Quetico Fault Zone, which is generally narrow, ranging in width from 10-300 m, but can locally attain widths of over 1 km (Pirie, 1978; Kennedy, 1984).

The Wabigoon Subprovince is 900 km in length by 150 km in width and is masked at both extremities by Phanerozoic sedimentary cover (Blackburn et al., 1985). Fenwick (1976), Pirie (1978), Schwerdtner et al. (1985), and Blackburn et

al. (1985) describe the subprovince as primarily consisting of large to batholithic, massive to foliated, felsic to intermediate bodies that intrude, and are generally surrounded by, a metamorphosed, supracrustal assemblage of major, curvilinear greenstone belts. The intrusive rocks, as outlined by Schwerdtner et al. (1985), generally consist of two main granitoid rock suites of approximately equal abundance. The earliest is a foliated to gneissic, tonalite-granodiorite suite, whereas the later suite consists of massive to foliated, mainly felsic granites. The older, gneissic rocks form complexes that host discrete plutons of massive to foliated rocks that increase in abundance toward the greenstone-gneissic complex boundary. The greenstone belts commonly exhibit a volcanic stratigraphy that Fenwick (1976) and Blackburn (1985) state is initiated by a lower mafic, tholeiitic metavolcanic sequence. This is overlain by felsic to intermediate, calc-alkaline to tholeiitic metavolcanic rocks, occasionally capped by a second mafic-tholeiitic succession, all of which are intercalated with assorted, subordinate, non-marine, clastic and chemical, metasedimentary rocks closely associated with volcanism. Metamorphic grade within the greenstone belt sequences range from lower greenschist to upper amphibolite facies.

The Quetico Subprovince is a broadly symmetrical, deformed, and variably metamorphosed belt of metasedimentary

rocks composed of a core of anatectic and magmatic granites that outwardly grade into migmatites and then medium- to low-grade metasedimentary schists at the margins of the belt (Stockwell et al., 1970; Blackburn and Mackasey, 1977; Percival et al., 1985; Percival and Williams, 1989; Percival, 1989). The subprovince is between 10 and 100 km in width, approximately 1200 km in length, and is observed to emerge from beneath the Paleozoic rocks of northern Minnesota and extend east-northeastwards until it is apparently truncated by the north-northeasterly-trending Kapuskasing Structural Zone. Where preserved, the metasedimentary rocks of the Quetico Subprovince are recognizable as rapidly deposited, deep water, turbiditic greywackes with subsidiary siltstones, mudstones, and rarely conglomerates. Close examination of these rocks suggest that they were derived from a mixed volcanic-plutonic terrain, such as that observed within the adjacent Wawa and Wabigoon Subprovinces (Percival and Williams, 1989; Blackburn et al., 1985). Percival and Williams (1989), Williams (1990), and Williams (1991) suggest that the subprovince was deposited as a fore-arc accretionary prism onto the margins of the older Wabigoon Subprovince. Metamorphic grade within the subprovince ranges from lower greenschist at belt margins, through amphibolite to migmatite facies, and locally granulite facies within the centre of the belt. The majority of the preserved

metasedimentary rocks occur in belts marginal to the subprovince boundaries. These marginal belts exhibit, on a regional scale, roughly symmetrical, prograde isograd sequences that are roughly proportional to the widths of the belts. Belt widths range from 6 km in the Crooked Pine Lake area to as much as 42 km in the Flanders-Lac La Croix area (Pirie and Mackasey, 1978; Percival et al., 1985; Card and Ciesielski, 1986). Metamorphic grade within these belts can range from lower greenschist to amphibolite facies. Away from the marginal belt the subprovince is composed of a highly variable mixture of migmatites intruded by relatively siliceous anatectic and magmatic granites, tonalite, diorite and occasionally alkalic syenite. Intrusions occurring within the marginal metasediments are usually granodioritic to dioritic, and occasionally mafic to ultramafic in composition (Percival and Stern, 1984).

The Quetico Subprovince in the Atikokan area is dominated by the intrusive rocks of the batholithic-sized Quetico Batholithic Complex (Figure 1.1). The complex is highly irregular in outline because of interfingering contacts and is composed of muscovite granite, biotite leucogranite, migmatite, K-feldspar porphyritic granite and minor tonalite and granodiorite (Percival and Stern, 1984; Percival, 1989). Migmatites associated with this complex tend to be formed by the injection of an intrusive mobilizate into pelitic schists, rather than being formed by

in situ anatectic melting. Anatectic migmatites are rare
west of the Shebandowan portion of the Quetico Subprovince
(Percival et al., 1985; Pirie, 1978). The metasedimentary
rocks surrounding the Quetico Park Complex are host to
numerous intrusions of intermediate composition, the most
notable is the Blaylock Pluton located a short distance
southwest of Crooked Pine Lake. These metasediments, and
the directly adjacent migmatitic and granitic rocks, host
the small dykes, plugs and stocks of the mafic to ultramafic
Quetico Intrusions. Most of the Quetico Intrusions are
associated with the narrow metasedimentary belt wedged
between the Quetico Batholithic Complex and the Quetico
Fault Zone east of Atikokan (Figure 1.1).

1.2.2 - Previous Studies:

The first government mapping in the area was completed
by Hawley (1929) and concentrated on the rocks of the
Wabigoon Subprovince. Moore (1939) examined a region
adjacent to Hawley's mapping that covered the western edge
of the thesis area and noted the presence of eight small
intrusions composed of what he referred to as gabbro,
usually altered to amphibolite. Moore's report specifically
described the Plateau Lake Intrusion, the westernmost of the
Quetico Intrusions studied in this thesis, as a small, oval,
very course-grained gabbro body. A sample from a small,
weathered zone containing blebs, fine stringers, and

disseminated pyrrhotite and chalcopyrite yielded 1.14% Ni and 0.01 oz/ton Pt.

Tanton (1940) of the Geological Survey of Canada produced the first regional geology map of the Atikokan-Quetico area. Tanton's mapping documents numerous small intrusions composed of granodiorite, diorite, and hornblende gabbro associated with the marginal areas of the Quetico Batholithic Complex and the surrounding metasedimentary remnants.

Irvine (1963) mapped the western Lac des Milles Lacs area and recognized 35 mafic to ultramafic intrusive bodies of highly variable size. These bodies, generally composed of feldspathic hornblendite, hornblendite and peridotite, occur within both the Quetico and Wabigoon Subprovinces. The three largest intrusions, two of which contain small Ni-Cu-PGE-rich sulphide zones, occur within the Quetico Subprovince. Irvine concluded that the relative age of the Quetico area intrusions was younger than the sedimentary rocks, but older than the granitic rocks. He arrived at this conclusion because the intrusions exhibit narrow chilled margins with the metasedimentary rocks, they are cut by granite and granite pegmatite dykes, and mafic to ultramafic inclusions and xenoliths are present within the granitic rocks.

Watkinson and Irvine (1964) made a study of the numerous small mafic to ultramafic intrusions in the Quetico

area and a similar, but compositionally different, cluster in the Shebandowan area. This work coined the term 'Quetico Intrusions' and proposed that the bodies formed by fractional crystallization of a tholeiitic olivine basalt liquid, possibly carrying suspended olivine and clinopyroxene when emplaced, at a P_{H2O} of at least 2500 bars, corresponding to a depth of 8 km. These rocks were shown to be very MgO-rich and relatively CaO-rich. The hornblende gabbros and feldspathic hornblendites contain 10-12% MgO and 10-11% CaO, and the hornblendites and hornblende peridotites contain 18.9-27% MgO, and 9-14% CaO.

A B.Sc. thesis by Larsen (1974) investigated the silicate and sulphide petrology of the Kawene Intrusion. He concluded that the intrusion was neither a 'stratiform-type' nor an 'Alpine-type' body. His study of the sulphides concluded that they were of primary magmatic origin.

The Sapawe Lake area, which includes the western 30% of the thesis area, was mapped and described by McIlwaine and Chorlton (1973), McIlwaine and Hillary (1974), and McIlwaine and Larsen (1981). They noted the presence of six small ultramafic bodies, composed of pyroxenite and hornblendite, intruding into the Quetico metasedimentary belt.

A B.Sc. thesis by Legault (1976) petrographically examined the Elbow Lake Stock. She described four main lithologic units composed of hornblende diorite, hornblende gabbro, feldspathic hornblendite and pyroxene-bearing

hornblendite, and concluded that they were emplaced in order of decreasing mafic mineral content.

The Crooked Pine Lake area, mapped by Pirie (1978), forms the central part of the thesis area. This mapping encountered 20 dioritic to peridotitic bodies, of Quetico Intrusion-type, ranging from outcrop-size to 3.3 km in diameter (South Elbow Lake Stock) and a large number of mafic to ultramafic sheets no more than 2 m in width. Pirie's descriptions suggest that a great similarity exists between the intrusive bodies, since most contain the same phases, albeit in different proportions. He notes that the Kawene, Mud Lake, and Abiwin Intrusions contain minor, very localized Cu-Ni mineralization consisting of irregular interstitial blebs and disseminations of pyrrhotite and chalcopyrite. Larger intrusions, such as the Heward Lake Complex and the Elbow Lake Stock, only contain very minor disseminated pyrrhotite and pyrite.

Finally, in 1984, a three-year program was initiated by the Resident Geologist's Branch of the Ontario Ministry of Natural Resources to examine cobalt, base metal and platinum group element (PGE) occurrences in the Atikokan area. This thesis is a direct result of the PGE portion of that study, which examined, mapped, sampled, or researched 22 bodies of Quetico Intrusion-type.

1.3: Thesis Objectives

The objectives of this thesis are to investigate the Quetico Intrusions by examining:

1)   General and detailed geology;

2)   Whole rock, mineral and trace element geochemistry; and

3)   Silicate, sulphide and platinum-group element (PGE) petrology.

To use the data obtained to attempt to determine:

1)   Whether the intrusions are genetically related and of a common origin.

2)   How the intrusions compare to other mafic/ ultramafic and sulphide/PGE-rich intrusions.

3)   Whether the Quetico Intrusions are Archean equivalents to either:

a)   the Alaskan-type ultramafic complexes; or

b)   the appinite suite rocks.

4)   The sulphide, oxide, and PGE mineral species present and the conditions that lead to their formation.

CHAPTER 2

THE GEOLOGY OF THE QUETICO INTRUSIONS

2.1: Location and Access

The fifteen Quetico Intrusions examined in this study are located within the northern portion of the Quetico Subprovince (Figure 1.1) within an east-west trending, 8 km wide, 53 km long zone, situated between the town of Atikokan to the west and Chief Peter Lake to the east. Many of the intrusions are accessible by highway, logging roads, or short boat rides.

2.2: Geology and Mineralization

2.2.1 - Introduction:

The Quetico Intrusions range in size from 3-5 m thick dykes, of limited extent, to a small, roughly elliptical stock 3300 m in length and up to 1800 m in width. They usually intrude the metaturbidites of the Quetico Subprovince in close proximity to the granitoid rocks of the Quetico Batholithic Complex; however, a few were observed within the marginal regions of the batholith and its associated migmatitic rocks. Irregular zones of copper-nickel sulphides and associated, highly variable PGE mineralization are present within nine of the intrusions examined. Three of the PGE-bearing bodies, the Kawene, Mud Lake, and Abiwin Intrusions, were mapped and sampled in

detail. The remainder were examined and locally sampled. Most of the data presented in this thesis will concern those intrusions hosting copper, nickel, and PGE-bearing sulphide zones.

The Quetico Intrusions exhibit a characteristic range of hornblende-rich lithologies. The smaller, dyke-like bodies are composed of diorite (dioritic appinite), hornblende leucogabbro to hornblende melagabbro, and hornblendite, with no observable zonation of lithologies. The larger bodies tend to encompass a wider suite of rock types that range from hornblende leucogabbro through hornblendite, hornblende clinopyroxenite, and hornblende wehrlite. Some of the larger intrusions exhibit a crude, gradational, multiphased zonation of lithologies, similar to that observed in the larger Alaskan-type ultramafic complexes (Ruckmick and Noble, 1959; Taylor, 1967; Irvine, 1974). In the Quetico examples either hornblende wehrlite or hornblende clinopyroxenite is situated in the core areas with clinopyroxene hornblendite, hornblendite, hornblende gabbro, and, occasionally, diorite, forming gradational, discontinuous envelopes. Cumulate layering is neither significant nor readily observable in most of the intrusions; however, weak, diffuse modal layering is present locally, and is occasionally well-developed in the Mud Lake and Kawene Intrusions.

The ubiquitous hornblende and the complex, but

characteristic textures observed within the Quetico
Intrusions are remarkably similar to those of the 'Appinite
Suite' rocks of Ireland, Great Britain and Italy (Read,
1961; Pitcher and Berger, 1972; Bowes and McArthur, 1976;
Key, 1977; Palicova, 1982; and Key, 1987), which occur as
minor, Caledonian-age, mafic to ultramafic intrusions
closely associated with granitic plutons and batholiths
(Bailey and Maufe, 1916; Read, 1960; Joplin, 1959; Roach,
1964; Pitcher and Berger, 1972).

Grain-sizes within the Quetico Intrusions range from
fine- to very coarse-grained, to locally pegmatitic. Large,
interstitial, optically continuous, poikilitic amphibole
grains (oikocrysts) occur within all ultramafic rock types,
Irregular feldspathic zones containing large, euhedral,
zoned, hornblende phenocrysts are also common. Coarse- to
very coarse-grained, locally pegmatitic diorite and gabbro
pods, patches, and veins occur within all rock types, and
typically exhibit skeletal, prismatic to acicular hornblende
grains often cored with plagioclase and quartz.

The above textures are also characteristic of the
intrusions of the appinite suite and are what distinguishes
the suite from other varieties of mafic to ultramafic
intrusions. The name for the suite was derived from the
term 'appinite', originally used to describe feldspar-rich
units, veins, patches, and pods that exhibit skeletal,
prismatic to acicular hornblende crystals, and was first

used by Bailey and Maufe (1916). The use of this term to distinguish a certain, characteristic textural type will be continued within this thesis.

PGE mineralization occurs within small, irregular zones of finely disseminated, blebby, occasionally net-textured copper-nickel sulphides. These zones contain between 1 and 30% chalcopyrite, pyrrhotite, pentlandite, magnetite and minor pyrite, with an overall average of 4-5% sulphides. The platinum-group minerals (PGM) only occur within the well-mineralized zones and usually in contact, or close association, with chalcopyrite, pyrrhotite or pentlandite. Some PGM were observed within, or interstitial to, the silicates. Sulphide and PGE mineralization will be discussed in detail in Chapter 5.

2.2.2 - The Kawene Intrusion:

The Kawene Intrusion is approximately 500 m in length, and between 70 and 130 m in width (Figure 2.1-in back pocket). The intrusion is crudely zoned and exhibits a wide range of lithologies including hornblende melagabbro, hornblendite, clinopyroxene hornblendite, hornblende clinopyroxenite and hornblende wehrlite. Wide variations of mineral content and textures are common throughout all the major rock types and sharp contacts between units are rare. The dominant lithologies, hornblende wehrlite and locally olivine-rich hornblende clinopyroxenite, form a diffuse,

irregular core surrounded by a modally variable, locally
discontinuous envelope of several varieties of hornblendite
and hornblende melagabbro. The hornblendites within this
envelope are usually clinopyroxene-rich, sometimes olivine-
rich, and locally feldspathic. Narrow hornblende
clinopyroxenite layers (Figures 2.2a and b), <10-20 cm in
thickness, occasionally occur within the hornblendites.
Feldspathic hornblendite and hornblende melagabbro are
rarely observed away from the outer edge of the intrusion,
while the content of olivine and clinopyroxene generally
increases with distance from the outer contact. The
hornblende melagabbro/hornblendite envelope is narrowest (2-
12 m) along the north and south contacts, and widest (20-55
m) along the east and west contacts of the intrusion.

Grain-size variations within the Kawene Intrusion range
from fine- to medium-grained to locally very coarse-grained
or porphyritic. Large oikocrysts of hornblende, which
occasionally reach 3 cm in diameter, are ubiquitous.
Narrow, sometimes pegmatitic veins, small pods, or irregular
patches of appinite occur within all rock types.

The weakly chilled contact between the intrusion and
the surrounding turbiditic, metasedimentary rocks is sharp,
undulatory, and commonly offset by faulting. A 2-10 m thick
contact metamorphic aureole is present and exhibits little
or no schistosity or preserved sedimentary structures.
Minor assimilation of the wall-rock sediments is sometimes

Figure 2.2a: Two narrow, shallow-dipping hornblende clinopyroxenite layers hosted by clinopyroxene hornblendite within the Kawene Intrusion.

Figure 2.2b: Hornblende clinopyroxenite layer; dark minerals are hornblende and the light-coloured minerals are diopside.

indicated by a narrow, discontinuous, 30-100 cm thick, plagioclase-rich reaction rim located at the contact. The absence of a significant contact-metamorphic aureole and a readily observable chilled margin suggests that the intrusion was probably emplaced into an already hot, dry, country rock. The heat of intrusion may have caused some partial melting of the overlying sediments, producing a narrow zone of lit-par-lit migmatite located directly north of the intrusion. A similar structure was observed at the Mud Lake Intrusion. Two hornblende melagabbro/clinopyroxene hornblendite dykes occur within the migmatite zone and are possibly apophyses of the main intrusion.

Field measurement and diamond drilling (Appendix 3, Drill Hole K-1-87, Fleck Resources/St. Joe Canada Joint Venture, 1987) show that the northern contact of the Kawene Intrusion dips 65-85° N, the southern contact 40-70° N, and the western contact at 60° E. The eastern contact could not be measured directly; however, nearby hornblende clinopyroxenite layers imply a westerly dip of 60-65°. These data suggest two possible morphologies, a canoe-shape or an elongated funnel-shape.

The contacts of the Kawene Intrusion are offset by numerous discrete, cross-cutting faults, with observed and apparent offsets in the order of 2-15 m. Observed, or inferred, orientations imply the presence of conjugate fault sets, with a dominant NNE-SSW set, and a subordinate NW-SE

set. Examination of mapping data suggests that some of the offsets were produced by vertical to oblique movement rather than strike-slip movement. A more diffuse shearing style occurs subparallel, or slightly oblique, to the long axis of the intrusion forming anastomosing, moderately to intensely sheared zones that tend to concentrate near the contacts of the intrusion. The density of these shears decreases toward the centre of the intrusion. Also, the cross-cutting conjugate fault sets apparently offset these shears suggesting that at least two periods of deformation acted upon the intrusion after its formation. The earlier shearing may have served to elongate the intrusion parallel to the regional, east-west trending, subvertical to steeply north-dipping, regional schistosity. Schistosities within 30-50 m of the intrusion roughly parallel its contacts and may have been produced as a result of emplacement.

Work by Pirie and Mackasey (1978) on the determination of metamorphic isograds within the pelitic metasedimentary rocks of the Kawene Lake/Crooked Pine Lake area places the Kawene Intrusion, and its nearby country rocks, near the boundary between mineral assemblages containing biotite-garnet-andalusite and biotite-garnet-staurolite. This would indicate P-T conditions of 2.5-3.2 kb and 450-525° C, which is near the boundary between upper greenschist and lower amphibolite facies (Winkler, 1974).

Very finely disseminated patches and zones containing

<1-3% pyrrhotite, pyrite, and some chalcopyrite occur throughout the intrusion. In addition, an irregular, elongated, Pt-Pd-Cu-Ni-rich zone containing 1-25% finely disseminated, blebby, and, occasionally, net-textured pyrrhotite, chalcopyrite and pentlandite is closely associated with the northern contact. Where exposed by surface trenching and stripping the mineralized zone is approximately 60 m in length and up to 30 m in width. Diamond drilling by the Fleck Resources/St. Joe Canada Joint Venture discovered that the mineralization remains closely associated with the contact, but eventually pinches out at 65-70 m depth below surface (Appendix 3). Precious and base metal contents within the mineralized zone range from 121-3942 ppb Pt, 173-1754 ppb Pd, 15-110 ppb Rh, 5-39 ppb Ir and 45-440 ppb Au, and up to 1.3% Cu, 4500 ppm Ni, and 9 ppm Ag.

2.2.3 - The Mud Lake Intrusion:

The Mud Lake Intrusion (Figure 2.10-in back pocket) is a comma-shaped, mafic to ultramafic body over 800 m in length and 10-100 m in width. It is composed of two distinct parts: a main, unzoned, ultramafic mass about 100 m in width and 375 m in length, and an east-west striking, dyke-like 'tail', 10-30 m in thickness and over 400 m in length, consisting of a lower ultramafic unit and an upper intermediate unit.

The main ultramafic mass is composed of feldspathic

hornblendite, hornblendite, and clinopyroxene hornblendite, with subordinate amounts of dioritic appinite (refer to Chapter 3 for classification system) and hornblende gabbro occurring along the western and northwestern contacts. The rocks are generally massive in character; however, weakly-developed igneous layering does occur within some of the feldspathic hornblendites. The tail of the intrusion is composed of two distinct, subparallel units. The lower unit is composed of often porphyritic hornblende melagabbro, feldspathic hornblendite, and hornblendite. Weak to well-developed layering is common throughout this unit. The upper unit is composed of massive, dioritic appinite (quartz diorite) and is identical to, and apparently continuous with similar rocks present along the western contacts of the main ultramafic mass. Thick units of dioritic appinite were not observed within any other Quetico Intrusions.

The ultramafic rocks (Figure 2.3) are dark green and tend to be fine- to medium-grained; however, large oikocrysts of hornblende are ubiquitous and reach diameters of greater than 3 cm. Also, numerous, irregular, feldspathic, coarsely hornblende-porphyritic zones occur throughout the ultramafic rocks (Figure 2.4). Occasionally the upper parts of the igneous layers are porphyritic. These zones consist of a fine- to medium-grained groundmass of subhedral hornblende and 5-20% plagioclase, with 30-70%, 0.5 to 2.0 cm in diameter, euhedral, zoned hornblende

Figure 2.3: Hornblendite located within the Mud Lake Intrusion. Note - the slightly lighter patches are oikocrysts of hornblende.
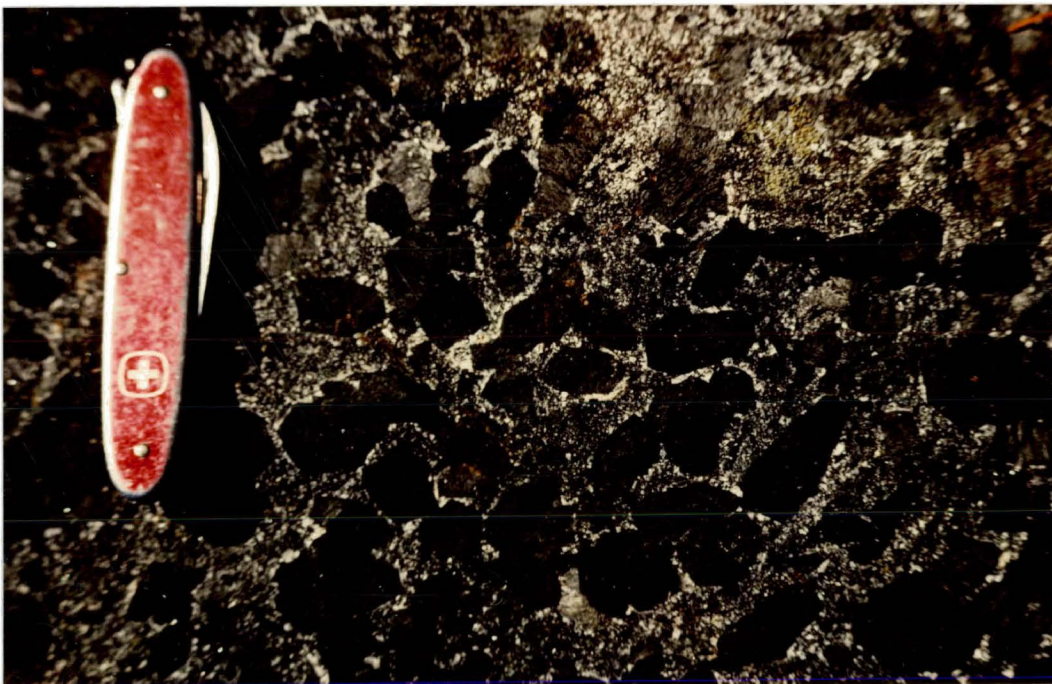
Figure 2.4: Zone of porphyritic feldspathic hornblendite to hornblende melagabbro within hornblendite. Mud Lake Intrusion.

phenocrysts. Contacts within the main ultramafic mass are generally gradational.

The appinitic diorites are massive, light green and generally fine- to medium-grained (Figure 2.5). Localized coarse-grained areas were observed. The sharp, lower contact of the unit is slightly chilled against the ultramafic rocks, suggesting that the ultramafic unit cooled to subsolidus temperatures before the appinite unit was emplaced. Numerous metasedimentary xenoliths in various stages of assimilation occur within the unit and suggest that it may be hybrid in nature.

Pods, patches, and veins of appinite (Figure 2.6a, b, c, and d) are common within all rock types, even the dioritic appinite unit, and often occur along contacts, shears, fractures and joints, but usually occur as isolated segregations and veins.

Emplacement of the Mud Lake Intrusion produced a narrow, 1-5 m thick, contact metamorphic aureole within the surrounding turbiditic metasedimentary rocks. This aureole is narrower than the one surrounding the Kawene Intrusion.

Regional dynamothermal metamorphism in the area of the Mud Lake Intrusion ranges between upper greenschist and lower amphibolite facies. The heat of the intrusion may have been responsible for the formation of a quartz monzonitic to granodioritic mobilizate. Injection of this mobilizate into the metasedimentary rocks in the immediate

Figure 2.5: Massive, fine- to medium-grained appinitic diorite within the Mud Lake Intrusion.
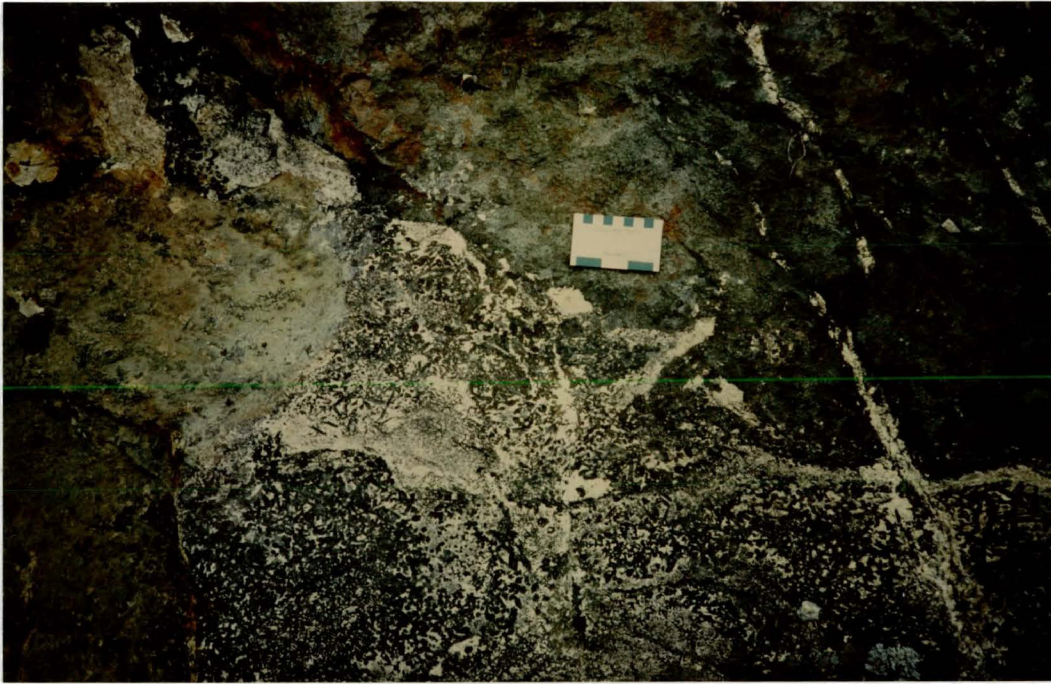
Figure 2.6a: Irregular, varitextured zone of appinite within hornblendite of the Mud Lake Intrusion.
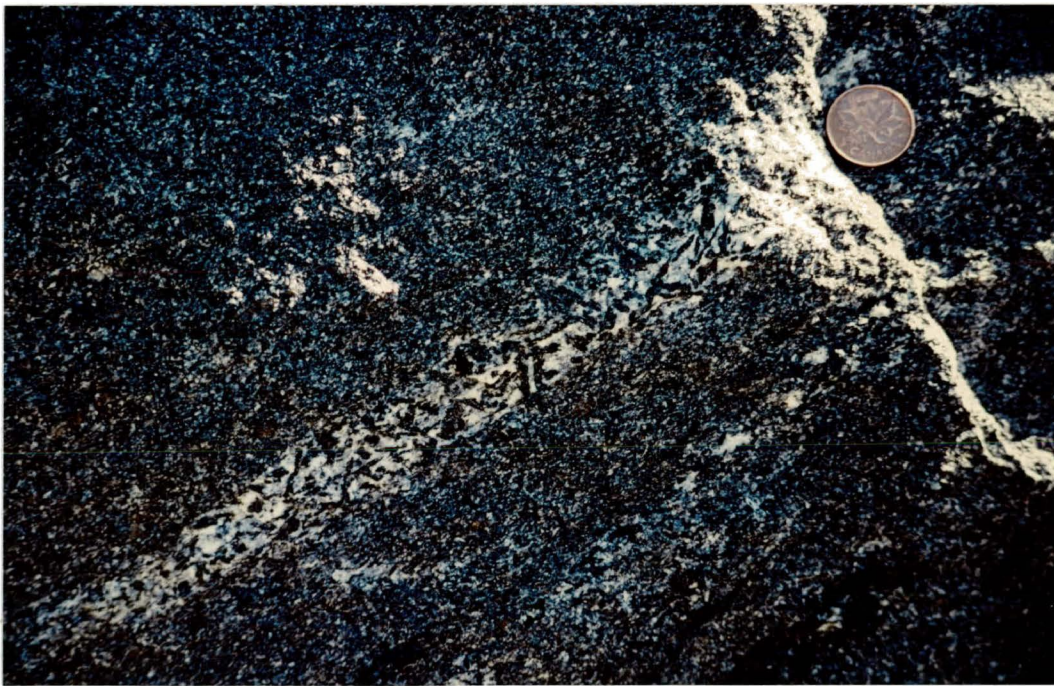
Figure 2.6b: Narrow vein of appinite within appinitic diorite unit of the Mud Lake Intrusion.
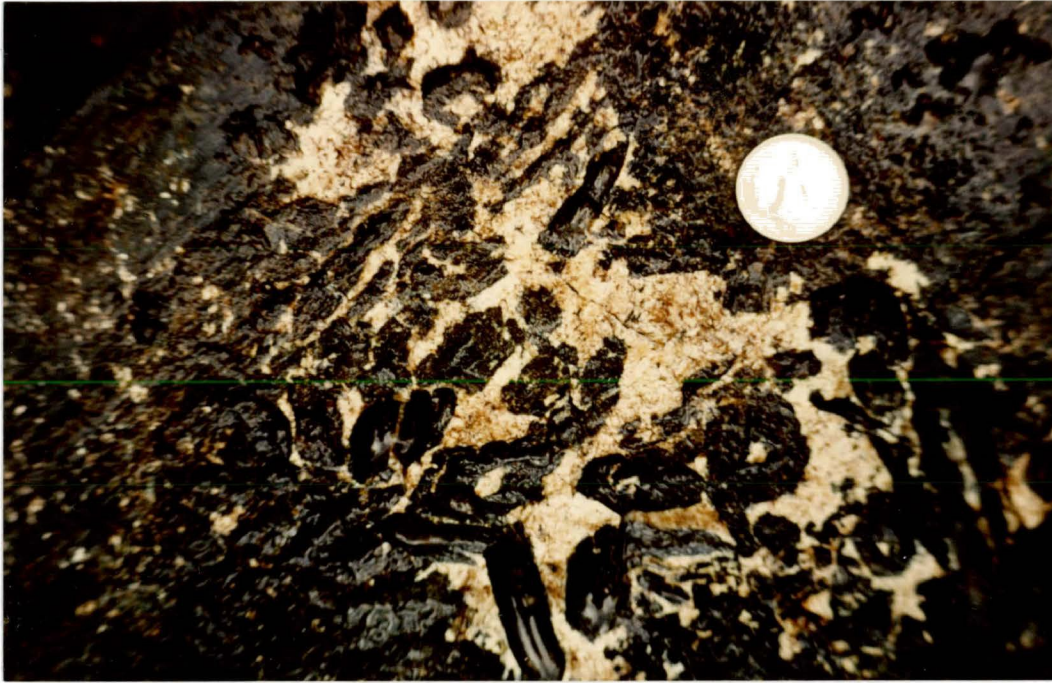
Figure 2.6c: Pod of appinite containing hornblende grains cored with plagioclase and quartz. Mud Lake Intrusion.
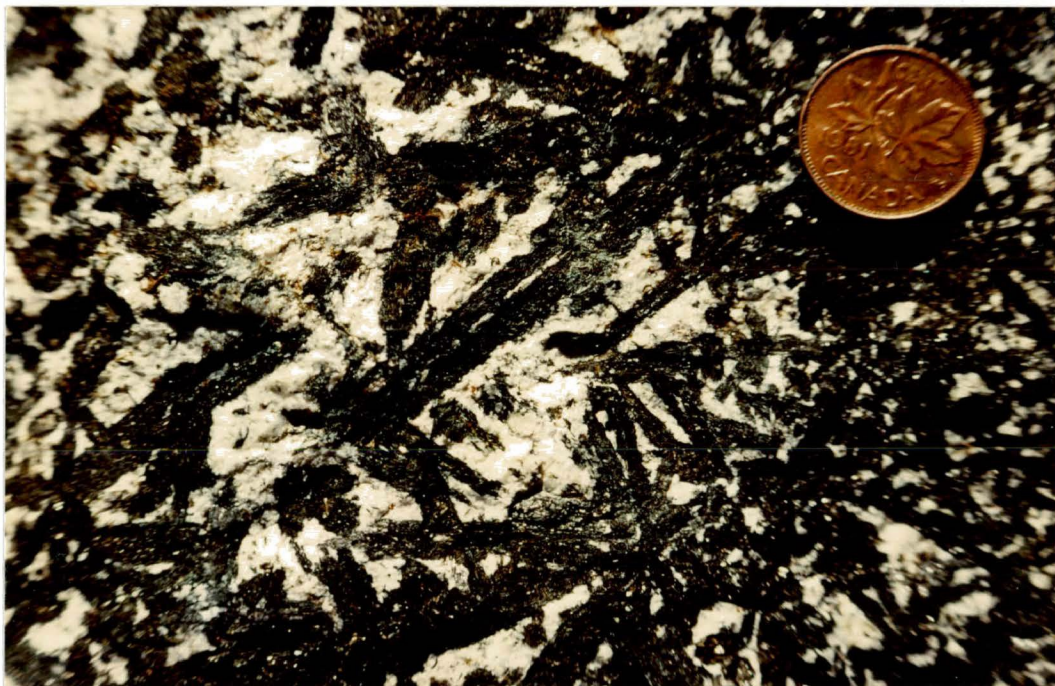
Figure 2.6d: Pod of appinite containing cored (split?) longitudinal hornblende grains infilled with plagioclase and quartz. Mud Lake Intrusion.

vicinity of the Mud Lake Intrusion produced a zone of migmatite (Figure 2.10) similar to that observed near the Kawene Intrusion. The surface exposure of the intrusion is relatively small; however, airborne magnetic data (ODM Map 1122G, 1961) implies the presence of a much larger body of mafic to ultramafic rock directly beneath the dyke-like tail of the intrusion. Much of the migmatite appears to lie within a concave depression located between the exposed and buried portions of the Mud Lake Intrusion.

Alteration is mainly due to regional metamorphism. It ranges from weak to strong and is strongly dependent upon rock type and proximity of contacts. Hornblendites are the most affected with primary hornblende altering to actinolite, biotite, and chlorite. Biotite and chlorite are most abundant near the contact with the surrounding metasedimentary rocks. Hornblende within the porphyritic and non-porphyritic varieties of feldspathic hornblendite, and the various gabbros, is usually less altered than hornblende within the non-feldspathic hornblendites. Most of the plagioclase has been heavily saussuritized.

Large- and small-scale faulting is readily evident. Two major, east-west-trending faults, one observed in outcrop and the other inferred from mapping and confirmed by diamond drilling (Resident Geologist's Assessment Files, Ministry of Northern Development and Mines, Thunder Bay), have been responsible for (Figure 2.10):

a)   A dextral offset of the northern limb of the Mud
     Lake Intrusion in the order of 125 to 150 m east;

b)   The formation of an intense, 30-50 m thick zone of
     mylonite 50 m south of the Mud Lake Intrusion; and

c)   The formation of a series of discrete, small-scale,
     mainly right-lateral faults within the intrusion,
     striking between 130° and 160°, with resulting
     offsets of 10 cm to 25 m.

Shearing is rare within the intrusion.

Much of the sulphide mineralization is confined to
small pods and patches within ultramafic rock types
adjacent to, or near, the contact with the surrounding
metasedimentary rocks. It consists of less than 1-5%, very
finely disseminated pyrrhotite, pyrite, and chalcopyrite.
The sulphides locally reach concentrations of 15% within
pegmatitic appinite veins.

The only significant surface concentration of PGE-
bearing base metal sulphides occurs within a small trench on
Discovery Island, located about 100 m east of the western
shore of Mud Lake (Figure 2.10). Platinum and base metals
were also encountered in diamond drill core from holes
completed on the mainland and on the lake ice by Ardel
Exploration in 1971. These drill results suggest that the
continuous mineralization present within the core for a
strike length of over 350 m is part of the same zone that
outcrops on Discovery Island (Resident Geologist's

Assessment Files, Ministry of Northern Development and
Mines, Thunder Bay). The sulphide content of the zone
ranges from 12-30% disseminated, net-textured, stringered,
and locally semi-massive pyrrhotite, chalcopyrite,
pentlandite, and some pyrite. Analytical results from this
study, and past exploration, yielded values of 33-3430 ppb
Pt, 50-525 ppb Pd, up to 8 g/ton Ag, 0.07% Ni, and 0.21% to
5.12% Cu.

It is interesting to note that some samples of
ultramafic rock from the intrusion contained between 175 and
2715 ppm tungsten. Close examination of these samples
revealed the presence of scheelite contained within 2-3 mm
thick quartz-carbonate stringers. These stringers occur
within hairline fractures and are due to late hydrothermal
fluids not related to the Mud Lake intrusive events.

2.2.4 - The Abiwin Intrusion:

The Abiwin Intrusion is a small, highly deformed body
approximately 200 m in length and up to 40 m in width
(Figure 2.11-in back pocket). The intrusion comprises two
main units composed of locally sheared, moderately to highly
altered feldspathic hornblendite to hornblendite and
hornblende gabbro to hornblende melagabbro, respectively.
The ultramafic rocks are massive, medium- to coarse-grained
and locally contain highly variable amounts of interstitial
plagioclase. The variation of the plagioclase content

locally produced irregular zones of hornblende melagabbro
within the ultramafic rock types. Well-developed patches
and zones of appinite are very common, particularly within
the feldspathic hornblendites. The mafic rocks (Figure 2.7)
are fine- to medium-grained and generally massive to
hornblende porphyritic; however, a weak to moderate igneous
foliation is developed locally.

Contacts between the main mafic and ultramafic rock
varieties within the intrusion are generally sharp, but
within each of the units contacts tend to be irregular and
gradational. Contacts between the intrusion and the
surrounding country rocks are sharp, but undulatory, and no
chilled margins were observed. Moderate to intense shearing
is often focused along external and internal contacts. Away
from these contacts the bulk of the intrusion is weakly
sheared to unsheared; however, some discrete, anastomosing
shear zones occur locally.

Regional, lower to upper amphibolite grade metamorphism
has had a marked effect upon the Abiwin Intrusion. The
resultant alteration ranges from moderate to intense with
hornblendite the most affected lithology. Hornblende within
all rock types is altered to actinolite and chlorite with
significant biotite occurring near contacts with the country
rock. Saussuritization of plagioclase is ubiquitous. The
turbiditic greywackes surrounding the intrusion are well-
foliated quartz-biotite schists that locally retain their

Figure 2.7: Porphyritic hornblende gabbro of the Abiwin Intrusion.

original, sedimentary textures. Locally they have been injected by a leucocratic, intrusive mobilizate. This mobilizate comprises between 25 and 50% of the country rock and takes the form of sheared, boudinaged, and disrupted, subconcordant veins and dykes of quartz monzonite and granodiorite. Pirie (1978) examined the mobilizate in this area and determined that the material originated elsewhere in an area of almost complete melting of the typical Quetico Subprovince wacke-mudstone.

The dynamic and thermal processes that formed, injected, and deformed the intrusive mobilizate reduced the once dyke-like Abiwin Intrusion to a complicated series of truncated, faulted, rotated, elongated, and possibly folded blocks and slices suggestive of pull-apart structures. Little lateral continuity of rock types is possible between most of the blocks and slices. Any evidence of a contact metamorphic aureole has been obliterated.

Mineralization within the intrusion consists of three small, irregular sulphide zones, the largest of which is approximately 40 m in length and up to 10 m in width. These zones occur within ultramafic rocks and contain 2-30% disseminated pyrrhotite, chalcopyrite, pentlandite, and minor pyrite. Two of the zones contain anomalous PGE and Cu-Ni values in the range of 0.30-2.04% Cu, 0.15-0.24% Ni, 55-720 ppb Pt, and 45-650 ppb Pd. One sample from the main zone returned 2.20% Cu, 0.08% Ni, 39.50 g/ton Pt, and 3.75

g/ton Pd.   The mineralized zones all occur near external or internal contacts.

2.2.5 - The Chief Peter Lake Intrusion:

The Chief Peter Lake Intrusion is poorly exposed.   Only the main sulphide exposure was observed and sampled in any detail.   The intrusion is an elongated, roughly lenticular plug approximately 760 m in length and up to 460 m in width. According to Irvine (1963) it is composed of a narrow northeast-trending, medium- to coarse-grained, serpentinized hornblende peridotite core surrounded by a main mass of medium- to coarse-grained, biotite-bearing, locally feldspathic hornblendite.   Irvine also states that the contact between the hornblende peridotite core and the outer hornblendite is gradational and marked by the decrease and eventual disappearance of clinopyroxene and olivine.   The reconnaissance examination completed during this study confirmed Irvine's statements, but noted that the hornblendites contain numerous coarse oikocrysts of hornblende, that the peridotite may best be termed hornblende wehrlite, and that appinitic pods and veins are present within the hornblende wehrlite.

Irvine (1963) classifies the enclosing metasedimentary rocks as a strongly foliated paragneiss.   The hornblendite/ metasediment contact was observed in one location by this author and proved to be sharp, undulatory, and apparently

unchilled. The metasediments at the contact are a contact
metamorphic, quartz-biotite fels with no foliation or
preserved primary features. Lack of exposure precluded the
determination of the thickness of a contact metamorphic
aureole.

Sulphide mineralization is exposed on surface at two
localities. Both occurrences are within hornblende wehrlite
and directly adjacent to the gradational contact with the
hornblendite envelope. Past diamond drilling encountered
appreciable sulphides, associated with this contact within
hornblende peridotite, at depth and along strike of the two
surface exposures (Resident Geologist's Assessment Files,
Thunder Bay). The 25 m long, 10 m wide western surface
showing examined during this study contained 1-8% finely
disseminated to locally net-textured pyrrhotite,
chalcopyrite, pentlandite, and minor pyrite. Two samples
contained appreciable PGE, gold and copper-nickel values in
the order of 0.39-0.63% Cu, 0.11-0.16% Ni, 1020-1500 ppb Pt,
1020-1050 ppb Pd, and 330-530 ppb Au.

2.2.6 - The Plateau Lake Intrusion:

The Plateau Lake Intrusion is a deformed body
approximately 650 m in length and 100 m in width. It is
composed of altered, medium- to coarse-grained hornblendite
with a small core of altered fine- to medium-grained,
hornblende clinopyroxenite. Both rock types contain large

oikocrysts of hornblende. A larger dioritic to gabbroic body occurs a short distance east of the ultramafic intrusion.

These two intrusions were emplaced into turbiditic sediments and appear subconcordant to bedding. Subsequent regional metamorphism, in the range of lower to mid-amphibolite facies, placed the Plateau Lake Intrusion into a P-T regime where the assemblage of biotite-andalusite-almandine +/- staurolite exists and well within the zone of almandine stability (Pirie and Mackasey, 1978). Rough calculation of the P-T conditions, based on the metamorphic isograds produced by Pirie and Mackasey's work, suggests approximately 3.0-3.2 kb and 525-550° C.

Sulphides were observed only within the ultramafic intrusion and are concentrated within altered hornblende clinopyroxenite. Sulphide content ranges from less than 10% to greater than 40% finely disseminated, locally net-textured chalcopyrite, pyrrhotite, pentlandite, and some pyrite. The average sulphide content is between 5% and 15% with chalcopyrite the dominant phase. Base and precious metal contents were 0.27-4.4% Cu, 0.06-0.73% Ni, 70-1028 ppb Pt, 69-686 ppb Pd, 86-686 ppb Au, and up to 20.5 g Ag.

2.2.7 - The Fire Lake Dykes:

The two deformed Fire Lake Dykes are about 400 m apart and were intruded subconcordantly into turbiditic metasediments. Regional metamorphism in the area is mid- to upper amphibolite grade. Both dykes are within 500 m of the irregular, migmatitic rim of the Quetico Batholithic Complex.

The western-most dyke is 3-4 m in thickness and was traced in outcrop for about 20-25 m. It is composed of altered, coarse-grained, locally feldspathic hornblendite and contains a small, finely disseminated sulphide zone of very limited extent. This zone comprises up to 1% chalcopyrite, pyrrhotite, and pyrite and contains 440 ppb Pt, 530 ppb Pd, and geochemically anomalous Cu and Ni values.

The eastern-most dyke is 20-40 m in width and is intermittently exposed along strike for about 650 m. It is composed of coarse, locally biotitic hornblendite and feldspathic hornblendite containing numerous, large, oikocrysts of hornblende. Much of the dyke is composed of very coarse-grained appinite with plagioclase-cored, or skeletal amphibole crystals up to 5 cm in length and 3 cm in diameter. Purely pegmatitic patches not exhibiting cored or skeletal amphiboles occur locally. One contact-related sulphide zone of very limited extend was observed. It contains 1-2% finely disseminated pyrrhotite and

chalcopyrite, with base and precious metal contents of 0.13% Cu, 0.15% Ni, 450 ppb Pt, and 99 ppb Pd.

2.2.8 - The Bergman Intrusion:

The Bergman Intrusion is partially exposed on a small island in Nym Lake. It is composed of massive, altered, locally biotitic, coarse-grained, hornblendite and feldspathic hornblendite. Common alteration products are actinolite and chlorite.

Field evidence suggests that the Bergman Intrusion is a rafted block or large xenolith contained within the varitextured to pegmatitic, quartz monzonitic border regions of the Quetico Batholithic Complex. Evidence to support this hypothesis is the presence of a thin wedge of clastic metasediments in contact with the hornblendite. This contact is sharp, undulatory, and weakly chilled and has, in turn, been cross-cut by the quartz monzonite country rocks. Additional supporting evidence is the lack of a pronounced, coincident, airborne magnetic anomaly (ODM Map 1122G, 1961) that is characteristic of the other intrusions previously described.

Finely disseminated pyrrhotite and chalcopyrite occur throughout the Bergman Intrusion. The average sulphide content is 1-2%; however, a poorly exposed, highly weathered, 3-6 m thick zone containing 2-10% disseminated to blebby pyrrhotite occurs near the southern contact. Samples

taken from this zone contain 0.13-0.28% Cu, up to 0.07% Ni, and in one case 180 ppb Pt and 75 ppb Pd.

2.2.9 - The Eva Lake Intrusion:

The Eva Lake Intrusion was not visited during this study; however, four sulphide-rich samples were made available by the Ontario Ministry of Northern Development and Mines. Aeromagnetic survey data (ODM Map 1122G, 1961) suggests the presence of a small, roughly circular body located in the area where the samples were taken.

The four samples are composed of weathered, moderately to strongly altered, hornblende peridotite and olivine-clinopyroxene hornblendite, and all contain numerous, large oikocrysts of hornblende. Common alteration products are actinolite, chlorite and serpentine. Sulphide content consists of 5-20% disseminated to blebby chalcopyrite and pyrrhotite along with considerable very finely disseminated magnetite. Two of the samples contain significant base and precious metal contents of 1.29% and 0.84% Cu, 0.39 and 0.26% Ni, 730 ppb and 430 ppb Au, 630 ppb and 225 ppb Pt, and 760 ppb and 840 ppb Pd.

2.2.10 - The North Elbow Lake Stock:

The North Elbow Lake Stock is the northern-most of two intrusions that comprise the Elbow Lake Mafic Complex. The stocks are separated by a 400 m wide screen of metasediments

bound on the south side by an inferred ENE-trending splay from the Elbow Lake Fault.

The roughly elliptical South Elbow Lake Stock is poorly exposed, and is 3300 m in length and up to 1800 m in width. This stock was described by Pirie (1978) and consists of medium-grained hornblende gabbro to diorite, with some medium- to coarse-grained blocks of biotitic hornblendite and rarely very coarse-grained, porphyritic hornblendite. No concentrations of sulphides were observed by Pirie (1978) nor this study.

The North Elbow Lake Stock measures 1900 m by 1500 m, and is much better exposed than the South Elbow Lake Stock. It is crudely zoned and consists of an irregular core of locally porphyritic hornblende clinopyroxenite, clinopyroxene hornblendite, hornblendite, and some slightly feldspathic hornblendite partially surrounded by often porphyritic, feldspathic hornblendite that locally exhibits weak layering (Figure 2.8). The core also contains isolated zones of hornblende websterite, which contains significant quantities of both clinopyroxene and orthopyroxene. Pirie (1978) and Legault (1976) believe that the ultramafic rocks are cumulates that were intruded by massive, non-cumulate, more normally-textured hornblende gabbro and diorite. The diorite is commonly hybridized and contains numerous, hornfelsic metasedimentary xenoliths in various stages of assimilation (Figure 2.9). The gabbro and the diorite also

Figure 2.8: Weakly layered, porphyritic feldspathic hornblendite of the North Elbow Lake Stock.

Figure 2.9: Foliated diorite containing recrystallized, partially assimilated xenolith. North Elbow Lake Stock.

contain numerous partially resorbed xenoliths derived from the earlier ultramafic phases of the intrusion. Porphyritic and appinitic textures are very common throughout the intrusion, particularly within the feldspathic hornblendites, and all ultramafic rock types contain large oikocrysts of hornblende.

The North Elbow Lake Stock exhibits a pronounced contact metamorphic aureole, with well-developed hornfelsic textures, that has been overprinted by later regional metamorphism. Deformed diorite, gabbro, and hornblendite dykes are common throughout this aureole. Also common are large numbers of irregular, boudinaged, and disrupted, locally pegmatitic, leucocratic quartz monzonite veins and dykes that have locally backveined the marginal rocks of the intrusion along joints, fractures, and discrete shears. Pirie (1978) notes that foliations observed within the metasedimentary rocks marginal to the contact metamorphic aureole are subparallel to the contacts of the intrusion. Where observed the intrusive/metasediment contact is cross-cutting and undulatory to irregular in appearance.

No PGE nor base metal-rich sulphide concentrations were observed during the examination undertaken by this study. Sulphide contents were usually much less than 1%, but rarely up to 3% of finely disseminated pyrrhotite and pyrite.

Legault (1976) notes the presence of a number of isolated lenses within the metasediments marginal to the

intrusion which she termed 'breccia-conglomerate'. These zones are up to 6 m in length and 4 m in width and consist of small, subround to subangular fragments, usually less than 10 cm in length, of clinopyroxene hornblendite and feldspathic hornblendite, within a groundmass of fine- to medium-grained hornblende gabbro and finely crushed biotite schist. Legault also notes that the fragments are locally aligned within the zones. These zones may be intrusion breccias similar in occurrence to the breccia pipes commonly associated with the appinite suite intrusions located in Ireland and Scotland (Bowes et al., 1964; French, 1966; Pitcher and Berger, 1972; Bowes and McArthur, 1976; French, 1976; Brindley et al., 1976; and French, 1977).

2.2.11 - Other Intrusions:

Four of the intrusions examined during this study contain no observed concentrations of base or precious metals, but do exhibit the same rock types and textures observed in the intrusions previously described in this chapter.

The largest of these intrusions, the Heward Lake Complex, is an elongated, deformed, dyke-like body approximately 1400 m in length and up to 150 m in width. It is composed of locally biotitic, porphyritic to massive hornblende melagabbro, with some locally porphyritic, feldspathic hornblendite and hornblendite. The ultramafic

rocks always contain large oikocrysts of hornblende.
appinitic pockets occur locally.

The Kawene Lake Mafic Complex is about 1700 m in
length, but is generally less than 100 m in thickness. It
exhibits a wider variety of medium- to coarse-grained
lithologies than the Heward Lake Complex with a range from
hornblende gabbro to hornblende wehrlite. The ultramafic
rock types predominate, and usually contain oikocrysts of
hornblende. The occasionally porphyritic, gabbroic rocks
occur as a narrow, 10-30 m thick zone along the northern
contract of the intrusion.

Two intrusions that occur north of the Plateau
Intrusion and are small, dyke-like and limited in extent.
Both are composed of medium- to coarse-grained biotitic
gabbro containing isolated appinite pockets and small
amounts of finely disseminated pyrrhotite and chalcopyrite.

CHAPTER 3

PETROGRAPHY OF THE SILICATE MINERALS

3.1: Introduction

The following chapter will describe the detailed petrography of the silicate minerals comprising the rocks of the Quetico Intrusions. This study deals with a group of related intrusive bodies that exhibit a range of very similar rock types and textures. It is necessary that the following discussion deal with the lithologies in general with notes on any intrusion- or site-specific variations, ie. differences of texture, mineral abundance, accessories or alteration styles.

3.2: Silicate Minerals

The examination of over 200 thin sections revealed a wide variety of hornblende-rich rock types that range from quartz diorite to hornblende wehrlite. The single most abundant lithology is clinopyroxene hornblendite. Hornblende, clinopyroxene, and plagioclase occur within all of the intrusions examined, olivine in three, and orthopyroxene in one. Weak to intense deuteric and metamorphic alteration processes are observed within all rock types.

The rock types described were identified using the IUGS system of rock classification and nomenclature (Streckeisen, 1976). Some texturally distinct rocks were further

subdivided using the nomenclature of the appinite suite
(Figure 3.1) developed by French (1966). This mainly
subjective nomenclature is based primarily on colour index
and amphibole habit and defines two contrasting textural
series. The dioritic series contains squat, stubby
amphiboles, sometimes occurring in aggregate form, whereas
the appinitic series contains long, prismatic to acicular
amphiboles. Amphiboles of both series are characterized by
large, ragged, cored and split grains that are generally
infilled by plagioclase and quartz. Figure 3.2 compares
amphibole textures from the Quetico Intrusions to those from
appinites of Great Britain (Roach, 1964). Some of the
normally textured diorites, gabbros, and feldspathic
hornblendites described below might be incipient dioritic or
appinitic series rocks as described by this classification
system; however, the term appinite within this thesis will
only refer to rocks with a colour index between 30 and 70
that exhibit the distinctive textures of the appinitic and
dioritic series. The subjective nature of the appinite
suite nomenclature was not suitable for application to all
of the rock types contained within the Quetico Intrusions.

The petrographic descriptions that follow will proceed
from the most mafic to the least mafic major rock divisions
observed, i.e. peridotite to diorite. The texturally
distinct appinites include rocks from more than one of the
IUGS fields and will be described last.

Nomenclature of the Appinite Suite
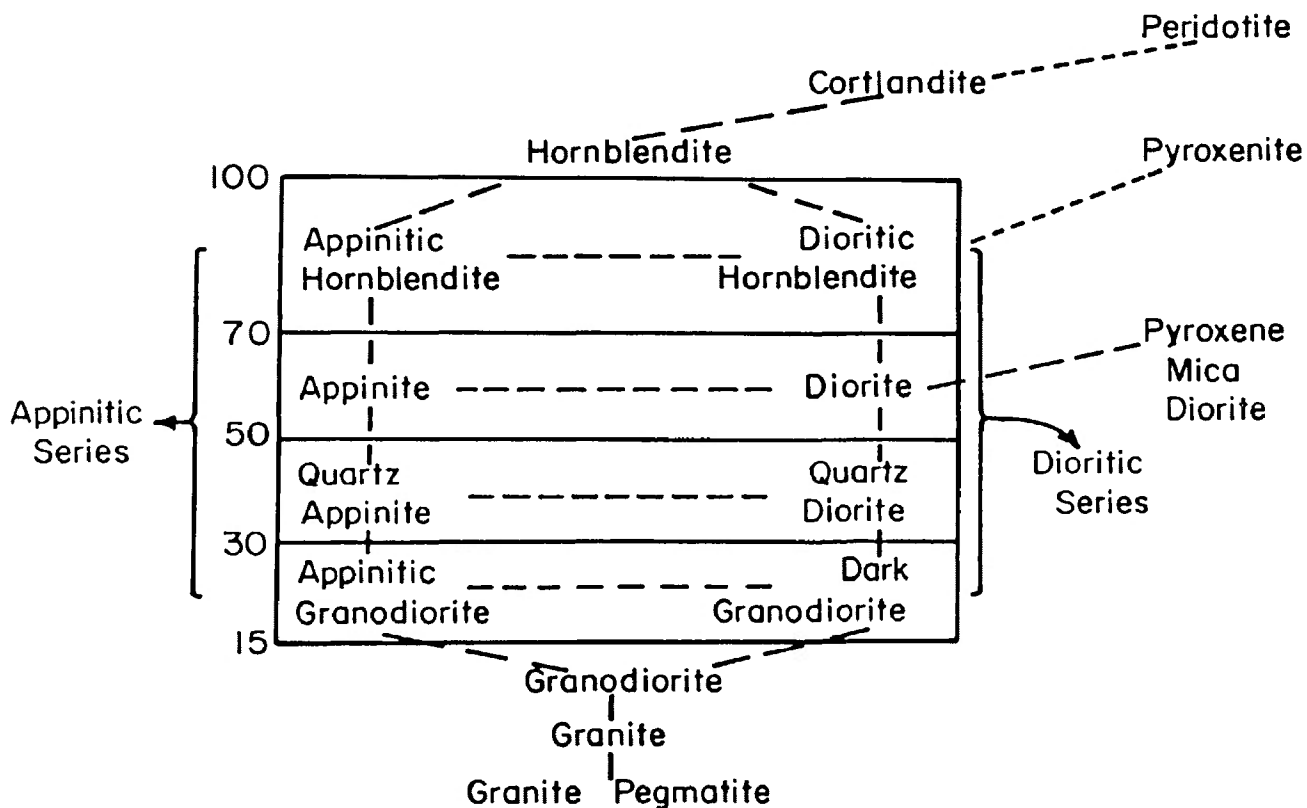
Figure 3.1: This mainly subjective nomenclature system (after French, 1966) is based primarily on colour index (numbers on diagram) and specific amphibole habit that defines two contrasting textural styles. The term appinite, as applied to the Quetico Intrusions, has been specifically defined using the portions of the above diagram that exhibit a colour index between 30 and 70.

Figure 3.2

Comparison of Amphibole Textures
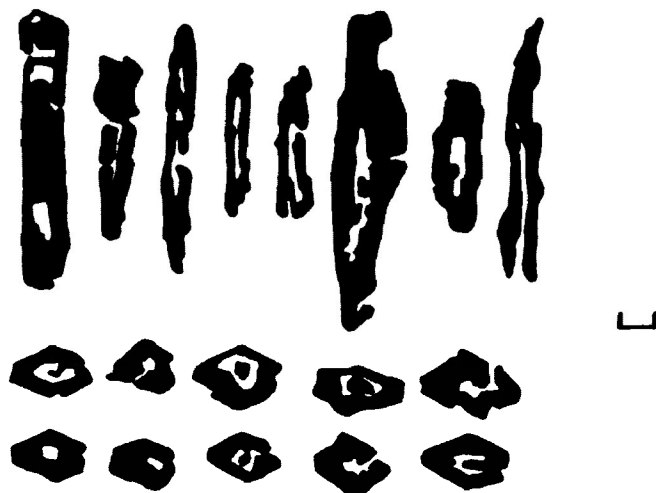
Figure 3.2a: Tracings from photographs illustrating the cored and split nature of amphiboles from appinites of Great Britain (Roach, 1964).
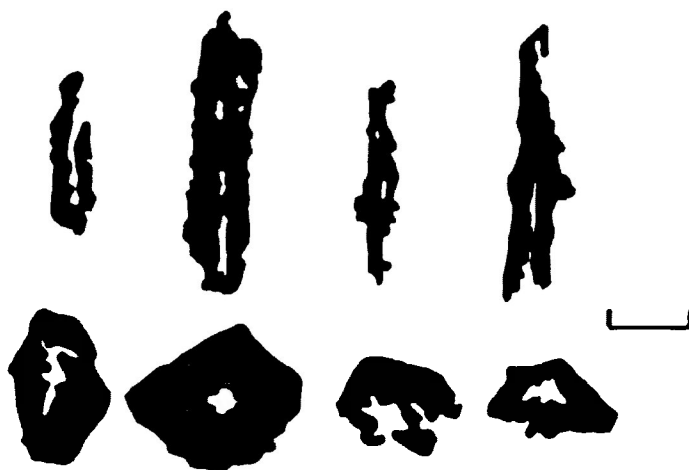
Figure 3.2b: Tracings from photographs and rock samples of appinites from the Quetico Intrusions. Note the similarity to the textures presented in Figure 3.2a.

SCALE BARS FOR BOTH FIGURES REPRESENT 1 CM.

Grain sizes were determined using the criteria of Williams et al. (1982): fine (<1 mm), medium (1-5 mm), coarse (5 mm - 3 cm).

3.2.1 - Peridotite:

Peridotite occurs within the Kawene, Chief Peter, and Eva Lake Intrusions. Two peridotite varieties were observed. The most abundant variety, hornblende wehrlite, is composed of olivine, clinopyroxene and hornblende. The second variety, hornblende peridotite, is observed only within the Eva Lake Intrusion and contains olivine and hornblende, but little or no clinopyroxene.

3.2.1.1 - Hornblende Wehrlite:

The hornblende wehrlite (Figure 3.3) present within the Kawene and Chief Peter Intrusions consists of fine- to medium-grained cumulus olivine and clinopyroxene commonly enclosed by large oikocrysts of medium- to coarse-grained hornblende. Biotite is locally a common intercumulus accessory, while apatite is rare. The modal percentage of olivine is 40-45%, while clinopyroxene and hornblende exhibit wider ranges of 10-40% and 15-35%, respectively. The crystallization sequence is apparently olivine and clinopyroxene, clinopyroxene, hornblende, biotite and apatite.

Olivine ($Fo_{78.65-80.53}$ $Fa_{18.96-20.83}Tp_{0.38-0.42}$) occurs as somewhat

rounded, 0.2-3 mm diameter grains that exhibit scalloped, corroded, sometimes embayed grain boundaries (Figure 3.4). The embayed boundaries are occasionally observed when in contact with clinopyroxene. The olivine grains commonly form 2-5 grain clusters (Figure 3.5).

Every olivine grain is fractured and serpentinized. Weakly altered grains exhibit narrow coronas and contain thin veinlets of serpentine and magnetite (Sample AK-40-86). As serpentinization proceeds the number and thickness of these veinlets increases, until the original grains are totally pseudomorphed by a mixture of colourless to yellowish-green serpentine (possibly antigorite), fine stringers and disseminated magnetite, sometimes colourless dolomite, and occasionally, light green actinolite. The best preserved olivines occur within the Kawene Intrusion, and the least preserved within the Chief Peter Intrusion.

Alteration haloes, or coronas, commonly develop around olivine grains enclosed by oikocrysts of hornblende, but rarely in contact with clinopyroxene. The best-developed coronas are observed within the Chief Peter Intrusion. They are up to 0.75 mm in thickness and consist of very fine-grained zones of actinolite-magnetite-serpentine+/-dolomite (Sample ACP-1-86). The least-developed coronas are observed within the Kawene Intrusion and are usually less than 0.20 mm in thickness.

Figure 3.3: Hornblende wehrlite (Sample AK-40-86). Note intense fracturing of minerals surrounding serpentinized olivine (FOV 2.7 mm).
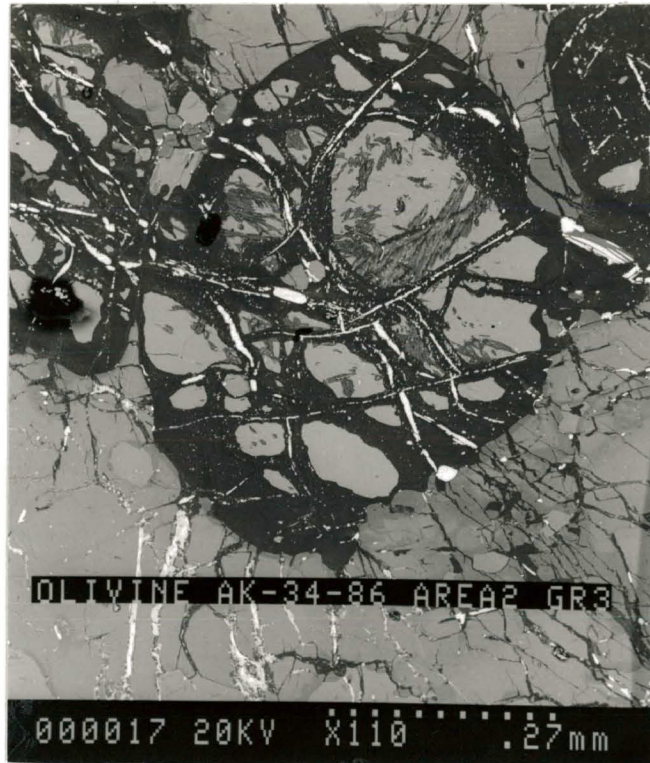
Figure 3.4: Strongly serpentinized, rounded olivine grain. Sample AK-34-86 from the Kawene Intrusion.
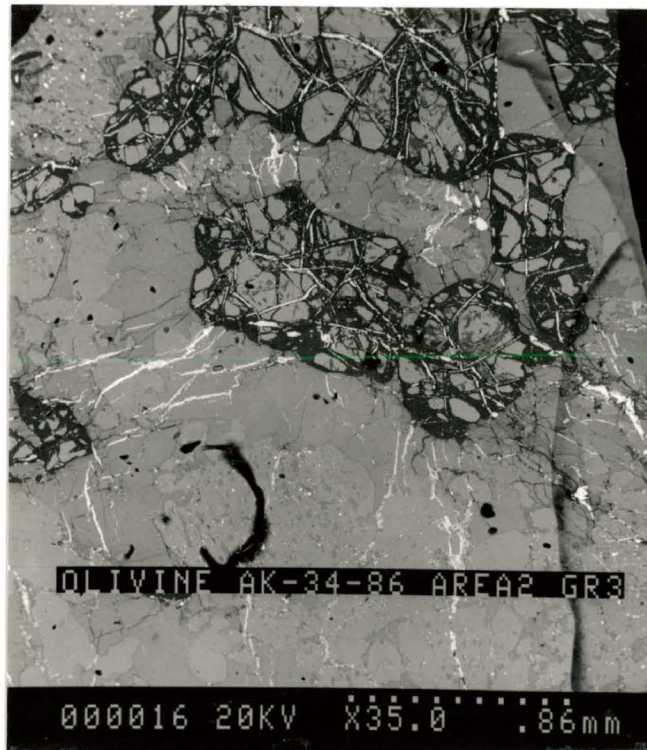
Figure 3.5: Cluster of round, serpentinized olivine grains within hornblende wehrlite. Sample AK-34-86.

Figure 3.6: Altered hornblende peridotite from the Eva Lake Intrusion (FOV 2.7 mm). Sample AKR-1-86.

The volume change accompanying serpentinization has fractured the silicate minerals surrounding the olivine grains. Serpentine and magnetite now occupy these fractures.

The <u>clinopyroxene</u> present is diopside and diopsidic augite (AK-34-86), with a composition of $Wo_{44.60-47.39}$, $En_{45.32-48.71}$, and $Fs_{6.39-7.30}$. The grains are colourless, non-pleochroic, generally subhedral, commonly twinned, variably uralitized, and <0.2-1.0 mm, but locally 2.0-3.0 mm, in diameter. A few grains are myrmekitically intergrown with magnetite. Grain boundaries, cleavage traces, and fractures are commonly uralitized. Within the Kawene Intrusion uralitization is progressive and produces increasingly corroded and sutured grain boundaries, eventually resulting in completely replaced pseudomorphs of actinolite and a very fine dusting of magnetite. The least altered grains are enclosed within large oikocrysts of hornblende. The most altered grains are interstitial to all other grains. Actinolite-rich coronas, up to 0.3 mm in thickness, surround many of the poikilitically enclosed grains. Most of the clinopyroxenes within the wehrlites of the Chief Peter Intrusion are almost completely uralitized to pseudomorphs of actinolite. There are few unaltered remnants. A few large grains have been partially replaced by hornblende. This may be due to resorption during late stage crystallization or subsolidus re-equilibration.

The two main varieties of <u>hornblende</u> are large, medium-
to coarse-grained, anhedral to subhedral, poikilitic,
intercumulus grains (oikocrysts) and small, fine-grained,
locally medium-grained, sometimes weakly poikilitic,
anhedral to subhedral cumulus grains. Both varieties are
pleochroic, pale green to brownish-green in colour and may
contain very fine-grained replacement magnetite along
cleavage traces.

The oikocrysts are 2-20 mm in diameter and optically
continuous, with scalloped, embayed, and locally corroded
grain boundaries. The numerous included grains
(chadacrysts) consist of olivine, clinopyroxene, and rarely
subhedral hornblende. Alteration to very pale green
actinolite and a very fine dusting of magnetite is common
along grain boundaries, fractures and cleavage planes, and
as narrow coronas surrounding the chadacrysts.

The considerably smaller, cumulus grains are usually
<2mm in diameter, commonly twinned, and exhibit sharp,
locally corroded, occasionally embayed grain boundaries.
Irregular, primary overgrowths of very pale green actinolite
occasionally form partial mantles on some of the grains.
Alteration to actinolite is generally more advanced than
alteration observed within oikocrysts.

The hornblendes of the Chief Peter Intrusion wehrlites
are much more altered than those of the Kawene Intrusion,
with many grains of both textural varieties almost totally

altered to an interlocking mass of anhedral to subhedral
actinolite and considerable very fine-grained magnetite.

Biotite is a relatively minor primary component that
locally comprises 5% of the rock. It occurs as discrete,
interstitial, anhedral to subhedral plates and books up to
1.5 mm in length. The grains are locally corroded, commonly
replaced by sulphides and oxides, and readily alter to
chlorite along grain boundaries and cleavage traces. Some
larger grains contain tiny chadacrysts of clinopyroxene and
hornblende.

Apatite is rare, but occurs locally as very fine to
fine-grained euhedral crystals usually < 0.1 mm in length.
It often occurs parallel to hornblende and actinolite
cleavage traces.

3.2.1.2 - Hornblende Peridotite:

Hornblende peridotite, composed essentially of fine- to
coarse-grained olivine and medium- to coarse-grained
oikocrysts of hornblende, with minimal identifiable
clinopyroxene, was only observed within the Eva Lake
Intrusion (Figure 3.6). Biotite is a significant primary
and secondary phase, clinopyroxene a minor accessory phase,
and apatite is rare. Little primary amphibole has survived
due to strong deuteric and metamorphic alteration. The
modal percentage of olivine, 45-65%, is greater than that
observed within the wehrlites described above; hornblende

comprises 25-35%; biotite 5-10%, and clinopyroxene less than 1%. Texturally the two peridotite varieties are almost identical. The principal differences are a general absence of clinopyroxene and an increase in the olivine content.

The <u>olivine</u> grains ($Fo_{78.03-79.42}$ $Fa_{20.11-21.66}Tp_{0.18-0.48}$) are up to 5 mm in diameter, rounded to subhedral in form, and often form multiple-grain aggregates. Serpentinization and subsequent replacement by actinolite is more advanced than observed within the wehrlites. No embayed grains were observed, but corroded grain boundaries and narrow 0.1-0.3 mm coronas composed of actinolite, serpentine, magnetite and sulphides are common (Figure 3.7).

Much of the original <u>hornblende</u> has subsequently altered to pale green, weakly pleochroic actinolite. Magnetite is a common replacement along fractures and cleavage traces. Partially replaced, irregular remnants within some grain centres are all that now remains of the original hornblende.

Altered hornblende locally forms pseudomorphs after <u>clinopyroxene</u>. Occasionally small, irregular clinopyroxene remnants are present within the cores of these pseudomorphs, implying that clinopyroxene was originally common within the melt, but was resorbed during the later stages of crystallization or replaced during subsolidus re-equilibration. Subsequent metamorphism has obliterated all traces of many of the pseudomorphs.
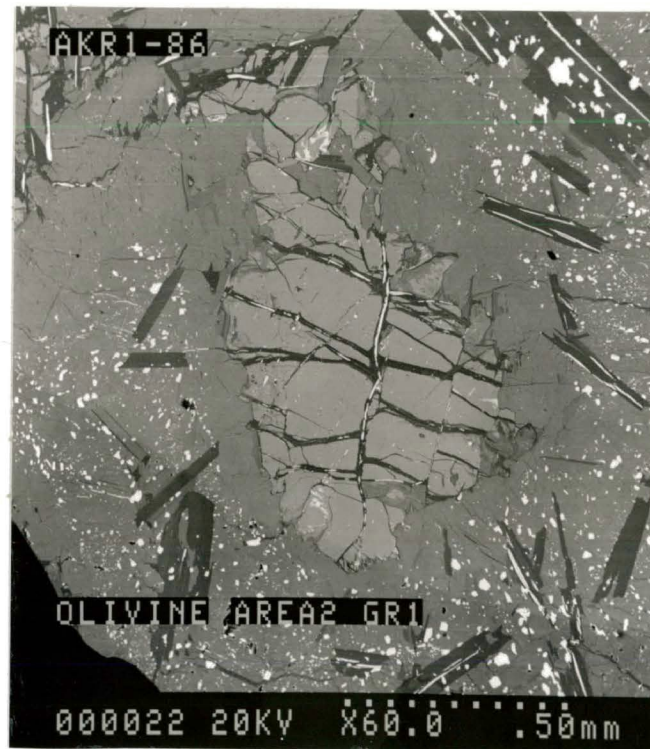
Figure 3.7: Actinolite corona surrounding a corroded olivine grain within hornblende peridotite of the Eva Lake Intrusion. Sample AKR-1-86.

Biotite occurs as both primary and secondary phases. The two varieties, often difficult to distinguish, are commonly twinned, slightly bent, partially altered to chlorite, and replaced by opaque minerals along cleavage traces. Formation as a late primary magmatic phase, contemporaneous with oikocrysts of hornblende, is suggested by larger, generally altered grains that are poikilitic, exhibit embayed grain boundaries, are included within oikocrysts of hornblende, or are interstitial to other primary phases. Secondary, metamorphic biotite is less altered, fine-grained, anhedral, and occurs as replacement ribbons along cleavage traces and fractures, or as randomly oriented flakes within other highly altered minerals. Grain size ranges from <0.1-4 mm in length.

Apatite is rare and occurs as isolated, euhedral blades and needles usually cross-cutting actinolite cleavage traces.

3.2.2 - Hornblende Pyroxenite:

Two varieties of hornblende pyroxenite were encountered. The most abundant is a moderately altered hornblende clinopyroxenite that is very common within the core of the Kawene Intrusion. The least abundant is a slightly altered, commonly porphyritic, feldspathic hornblende websterite, is only present within the North Elbow Lake Stock.

3.2.2.1 - Hornblende Clinopyroxenite:

The hornblende clinopyroxenite (Figure 3.8) is fine- to coarse-grained and consists of 40-65% clinopyroxene, 30-45% hornblende, trace-10% biotite, and occasionally 5-25% olivine. The IUGS System classifies olivine-bearing varieties as olivine-hornblende clinopyroxenite (Streckeisen, 1976).

Clinopyroxene ($Wo_{43.98-48.78}$ $En_{45.83-49.02}$ $Fs_{5.39-7.93}$) occurs as commonly twinned, variably uralitized, subhedral to euhedral cumulus grains with sharp, locally embayed, commonly corroded boundaries. Myrmekitic intergrowths with magnetite are observed. Grains range from 0.04-2.00 mm, but average 0.30-0.65 mm in diameter. Many grains are totally or partially enclosed within large oikocrysts of hornblende, and are often partially to totally replaced by actinolite and a very fine dusting of magnetite. Alteration coronas within the hornblende are common. Clinopyroxene within olivine-rich hornblende clinopyroxenites contains less magnesium and more calcium ($Wo_{47.13-48.44}$ $En_{45.25-47.30}$ $Fs_{5.00-6.45}$).

Hornblende generally occurs as large, 2-10 mm, anhedral to subhedral, poikilitic, intercumulus grains. Smaller, 0.05-3 mm diameter, non-poikilitic, subhedral to euhedral, cumulus grains are also common and are sometimes enclosed by the larger oikocrysts. Unaltered grains are yellowish-green to olive-green, blue-green or brownish-green. Actinolite and biotite are common alteration products along grain

boundaries, cleavage traces, or as narrow coronas around clinopyroxene chadacrysts.

Olivine ($Fo_{78.25-80.89}$ $Fa_{18.6-20.99}Tp_{0.51-0.72}$) is generally absent, but where observed (Figure 3.9) forms rounded to subhedral, highly fractured and serpentinized grains 0.25-0.80 mm in diameter. Serpentine and magnetite comprise between 30 and 100% of any particular grain.

Biotite is common as both an intercumulus, late magmatic, accessory mineral and as a metamorphic alteration product of hornblende. The primary grains are generally larger than the secondary grains, but the overall size-range is from <0.1-0.75 mm. Biotite is rare to absent within the olivine-rich hornblende clinopyroxenites.

Zircon is a rare accessory associated with primary biotite. Apatite forms a few acicular, euhedral crystals up to 0.2 mm in length that are closely associated with hornblende and actinolite. Calcite sometimes occurs as a minor alteration product of clinopyroxene in olivine-bearing varieties of hornblende clinopyroxenite.

3.2.2.2 - Feldspathic Hornblende Websterite:

The only orthopyroxene-bearing lithology observed within the Quetico Intrusions is a feldspathic hornblende websterite that occurs within the North Elbow Lake Stock (Figure 3.10). It is hornblende-porphyritic with a fine- to medium-grained groundmass and contains numerous medium- to

Figure 3.8: Hornblende clinopyroxenite (FOV 2.7 mm). Sample AK-2-86, Kawene Intrusion.

Figure 3.9: Olivine hornblende clinopyroxenite (FOV 2.7mm). Sample AK-12-86, Kawene Intrusion.
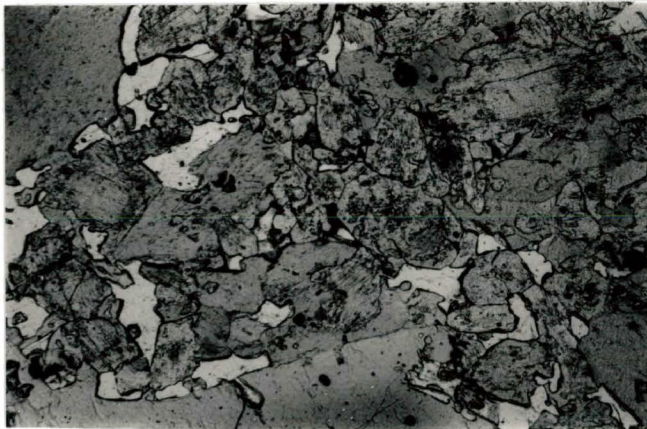
Figure 3.10: Feldspathic hornblende websterite (FOV 2.7 mm). Sample AEN-7-84, North Elbow Lake Stock.

coarse-grained oikocrysts of hornblende. Mineral content is 30-40% clinopyroxene, 15-35% orthopyroxene, 12-40% hornblende, 7-10% plagioclase, and 2-5% quartz. The two samples studied (AEN-7 and 9-84) show a wide range in hornblende and orthopyroxene content, with an apparent increase in orthopyroxene and a decrease in hornblende toward the centre of the intrusion.

Clinopyroxene is colourless to pinkish, <0.1-1 mm in diameter, anhedral to euhedral with subhedral shapes dominant, and commonly twinned. Grain boundaries are sharp to embayed and exhibit very narrow actinolite coronas when in contact with hornblende. Some grains are weakly uralitized.

The orthopyroxene is colourless to pale pink, slightly pleochroic hypersthene with extinction parallel to cleavage traces. The grains range from <0.1-1.2 mm in diameter, are subhedral to euhedral, with sharp, commonly embayed grain boundaries. Hypersthene in contact with hornblende is moderately to heavily corroded and skeletal in appearance.

Hornblende forms poikilitic, intercumulus grains (oikocrysts) up to 5 mm in diameter, and weakly zoned, moderately poikilitic phenocrysts up to 6 mm in diameter. The phenocrysts are subhedral to euhedral, with sharp, commonly embayed grain boundaries that are sutured when in contact with other hornblende grains. A weak zonation is implied by reddish-green to brownish-green cores and pale

green to bluish-green rims. The oikocrysts are pale
yellowish-green to brownish-green or pale greenish-brown to
reddish-green and anhedral to locally subhedral.

Plagioclase occurs as an anhedral, locally poikilitic,
intercumulus phase usually much less than 2 mm in length.
Most grains, particularly the larger ones, are heavily
saussuritized. Some of the smaller grains are preserved and
exhibit two apparent compositional ranges from the
measurement of albite twins. The least calcic is An_{36-40} and
the most calcic is An_{48-62}.

Accessory quartz occurs as small, anhedral,
interstitial grains, usually less than 0.2 mm in diameter.

No biotite, apatite, nor zircon were observed.

3.2.3 - Hornblendite:

The hornblendites are the most abundant lithologic
group occurring within the Quetico Intrusions examined. The
five varieties observed all contain greater than 50%, and
usually greater than 80%, hornblende and are subdivided on
the additional presence or absence, of clinopyroxene,
olivine and plagioclase. Sub-types are often gradational
and include feldspathic hornblendite, hornblendite (sensu
stricto), feldspathic clinopyroxene hornblendite,
clinopyroxene hornblendite, and olivine hornblendite. The
feldspathic varieties are slightly to moderately
porphyritic, and all varieties contain medium- to very

coarse-grained oikocrysts of hornblende. Alteration varies from slight to intense. Mineral habit, form, and size-range are practically identical from variety to variety. To avoid repetition the constituent minerals will be described once, in detail, after the rock-descriptions.

3.2.3.1 - Hornblendite (sensu stricto) and Feldspathic Hornblendite:

Hornblendite (sensu stricto) is fine- to coarse-grained and contains 80-97% hornblende, less than 10% clinopyroxene, 1-3%, occasionally up to 10%, biotite, and <1% plagioclase (Figure 3.11). Apatite usually occurs in trace amounts of 1% or less, but can locally comprise 2-3%. Trace titanite (sphene) and zircon occur locally.

Feldspathic hornblendite is fine- to coarse-grained and similar to non-feldspathic hornblendite, but tends to contain both phenocrysts and oikocrysts of hornblende. It is comprised of 67-90% hornblende, 2-10% plagioclase, 1-5%, locally up to 20%, biotite, 1-3% apatite, and trace quartz and zircon.

3.2.3.2 - Clinopyroxene Hornblendite and Feldspathic Clinopyroxene Hornblendite:

Clinopyroxene hornblendite is fine- to coarse-grained and consists of highly variable amounts of hornblende, clinopyroxene and biotite (Figure 3.12). Estimated modal abundances of the constituent minerals are 50-85%

hornblende, 10-40% clinopyroxene, trace to 6%, and locally
up to 20%, biotite; trace to 3% apatite, and rare
plagioclase.

The feldspathic varieties of clinopyroxene hornblendite
observed within the Kawene Lake Mafic Complex and the Mud
Lake Intrusion contain 63-86% hornblende, 10-25%
clinopyroxene, 2-6% plagioclase, trace to 3% biotite, and
trace to 2% apatite. Like the feldspathic hornblendite
described previously, this rock is hornblende porphyritic.

3.2.3.3 - Olivine Hornblendite:

Olivine hornblendite is present within two samples (AK-
19-86 and AK-43-86) within the Kawene Intrusion. It is
similar to the hornblendite (sensu stricto) described
previously except for the presence of about 10% cumulus
olivine and a few scattered remnants of clinopyroxene (<1%).
This rock is also quite altered and contains 10-15%
secondary carbonate, possibly dolomite. Apatite is rare.

The mineral descriptions for the five varieties of
hornblendite just described are presented below:

Hornblende occurs as both cumulus and intercumulus
varieties. The main difference between the hornblendites
and the more primitive rock types previously described is
the presence of a porphyritic cumulus phase within the
feldspathic varieties.

Cumulus hornblende grains are commonly twinned, often crudely zoned, subhedral to euhedral, and slightly to moderately poikilitic (Figure 3.13). They average 0.05-4 mm in diameter, but phenocrysts within the feldspathic rocks may reach 15 mm in diameter. Grain boundaries are sharp, commonly embayed, and locally exhibit sutured boundaries with adjacent grains. Colour is variable, but is usually brownish-green or olive-green to green or bluish-green. Occasionally light buff-brown to olive-green is observed. Grain zonation is diffuse, subtle, and is observed as a gradual colour change from core to rim. Cores tend to be greenish or brownish-green and rims bluish-green or olive-green. A few larger grains, primarily phenocrysts, exhibit narrow, irregular to asymmetric, primary overgrowths of pale green actinolite and green hornblende. Similar overgrowths are a common within some of the appinite suite intrusions of the British Isles (Bowes et al., 1964). Narrow reaction rims of pale green actinolite are common when cumulus hornblende is in contact with intercumulus hornblende.

Clinopyroxene (variety diopside - $Wo_{49.33-50.03}$ $En_{40.92-44.62}$ $Fs_{5.35-9.31}$) forms colourless, subhedral to euhedral, locally twinned, cumulus grains that average 0.10- 0.50 mm, but range from 0.01-2.0 mm in diameter. They occur in loose, multi-grain aggregates, or as single-grain chadacrysts

Figure 3.11: Slightly recrystallized hornblendite (FOV 2.7 mm). Sample AAb-10-85, Abiwin Intrusion.

Figure 3.12: Clinopyroxene hornblendite (FOV 2.7 mm). Sample AK-49-86, Kawene Intrusion.

Figure 3.13: Weakly zoned hornblende within clinopyroxene hornblendite (FOV 2.7 mm). Sample AM-3-85, Mud Lake Intrusion.

within poikilitic cumulus and intercumulus hornblende.
Uralitization is highly variable and can range from a slight
alteration along cleavage traces and grain boundaries to
complete or almost complete replacement of individual
grains. Moderate to strong alteration is the norm and
produces partially preserved, anhedral remnants exhibiting
corroded, scalloped grain boundaries, and a very fine
dusting of secondary magnetite. Pale green actinolite is
the most common alteration product, but carbonate (possibly
dolomite, or Mg-calcite) is sometimes present. Actinolite
+/- carbonate pseudomorphs are common, particularly after
clinopyroxene chadacrysts within large oikocrysts of
hornblende (Figure 3.14). Chadacrysts within large cumulus
hornblende grains are commonly less altered. The abundance
of actinolite pseudomorphs suggests that clinopyroxene was
initially much more abundant.

Biotite is common, but not always present. It occurs
as both primary intercumulus and secondary phases. The
primary phase is usually <1 mm, but occasionally as much as
2 mm in length, generally subhedral, light brown or tan to
reddish-brown, and randomly distributed. It is generally
interstitial to cumulus clinopyroxene and hornblende, but
locally forms embayments or chadacrysts within oikocrysts of
hornblende, suggesting contemporaneous crystallization. The
secondary phase commonly occurs as a very fine-grained,
anhedral replacement of hornblende along fractures and

cleavage traces. Both phases commonly alter to very pale green chlorite.

Apatite is a common accessory phase that forms clusters or aggregates of subhedral to euhedral grains. Basal sections range from <0.1-0.75 mm in diameter, while longitudinal or oblique sections can be up to 1.5 mm in length. There may be a preferred association with plagioclase and interstitial sulphides.

Olivine ($Fo_{77.55-78.88}Fa_{20.49-21.68}Tp_{0.47-0.63}$ occurs as scattered, irregular, almost completely altered remnants that form distorted, but distinctive, serpentine-magnetite pseudomorphs up to 1.75 mm in diameter. Volume change during serpentinization fractured many surrounding hornblende grains. The fractures were subsequently occupied by serpentine-magnetite veinlets. Serpentine is commonly replaced by Mg-carbonate.

Plagioclase occurs as small, anhedral grains, usually interstitially to cumulus clinopyroxene and hornblende. It is never observed within intercumulus hornblende; however, it locally forms embayments of the grain boundaries. Most grains are moderately to completely saussuritized. Twinning is rare. Some metamorphic recrystallization to albite or oligoclase is possible.

Quartz and zircon are rare.

3.2.4 - Gabbro:

Highly variable amounts of hornblende melagabbro and hornblende gabbro are present within many of the Quetico Intrusions (Figure 3.15). These rocks are sometimes fine-grained, usually medium- to coarse-grained, often porphyritic (Figure 3.16) and display a wide range in primary mineral content. A weak to moderate igneous foliation is displayed locally. The percentage of hornblende (30-80%) is always greater than clinopyroxene, which is sometimes absent altogether (0- 30%). In many instances the clinopyroxene content appears to decrease with an increase in the hornblende content, suggesting that amphibole formed at the expense of clinopyroxene. Plagioclase, apatite, and titanite are always present, and comprise 10-45%, <1-4% (rarely 8-10%), and trace to 3%, respectively. Biotite is common (1-18%), but is locally absent in some intrusions. Potassium-feldspar (trace to 2%, rarely 5-10%) and quartz (1-6%) are relatively minor components that may represent contamination by the enclosing metasedimentary rocks. Zircon is a common accessory phase.

Hornblende is ubiquitous, usually occurs as poikilitic cumulus grains, but rarely forms poikilitic intercumulus grains. The grains are subhedral to euhedral with sharp, often embayed boundaries. Ragged, locally corroded boundaries are also common when in contact with biotite or

Figure 3.14: Actinolite/carbonate pseudomorphs after clinopyroxene enclosed in an oikocryst of hornblende (FOV 2.7 mm). Sample AM-4-85.
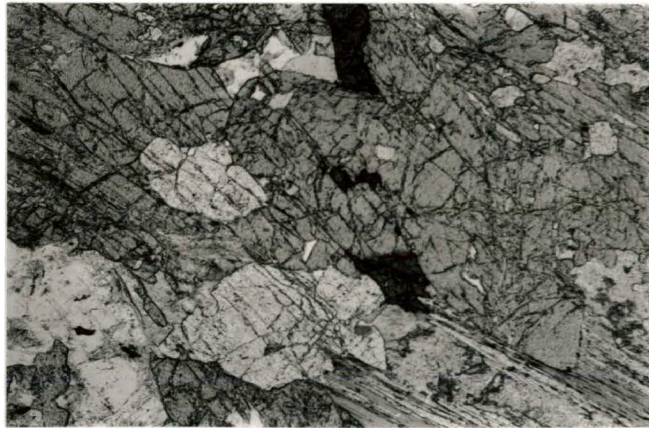
Figure 3.15: Hornblende melagabbro (FOV 2.7 mm). Sample AK-41-86.
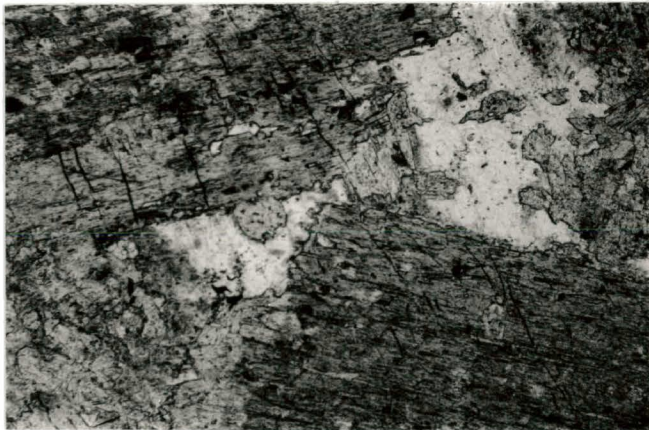
Figure 3.16: Porphyritic hornblende melagabbro (FOV 2.7 mm). Sample AM-8-84.

altered plagioclase. Grain size is widely variable and phenocrysts are common. The phenocryst phases are always moderately to heavily poikilitic, locally twinned, sometimes exhibit a subtle zonation, and range from 2-15 mm in diameter. Grains that occur within the groundmass are often corroded, locally skeletal, slightly to moderately poikilitic, and up to 4 mm in diameter. The skeletal grains are intergrown with or replaced by plagioclase. A few smaller grains have cores of plagioclase. All textural varieties of gabbro contain tiny euhedral grains that are less than 0.1 mm in diameter. Phenocrysts commonly contain chadacrysts of altered or resorbed, earlier-formed hornblende grains, whereas both oikocrysts and poikilitic phenocrysts contain clinopyroxene, biotite or apatite chadacrysts. The few oikocrysts observed (Samples AM-21-85 and AAb-23-85) are anhedral, heavily poikilitic, and up to 6 mm in diameter. Pleochroism within all varieties of hornblende is pronounced and easy to observe with light brownish-green, tan, olive-green, or greenish-brown grains becoming green, dark olive-green, or blue-green. The most common alteration is replacement along cleavage traces by reddish-brown flakes and ribbons of biotite. Pale green actinolite commonly pseudomorphs hornblende chadacrysts or forms irregular reaction rims when in contact with clinopyroxene, plagioclase, or primary biotite. A few irregular overgrowths of pale green actinolite and green

hornblende were observed.

Clinopyroxene (diopside: $Wo_{48.51-50.53}$, $En_{39.03-42.08}$, $Fs_{9.13-11.31}$) crystallized before and during the formation of much of the hornblende, but is always less abundant, and locally absent. Grains are colourless to pale pinkish, non-pleochroic, sometimes twinned, often corroded, variably altered, and often replaced by hornblende and sometimes plagioclase. Some grains are embayed by small grains of hornblende. The larger, early-forming clinopyroxene grains range from 2-8 mm in diameter (average 2-4 mm) and tend to occur as anhedral to subhedral, often granular, optically continuous remnants that have been partially replaced (AKL-2-84) or completely pseudomorphed by hornblende (AAb-1-85) and, occasionally, plagioclase. Some of these earlier grains form embayments within adjacent, often larger hornblende grains. The smaller, late-forming, subhedral to euhedral grains, with a size range of <0.05-1 mm in diameter, usually occur within the groundmass as loose clusters or multigrain aggregates, but may also occur singly to form embayments or chadacrysts within hornblende and, occasionally, plagioclase grains. These smaller grains are rarely replaced by hornblende, suggesting equilibrium conditions. Most clinopyroxene grains are uralitized along cleavage traces or grain boundaries, producing fibrous, pale-green actinolite and an extremely fine dusting of magnetite. Actinolite pseudomorphs are common where

clinopyroxene forms chadacrysts within hornblende. A few samples exhibit advanced replacement along cleavage traces that produces a delicate skeletal remnant.

Plagioclase always occurs as an anhedral intercumulus phase, usually <3 mm in diameter, but with a range of <0.1-5 mm in diameter. Most grains have been heavily to totally saussuritized. Twinning is usually obliterated or obscured and determination of anorthite content is difficult and often impossible. A few, quite small, remnant grains allow the determination of An_{11-41} (oligoclase to andesine). This range is often observed within a single sample, although a few samples exhibit a tighter range of An_{30-40} (andesine). These remnant grains may be younger than the larger, totally saussuritized grains and may be less calcic in composition.

Biotite occurs as both primary and secondary varieties within most, but not all of the gabbro samples examined. Metamorphic biotite usually occurs as tiny (<0.3 mm in length) replacement flakes and ribbons along hornblende cleavage traces. Primary, intercumulus biotite occurs as anhedral to subhedral, often twinned grains, 0.1-4 mm in length, occurring interstitially to cumulus hornblende and clinopyroxene, but occasionally forming chadacrysts within large poikilitic hornblende grains. All of the biotite grains observed are light tan to dark reddish-brown and commonly alter to pale green chlorite.

Apatite is ubiquitous and averages between 1 and 3%; however, in sample AK-41-86 it constitutes 8-10% of the rock. It usually occurs as tiny, subhedral to euhedral needles, blades and hexagonal basal sections (Figure 3.17), averaging 0.1-0.5 mm in diameter or length, but ranging from <0.01-2.30 mm in length or 1.5 mm in diameter. Elongated aggregates of two or more longitudinal grains are common, as are loose clusters. Apatite occurs most commonly as an interstitial phase closely associated with plagioclase; however, specimens with higher percentages of the mineral exhibit larger grains that are poikilitically enclosed within hornblende.

Potassic feldspar is not often present, but when observed, forms small, anhedral to subhedral, usually sericitized, intercumulus grains up to 0.3 mm in diameter that sometimes exhibit polysynthetic twinning, and are often associated with clusters of biotite.

Quartz is a localized, interstitial accessory in some samples, often exhibits undulose extinction, and locally appears to replace plagioclase. Titanite is always present as pleochroic, light brown, subhedral to euhedral grains <0.01-0.5 mm in diameter. Zircon forms very tiny, euhedral to subhedral grains that are usually <0.01 mm, but sometimes approach 0.3 mm, in length.

Opaque minerals are usually present as a fine dusting of magnetite in hornblende, sometimes as interstitial, magmatic sulphides, and rarely as replacement of silicates.

3.2.5 - Diorite:

The diorites are the least common lithology observed and, in part, include rocks of appinitic texture. The appinites will be discussed as a group in the following subsection. Classification of the diorites is difficult due to ubiquitous, moderate to locally intense saussuritization of plagioclase that makes determination of anorthite content difficult. The mostly subjective classification used here is modified after Williams et al. (1982). It is based on an equant rock composed of weakly zoned, moderately saussuritized oligoclase or andesine, green occasionally brownish hornblende, subordinate, pale to dark brown biotite that increases in content with the presence of quartz, traces of interstitial quartz and orthoclase, and a colour index that is usually less than 40. Classification of the more basic diorites becomes more difficult with the increase in colour index. The presence of weakly zoned plagioclase and less intense saussuritization (suggesting less calcic compositions) is used to categorize the more basic rocks into the diorite field.

Non-appinitic diorites occur within three intrusions: the Kawene Lake Igneous Complex; the Heward Lake Igneous

Complex, and both parts of the Elbow Lake Intrusion. These rocks are fine- to medium-grained and roughly equant, with a few weakly hornblende-porphyritic zones. Content of all minerals is widely variable. Hornblende content is usually 20-40%, plagioclase 25-48%, biotite 7-10%, quartz 5-20%, potassium feldspar 8-10%, apatite 1-4%, titanite <1-4%, and trace zircon. Two localities within the North Elbow Lake Stock exhibit a basic variety of diorite that verges on gabbro. In these rocks hornblende content was 45-60%, plagioclase content as low as 10%, and quartz 1-2%.

Hornblende is light brownish- or light olive-green to dark green or blue-green, subhedral to euhedral, commonly twinned, often moderately poikilitic, and tends to form clusters or aggregates of various sized grains. Average grain-size is 0.5-2.0 mm; however, some grains can be up to 5.0 mm in length or 2.5 mm in diameter. Grain boundaries are sharp, embayed, occasionally ragged, and locally corroded. A weak zonation, characterized by a subtle colour change, occurs locally. A few samples (particularly AEN-2-84) contain grains that exhibit longitudinal or transverse splitting, or cores filled with plagioclase+/-quartz and K-spar. This may indicate an incipient appinite texture. Poikilitic grains may contain chadacrysts of apatite, biotite, and possibly plagioclase. Secondary replacement by biotite is very common. Alteration to pale green actinolite is uncommon. A few grains may have been partially replaced

by plagioclase.

Plagioclase occurs as an interstitial, moderately saussuritized, anhedral component. Average grain-size is 0.5-1.25 mm; however, a few grains can be as large as 5.0 mm in diameter. Twinning is common, but is usually obscured by alteration. The few extinction angles measured resulted in an anorthite content, within single samples, of An_{4-44}. A few grains are totally saussuritized. Alteration is often confined to the cores of grains, suggesting a zonation that is not readily apparent optically. Poikilitic grains containing chadacrysts of biotite and apatite are sometimes observed. Some grains are partially rimmed by quartz and/or K-spar.

Light brown to dark brown, anhedral to subhedral biotite is commonly associated with grains of hornblende. It averages 0.5-1.25 mm in length or diameter, but is occasionally up to 2.25 mm in length. The brown biotite grains occurring within diorite exhibit a definite colour-difference when compared with the reddish-brown biotite grains present within gabbro. This observation suggests a change in the overall chemistry of the biotite grains with continued fractionation. Fine-grained ribbons of secondary biotite replace hornblende along cleavage traces in some samples.

Quartz occurs as small anhedral, interstitial grains averaging 0.2-0.5 mm, and locally 1.0 mm in diameter. Many grains have been weakly strained and exhibit slightly undulose extinction.

Potassium feldspar, comprising orthoclase and some microcline, forms moderately sericitized, anhedral, interstitial grains usually <1 mm, but occasionally up to 3 mm in diameter. It is often observed, along with quartz, forming discontinuous rims around plagioclase grains.

Apatite and titanite are ubiquitous accessories. Apatite forms euhedral blades, needles and basal sections up to 0.75 mm in diameter or length; and titanite forms brown, pleochroic, subhedral to euhedral grains up to 0.5 mm in length.

Clinopyroxene is rare and was observed in only one sample (AEN-2-84) as a few small, corroded, rounded, uralitized remnants enclosed within plagioclase.

Zircon is rare.

3.2.6 - Appinite:

Appinites, as described by Read (1961), French (1966), Pitcher and Berger (1972), Bowes and McArthur (1976), Key (1977), Palicova (1982), and Key (1987), occur within every intrusion examined. Volumetrically, they comprise minor amounts of each intrusion, but their characteristic appearance and ubiquitous nature are an important tool in

classifying the Quetico Intrusions as a suite of genetically related rocks.

The appinites are fine- to very coarse-grained, usually porphyritic, and occasionally pegmatitic. They are often dioritic in composition, but as a group can exhibit a wide compositional range from granodioritic to gabbroic. They essentially consist of prismatic to acicular hornblende, and altered plagioclase, with subordinate, highly variable amounts of interstitial biotite, quartz, potassium feldspar (orthoclase and microcline), and apatite. Accessories such as clinopyroxene, titanite, zircon, and calcite are common locally, but not always present. The most characteristic appinite features are illustrated by the amphiboles. The **dioritic series** is typified by squat hornblende grains (often cored by plagioclase, quartz, and sometimes K-spar), and multigrain aggregates of hornblende, whereas the **appinitic series** is identified by long prismatic hornblende crystals that often exhibit longitudinal or basal splitting. Skeletal, cored, and split hornblende crystals are common to both series (Figure 3.18).

Most of the appinites identified belong to the appinite series; however, dioritic series appinites are common within the Mud Lake Intrusion, where they form a complete unit up to 10 m in thickness.

Mineral abundances are widely variable; hornblende has a range of 15-45%, plagioclase a wider range of 15-70%,

biotite tends to occur in lower amounts of 1-8%, but occasionally reaches 15%, apatite is present in significant quantities ranging from 2-8% (Figure 3.19), potassium feldspar ranges from 1-15%, quartz has a range of nil-25%, clinopyroxene <1-10%, titanite trace-2%, zircon <1%, the opaques trace-1%, and calcite is rare, but locally reaches 1-2%.

Hornblende commonly forms subhedral to euhedral, prismatic to acicular phenocrysts, usually less than 10 mm in diameter or length, but occasionally as large as 10 mm in diameter, or 22 mm in length. The grains are light brownish-green or olive-green to blue-green, often twinned and poikilitic, with embayed, ragged, and locally corroded boundaries. Some grains are weakly zoned, with brownish-green to olive-green cores and green to bluish-green rims. Basal cross-sections are often cored with felsic minerals, such as quartz and plagioclase, and longitudinal sections are commonly split along or across their length. The cored or split grains are infilled with a mixture of plagioclase, quartz, K-spar, and, sometimes, apatite or biotite. Larger grains are typically surrounded by numerous small grains of hornblende and biotite. Biotite often appears to be intergrown with hornblende. Irregular overgrowths of green actinolite and hornblende are sometimes present. Alteration tends to be slight. Fibrous, pale green actinolite and fine-grained flakes and ribbons of biotite are common as

Figure 3.17: Hexagonal apatite grains within biotite-hornblende melagabbro (FOV 2.7 mm). Sample AK-41-86.

Figure 3.18: Cored hornblende grain within appinite (FOV 2.7 mm). Sample AML-6-85.

Figure 3.19: Large apatite within appinite (FOV 2.7 mm). Sample AML-6-85.

replacement along cleavage traces. Many grains contain a fine dusting of secondary magnetite, and a few exhibit narrow, discontinuous coronas of actinolite. A few grains are partially replaced by sulphides.

Plagioclase is anhedral to subhedral and usually interstitial; however, a few subhedral grains may be cumulus in nature. Grains are usually <1 mm, but occasionally reach 3-5 mm in diameter. Saussuritization, ranging from moderate to intense, affects every grain and commonly obscures or obliterates twinning. Weak to moderately developed zonation is indicated by the preferential alteration of grain centres and the presence of localized rims of orthoclase. Some grains have been partially replaced or rimmed by quartz. Determination of anorthite content was possible in only two samples, indicating a wide, probably misleading range of An_{5-44}.

Biotite forms anhedral to subhedral, locally twinned, tan to reddish-brown, interstitial grains averaging <1.0 mm, but locally attaining lengths of up to 5 mm. It commonly clusters around, and is often intergrown with, hornblende and interstitial sulphides. It is also common as a fine-grained replacement along hornblende cleavage traces, and alters readily to light green chlorite.

Fine-grained, anhedral, interstitial quartz, with embayed and scalloped grain boundaries is associated with plagioclase and sometimes hornblende. It occasionally

partially replaces or occurs as discontinuous rims around plagioclase and often forms part of the felsic material that infills cored and split hornblende grains.

Potassic feldspar always forms anhedral, moderately to strongly sericitized, interstitial grains. Their average size is <0.5 mm, but can attain diameters of up to 4 mm. The most common variety is orthoclase, but microcline occurs locally.

Apatite is present in significant quantities and forms euhedral to anhedral blades and basal cross-sections that occur within loose clusters or as single isolated grains. It is most commonly associated with plagioclase, but often forms near or within hornblende. The average grain is <0.25 mm in diameter, but some are up to 0.8 mm in diameter, or 3.5 mm in length.

Titanite is a common accessory, forming subhedral to euhedral grains up to 1.9 mm in length, with most grains less than 0.6 mm. Zircon is a minor accessory and forms multiple-grain clusters of very tiny grains.

CHAPTER 4

WHOLE ROCK, TRACE ELEMENT, AND MINERAL GEOCHEMISTRY

4.1: Introduction

The effects of alteration and the cumulus nature of the Quetico rocks does not allow the use of whole rock data to show definitive fractionation trends. Instead, emphasis will be placed on the quantitative mineral chemistry of olivine and clinopyroxene.

The sub-section on quantitative mineral chemistry will include comparisons with other mafic to ultramafic intrusions, particularly the appinite suite and the Alaskan-type complexes, in an attempt to characterize the Quetico Intrusions within the known spectrum of mafic/ultramafic rocks.

4.2: Whole Rock and Trace Element Chemistry

Thirty samples, taken from all rock types present within the Quetico Intrusions, except for the hornblende websterite identified within the North Elbow Lake Stock, were analyzed for major oxides and trace elements (Table 4.1).

The whole rock analyses were completed in two batches at outside laboratories. The first batch of 19 samples were analyzed by the Geoscience Laboratory of the Ontario Geological Survey, and the second batch of 13 samples were

analyzed by Chemex Labs Ltd. All trace element analyses
were completed by Chemex Labs Ltd. Determination of H_2O+
for the batch of 13 samples analyzed by Chemex were
completed at Lakehead University by the CHN elemental
analyzer.

The OGS Geoscience Laboratory determined most of the
major oxides by XRF. FeO was determined by titration; S and
CO_2 by the Leco Infrared Absorption Detector; and H_2O by the
Beckman Infrared Absorption Analyzer.

Chemex Labs Ltd. determined most of the major oxides by
Inductively Coupled Plasma-Atomic Emission Spectrometry
(ICP-AES). FeO was determined by titration, S by Leco
Infrared Absorption, and CO_2 by Leco-Gasometric.

In both cases ferric iron was calculated from
chemically determined FeO and Total Iron and then expressed
as Fe_2O_3.

Trace elements were determined by ICP-AES, except for
Nb, Y, and Zr, which were determined by XRF, and Rb by
Atomic Absorption Spectrometry.

4.2.1 - Major Oxides:

The Quetico Intrusions are composed of mainly cumulate
rocks that have been subjected to regional metamorphism
ranging from upper greenschist to upper amphibolite facies.
Serpentinization of olivine and saussuritization of
plagioclase are ubiquitous, most clinopyroxenes are

uralitized to some extent, and partial replacement of hornblende by actinolite and biotite is common. This alteration may have had a significant effect upon major oxide distributions, therefore an attempt was made to choose the least altered samples for the whole rock analyses (Table 4.1). CIPW norm calculations were not carried out because the presence of significant secondary minerals and an accompanying modification of the overall chemistry of the rock would produce inaccurate and misleading normative mineralogy.

Barker (1978) states that the compositions of cumulus rocks lie on lines of mixing, not of fractionation. This is due to the presence of variable proportions of usually magnesian cumulus crystals within a groundmass of more alkali-rich, formerly liquid, intercumulus material. It is the residual liquids formed during the fractionation process that define fractionation trends. The rocks of the Quetico Intrusions are mainly medium- to coarse-grained cumulates and, therefore, should not be used to define fractionation trends on an AFM diagram. The AFM diagram can be used to provide an overall picture of the present chemistry of these rocks and to possibly hint at their magmatic affinity, but cannot provide definitive answers.

TABLE 4.1

WHOLE ROCK AND TRACE ELEMENT CHEMISTRY OF THE QUETICO INTRUSIONS

A:Appinite   G:Gabbro   H:Hornblendite   C:Clinopyroxenite   W:Wehrlite

Sample	AML-1 -85	AML-2 -85	AM-1 -85	AM-23 -85	AM-27 -85	AM-30 -85	AM-38 -85
Rock	A	H	H	A	A	H	H
SiO2	46.90	48.90	47.60	47.90	49.80	48.00	47.90
TiO2	1.49	0.64	0.43	0.90	0.75	0.61	0.82
Al2O3	13.50	9.57	6.45	18.80	18.70	7.16	9.12
Fe2O3	2.70	1.94	2.05	1.91	1.42	2.34	2.40
FeO	12.30	8.84	8.37	7.18	5.55	8.59	9.70
MnO	0.17	0.18	0.19	0.14	0.15	0.17	0.20
MgO	7.28	11.00	16.00	5.05	3.41	15.30	12.60
CaO	7.71	11.00	13.00	8.23	8.75	12.00	12.30
Na2O	2.03	2.02	0.50	3.55	2.69	0.97	1.16
K2O	2.21	1.18	0.41	2.05	2.03	0.65	0.59
P2O5	0.04	0.08	0.12	0.55	0.78	0.08	0.14
CO2	0.16	2.09	2.59	0.46	0.24	0.67	0.38
S	0.73	0.06	0.19	0.54	0.25	0.12	0.07
H2O+	1.49	0.00	2.83	1.77	2.33	1.82	1.82
TOTAL	98.71	97.50	100.73	99.03	96.95	98.48	99.20
Ba	320	110	30	190	200	50	30
Cr	3	40	278	115	<1	94	38
Ni	17	13	203	34	<1	34	11
Cu	206	54	261	86	6	23	25
Pb	<2	<2	12	18	10	18	10
Sr	22	70	64	61	147	30	40
Co	34	27	26	15	11	21	24
Sc	11	9	5	7	3	6	9
V	199	104	59	89	54	63	84
Zr	130	85	40	120	125	50	60
Nb	10	5	5	10	5	<5	5
Y	25	15	5	20	20	5	15
Zn	54	18	20	38	68	8	16
Rb	80	55	9	90	75	20	12
La	30	10	10	30	20	<10	<10

Ternary Plotting Parameters

A	16.15	12.91	3.40	28.64	31.60	5.90	6.70
F	56.11	42.72	37.70	45.52	45.60	38.70	45.20
M	27.73	44.38	59.00	25.83	22.80	55.40	48.10

TABLE 4.1 (Cont'd)

WHOLE ROCK AND TRACE ELEMENT CHEMISTRY OF THE QUETICO INTRUSIONS

A:Appinite   G:Gabbro   H:Hornblendite   C:Clinopyroxenite   W:Wehrlite

Sample	AM-39 -85	AAB-1 -85	AAB-4 -85	AAB-6 -85	AAB-13 -85	AAB-15 -85	AAB-23 -85
Rock	A	G	H	H	H	G	G
SiO2	49.20	50.20	48.70	46.90	48.20	50.30	51.70
TiO2	0.73	0.56	0.36	0.94	0.54	0.54	0.51
Al2O3	19.10	10.50	5.81	8.48	7.30	11.60	7.34
Fe2O3	1.44	1.51	2.26	1.85	1.86	1.80	1.43
FeO	5.85	7.11	7.26	8.51	7.40	7.33	5.85
MnO	0.13	0.16	0.17	0.17	0.18	0.16	0.14
MgO	3.29	11.60	18.40	15.60	17.10	11.10	14.60
CaO	8.84	13.00	13.00	12.40	13.10	10.80	14.30
Na2O	2.78	1.80	0.40	0.87	0.50	1.86	1.12
K2O	2.22	0.93	0.31	0.58	0.38	1.36	0.94
P2O5	0.73	0.14	0.08	0.08	0.10	0.18	0.24
CO2	0.61	0.13	0.50	0.22	0.21	0.11	0.71
S	0.32	0.13	0.30	0.09	0.02	0.04	0.03
H2O+	2.49	2.06	2.34	2.22	2.21	2.20	1.15
TOTAL	97.73	99.83	99.89	98.91	99.10	99.38	100.06
Ba	30	20	<10	20	10	20	20
Cr	14	52	191	203	198	111	109
Ni	14	47	131	88	64	32	28
Cu	6	124	172	102	25	106	264
Pb	<2	12	6	26	18	28	10
Sr	139	27	14	32	57	29	51
Co	13	15	28	19	14	8	2
Sc	4	3	3	6	5	2	2
V	62	39	32	64	45	34	14
Zr	145	50	40	45	45	80	80
Nb	10	<5	<5	5	5	5	5
Y	20	5	5	10	5	10	5
Zn	52	8	8	16	10	6	2
Rb	75	30	<5	<5	<5	55	38
La	30	10	<10	<10	<10	10	20

Ternary Plotting Parameters

A	32.40	12.00	2.50	5.30	3.30	13.80	8.70
F	46.30	37.10	32.70	37.40	33.50	38.50	30.00
M	21.30	50.90	64.80	57.30	63.20	47.70	61.40

TABLE 4.1 (Cont'd)

WHOLE ROCK AND TRACE ELEMENT CHEMISTRY OF THE QUETICO INTRUSIONS

A:Appinite G:Gabbro H:Hornblendite C:Clinopyroxenite W:Wehrlite

Sample	APL-2 -84	APL-3 -84	API-3 -84	ACP-4 -86	ACP-7 -86	ACP-9 -86	AEN-1 -86
Rock	G	A	C	A	H	H	A
SiO2	53.30	52.40	47.90	51.58	46.33	44.97	57.00
TiO2	0.85	0.85	0.85	0.76	1.02	0.51	0.41
Al2O3	13.50	17.10	10.40	17.96	7.16	9.10	16.01
Fe2O3	2.40	2.30	2.30	1.65	5.02	3.43	2.30
FeO	6.59	7.19	8.73	5.08	8.43	7.51	3.68
MnO	0.15	0.13	0.17	0.14	0.18	0.20	0.08
MgO	8.02	4.69	14.20	6.88	15.14	16.78	4.79
CaO	8.92	8.06	9.80	8.18	11.30	11.92	5.00
Na2O	2.69	2.58	1.65	4.85	1.77	2.42	5.69
K2O	1.51	2.82	1.43	1.96	1.06	0.73	2.21
P2O5	0.18	0.37	0.05	0.31	0.04	0.24	0.46
CO2	0.08	0.07	0.11	0.40	0.29	0.30	0.30
S	0.01	0.66	0.17	0.04	0.61	0.04	0.24
H2O+	0.74	0.77	1.45	1.36	1.45	1.82	1.54
TOTAL	98.94	99.99	99.21	101.15	99.80	99.97	99.71
Ba	200	180	240	290	170	30	60
Cr	336	20	396	95	178	434	61
Ni	36	15	121	41	56	88	17
Cu	37	133	129	99	168	27	134
Pb	<2	<2	<2	4	<2	<2	14
Sr	28	95	19	11	21	17	4
Co	16	31	28	19	44	22	17
Sc	5	5	6	11	21	17	4
V	80	108	76	83	180	78	49
Zr	85	110	60	95	30	55	395
Nb	5	5	<5	<5	<5	<5	<5
Y	10	15	10	5	5	10	10
Zn	28	54	14	34	28	30	32
Rb	38	85	41	34	10	3	38
La	10	20	<10	10	<10	<10	20

Ternary Plotting Parameters

A	20.00	27.90	11.00	26.87	7.19	8.32	35.71
F	41.70	47.90	38.50	45.97	54.33	47.86	42.63
M	38.20	24.20	50.60	27.15	38.48	43.82	21.65

TABLE 4.1 (Cont'd)

WHOLE ROCK AND TRACE ELEMENT CHEMISTRY OF THE QUETICO INTRUSIONS

A:Appinite G:Gabbro H:Hornblendite C:Clinopyroxenite W:Wehrlite

Sample	AEN-2 -86	AK-16 -86	AK-18 -86	AK-34 -86	AK-40 -86	AK-43 -86	AK-47 -86
Rock	H	C	H	W	W	H	H
SiO2	49.76	46.51	47.94	46.04	46.02	43.85	48.58
TiO2	0.36	0.23	0.21	0.20	0.21	0.18	0.37
Al2O3	6.03	3.59	3.30	2.96	3.07	2.84	6.05
Fe2O3	2.77	4.01	2.27	4.03	3.97	4.23	1.90
FeO	6.65	5.28	5.31	5.06	5.23	4.43	7.27
MnO	0.21	0.15	0.16	0.16	0.17	0.14	0.19
MgO	17.03	22.51	21.30	23.38	23.72	23.07	16.43
CaO	13.46	12.64	13.29	13.26	12.85	11.63	13.70
Na2O	1.11	0.67	0.47	0.58	0.62	0.35	1.01
K2O	0.76	0.61	0.85	0.64	0.63	1.39	0.59
P2O5	0.08	0.04	0.04	0.03	0.02	0.03	0.12
CO2	0.30	0.90	2.40	0.30	0.40	3.70	0.44
S	0.25	0.21	0.32	0.06	0.07	0.15	0.05
H2O+	1.09	2.09	1.73	3.09	2.54	2.63	1.63
TOTAL	99.86	99.44	99.59	99.79	99.52	98.62	98.33
Ba	50	50	60	60	60	100	50
Cr	232	915	1090	585	653	1245	444
Ni	91	299	242	260	267	259	96
Cu	96	330	161	65	16	28	77
Pb	4	2	2	<2	2	<2	4
Sr	35	58	43	37	47	149	84
Co	25	55	43	54	53	51	24
Sc	8	5	4	6	6	6	13
V	40	56	57	31	32	45	55
Zr	40	20	15	20	20	15	30
Nb	<5	<5	<5	<5	<5	<5	5
Y	5	<5	<5	<5	<5	<5	5
Zn	14	36	22	38	40	36	30
Rb	3	4	11	9	4	78	5
La	<10	<10	<10	<10	<10	<10	<10

Ternary Plotting Parameters

A	6.60	3.87	4.37	3.62	3.66	5.20	5.88
F	33.26	28.08	25.10	26.98	26.92	26.47	33.71
M	60.13	68.05	70.53	69.40	69.42	68.93	60.40

TABLE 4.1 (Cont'd)

WHOLE ROCK AND TRACE ELEMENT CHEMISTRY OF THE QUETICO INTRUSIONS

A:Appinite   G:Gabbro   H:Hornblendite   C:Clinopyroxenite   W:Wehrlite
P:Peridotite

Sample	AK-49-86	AKR-1-86
Rock	H	P
SiO2	48.37	40.77
TiO2	0.29	0.16
Al2O3	5.33	4.07
Fe2O3	1.15	5.15
FeO	6.54	8.37
MnO	0.16	0.19
MgO	16.75	29.01
CaO	15.21	4.30
Na2O	1.02	0.44
K2O	0.50	0.64
P2O5	0.10	0.02
CO2	1.10	0.18
S	0.03	0.10
H2O+	1.45	4.54
TOTAL	98.00	97.94

Ba	30	130
Cr	391	643
Ni	24	576
Cu	8	350
Pb	4	8
Sr	109	29
Co	14	95
Sc	8	3
V	36	34
Zr	40	30
Nb	10	<5
Y	5	<5
Zn	16	70
Rb	6	10
La	<10	<10

Ternary Plotting Parameters

A	5.86	2.48
F	29.62	31.00
M	64.52	66.52

The ternary AFM plot of the Quetico data shows a clearly evident scatter (Figure 4.1). Most of the data points form a cluster near the $(FeO+Fe_2O_3)$-MgO boundary of the diagram with no clear association with either the tholeiitic or the calc-alkaline field, whereas the remaining points form a scattered, diffuse cluster clearly within the calc-alkaline field. The former cluster represents mafic and ultramafic rock types and the latter cluster the appinitic rock types. Alteration of olivine, clinopyroxene, and hornblende within the mafic and ultramafic rocks would tend to deplete magnesium and enrich iron producing an apparent, but possibly misleading trend toward the tholeiitic field. Alteration within the appinites, which are not cumulates, is usually confined to saussuritization of plagioclase feldspars, suggesting that the chemistry reflected by the diagram may be fairly accurate with a slight shift toward the alkalis. The volatile and incompatible element-rich appinites may represent end-stage rocks produced by a fractionation trend toward, or within, the calc-alkaline field.

Figure 4.2 compares the Quetico Intrusions with the appinite suite and the Alaskan-type complexes. These data represent an almost complete suite of the least evolved to the most evolved rock types from each group of intrusions. All three groups are initially very rich in MgO. The Alaskan-type complexes exhibit little eventual enrichment in

AFM Diagram for the Quetico Intrusions
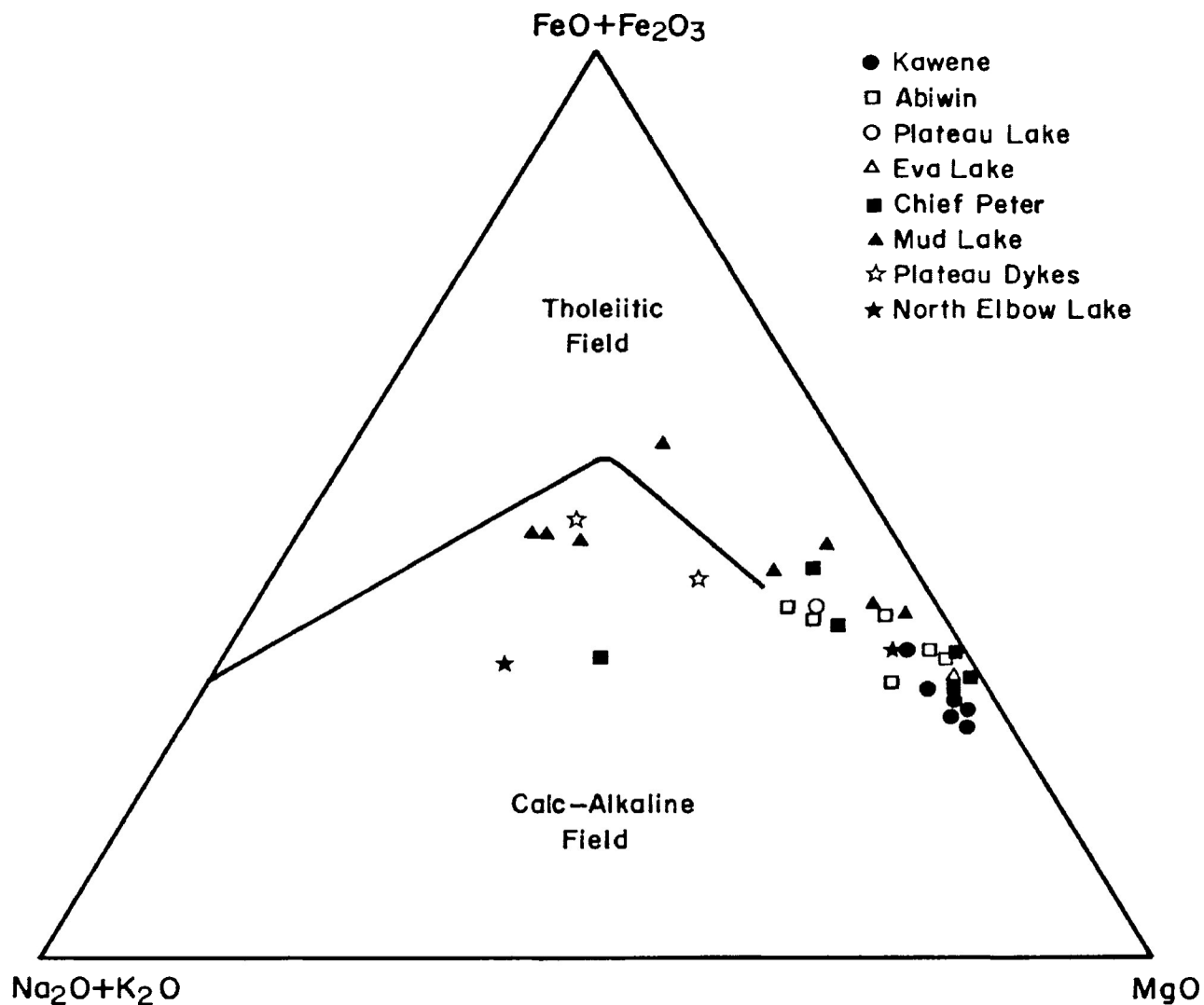
Figure 4.1: The ternary AFM plot of whole rock data shows a clearly evident scatter with no clear association with either the tholeiitic or the calc-alkaline field. The cumulus nature of these rocks precludes the use of this diagram for any purpose other than to illustrate present chemistry. Additional whole rock data for the Chief Peter Intrusion was taken from Watkinson and Irvine (1964).

Quetico Intrusions vs Appinite Suite and Alaskan-type Complexes
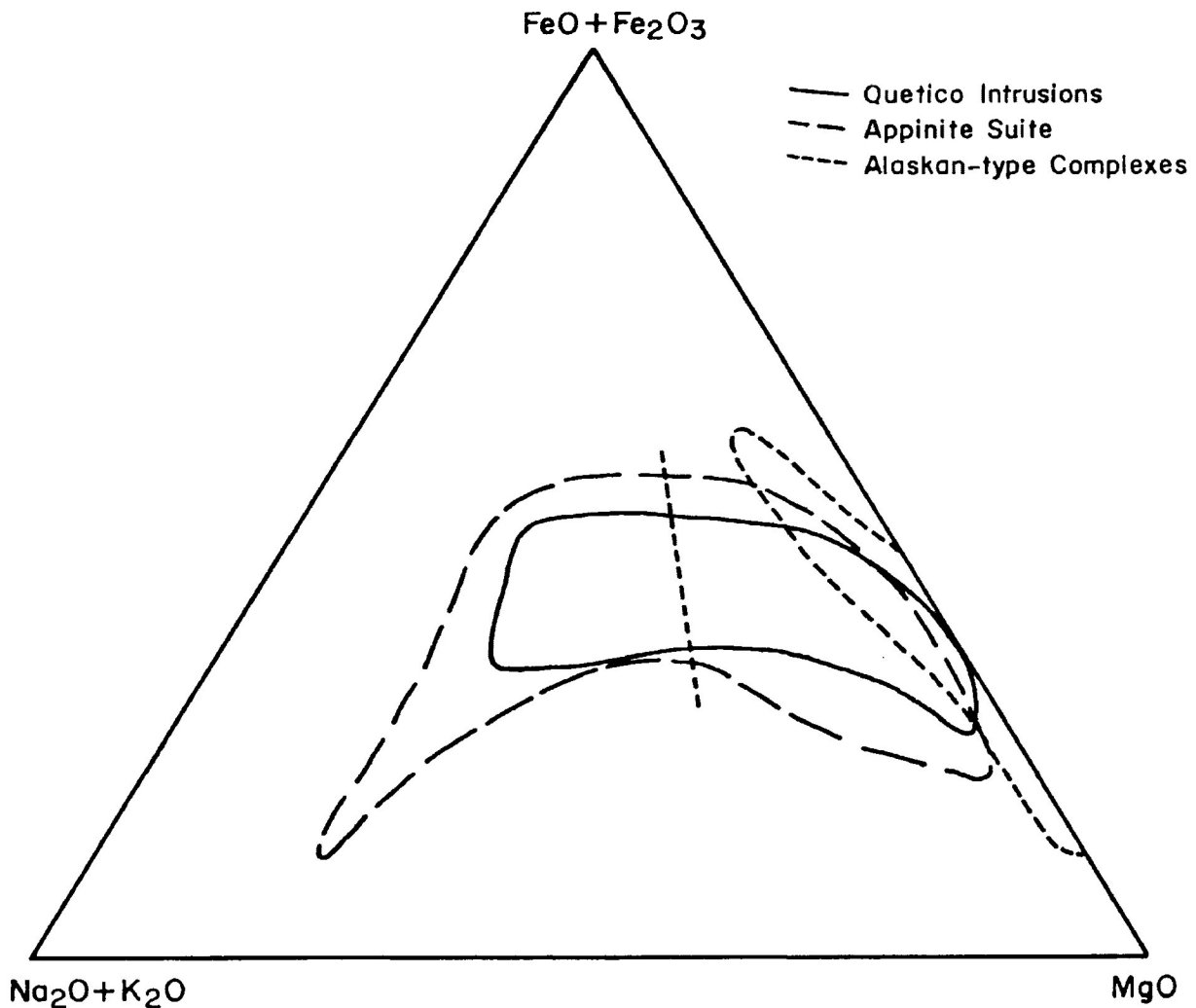
Figure 4.2: The Quetico Intrusions are chemically similar to the appinite suite, and quite dissimilar to the Alaskan-type Complexes. Appinite Suite data was from Haslam(1970), Hall(1967), Wright and Bowes (1979), Bowes et al.(1964), Brooks et al.(1981), Stephens and Halliday (1984), French(1978), Bowes and McArthur(1976), Key(1977), and Jennings and Sutherland(1969); Alaskan-type data was from Taylor(1967), Clark (1980), Findlay(1969), Irvine(1974), and Ruckmick and Noble(1959).

alkalis, whereas the appinite suite and the Quetico
Intrusions become considerably enriched in alkalis. The
field of the Quetico Intrusions has a similar shape and is
almost completely contained within the appinite suite field.
The near vertical line through the two fields separates
rocks exhibiting the distinctive appinite texture from those
of more normal texture. The appinites plot left of the line
and all other rocks plot to the right. The Alaskan-type
complexes overlap the Quetico and appinite suite fields at
the extreme right of the diagram. This zone of overlap
contains approximately 33% of the Quetico data points.

Harker variation diagrams (Figure 4.3) illustrate some
rough trends, often with a separate trend for the appinitic
rocks (solid triangles). When the major oxides from
normally-textured mafic and ultramafic rocks are compared
against increasing SiO_2 content the following observations
can be made: MgO is initially very high and scattered but
decreases quickly, FeO exhibits a relatively flat, well-
defined profile, CaO is relatively high and constant and may
exhibit a slight increase, TiO_2 is slightly more diffuse but
also increases gradually, and Al_2O_3, Na_2O and K_2O are widely
scattered with an apparent increase. The appinites exhibit
relatively flat, well-defined, depleted profiles for FeO,
MgO, and CaO, and enriched, slightly positive profiles for
TiO_2, Al_2O_3, Na_2O, and K_2O.

Harker Variation Diagrams
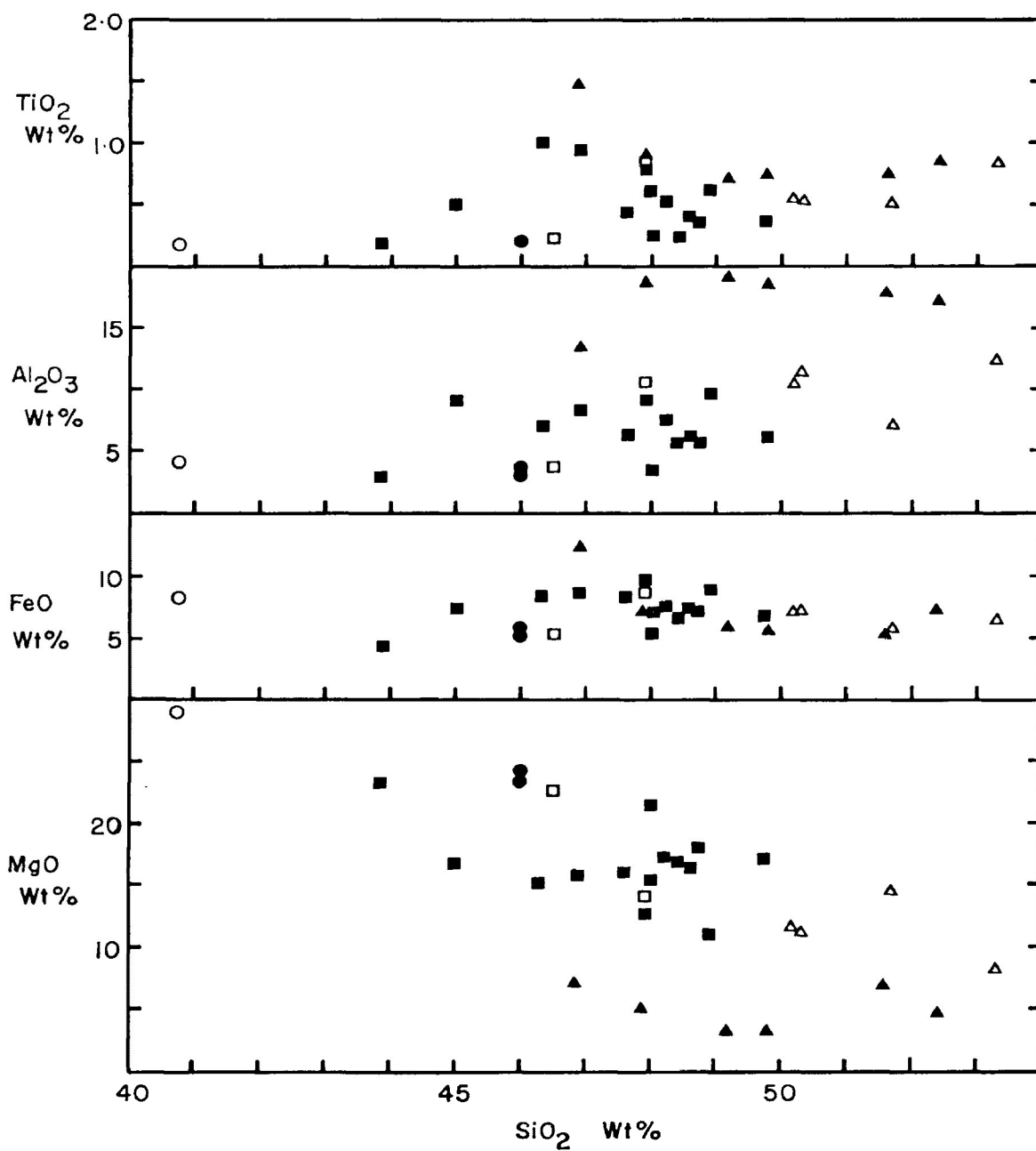
Figure 4.3: Harker variation diagrams for the Quetico Intrusions illustrate some rough trends, often with a separate trend for the appinites. Note the relatively flat FeO profile and the high MgO content.

Harker Variation Diagrams (Cont'd)
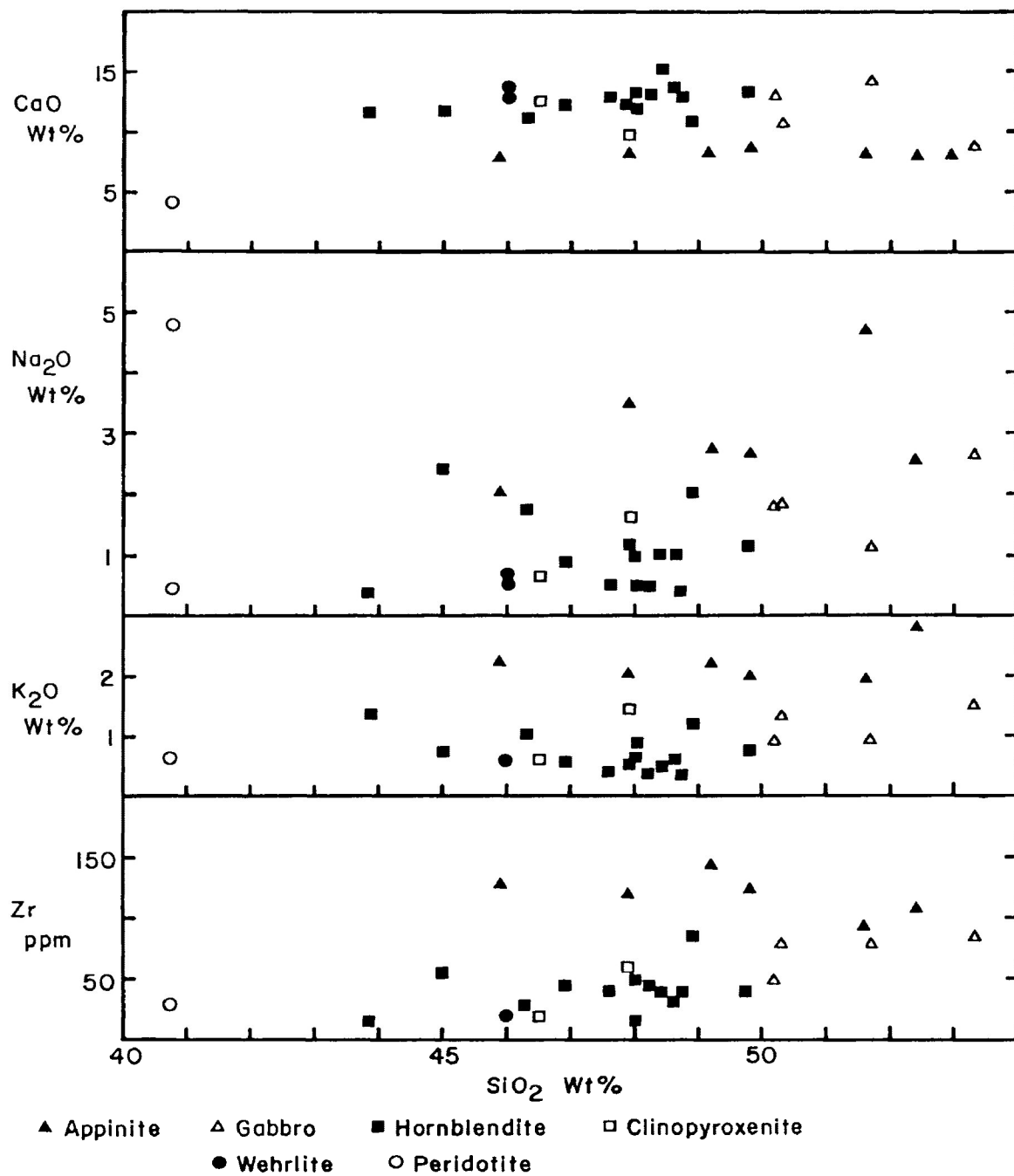
Figure 4.3 (Cont'd): Note the high, but relatively constant CaO content and the increasing Zr content with increasing SiO2.

4.2.2 - Trace Elements:

Trace element abundances are presented in Table 4.1. The concentrations of incompatible elements such as Rb, Y, Nb, Zr, and Ba may not have been as greatly affected by metamorphism as have compatible elements such as Sr, Ni, Co, Cr, and Sc.

Rubidium content is relatively constant within the ultramafic rock types, averaging less than 15 ppm, and usually less than 10 ppm. There is an abrupt increase within the gabbros (40 ppm), and a further increase within the appinitic rocks (68 ppm). The K/Rb ratios are highly variable ranging from 13 to 420 and may have been modified by metamorphism. As would be expected, biotitic rocks tend to exhibit higher ratios.

Barium content is low, but highly variable throughout most rock types with a range of 10 to 320 ppm. The highest average Ba content (181 ppm) is noted within appinite and the lowest (38 ppm) within hornblendite.

Yttrium content is below detection limit (5 ppm) within the peridotites and the clinopyroxenites. The least evolved varieties of hornblendite, i.e. those that contain olivine and considerable quantities of clinopyroxene, contain Y at, or below, detection limit. Hornblendite (sensu stricto), feldspathic hornblendite, and gabbro contain 5-20 ppm, with an average of 8.6 ppm. Appinite can contain up to 25 ppm Y, but averages 16.4 ppm.

Niobium contents are usually less than detection limit (5 ppm) and never exceed 10 ppm. The 10 ppm values occur within the appinites. Although the amounts of Nb are very low there is still an apparent increase in concentration with increasing differentiation of the rocks.

The content of zirconium exhibits a gradual, relatively systematic increase throughout the differentiation of the Quetico rocks (Figure 4.3). The values average 22.5 ppm within the peridotites and clinopyroxenites (20-30 ppm range), 31 ppm within the least evolved hornblendites (15-40 ppm range), 54.3 ppm within hornblendite (sensu stricto) and feldspathic hornblendite (40-85 ppm range), 73.8 ppm within the gabbros (50-85 ppm range), and 160 ppm within the appinites (95-395 ppm range).

There is a systematic, sometimes subtle increase in the incompatible trace element concentrations of the host rocks with increasing SiO_2 content. This apparent trend is difficult to assess due to the lack of reliable analyses from a complete suite of rocks within each of the Quetico Intrusions and may be real or due to changes in the modal mineralogy of the rock suite.

4.3:   Quantitative Mineral Chemistry:

Quantitative mineral chemistry of unaltered grains and mineral remnants may provide a way to determine the overall geochemical affinity of the Quetico Intrusions without the uncertainty produced by whole rock and trace element analyses of altered cumulus rocks.   Quantitative analyses of olivine (Table 4.2) and clinopyroxene (Table 4.4) were completed using an X-ray energy dispersive analyzer (EDS) attached to a scanning electron microscope (SEM). Hornblende and biotite were considered to be too difficult to analyze with the equipment available.

4.3.1 - Olivine:

A total of 34 analyses were completed on 18 partially serpentinized olivine grains contained within 6 samples from the Kawene and Eva Lake Intrusions.   The three samples from the Eva Lake Intrusion were all hornblende peridotite.   The three samples from the Kawene Intrusion were hornblende wehrlite, olivine-hornblende clinopyroxenite, and clinopyroxene-olivine hornblendite, which is transitional to wehrlite.   Multiple analyses were completed on heavily fractured grains and the results averaged.   The cores and rims of the better preserved grains were analyzed in order to test for zoning.   Olivines from the Chief Peter Intrusion were too altered to be accurately analyzed.

Major oxide contents (Table 4.2A and B) are quite

uniform and exhibit an overall range of 38.19-40.07 Wt.% SiO_2, 40.95-43.45 Wt.% MgO, 17.37-20.46 Wt.% FeO, and 0.24-0.69 Wt.% MnO. NiO was detected only at the MnO-poor core of one grain (0.36 Wt.%) within Eva Lake Intrusion Sample AKR-2-86. The Kawene Intrusion exhibits a wider range of MgO, FeO, and MnO contents, whereas the Eva Lake Intrusion shows a wider range of SiO_2. There are slight, but not necessarily significant variations in major oxide content between the cores and rims of some grains, usually consisting of an increase in silica (0.89-1.69 Wt.%) and MgO (0.33-1.69 Wt.%). One grain within the Eva Lake Intrusion (Sample AKR-2-86) exhibits a 1.31 Wt.% decrease in SiO_2, whereas another (Sample AKR-3-86) shows a 1.26 Wt.% decrease in MgO. Table 4.3 shows the average EDS analyses for each olivine grain examined.

The relative uniformity of major oxide contents within the Quetico Intrusions is further illustrated by the narrow compositional range of averaged forsterite (77.55-80.89), fayalite (18.60-21.68), and tephroite (0.18-0.72) presented in Table 4.3. There is also little apparent difference in olivine compositions between the three rock types examined, but the hornblende peridotites of the Eva Lake Intrusion exhibit a slightly narrower range of forsterite and fayalite and a lower overall tephroite range than was observed within the rocks of the Kawene Intrusion.

TABLE 4.2A

Quantitative EDS Analyses of Olivine

Kawene Intrusion   C:Core R:Rim   N.D:Not Detected

Sample	AK-16-86	AK-16-86	AK-16-86	AK-16-86	AK-16-86	AK-16-86
Grain	1-1	1-2	2-3	2-3	3-1	3-1
SiO_2	39.83	39.26	39.58	39.51	39.68	39.06
MgO	43.08	42.40	41.90	42.11	41.78	42.07
FeO	17.66	19.64	19.75	19.70	19.67	20.10
MnO	0.47	0.69	0.61	0.59	0.66	0.60
NiO	N.D	N.D	N.D	N.D	N.D	N.D
TOTAL	101.04	101.99	101.85	101.91	101.80	101.84

Structural Formula Based on Four Oxygens

Si	1.002	0.989	0.996	0.994	0.999	0.983
Mg	1.615	1.592	1.572	1.580	1.569	1.578
Fe^{2+}	0.371	0.414	0.416	0.414	0.414	0.423
Mn	0.010	0.015	0.013	0.012	0.014	0.013
Ni	N.D	N.D	N.D	N.D	N.D	N.D

Mol. Percent End Members (Plotting Parameters)

Fo	80.89	78.70	78.57	78.53	78.41	78.36
Fa	18.60	20.45	20.77	20.60	20.71	21.01
Tp	0.51	0.72	0.65	0.62	0.70	0.63

TABLE 4.2A (Cont'd)

Quantitative EDS Analyses of Olivine

Kawene Intrusion   C:Core R:Rim   N.D:Not Detected

Sample	AK-16-86	AK-16-86	AK-19-86	AK-19-86	AK-19-86	AK-19-86
Grain	3-1	3-1	2-1	3-1	3-2C	3-2R
SiO_2	39.73	39.40	39.29	39.60	38.79	39.68
MgO	41.40	41.73	40.95	41.95	41.50	41.83
FeO	20.21	19.84	20.41	19.43	19.85	19.59
MnO	0.66	0.62	0.54	0.58	0.45	0.41
NiO	N.D	N.D	N.D	N.D	N.D	N.D
TOTAL	101.99	101.60	101.19	101.56	100.60	101.51

Structural Formula Based on Four Oxygens

Si	1.002	0.996	0.999	0.999	0.991	1.002
Mg	1.556	1.572	1.553	1.579	1.580	1.574
Fe^{2+}	0.426	0.419	0.434	0.410	0.424	0.414
Mn	0.014	0.013	0.012	0.013	0.010	0.009
Ni	N.D	N.D	N.D	N.D	N.D	N.D

Mol. Percent End Members (Plotting Parameters)

Fo	77.95	78.27	77.55	78.88	78.45	78.84
Fa	21.35	20.88	21.68	20.49	21.05	20.71
Tp	0.70	0.66	0.58	0.63	0.49	0.45

TABLE 4.2A (Cont'd)

Quantitative EDS Analyses of Olivine

Kawene Intrusion   C:Core R:Rim   N.D:Not Detected

Sample	AK-34-86	AK-34-86	AK-34-86	AK-34-86	AK-34-86	AK-34-86	AK-34-86
Grain	2-1	2-1	2-1	2-2	2-2	2-3	2-3
SiO_2	39.33	39.93	40.17	39.95	39.26	39.62	39.38
MgO	43.45	43.42	42.19	43.22	42.73	41.09	41.50
FeO	17.37	17.94	18.85	17.94	18.58	19.64	19.32
MnO	0.36	0.37	0.33	0.39	0.39	0.29	0.42
NiO	N.D	N.D	N.D	N.D	N.D	N.D	N.D
TOTAL	100.50	101.66	101.53	101.07	100.96	100.64	100.63

Structural Formula Based on Four Oxygens

Si	0.993	0.998	1.008	1.000	0.992	1.008	1.002
Mg	1.636	1.618	1.578	1.614	1.610	1.558	1.574
Fe^{2+}	0.367	0.375	0.396	0.376	0.393	0.418	0.411
Mn	0.008	0.008	0.007	0.008	0.008	0.006	0.009
Ni	N.D	N.D	N.D	N.D	N.D	N.D	N.D

Mol. Percent End Members (Plotting Parameters)

Fo	81.27	80.75	79.56	80.71	79.89	78.48	78.81
Fa	18.22	18.72	19.94	18.79	19.49	21.05	20.60
Tp	0.39	0.39	0.35	0.41	0.42	0.32	0.46

TABLE 4.2B

Quantitative EDS Analyses of Olivine

Eva Lake Intrusion   C:Core R:Rim   N.D:Not Detected

Sample	AKR-1-86	AKR-1-86	AKR-1-86	AKR-1-86	AKR-1-86
Grain	1-2	1-2	1-2	2-1	2-2
SiO_2	39.51	39.45	39.17	39.25	40.07
MgO	41.72	40.70	41.05	41.74	41.57
FeO	20.46	20.29	20.33	19.96	20.06
MnO	N.D	0.32	0.24	0.40	0.34
NiO	N.D	N.D	N.D	N.D	N.D
TOTAL	101.61	100.76	100.78	101.35	101.90

Structural Formula Based on Four Oxygens

Si	0.997	1.006	1.000	0.995	1.006
Mg	1.569	1.548	1.562	1.576	1.556
Fe^{2+}	0.432	0.433	0.434	0.423	0.421
Mn	N.D	0.007	0.005	0.009	0.007
Ni	N.D	N.D	N.D	N.D	N.D

Mol. Percent End Members (Plotting Parameters)

Fo	78.15	77.88	78.07	78.37	78.29
Fa	21.51	21.78	21.68	21.02	21.20
Tp	---	0.34	0.25	0.42	0.37

TABLE 4.2B (Cont'd)

Quantitative EDS Analyses of Olivine

Eva Lake Intrusion   C:Core R:Rim   N.D:Not Detected

Sample	AKR-1-86	AKR-2-86	AKR-2-86	AKR-2-86	AKR-2-86
Grain	3-3	1-1R	1-1C	1-2C	1-2
SiO_2	39.20	39.98	38.34	39.69	38.19
MgO	41.71	42.02	40.33	42.09	41.27
FeO	19.65	19.11	19.39	19.52	19.19
MnO	0.28	0.33	N.D	0.32	0.37
NiO	N.D	N.D	0.36	N.D	N.D
TOTAL	100.85	101.41	98.41	101.63	99.01

Structural Formula Based on Four Oxygens

Si	0.992	1.005	0.999	0.998	0.989
Mg	1.574	1.575	1.567	1.578	1.593
Fe^{2+}	0.416	0.402	0.423	0.410	0.416
Mn	0.006	0.007	N.D	0.007	0.008
Ni	N.D	N.D	0.007	N.D	N.D

Mol. Percent End Members (Plotting Parameters)

Fo	78.85	79.38	78.47	79.08	78.74
Fa	20.84	20.26	21.16	20.57	20.54
Tp	0.31	0.36	---	0.35	0.40

TABLE 4.2B (Cont'd)

Quantitative EDS Analyses of Olivine

Eva Lake Intrusion   C:Core R:Rim   N.D:Not Detected

Sample	AKR-2-86	AKR-2-86	AKR-2-86	AKR-3-86	AKR-3-86
Grain	1-2R	1-3R	1-3C	1-1C	1-1R
SiO_2	38.38	39.82	38.63	39.64	39.57
MgO	40.62	41.98	40.96	42.65	41.39
FeO	19.95	19.49	19.64	18.95	18.97
MnO	0.29	0.40	0.37	0.35	0.54
NiO	N.D	N.D	N.D	N.D	N.D
TOTAL	99.24	101.71	99.61	101.59	100.47

Structural Formula Based on Four Oxygens

Si	0.995	1.003	0.997	0.997	1.005
Mg	1.570	1.576	1.575	1.599	1.568
Fe^{2+}	0.433	0.411	0.424	0.399	0.403
Mn	0.007	0.009	0.008	0.007	0.012
Ni	N.D	N.D	N.D	N.D	N.D

Mol. Percent End Members (Plotting Parameters)

Fo	78.15	78.99	78.49	79.75	79.08
Fa	21.53	20.58	21.12	19.88	20.34
Tp	0.32	0.43	0.39	0.37	0.58

TABLE 4.3 Average Mol.% Fo:Fa:Tp in Olivine					
H:Hornblendite C:Clinopyroxenite P:Peridotite W:Wehrlite					
Intrusion	Sample #	Spots	Fo	Fa	Tp
KAWENE	AK-16-86 (C)	1	80.89	18.60	0.51
		1	78.70	20.45	0.72
		4	78.25	20.99	0.67
		2	78.55	20.69	0.64
KAWENE	AK-19-86 (H)	1	77.55	21.68	0.58
		1	78.88	20.49	0.63
		2	78.65	20.88	0.47
KAWENE	AK-34-86 (W)	3	80.53	18.96	0.38
		2	80.30	19.14	0.42
		2	78.65	20.83	0.39
EVA LAKE	AKR-1-86 (P)	3	78.03	21.66	0.20
		1	78.37	21.02	0.42
		1	78.29	21.20	0.37
		1	78.85	20.84	0.31
EVA LAKE	AKR-2-86 (P)	2	78.93	20.71	0.18
		3	78.66	20.88	0.36
		2	78.74	20.85	0.41
EVA LAKE	AKR-3-86 (P)	2	79.42	20.11	0.48

Comparisons of olivine mineral chemistry within the literature commonly plot Wt.% CaO and NiO against Mol.% forsterite content; however, the olivines of the Quetico Intrusions contain no detectable CaO and minimal detectable NiO and cannot be examined in this manner.

Figure 4.4 presents a comparison of the percent forsterite range between the Quetico Intrusions and similar hornblende-rich rock types occurring within other intrusions often of widely varying chemical affinities. Olivine-rich, hornblende-poor ultramafic rocks from the Stillwater (Czamanske and Zientek, 1985; Barnes and Naldrett, 1986), Bushveld (Scoon and De Klerk, 1987) and Lac des Iles complexes (Sutcliffe et.al., 1989) are included for added comparison. The olivines from this study exhibit a narrower range of forsterite than all but the Bear Mountain calc-alkaline complex (Snoke et.al., 1981) and the less evolved Basal Series rocks of the Bushveld complex (Atkins, 1969). They appear to be more evolved than most of the Alaskan-type complexes, except possibly the Duke Island complex (Findlay, 1969; Irvine, 1974; Cawthorn, 1975; Clark, 1980; and Himmelberg, 1986). The Tapia-Asturias cortlandite enclaves associated with Spanish calc-alkaline granites are initially slightly less evolved but exhibit a similar lower forsterite content boundary (Galan and Suarez, 1989). These enclaves are texturally and lithologically similar in some respects to the rocks of the Quetico Intrusions, and, chemically, the

Figure 4.4   Olivine Fo Contents of the Quetico and Other Intrusions
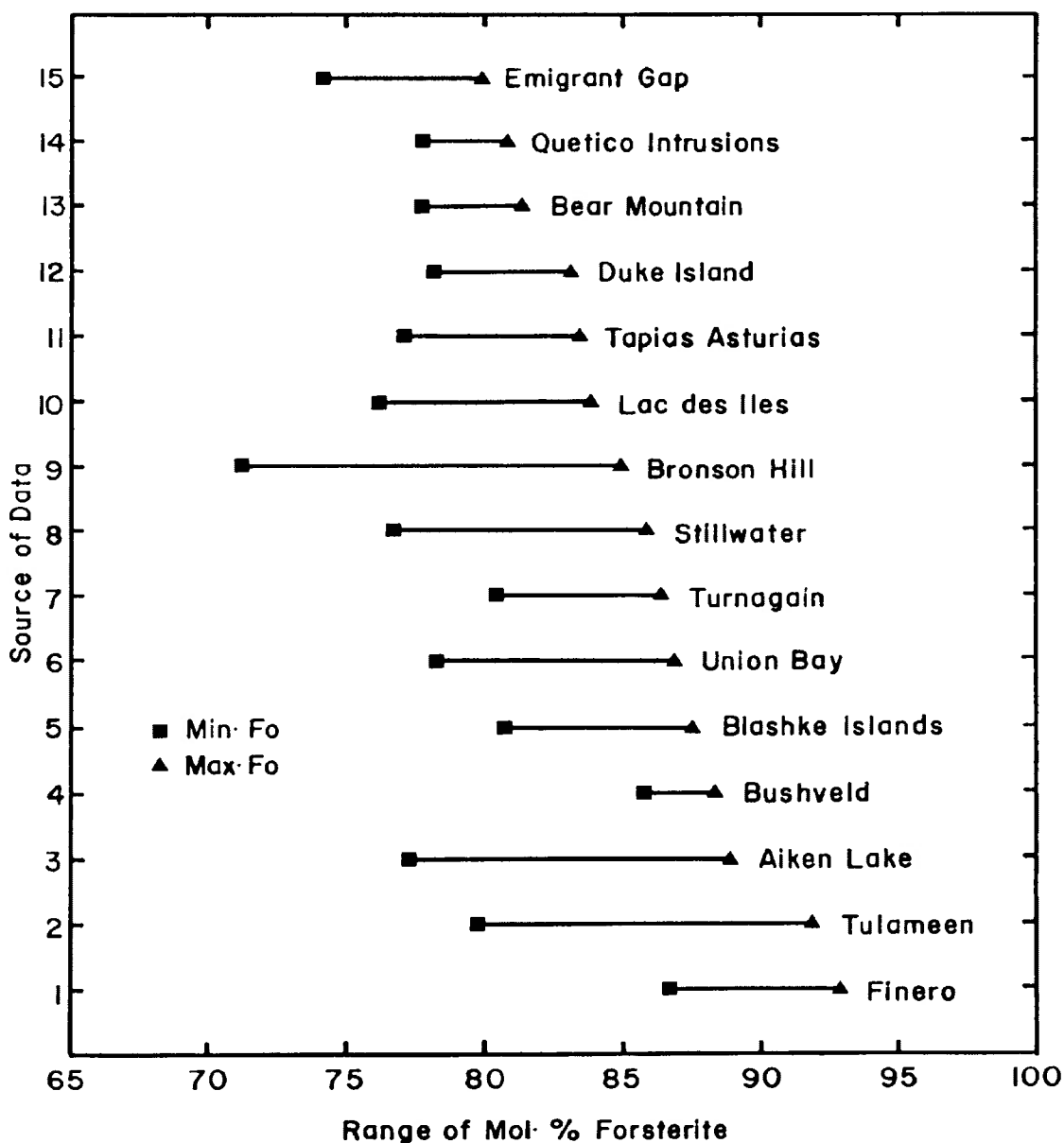
Data Sources: 1. Cawthorn (1975); 2. Findlay (1969); 3. Irvine (1974); 4. Atkins (1969), Scoon and De Klerk (1987); 5. Himmelberg et al. (1986); 6. Taylor and Noble (1969); 7. Clark (1980); 8. Czamanske and Zientek (1985), Barnes and Naldrett (1986); 9. Tracey et al. (1984); 10. Sutcliffe et al. (1989); 11. Galan and Suarez (1989); 12. Irvine (1974); 13. Snoke et al. (1981); 14. This Study; 15. James (1971).

olivines are almost identical. Various workers (French, 1966; Pitcher and Berger, 1972) suggest that some cortlandites (olivine-pyroxene hornblendites) may be members of the appinite suite. The Lac des Iles, Bronson Hill (Tracy et.al., 1984), and Stillwater complexes exhibit wider, generally more evolved ranges straddling the Quetico range. The Emigrant Gap complex is more evolved, but overlaps at lower forsterite contents (James, 1971).

4.3.2 - Clinopyroxene:

A total of 48 analyses were completed on 28 clinopyroxene grains from 9 samples taken from the Abiwin and Kawene Intrusions. Some grains were subjected to 2 or more analyses in an effort to determine the presence of zonation. Analyses were also attempted on clinopyroxene grains from the Mud Lake, Eva Lake, and Chief Peter Intrusions; however, the grains are too uralitized to provide reliable quantitative results. The three samples from the Abiwin Intrusion are all hornblende melagabbro, whereas the Kawene Intrusion is represented by two samples each of hornblende wehrlite and hornblende clinopyroxenite, one of clinopyroxene hornblendite, and one of clinopyroxene-olivine hornblendite that is transitional to hornblende wehrlite. Accurate clinopyroxene analyses from less mafic rock types were not possible owing to strong alteration.

Clinopyroxene compositions and structural formulas are

presented in Table 4.4A and B. Fe^{3+} concentrations were calculated using the method devised by Droop (1987). This indirect method is sensitive to errors in concentrations of the most abundant elements present; therefore, an effort was made to use the best quality analyses. Average Mol.% wollastonite (Wo), enstatite (En), and ferrosilite (Fs) contents are listed in Table 4.5.

The system of Morimoto (1989) classifies most of the clinopyroxenes of the Quetico Intrusions as diopside, with some calcium-rich augite grains occurring in less evolved rock types such as hornblende wehrlite and hornblende clinopyroxenite (Figure 4.5). The older and more familiar system of Deer et al. (1978) also classifies many of the Quetico clinopyroxenes as diopside; however, the less calcic grains are classified as calcic endiopside and the more iron-rich grains, occurring within hornblende melagabbro, are classified as calcic salite.

Some clinopyroxenes, particularly larger grains, exhibit a weak zonation that is somewhat variable between rock types and rarely exceeds an increase or decrease of 1 Mol.% Wo, En, or Fs. Measured core-to-rim variations are:

Melagabbro: $Wo_{49.91}En_{39.17}Fs_{10.93}$ to $Wo_{49.28}En_{39.70}Fs_{11.08}$;

Clinopyroxenite: $Wo_{44.44}En_{48.30}Fs_{7.26}$ to $Wo_{43.57}En_{49.22}Fs_{7.21}$;

Wehrlite: $Wo_{46.21}En_{47.80}Fs_{5.99}$ to $Wo_{46.73}En_{46.33}Fs_{6.94}$;

$Wo_{47.52}En_{45.54}Fs_{6.94}$ to $Wo_{47.25}En_{45.10}Fs_{7.65}$; and

$Wo_{44.70}En_{48.62}Fs_{6.73}$ to $Wo_{44.88}En_{48.08}Fs_{7.04}$.

TABLE 4.4A

Quantitative EDS Analyses of Clinopyroxene

Abiwin Intrusion   C:Core R:Rim   N.D:Not Detected

Sample	AAb-1-85	AAb-1-85	AAb-1-85	AAb-1-85	AAb-1-85	AAb-1-85	AAb-8-85
Grain	1-1R	1-1	1-1C	1-2R	1-3	1-4	1-2R
SiO_2	52.64	53.54	53.74	53.79	53.49	53.01	53.44
Al_2O_3	N.D	N.D	N.D	N.D	N.D	N.D	N.D
MgO	14.29	13.88	14.35	14.59	14.21	14.48	14.94
CaO	24.68	25.23	25.43	24.73	25.17	25.26	24.51
FeO	5.73	6.90	6.08	6.68	6.08	5.18	5.84
Fe_2O_3	1.48	0.86	1.19	0.75	0.21	1.17	0.96
Cr_2O_3	0.24	N.D	N.D	N.D	N.D	N.D	N.D
MnO	N.D	N.D	N.D	N.D	0.28	N.D	N.D
TiO_2	N.D	N.D	N.D	N.D	N.D	N.D	N.D
TOTAL	99.06	100.41	100.79	100.54	99.44	99.10	99.69

Structural Formula Based on Six Oxygens

Si	1.977	1.989	1.984	1.989	1.997	1.984	1.987
Al(iv)	---	---	---	---	---	---	---
Al(vi)	---	---	---	---	---	---	---
Fe^{3+}(iv)	0.023	0.011	0.016	0.011	0.003	0.016	0.013
Fe^{3+}(vi)	0.019	0.013	0.017	0.010	0.003	0.017	0.014
Ti	---	---	---	---	---	---	---
Cr	0.007	---	---	---	---	---	---
Mg	0.800	0.769	0.790	0.804	0.791	0.808	0.828
Fe^{2+}	0.180	0.215	0.188	0.207	0.190	0.163	0.182
Mn	---	---	---	---	0.009	---	---
Ca	0.994	1.004	1.006	0.980	1.008	1.013	0.977

Mol. Percent End Members (Plotting Parameters)

Wo	49.28	49.93	49.90	48.72	50.53	50.25	48.51
En	39.70	38.21	39.17	39.95	39.65	40.06	41.13
Fs	11.02	11.86	10.93	11.33	9.82	9.70	10.36

TABLE 4.4A (Cont'd)

Quantitative EDS Analyses of Clinopyroxene

Abiwin Intrusion   C:Core R:Rim   N.D:Not Detected

Sample	AAb-8-85	AAb-23-85	AAb-23-85	AAb-23-85	AAb-23-85	AAb-23-85	AAb-23-85
Grain	1-5C	1-1	1-1	1-2C	1-3	1-3	1-4
SiO_2	53.51	53.82	54.29	53.69	54.42	53.92	54.57
Al_2O_3	N.D	N.D	N.D	N.D	N.D	N.D	N.D
MgO	14.16	14.33	14.70	15.00	15.28	15.30	14.62
CaO	24.35	24.52	24.72	24.18	24.81	24.64	24.81
FeO	6.99	6.18	6.02	5.81	5.75	5.58	6.23
Fe_2O_3	N.D	N.D	N.D	N.D	0.11	0.75	N.D
Cr_2O_3	N.D	N.D	N.D	N.D	N.D	N.D	N.D
MnO	0.34	0.29	N.D	0.28	0.24	N.D	0.33
TiO_2	N.D	N.D	N.D	N.D	N.D	N.D	N.D
TOTAL	99.35	99.14	99.73	98.96	100.61	100.19	100.56

Structural Formula Based on Six Oxygens

Si	2.002	2.010	2.011	2.004	2.000	1.991	2.009
Al(iv)	---	---	---	---	---	---	---
Al(vi)	---	---	---	---	---	---	---
Fe^{3+}(iv)	---	---	---	---	---	0.009	---
Fe^{3+}(vi)	---	---	---	---	0.003	0.012	---
Ti	---	---	---	---	---	---	---
Cr	---	---	---	---	---	---	---
Mg	0.790	0.797	0.811	0.834	0.837	0.842	0.802
Fe^{2+}	0.219	0.193	0.186	0.181	0.177	0.173	0.192
Mn	0.011	0.009	---	0.009	0.007	---	0.006
Ca	0.976	0.981	0.981	0.967	0.977	0.974	0.979

Mol. Percent End Members (Plotting Parameters)

Wo	49.17	49.77	49.60	48.52	49.01	48.48	49.62
En	39.80	40.44	41.00	41.91	41.98	41.88	40.65
Fs	11.03	9.79	9.40	9.56	9.03	9.64	9.73

TABLE 4.4B

Quantitative EDS Analyses of Clinopyroxene

Kawene Intrusion   C:Core R:Rim   N.D:Not Detected

Sample	AK-47-86	AK-47-86	AK-47-86	AK-47-86	AK-47-86	AK-12-86	AK-12-86
Grain	1-1C	1-1	1-3	1-3	2-1	1-1	1-1R
SiO_2	53.79	53.52	53.84	54.58	53.70	53.68	53.78
Al_2O_3	N.D	N.D	N.D	N.D	N.D	0.72	0.54
MgO	14.64	14.69	14.94	16.16	15.60	17.89	17.98
CaO	24.75	24.87	25.29	24.88	25.18	22.43	22.14
FeO	5.94	5.58	5.39	4.54	3.70	3.73	4.01
Fe_2O_3	N.D	0.43	0.22	0.55	1.29	1.20	0.76
Cr_2O_3	0.35	0.32	N.D	N.D	0.37	N.D	N.D
MnO	0.33	0.32	N.D	N.D	0.37	N.D	N.D
TiO_2	N.D	N.D	N.D	N.D	N.D	0.25	N.D
TOTAL	99.80	99.41	99.68	100.71	99.84	100.22	99.68

Structural Formula Based on Six Oxygens

Si	1.997	1.995	1.997	1.993	1.983	1.958	1.970
Al(iv)	---	---	---	---	---	0.031	0.023
Al(vi)	---	---	---	---	---	---	---
Fe^{3+}(iv)	---	0.005	0.030	0.007	0.017	0.011	0.007
Fe^{3+}(vi)	---	0.007	0.030	0.008	0.019	0.022	0.014
Ti	---	---	---	---	---	0.007	---
Cr	0.010	---	---	---	---	0.009	0.014
Mg	0.810	0.816	0.826	0.880	0.858	0.972	0.981
Fe^{2+}	0.184	0.174	0.167	0.139	0.115	0.114	0.123
Mn	0.010	0.010	---	---	0.012	---	---
Ca	0.985	0.993	1.005	0.974	0.996	0.877	0.869

Mol. Percent End Members (Plotting Parameters)

Wo	49.77	49.77	50.15	48.51	49.67	43.93	43.57
En	40.93	40.91	41.22	43.83	42.82	48.72	49.22
Fs	9.30	9.31	8.63	7.66	7.51	7.35	7.21

TABLE 4.4B (Cont'd)

Quantitative EDS Analyses of Clinopyroxene

Kawene Intrusion   C:Core R:Rim   N.D:Not Detected

Sample	AK-12-86	AK-12-86	AK-12-86	AK-12-86	AK-12-86	AK-12-86	AK-12-86
Grain	1-1C	1-2R	1-3R	1-3	2-1	2-1	2-2
SiO_2	53.80	52.51	53.34	53.93	53.44	53.04	54.00
Al_2O_3	0.88	2.01	1.07	0.82	1.44	1.49	N.D
MgO	17.36	16.66	17.51	17.24	16.85	17.07	17.78
CaO	22.21	22.34	22.38	22.63	22.68	22.78	22.17
FeO	4.66	4.92	4.19	3.97	4.69	3.70	4.41
Fe_2O_3	N.D	0.11	0.22	N.D	N.D	0.65	0.22
Cr_2O_3	0.39	0.46	0.41	0.52	0.70	0.67	0.58
MnO	N.D	N.D	N.D	N.D	N.D	N.D	N.D
TiO_2	N.D	0.33	0.27	N.D	N.D	N.D	N.D
TOTAL	99.30	99.34	99.39	99.11	99.80	99.40	99.16

Structural Formula Based on Six Oxygens

Si	1.978	1.938	1.960	1.983	1.960	1.950	1.989
Al(iv)	0.022	0.062	0.040	0.017	0.040	0.050	---
Al(vi)	0.016	0.025	0.006	0.019	0.022	0.015	---
Fe^{3+}(iv)	---	---	---	---	---	---	0.060
Fe^{3+}(vi)	---	0.003	0.006	---	---	0.018	---
Ti	---	0.009	0.007	---	---	---	---
Cr	0.011	0.013	0.012	0.015	0.020	0.020	0.017
Mg	0.951	0.916	0.959	0.945	0.921	0.936	0.977
Fe^{2+}	0.143	0.152	0.129	0.122	0.144	0.114	0.136
Mn	---	---	---	---	---	---	---
Ca	0.875	0.883	0.882	0.892	0.891	0.898	0.876

Mol. Percent End Members (Plotting Parameters)

Wo	44.44	45.19	44.60	45.53	45.55	45.68	43.91
En	48.30	46.88	48.57	48.24	47.09	47.61	48.97
Fs	7.26	7.93	6.82	6.22	7.36	6.71	7.12

TABLE 4.4B (Cont'd)

Quantitative EDS Analyses of Clinopyroxene

Kawene Intrusion   C:Core R:Rim   N.D:Not Detected

Sample	AK-12-86	AK-16-86	AK-19-86	AK-27-86	AK-27-86	AK-27-86	AK-27-86
Grain	2-2	2-2	1-4C	1-4C	1-4	1-4	1-4
SiO_2	54.62	53.65	53.75	54.01	54.71	54.39	54.25
Al_2O_3	N.D	0.57	N.D	0.96	0.96	0.81	1.06
MgO	18.12	16.70	16.33	17.17	17.13	17.31	17.63
CaO	23.46	24.72	25.46	23.08	23.26	23.25	22.98
FeO	2.97	3.50	2.55	3.84	4.18	4.25	4.00
Fe_2O_3	0.55	0.87	1.05	N.D	N.D	N.D	0.09
Cr_2O_3	0.47	0.24	0.36	0.94	0.76	1.12	1.01
MnO	N.D	N.D	N.D	N.D	N.D	N.D	N.D
TiO_2	N.D	N.D	N.D	N.D	N.D	N.D	N.D
TOTAL	100.19	99.47	99.50	100.00	101.00	101.14	101.02

Structural Formula Based on Six Oxygens

Si	1.986	1.972	1.980	1.972	1.978	1.968	1.962
Al(iv)	---	0.025	---	0.028	0.022	0.032	0.038
Al(vi)	---	---	---	0.013	0.019	0.002	0.007
Fe^{3+}(iv)	0.014	0.003	0.020	---	---	---	---
Fe^{3+}(vi)	0.001	0.021	0.009	---	---	---	0.002
Ti	---	---	---	---	---	---	---
Cr	0.014	0.007	0.011	0.027	0.022	0.032	0.029
Mg	0.982	0.915	0.897	0.934	0.923	0.934	0.950
Fe^{2+}	0.090	0.108	0.079	0.117	0.126	0.129	0.121
Mn	---	---	---	---	---	---	---
Ca	0.914	0.934	1.005	0.903	0.901	0.902	0.891

Mol. Percent End Members (Plotting Parameters)

Wo	45.68	48.77	50.03	46.21	46.20	45.91	45.33
En	49.06	45.85	44.62	47.80	47.32	47.54	48.39
Fs	5.24	5.39	5.35	5.99	6.48	6.55	6.28

TABLE 4.4B (Cont'd)

Quantitative EDS Analyses of Clinopyroxene

Kawene Intrusion   C:Core R:Rim

Sample	AK-27-86	AK-27-86	AK-27-86	AK-27-86	AK-27-86	AK-27-86	AK-27-86
Grain	1-4	1-4R	2-1C	2-1R	3-1R	1-1C	1-1R
SiO_2	54.94	54.16	54.55	54.10	54.20	54.25	53.86
Al_2O_3	0.68	0.67	0.90	1.06	1.13	0.81	1.13
MgO	17.34	16.79	17.34	16.87	17.14	16.83	16.12
CaO	23.43	23.55	22.95	23.28	23.84	24.43	23.49
FeO	4.19	4.48	4.07	4.60	3.71	3.57	4.87
Fe_2O_3	N.D	N.D	N.D	N.D	0.51	1.11	N.D
Cr_2O_3	0.78	0.60	0.79	0.58	0.27	0.59	0.77
MnO	N.D	N.D	N.D	N.D	N.D	N.D	N.D
TiO_2	N.D	N.D	N.D	N.D	N.D	N.D	N.D
TOTAL	101.36	100.25	100.59	100.48	100.81	100.59	100.23

Structural Formula Based on Six Oxygens

Si	1.980	1.979	1.978	1.971	1.965	1.959	1.972
Al(iv)	0.020	0.021	0.022	0.029	0.035	0.034	0.028
Al(vi)	0.009	0.008	0.017	0.017	0.013	---	0.021
Fe^{3+}(iv)	---	---	---	---	---	0.007	---
Fe^{3+}(vi)	---	---	---	---	0.014	0.023	---
Ti	---	---	---	---	---	---	---
Cr	0.022	0.017	0.023	0.017	0.008	0.017	0.023
Mg	0.932	0.914	0.937	0.916	0.926	0.906	0.879
Fe^{2+}	0.126	0.137	0.123	0.140	0.1126	0.108	0.149
Mn	---	---	---	---	---	---	---
Ca	0.905	0.922	0.892	0.909	0.926	0.954	0.921

Mol. Percent End Members (Plotting Parameters)

Wo	46.10	46.73	45.68	46.25	46.81	47.52	47.25
En	47.45	46.33	48.01	46.62	46.81	45.54	45.10
Fs	6.44	6.94	6.31	7.13	6.39	6.94	7.65

TABLE 4.4B (Cont'd)

Quantitative EDS Analyses of Clinopyroxene

Kawene Intrusion   C:Core R:Rim   N.D:Not Detected

Sample	AK-34-86	AK-34-86	AK-34-86	AK-34-86	AK-34-86	AK-34-86
Grain	1-1C	1-1R	1-2R	1-3	1-3	1-6
SiO_2	53.66	54.10	53.99	53.61	53.11	53.43
Al_2O_3	0.77	1.10	0.63	0.88	1.48	0.85
MgO	17.69	17.54	17.51	18.24	17.21	17.87
CaO	22.64	22.77	22.51	22.91	22.29	22.78
FeO	3.96	4.47	4.31	2.24	4.22	2.85
Fe_2O_3	0.46	0.12	N.D	1.82	0.52	1.73
Cr_2O_3	0.48	0.56	0.70	0.84	0.75	0.53
MnO	N.D	N.D	N.D	N.D	N.D	N.D
TiO_2	0.38	0.25	N.D	N.D	N.D	N.D
TOTAL	100.04	100.91	99.65	100.54	99.59	100.03

Structural Formula Based on Six Oxygens

Si	1.960	1.960	1.978	1.945	1.951	1.950
Al(iv)	0.033	0.040	0.022	0.038	0.049	0.037
Al(vi)	---	0.007	0.005	---	0.015	---
Fe^{3+}(iv)	0.007	---	---	0.017	---	0.013
Fe^{3+}(vi)	0.006	0.003	---	0.033	0.014	0.034
Ti	0.011	0.007	---	---	---	---
Cr	0.014	0.016	0.020	0.024	0.022	0.015
Mg	0.963	0.947	0.956	0.944	0.942	0.950
Fe^{2+}	0.121	0.135	0.132	0.068	0.130	0.087
Mn	---	---	---	---	---	---
Ca	0.886	0.884	0.884	0.890	0.878	0.891

Mol. Percent End Members (Plotting Parameters)

Wo	44.70	44.88	44.81	44.65	44.69	44.60
En	48.62	48.08	48.49	49.45	47.97	48.66
Fs	6.73	7.04	6.70	5.90	7.34	6.74

TABLE 4.5	Average Mol.% Wo:En:Fs in Clinopyroxene					
G:Melagabbro H:Hornblendite C:Clinopyroxenite W:Wehrlite						
Intrusion	Sample #	Spots	Wo	En	Fs
ABIWIN	AAb-1-85 (G)	3	49.70	39.03	11.27
		1	48.73	39.95	11.31
		1	50.53	39.65	9.82
		1	50.25	40.06	9.70
ABIWIN	AAb-8-85 (G)	1	48.51	41.13	10.36
		1	49.17	39.80	11.03
ABIWIN	AAB-23-85 (G)	2	49.69	40.72	9.60
		1	48.79	42.08	9.13
		2	48.75	41.93	9.34
		1	49.62	40.65	9.73
KAWENE	AK-12-86 (C)	3	43.98	48.75	7.27
		1	45.19	46.88	7.93
		2	45.09	48.39	6.53
		2	46.62	47.35	7.04
		2	44.80	49.02	6.18
KAWENE	AK-16-86 (C)	1	48.78	45.83	5.39
KAWENE	AK-19-86 (H)	1	50.03	44.62	5.35
KAWENE	AK-27-86 (W)	2	47.39	45.32	7.30
		1	46.81	46.81	6.39
		6	46.08	47.47	6.45
		2	45.97	47.32	6.72
KAWENE	AK-34-86 (W)	2	44.79	48.35	6.89
		1	44.81	48.49	6.70
		2	44.67	48.71	6.62
		1	44.60	48.66	6.74
KAWENE	AK-47-86 (H)	2	49.77	40.92	9.31
		2	49.33	42.53	8.14
		1	49.67	42.82	7.51

Figure 4·5   Clinopyroxenes - Quetico Intrusions

Wo

Di 50   50 Hd

        Diopside   Hedenbergite

45   45

                          Augite

20   20

                          Pigeonite

5   5

        Enstatite   Ferrosilite

En   Fs
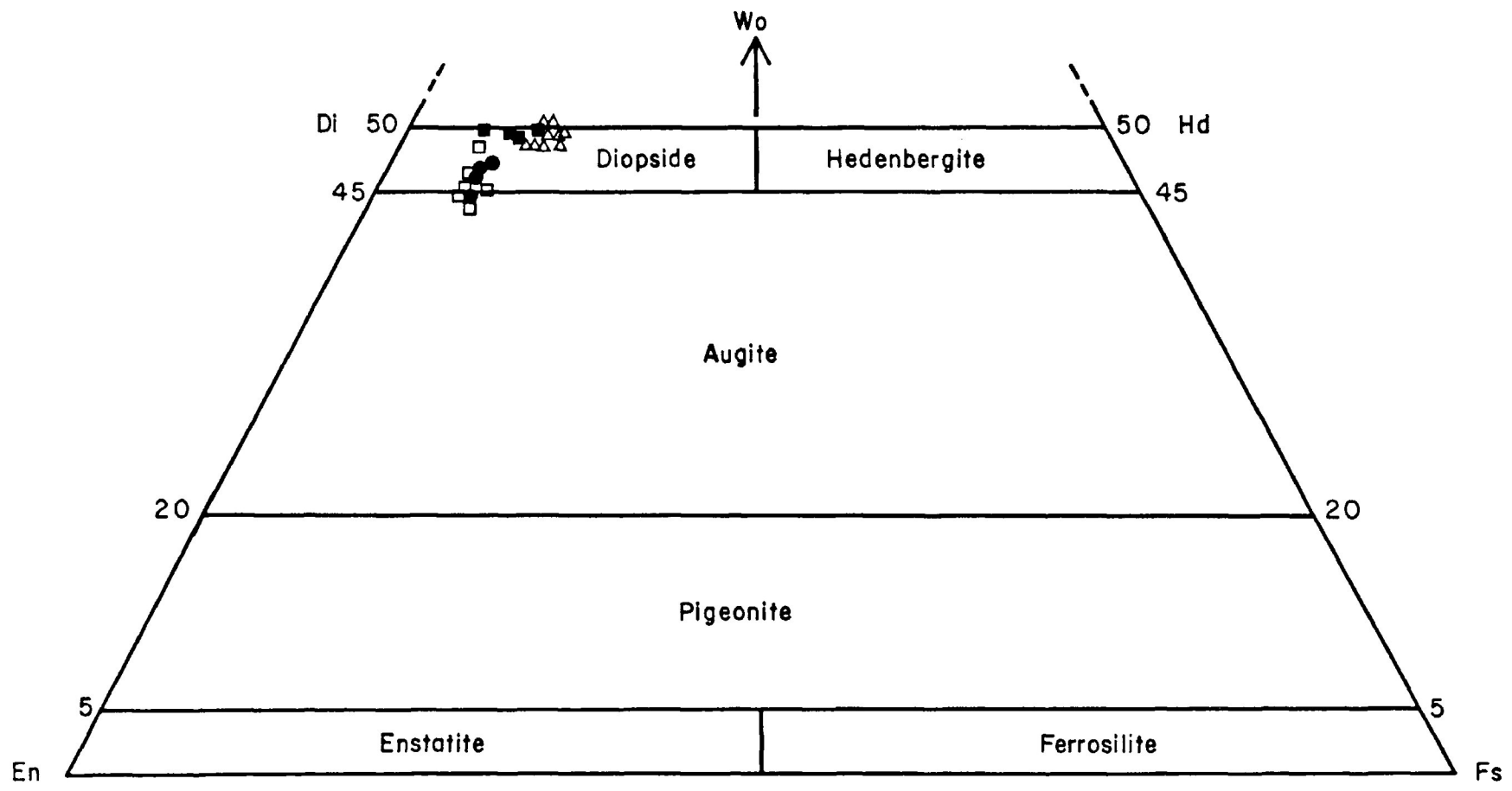
Classification after Morimoto (1989)

● Wehrlite   □ Clinopyroxenite   ■ Hornblendite   △ Melagabbro

Figures 4.6A and 4.6B illustrate the zonation observed within two grains from the Kawene Intrusion.

When the data from Table 4.5 are plotted on the pyroxene quadrilateral (Figure 4.5) they form a small, well-defined field representing an apparent fractionation trend initially exhibiting a steep slope that quickly flattens near the Wo_{50} line. Many grains cluster within the Mg- or Fe-rich portions of this field, while most of the remaining points are centrally scattered. A few grains plot just above the Wo_{50} line. The central part of the field may represent where clinopyroxenes from the hornblendite lithologies would plot; however, few unaltered grains remain.

Clinopyroxene compositions from the Quetico Intrusions are compared with other intrusions in Figure 4.7. Analyses from the full range of clinopyroxene-bearing lithologies present within the appinite suite are not available, particularly from the less evolved olivine-rich rock types. It is immediately apparent that the shape and location of the Quetico trend is totally unlike the tholeiitic Stillwater and Bushveld trends, as well as the mildly alkaline Shiant Isles trend, but is similar in shape and considerably overlaps the Alaskan-type trend. The few available clinopyroxene analyses from rocks of the appinite suite plot within or slightly to the right of the Quetico field. The points located near the right side of the field

Figure 4.6A

Zoning Within Clinopyroxene
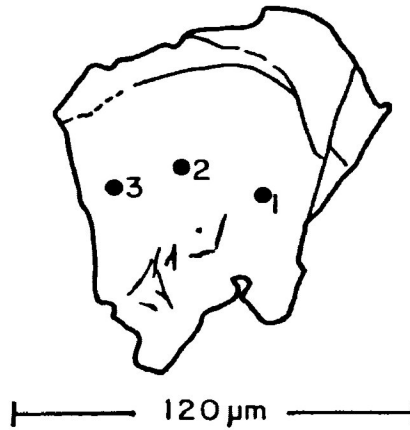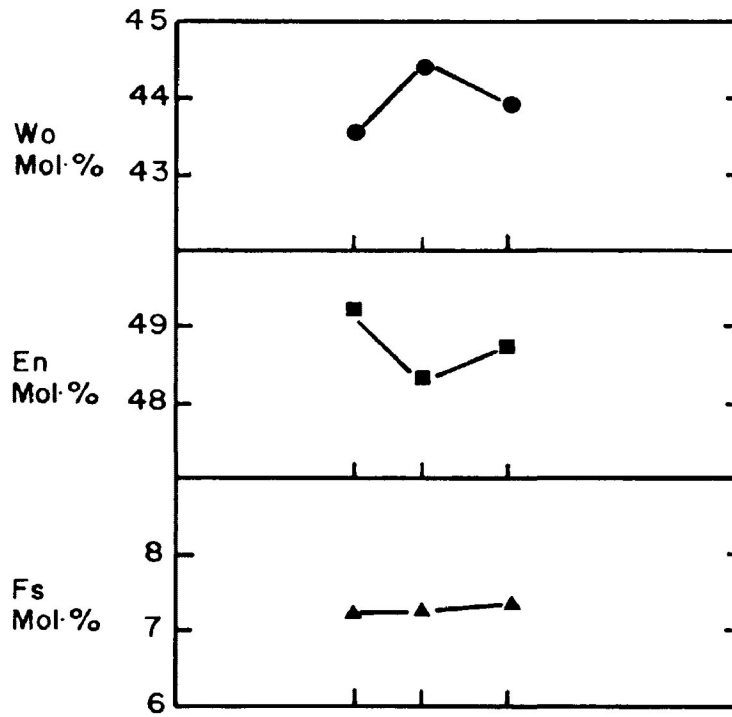
Sample AK-12-86

Figure 4.6B

Zoning within Clinopyroxene

500µm
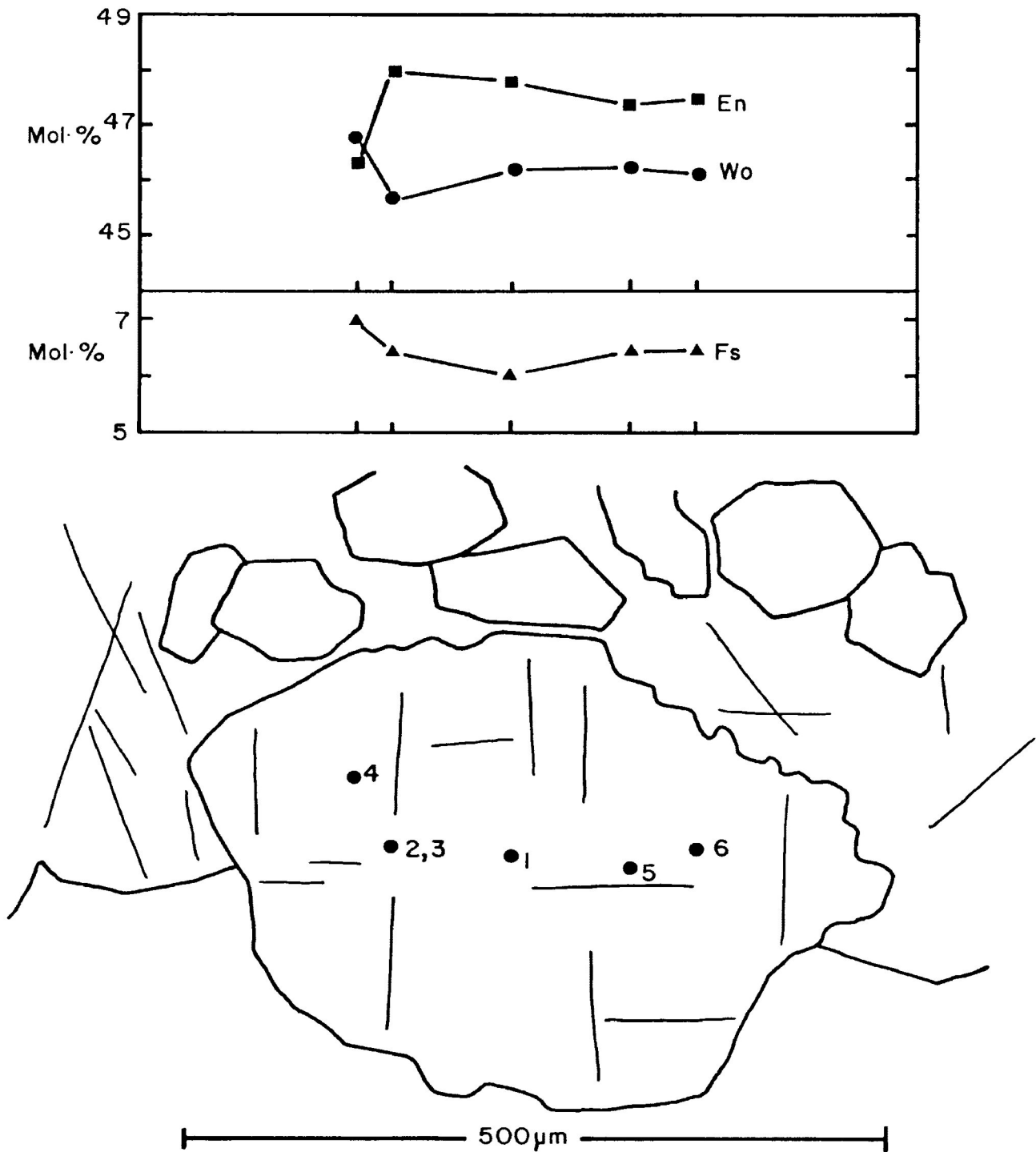
Sample AK-27-86

Figure 4·7   Comparison of Clinopyroxene Compositions

Legend:
- ⬭ Quetico Intrusions
- ⬭ Alaskan-type
- ● Appinite Suite
- —— Bushveld
- ---- Stillwater
- ~—~ Black Jack
- ~—~ Shiant Isles

Wo

Di   Hd

En   Fs

After Morimoto (1989)
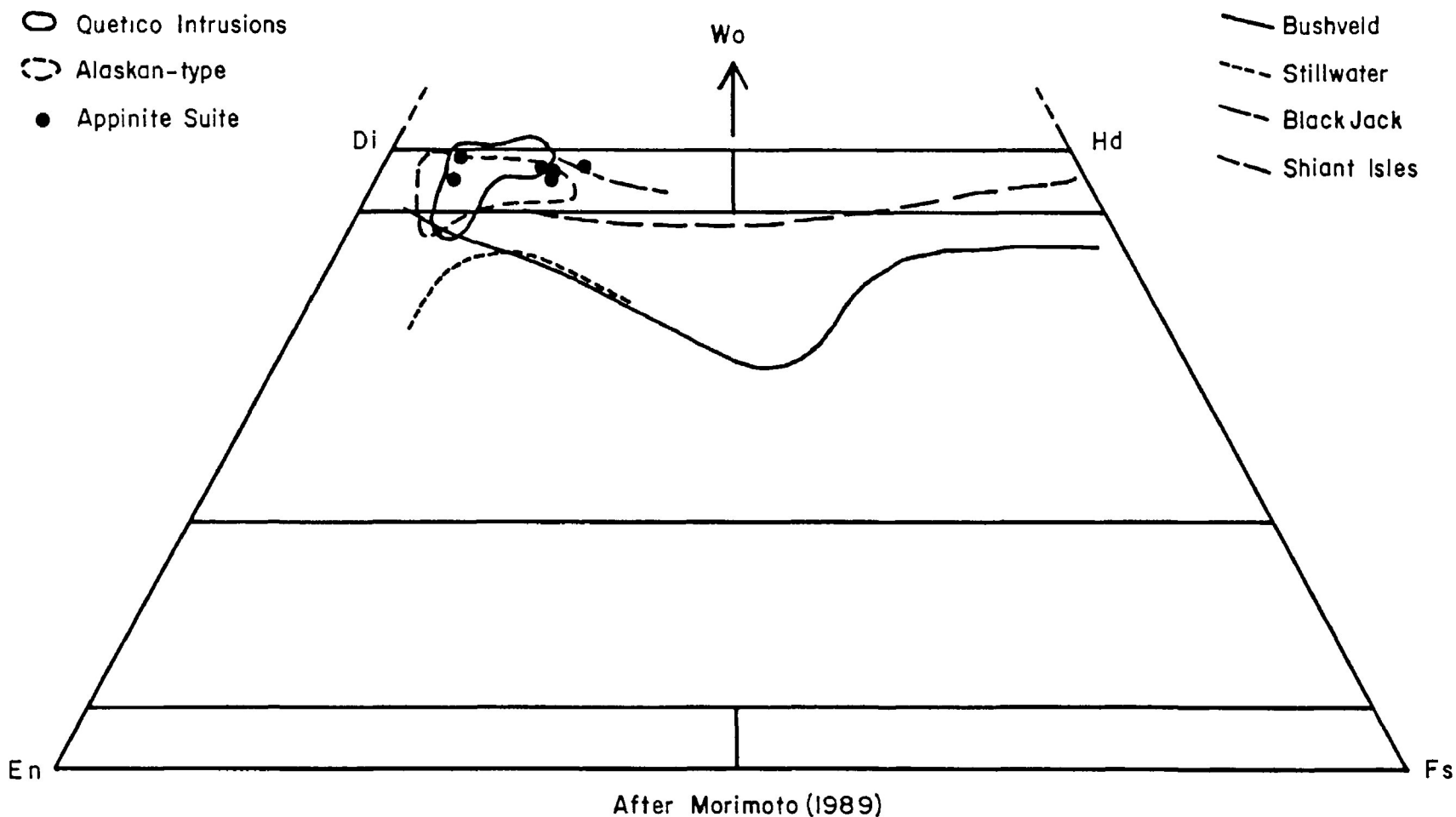
Data Sources – Himmelberg et al· (1986); Wilkinson (1956); Clark (1980); Ruckmick & Noble (1959); Hess (1960);
                Gibb (1973); Findlay (1969); Irvine (1974); Galan & Suarez (1989); Haslam (1970);
                Bishop & Key (1983); Atkins (1969)·

are from dioritic appinites and hornblende gabbros and lie directly in the path of the Quetico data trend, if it was extrapolated to include less mafic rock types. The points near the left edge of the field are from hornblende clinopyroxenites and olivine-pyroxene hornblendites and match similar Quetico rock types rather well. The trend for the strongly alkaline Black Jack Intrusion, Australia, appears to closely parallel the extrapolation of the Quetico Intrusions trend, but does not exhibit any overlap.

Figure 4.8 compares the relationship of Al_2O_3, TiO_2, and Cr_2O_3 to Mg/(Mg+Fe) between the Quetico Intrusions and other intrusions. This diagram shows that with increasing Fe/Mg ratio the contents of the three oxides initially increases, but then abruptly decreases to below detection limit at about 96 At.% Mg/(Mg+Fe). The Al_2O_3 and TiO_2 contents are similar to those of the appinite suite, but generally lower than those of the Alaskan-type or Bushveld complexes. Cr_2O_3 shows considerable overlap with the Alaskan-type complexes and rocks of the appinite suite, and minor overlap with the Bushveld complex.

Work by Kushiro (1960) determined that the alumina content of Na-poor clinopyroxene increases with the alkalinity of the magma type and that Si and Al behave in an inverse manner. These ideas were independently confirmed and taken a step further by LeBas (1962), who determined that the Al, Si, and Ti content of clinopyroxene might be

Comparisons of the Variation in Al2O3 and Mg/(Mg+Fe) in Clinopyroxenes

△ Melagabbro
■ Hornblendite
□ Clinopyroxenite
● Wehrlite

Quetico Intrusions
Appinite Suite
Alaskan-type
Bushveld
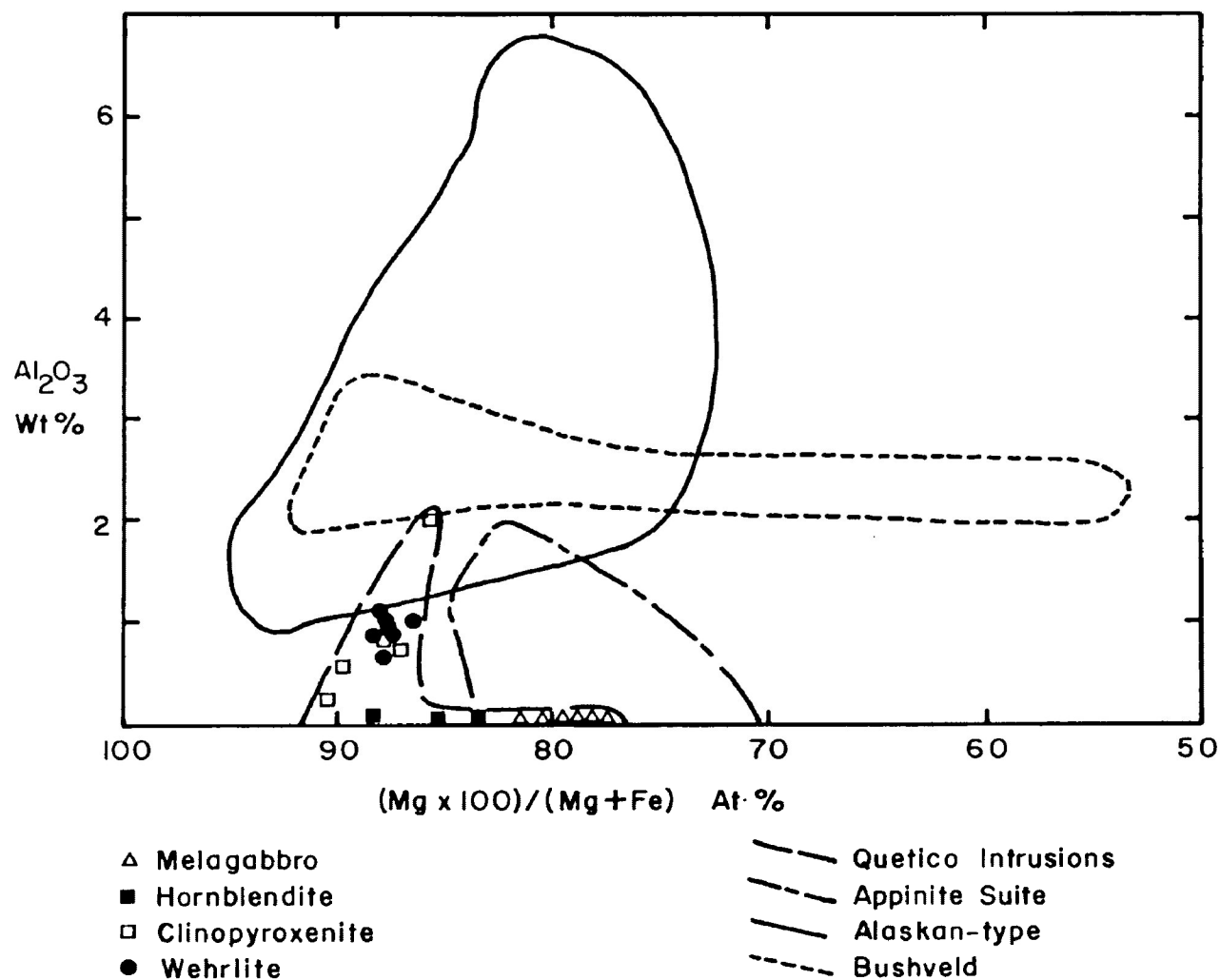
After Irvine (1973)

Figure 4.8A: Comparison of Al2O3 to Mg/(Mg+Fe) between the Quetico Intrusions and other intrusions. The Alaskan-type and the Bushveld Complex are considerably more alumina-rich, and the Quetico and appinite fields only partially overlap.

Data Sources: Haslam (1970); Galan and Suarez (1989); Bishop and Key (1983); Himmelberg et al. (1986); Clark (1980); Cawthorn (1975); Findlay (1969); Irvine (1974); Atkins (1969).

Comparisons in the Variations in TiO2, Cr2O3, and Mg/(Mg+Fe) in
Clinopyroxenes
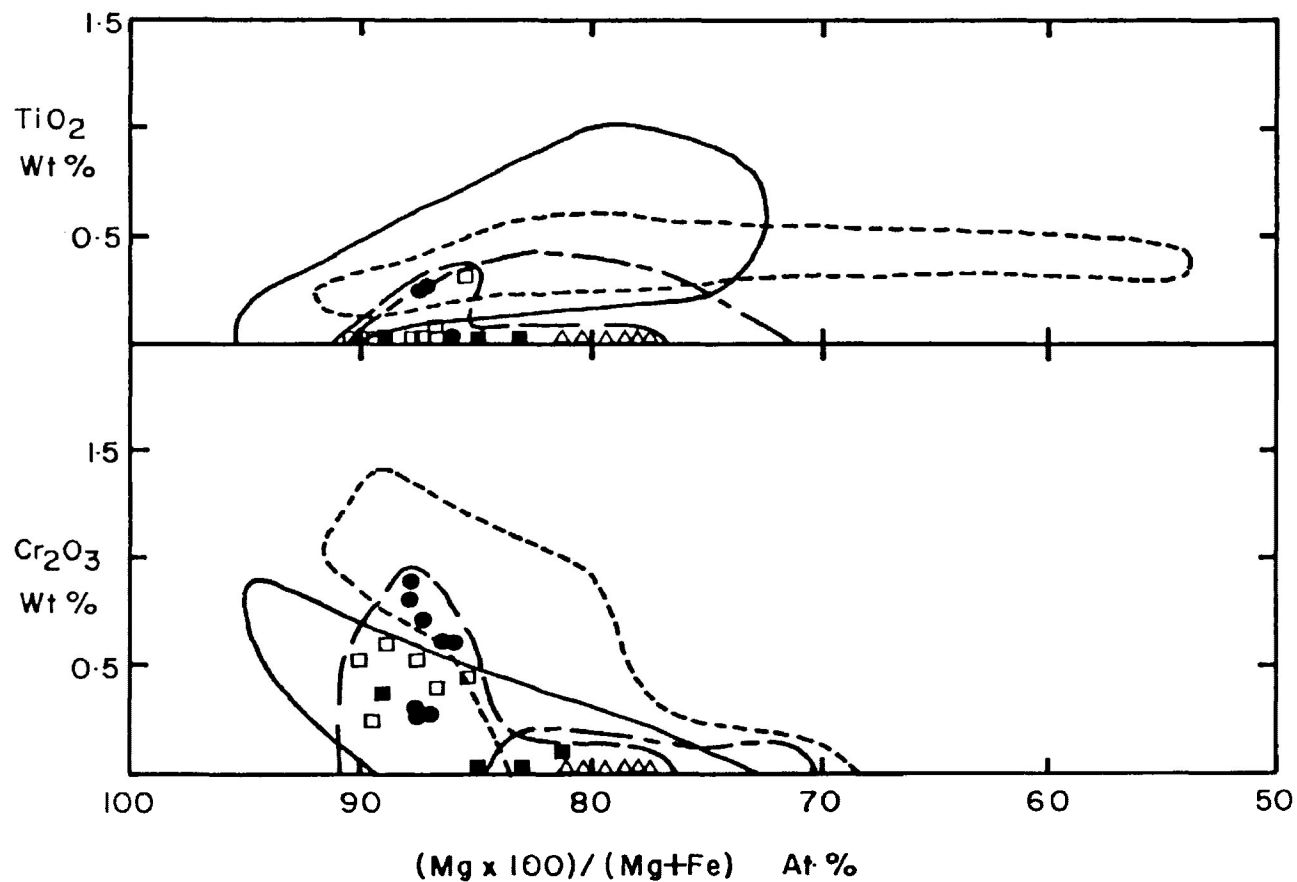
After Irvine (1973)

Figure 4.8B: Comparison of TiO2 and Cr2O3 to Mg/(Mg+Fe). All fields
show considerable overlap. The Bushveld and Alaskan-type complexes
contain more TiO2 and the Bushveld Complex contains more Cr2O3.
Data sources and symbols are the same as in Figure 4.8A.

used to determine magmatic affinity irrespective of whether the host rock is plutonic or volcanic in nature. This technique can determine whether a parent magma was sub-alkaline, normal-alkaline or per-alkaline in nature, but cannot distinguish between the tholeiitic and calc-alkaline varieties of sub-alkaline magma. Leterrier et al. (1982) derived a set of discrimination diagrams from a statistical study of the Ti, Cr, Ca, Al, and Na contents of volcanic clinopyroxenes from various magma types and tectonic settings. This method, which can also be used to identify magmatic affinities, is primarily used in the study of volcanic rocks. It has recently seen some use in the study of plutonic rocks (Himmelberg et al., 1986) and can sometimes distinguish between clinopyroxenes that have crystallized from tholeiitic or calc-alkaline magmas.

Figure 4.9A is a comparison plot of Wt.% Al_2O_3 against Wt.% SiO_2 that suggests a sub-alkaline nature for the Quetico Intrusions and illustrates their similarity to clinopyroxenes of the appinite suite. The Quetico field shows some overlap and a similarity in trend with the Alaskan-type complexes. The Bushveld complex field exhibits a different trend direction and no apparent overlap.

Figure 4.9B plots the proportion of Al^{iv} present within the tetrahedral Z-site, per clinopyroxene formula (Al_z), against Wt.% TiO_2. Data sources are the same as those for Figure 4.9A. The Quetico data support the inference of sub-

Comparison Plot of SiO2/Al2O3 in Clinopyroxene of the Quetico and Other
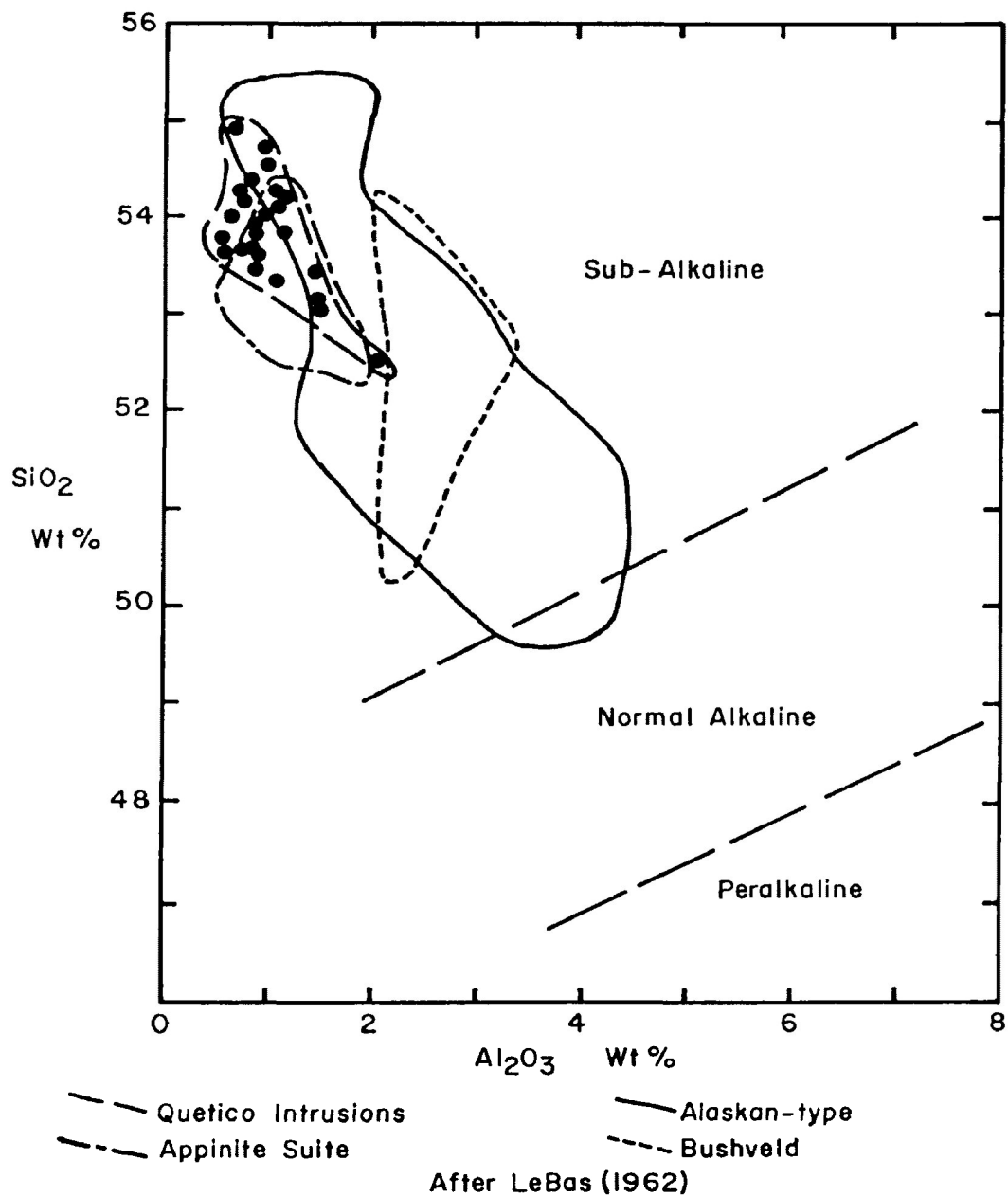
Intrusions

Figure 4.9A: Comparison plot of Al2O3/SiO2. Diagram illustrates the similarity and sub-alkaline nature of the Quetico Intrusions and the appinite suite. Note the Alaskan-type Complexes trend toward the normal alkaline field. Data sources the same as Figure 4.8.

Comparison Plot of Alz/TiO2 in Clinopyroxene from the Quetico

and Other Intrusions
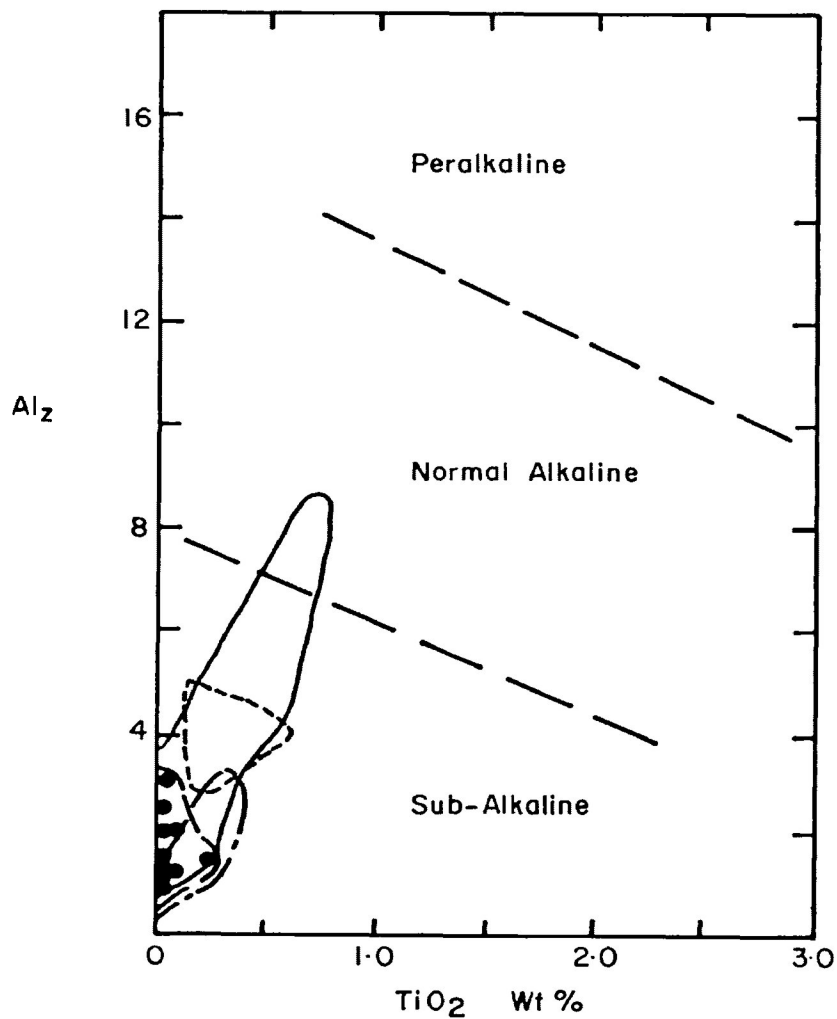
After LeBas (1962)

Figure 4.9B: Comparison plot of Alz/TiO2 in clinopyroxene. Alz is the proportion of Al^{iv} present within the tetrahedral Z-site per clinopyroxene formula. The Quetico Intrusions and the appinite suite contain little Al in the Z-site, whereas the Alaskan-type contain considerable Al and exhibit a trend toward the normal alkaline field. Data sources and symbols are the same as in Figure 4.9A.

alkaline affinity that was suggested in diagram 4.9A,
illustrate the Al- and titania-poor nature of the
clinopyroxenes, and confirm their similarity to the appinite
suite. The Alaskan-type complexes contain a range of
clinopyroxene-bearing rock types that are superficially
similar to the Quetico Intrusions, but exhibit a much wider
range of Al and Ti content and form a well-defined trend
extending into the normal alkaline field. Clinopyroxenes
from the Bushveld complex contain slightly more Al_z and Ti,
in the range of 3-5, and 0.25-0.6 Wt.%, respectively, than
the Quetico Intrusions or the appinite suite. LeBas (1962)
states that clinopyroxenes crystallizing from magmas of
tholeiitic or calk-alkaline affinity would tend to develop a
trend toward the lower right hand corner of the diagram,
whereas the alkaline rocks would form a trend extending
toward the upper right hand portion of the diagram. There
are not enough titania-bearing clinopyroxene analyses from
the Quetico Intrusions or the appinite suite to produce a
well-defined trend; however, the Quetico data apparently
form a weak trend toward the lower right hand corner of the
diagram.

Figure 4.10 is a plot of the relationship of the Ti and
Al present within the clinopyroxene formula. It is a
discrimination diagram generally used in the study of
volcanic rocks that attempts to separate clinopyroxenes that
have formed from calc-alkaline or tholeiitic magmas

Discrimination Plot of (Ti per formula)/(Total Al per formula) within

Clinopyroxene
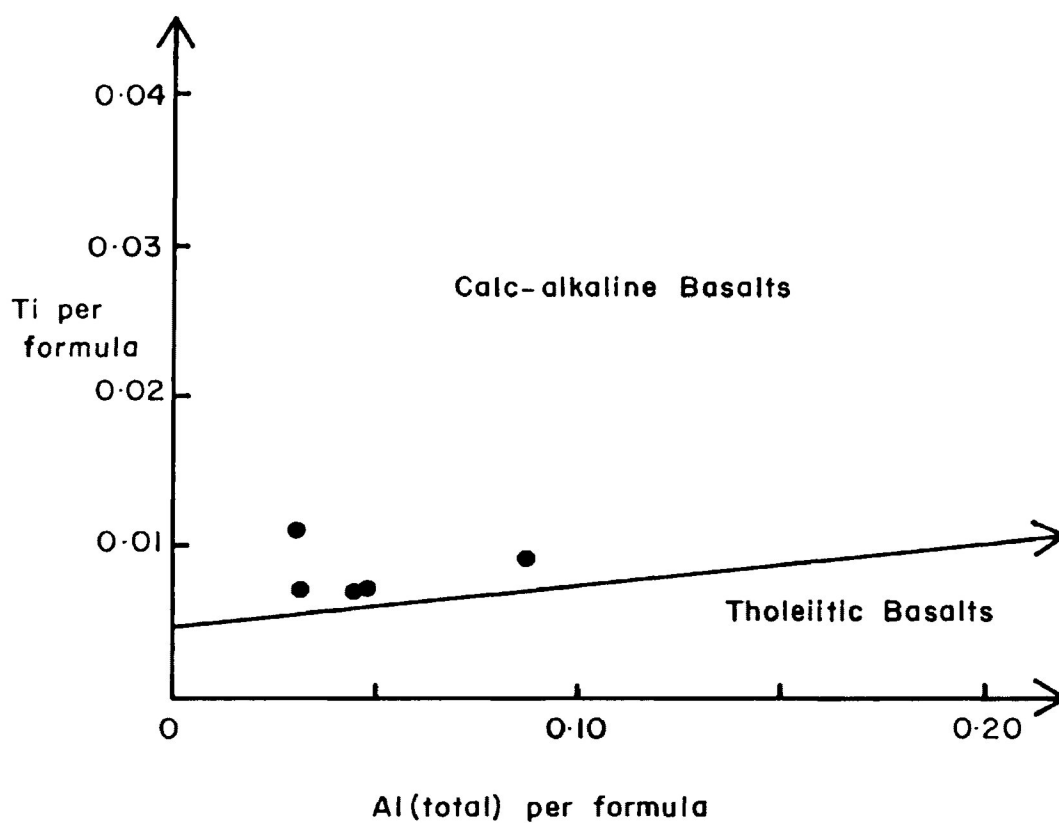
After Leterrier et al· (1982)

Figure 4.10: Discrimination plot of the relationship between Al and Ti present within the clinopyroxene formula. Both Al and Ti were detected in only 5 grains, all of which plot in the calc-alkaline field. This data only hints at a possible affinity, because 5 points are not enough in this case to properly place the intrusions into one field or another.

(Leterrier et al., 1982). Both Ti and Al were detected in only five clinopyroxenes, all of which plot within the calc-alkaline field. Five data points cannot properly define whether the Quetico clinopyroxenes actually formed from a calc-alkaline magma, but they do hint at a possible affinity. This supposition is supported by the dioritic and gabbroic appinites that plot well within the calc-alkaline field of the AFM diagram in Figure 4.1, the lack of a marked Fe-enrichment with fractionation, and the calc-alkaline nature of closely associated, possibly coeval, syntectonic, felsic to intermediate intrusions that locally intrude and are often, in turn, intruded by the Quetico Intrusions. The lack of iron enrichment may be explained by the occasional observation of myrmekitic intergrowths between magnetite and clinopyroxene (Chapter 3), suggesting that magnetite was a stable phase at early magmatic temperatures. Experimental evidence (Osborn, 1959) shows that the early crystallization of magnetite under magmatic conditions is a characteristic of calc-alkaline affinity. This stability is the result of a high, relatively constant oxygen fugacity which allows magnetite to crystallize from the liquid along with olivine and then clinopyroxene thereby depleting the residual liquid of iron oxides (Kushiro, 1979).

CHAPTER 5

SULPHIDE, OXIDE AND PLATINUM-GROUP ELEMENT MINERALIZATION

5.1: Introduction

Examination of more than 40 samples from surface and diamond drill core, has identified a variety of sulphides, oxides, sulpharsenides, tellurides, antimonides, alloys, native metals, and platinum group minerals (PGM). Coarser sulphides and oxides were identified by reflected light microscopy, whereas the remaining phases were identified by back-scattered electron (BSE) imagery and semi-quantitative energy dispersive X-ray spectrometry (SQ-EDS).

This chapter describes the occurrence, texture, petrography, mineral chemistry, and PGE/base metals geochemistry of the mineralized zones. All mineral chemistry was by SQ-EDS methods. During ZAF Correction the SQ-EDS software utilizes a set of internal standards and then automatically normalizes all weight percent totals to 100.00%. Trace element geochemistry of mineralized surface samples was completed by the Ontario Geological Survey Geoscience Laboratory; similar diamond drill core analyses were completed by Bondar-Clegg and Company and made available to the author by Fleck Resources Ltd. PGE analyses were completed by X-Ray Assay Laboratories Limited and made available by the Ontario Geological Survey. All samples, except those from the Eva Lake Intrusion, were collected by the author.

5.2: Occurrence and Style of Mineralization

Significant copper, nickel, and platinum-group mineralization is present within six of the Quetico Intrusions as small, irregular, contact-related zones of disseminated, occasionally net-textured chalcopyrite, pyrrhotite, and pentlandite. The style of mineralization within each zone is practically identical. Average sulphide content is 2-10%, but an overall range of 1-40% and, rarely, 50-70% is observed. Mineralization commonly crosscuts internal contacts, shows a preference for ultramafic rock types, usually decreases towards the centre of, and is always confined to, the host intrusion. Most zones occur at country-rock contacts; however, the Chief Peter Intrusion mineralization is associated with a gradational internal contact. Rocks not associated with well-mineralized zones always contain trace to 1% finely disseminated magnetite, pyrrhotite, and chalcopyrite.

The petrology and mineralogy of the dominant sulphide and oxide minerals is quite simple. The primary phases generally occur interstitially to the silicate gangue and the effects of regional metamorphism are not readily apparent. Grain-size ranges from less than 10 μm in diameter up to 8.0 mm in diameter or 16 mm in length. Average grain-size tends to decrease as sulphide content decreases. The most common sulphide and oxide phases are, in descending order of abundance:

1) Pyrrhotite $(Fe_{1-x}S)$;

2) Chalcopyrite $(CuFeS_2)$;

3) Magnetite (Fe_3O_4); and

4) Pentlandite $((Fe,Ni)_9S_8)$.

The petrology of the minor phases tends to be more complex than that of the major phases possibly due to the effects of deuteric and metamorphic processes. Average grain-size is usually much less than 1 mm with many PGM grains <1 μm in diameter. The identified minor phase minerals are:

1) The Platinum-group Minerals: michenerite (PdBiTe), hollingworthite (RhAsS), sobolevskite (PdBi), froodite $(PdBi_2)$, sperrylite $(PtAs_2)$;

2) Pyrite (FeS_2);

3) Tellurides: altaite (PbTe), empressite (AgTe), hedleyite (Bi_2Te);

4) Cubanite $(CuFe_2S_3)$;

5) Nickeliferous cobaltite $((Co,Ni)AsS)$;

6) Violarite $(FeNi_2S_4)$;

7) Covellite (CuS);

8) Breithauptite (NiSb);

9) Bismuthinite (Bi_2S_3);

10) Alloys: Pd-Au, Au-Ag-Hg-Bi, Ag-Cd, Ni-Bi-(S);

11) Native Metals: Bi, Sb, Ag.

Most minor phase minerals are closely associated with chalcopyrite, pyrrhotite, or pentlandite. Alloys and PGM are intimately associated with the copper-nickel sulphides and are occasionally observed within the silicate gangue adjacent to the copper-nickel sulphides. Native metals often occur within strongly serpentinized olivine grains. Covellite and violarite occur as minor alteration products of chalcopyrite, pyrrhotite, and pentlandite. Magnetite occurs everywhere, but is only dominant within the weakly mineralized rocks.

5.3: Petrography and Mineral Chemistry

This section will deal with the mineral groups in descending order of relative abundance, and will examine each mineral in terms of its detailed petrography, mineral chemistry, and relationship with other minerals. The similarity of the mineralization between intrusions greatly simplifies the description process; however, intrusion-specific differences, or variations, will be included to insure that the general descriptions are as complete and accurate as possible.

Most of the SQ-EDS work presented below was completed on drill core samples taken from the Kawene Intrusion because of the similarity of the Kawene Main Zone to the other mineralized zones, the absence of weathering, and the significant Cu-Ni-PGE values intersected within the core.

5.3.1 - Sulphides:

Sulphides are present within all rock types and are the most dominant opaque phase. Much of the mineralization is composed of disseminated, interstitial, single grains, and monomineralic aggregates. Multigrain aggregates and composite grains composed of pyrrhotite-chalcopyrite-pentlandite+/-magnetite (Figure 5.1) are abundant within well-mineralized rocks, but are much less abundant within weakly mineralized rocks and usually do not contain pentlandite. Progressive replacement along grain boundaries, cleavage planes, and fractures by magnetite, and rarely pyrite has often affected the three most abundant sulphides, pyrrhotite, chalcopyrite, and pentlandite. Annealing textures and most other indications of the effects of metamorphism were not observed. Remobilization of chalcopyrite and pyrrhotite into narrow veinlets and the fracturing and interpenetration of opaque grains by the growth of acicular actinolite occurs within all mineralized intrusions and is the only apparent evidence of applied stress and/or metamorphism.

Pyrrhotite ($Fe_{1-x}S$) is the most abundant sulphide and occurs within every rock type. It is the dominant sulphide phase within weakly mineralized rocks and is slightly subordinate to chalcopyrite within well-mineralized rocks. Fractured grains are common locally. Remobilization, along with chalcopyrite, into narrow, discontinuous veinlets

po = pyrrhotite   cp = chalcopyrite   mag = magnetite
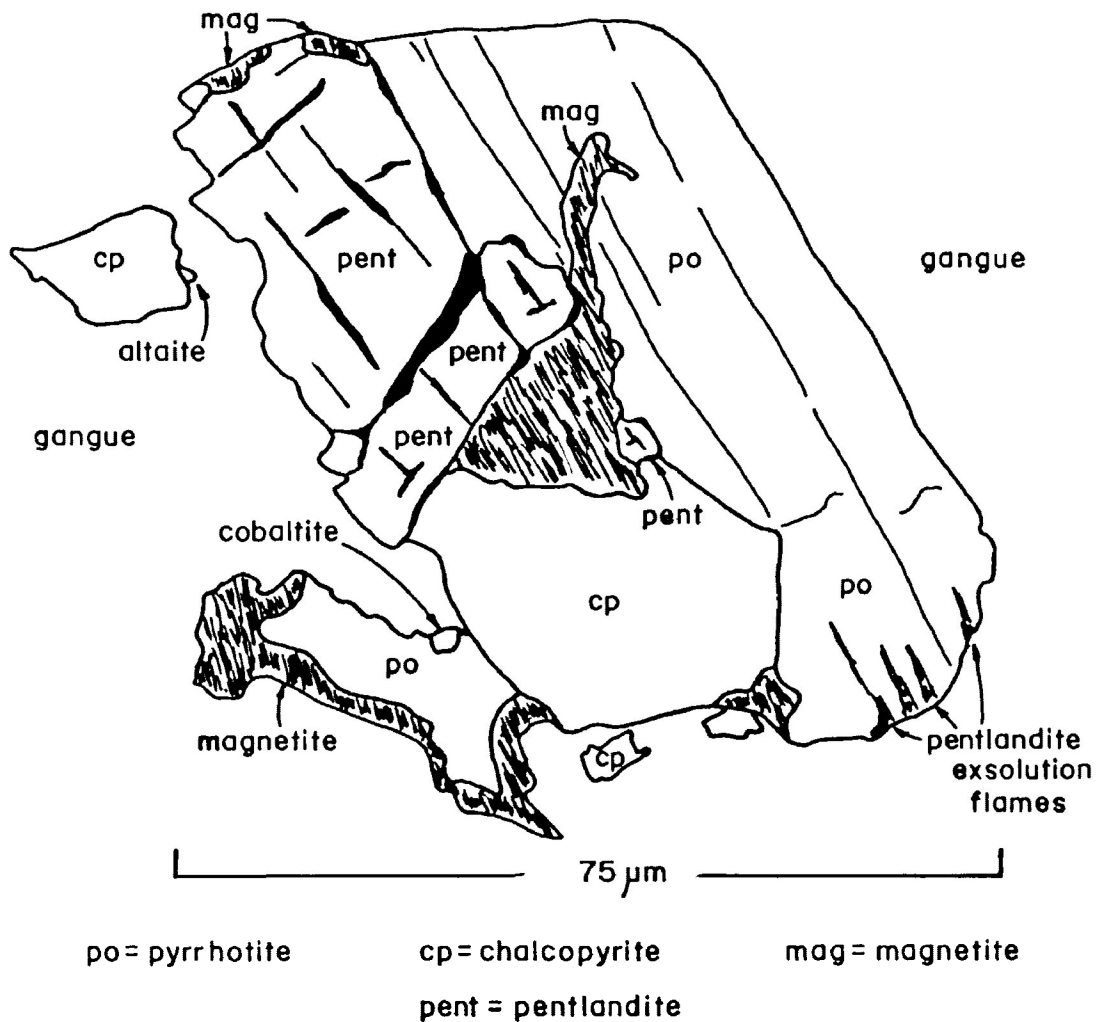
pent = pentlandite

Figure 5.1: Typical composite grain composed of pyrrhotite, chalcopyrite, and pentlandite, +/- magnetite, altaite, cobaltite, etc. In this example magnetite appears to be secondary in nature. Sample AK-16-86.

occurs locally within the Kawene Intrusion, but is quite common within the Eva Lake, Chief Peter, and Abiwin Intrusions.

Pyrrhotite within well-mineralized rocks is anhedral to subhedral, highly variable in size, with a range of <0.01-6.0 mm in diameter and often forms multigrain aggregates up to 15 mm in length and 5 mm in width. It commonly forms partial or complete rims surrounding chalcopyrite. Tiny, anhedral to euhedral grains often occur within the silicate gangue, occasionally included within the silicates. Most grains exhibit sharp boundaries that are often straight to curved, locally irregular, or occasionally embayed. Boundaries with other opaque phases tend to be sharp and straight; however, doubly penetrative, intergrown boundaries with chalcopyrite are apparent locally.

Progressive replacement by magnetite is common within the Mud Lake Intrusion, but less common within the Kawene and Chief Peter Intrusions. The development of bird's-eye texture is common within surface-weathered samples from the Kawene and Mud Lake Intrusions. Weakly developed growth twins and narrow streaks of monoclinic pyrrhotite along fracture surfaces occur locally. Skeletal grains develop along the margins of multigrain aggregates and are confined to rocks containing >30% net-textured sulphides (Kawene and Plateau Intrusions).

Exsolution flames, granular veinlets, and robust grains

(eyes) of pentlandite are common within pyrrhotite grains and aggregates. Some contain inclusions of chalcopyrite. Minor alteration to violarite occurs along some grain boundaries and fracture surfaces of a few weathered samples from the Kawene and Mud Lake Intrusions.

Many of the identified PGM are associated with pyrrhotite and occur between adjacent grains, along grain margins, within fractures, or as isolated inclusions.

Weakly mineralized rocks contain finely disseminated pyrrhotite, usually much less than 2 mm in diameter, as isolated, anhedral to subhedral and locally euhedral, interstitial grains with straight to curved boundaries. It is occasionally replaced by magnetite along grain boundaries. Minor monoclinic pyrrhotite is present along some fractures. A few isolated exsolution flames of pentlandite were observed.

An SQ-EDS analysis of one pyrrhotite grain (Table 5.1) detected approximately 0.48 Wt.% Ni. Other analyses were deemed unreliable due to the presence of >1 Wt.% Bi.

Chalcopyrite (CuFeS$_2$) is usually intimately associated with pyrrhotite, and exhibits many of the same textural features. It differs from pyrrhotite by exhibiting a slightly smaller average grain-size (<0.01-6.0 mm), a tendency to occur in subordinate amounts within weakly mineralized rocks and a slightly greater abundance within well-mineralized rocks. Some grains are well-zoned, but this

Table 5.1

Semi-quantitative EDS Pyrrhotite Analysis

Sample	AK-16-86	
	At.%	Wt.%
Fe	46.84	60.42
Ni	0.35	0.48
S	52.80	39.10
TOTAL Wt.%		100.00

is evident only after the grains have tarnished. Inclusions within pyrrhotite and, rarely, pentlandite are sometimes observed. Some large chalcopyrite grains contain pyrrhotite, pentlandite, and silicate inclusions. Skeletal textures are sometimes present within the net-textured sulphides of the Kawene and Plateau Lake Intrusions. Elsewhere, small grains are locally observed as inclusions within silicates. A few, myrmekitic intergrowths were observed within cumulus hornblendes of the Kawene Intrusion. It readily remobilizes, often infills narrow fractures, and occasionally invades biotite cleavage planes. Minor alteration to covellite occurs within weathered surface samples from the Mud Lake and Kawene Intrusions. PGM are often closely associated with chalcopyrite.

SQ-EDS analyses of chalcopyrite determined that the grains contain no detectible impurities.

Pentlandite ((Fe,Ni)$_9$S$_8$) occurs as large, robust grains closely associated with pyrrhotite and chalcopyrite, fine-grained, granular veinlets associated with pyrrhotite grains, and delicate exsolution flames within pyrrhotite. The coarser pentlandite varieties only occur within well-mineralized zones and are occasionally fractured and penetrated by acicular actinolite grains. Exsolution flames are more abundant within well-mineralized zones, but occur wherever there is pyrrhotite. Pentlandite is always subordinate to pyrrhotite and chalcopyrite and is rare in

the Mud Lake Intrusion.

Robust pentlandite grains (Figure 5.2a) are subround, subhedral to euhedral, and usually between 0.25 and 2.0 mm in diameter. They often occur in large composite grains with chalcopyrite and pyrrhotite, irregular, multigrain aggregates with pyrrhotite, and rarely, isolated grains within the silicate gangue. All grains are heavily fractured from the effects of considerable shrinkage during cooling. Grain boundaries are curved, often undulose, and locally ragged.

Granular pentlandite veinlets (Figure 5.2b) are irregular aggregates composed of anhedral to subhedral grains that form along pyrrhotite grain boundaries, between pyrrhotite and chalcopyrite grains, and along fractures in pyrrhotite. Grains are usually <0.25 mm and are often less than 50 μm in diameter. They have sharp, curved, or irregular boundaries when in contact with chalcopyrite, silicates, or other pentlandite grains and often diffuse boundaries when in contact with pyrrhotite. Cooling and shrinkage features are ubiquitous.

Exsolution flames (Figure 5.2c) occur only in a crystallographically controlled direction in pyrrhotite and are <0.1 mm, and often <25 μm in length.

Minor alteration to violarite $(FeNi_2S_4)$ is present in some surface-weathered samples from the Kawene Intrusion. Only a few PGM are associated with pentlandite.
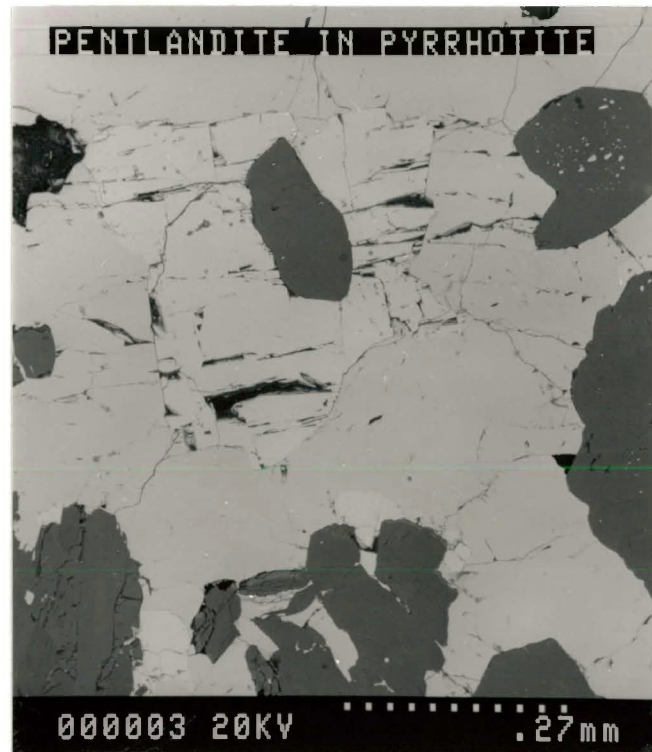
Figure 5.2a: Robust pentlandite grains within pyrrhotite. Sample AK-16-86.
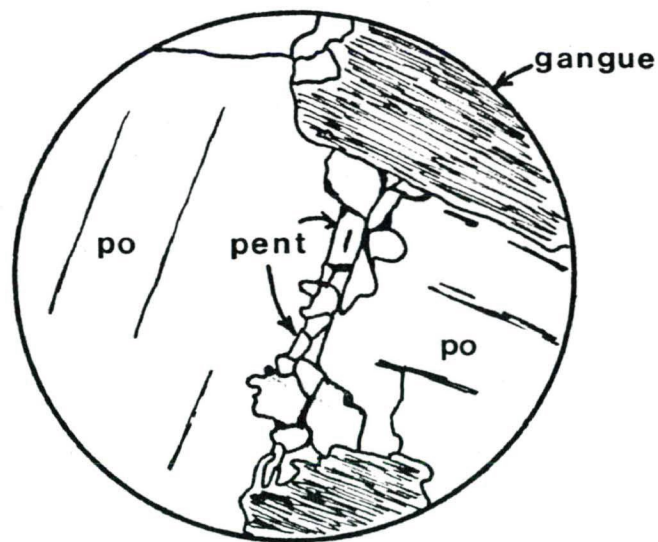
Figure 5.2b: Granular pentlandite veinlet within pyrrhotite; field of view is 1.0 mm; po =pyrrhotite; pent = pentlandite.   Sample #15A, Drill Hole K-1-87.

Figure 5.2c: Cluster of pentlandite exsolution flames within
pyrrhotite. Sample #17, Drill Hole K-1-87.

SQ-EDS analyses (Tables 5.2a, b and c) of pentlandite exsolution flames detected 1.58-3.18 Wt% Co. Similar analyses of robust single grains detected 6.89-7.79 Wt% Co, with one grain containing 0.60 Wt% Te. Smaller grains within granular veinlets contained 2.56-3.57 Wt% Co.

Pyrite (FeS$_2$) is not common and, when present, tends to occur within weakly mineralized rocks where magnetite is the dominant opaque phase, or strongly altered rocks. It forms anhedral to euhedral and occasionally skeletal grains up to 3 mm in diameter that are finely disseminated throughout the rock and often partially replaced by magnetite. The few pyrite grains observed within well-mineralized rocks are closely associated with pyrrhotite and chalcopyrite. The presence of pyrrhotite exhibiting well-developed birds-eye texture suggests that some pyrite formed at the expense of pyrrhotite in weathered surface samples.

A few tiny grains of what may be cubanite (CuFe$_2$S$_3$) were observed within the weakly mineralized rocks of the Kawene Intrusion. These fractured, irregular, strongly anisotropic, creamy-grey grains, with distinct greyish to brown bireflectance, associate closely with chalcopyrite and pyrrhotite within a weakly mineralized biotitic hornblende wehrlite. Magnetite partially replaces one grain.

One tiny grain of bismuthinite (Bi$_2$S$_3$) was observed within gangue near a pyrrhotite grain (Drill Hole K-1-87, Sample 15A).

Table 5.2a

Semi-quantitative EDS Analyses of Robust Pentlandite

Sample	AK-16-86		AK-16-86		*AK-16-86	
	At.%	Wt.%	At.%	Wt.%	At.%	Wt.%
Ni	26.12	33.40	26.91	34.43	27.17	35.80
Fe	22.06	26.83	21.59	26.28	16.08	20.16
Co	5.37	6.89	5.66	7.27	5.30	7.02
Te	0.22	0.60	N.D	N.D	N.D	N.D
S	46.24	32.29	45.83	32.02	51.44	37.02
TOTAL Wt.%		100.00		100.00		100.00

Sample	*AK-16-86		*AK-16-86	
	At.%	Wt.%	At.%	Wt.%
Ni	21.96	29.80	23.07	29.36
Fe	16.61	21.45	26.43	31.99
Co	5.18	7.06	6.10	7.79
Te	N.D	N.D	N.D	N.D
S	56.25	41.69	44.41	30.87
TOTAL Wt.%		100.00		100.00

NOTE: Analyses with an asterix (*) were taken from altered grains, sometimes partially replaced by magnetite.

N.D = Not Detected

Table 5.2b

Semi-quantitative EDS Analyses of Granular Pentlandite

Sample	K87-1 #15A		K87-1 #17		K87-1 #17	
	At.%	Wt.%	At.%	Wt.%	At.%	Wt.%
Ni	28.39	36.18	30.41	38.09	30.20	37.82
Fe	24.35	29.52	25.33	30.18	25.21	30.05
Co	2.40	3.07	2.52	3.17	2.84	3.57
S	44.86	31.22	41.75	28.56	41.75	28.56
TOTAL Wt.%		100.00		100.00		100.00

Sample	K87-1 #17		K87-1 #17	
	At.%	Wt.%	At.%	Wt.%
Ni	30.05	37.71	28.44	36.32
Fe	25.38	30.30	24.37	29.61
Co	2.52	3.17	1.99	2.56
S	42.06	28.83	45.19	31.51
TOTAL Wt.%		100.00		100.00

Table 5.2c

Semi-quantitative EDS Analyses of Pentlandite Exsolution

Flames

Sample	K87-1 #15A		K87-1 #15A	
	At.%	Wt.%	At.%	Wt.%
Ni	28.44	36.23	24.61	31.72
Fe	24.28	29.42	27.75	34.02
Co	2.48	3.18	1.22	1.58
S	44.81	31.18	46.41	32.67
TOTAL Wt.%		100.00		100.00

5.3.2 - Oxides:

Magnetite (Fe_3O_4) is the only observed opaque oxide. It occurs within all rock types, but is not common within well-mineralized rocks. It is often the dominant opaque phase within weakly mineralized rocks and occurs as both primary and secondary phases. Some magnetite appears to replace fibrous amphiboles within the Mud Lake Intrusion.

Primary magnetite occurs as: subhedral to euhedral, finely disseminated grains interstitial to silicates; subhedral to euhedral inclusions within clinopyroxene, chalcopyrite, and sometimes pyrrhotite; myrmekitic intergrowths with clinopyroxene; anhedral grains within composite sulphide grains and aggregates; and, rarely, partial or complete rims around sulphides, particularly pyrrhotite. Most grains are commonly <1 mm and usually <0.1 mm in diameter with sharp, usually straight to curved, sometimes irregular or ragged margins. Ilmenite exsolution lamellae were not observed by any optical or SEM methods.

Secondary magnetite often occurs as a progressive, sometimes complete replacement of sulphides and is the most common alteration product of pentlandite. Alteration of clinopyroxene and hornblende commonly produces a very fine dusting of magnetite. Serpentinization of olivine produces considerable disseminated and stringered magnetite, which is often remobilized along fractures within the surrounding silicates. It commonly replaces hornblende along cleavage

traces within olivine-rich ultramafic rocks.

SQ-EDS analyses (Table 5.3) detected no ilmenite exsolution nor chromium-rich spinels even though Cr and Ti are present in most grains. In contrast AKR-3-86 is apparently secondary as seen in its lack of Cr and Ti.

5.3.3 - Tellurides and Antimonides:

One tiny grain each of breithauptite, altaite, and empressite and a few grains of either hedleyite or pilsenite were encountered during examination by EDS and backscattered electron methods. All other tellurium-rich, or tellurium-bearing minerals encountered were PGM. No other antimony-rich minerals were observed.

A breithauptite (NiSb) (Table 5.4) grain 2 μm in diameter occurs within a large pyrrhotite grain in the main mineralized zone of the Kawene Intrusion (K-1-87, Sample #17). SQ-EDS analysis determined that the grain was essentially pure with no detectable trace elements.

An altaite (PbTe) grain (Table 5.4), <5 μm in diameter in contact with a small chalcopyrite grain occurs proximal to a composite pyrrhotite-pentlandite-chalcopyrite-magnetite grain (Sample AK-16-86). SQ-EDS analysis determined the additional presence of 6.10 Wt% Ag. Garuti and Rinaldi (1986) state that altaite can contain up to 9.0 Wt% Ag; however, Kissin (personal communication, 1991) states that

Table 5.3

Semi-quantitative EDS Analyses of Magnetite

Sample	AK-16-86		AK-16-86		AKR-3-86	
	At.%	Wt.%	At.%	Wt.%	At.%	Wt.%
Fe	41.58	70.41	38.28	65.44	42.86	72.36
Mn	0.00	0.00	1.08	1.81	0.00	0.00
Ti	0.16	0.24	2.07	3.03	0.00	0.00
Cr	1.00	1.57	0.93	1.48	0.00	0.00
O	57.26	27.78	57.65	28.23	57.14	27.64
Total Weight %		100.00		100.00		100.00

Table 5.4

Semi-quantitative EDS Analyses of Breithauptite, Altaite, and Empressite

Mineral	Breithauptite		Altaite		Empressite	
Sample	K87-1 #17		AK-16-86		AKR-3-86	
	At.%	Wt.%	At.%	Wt.%	At.%	Wt.%
Sb	44.04	62.01	N.D	N.D	N.D	N.D
Te	N.D	N.D	44.69	35.09	54.23	58.36
Ag	N.D	N.D	9.18	6.10	45.77	41.64
Pb	N.D	N.D	46.13	58.82	N.D	N.D
Ni	55.96	37.99	N.D	N.D	N.D	N.D
TOTAL Wt.%		100.00		100.00		100.00

N.D = Not Detected

ionic substitution of Ag into the galena-like altaite structure would be unlikely. The silver may be present as a separate telluride phase, such as hessite or empressite.

Empressite (AgTe) (Table 5.4) was observed (Sample AKR-3-86) as a 1.5 μm grain within fractured, corroded pyrrhotite enclosed by serpentinized olivine. SQ-EDS analyses indicate no detectable impurities. Hessite (AgTe$_2$) was not observed as a separate phase.

An irregular, somewhat rounded, 1.5 μm grain of bismuth telluride, possibly hedleyite (Bi$_2$Te), or pilsenite (Bi$_4$Te$_3$) occurs interstitially to clinopyroxene and amphibole in close proximity to pyrrhotite and native Bi (DDH K-1-87, Sample #15A).

5.3.4 – Sulpharsenides:

The only non-PGM sulpharsenide mineral identified was nickeliferous cobaltite, (Co,Ni)AsS. It occurs as a euhedral, 5-7 μm grain that forms an embayment within pyrrhotite (Sample AK-16-86). SQ-EDS analyses (Table 5.5) also indicate the presence of some Fe, suggesting that the mineral may be intergrown with bravoite, (Fe,Ni,Co)S$_2$).

Table 5.5

Semi-quantitative EDS Analysis of Nickeliferous Cobaltite

Sample	AK-16-86	
	At.%	Wt.%
Co	22.26	25.19
As	21.37	30.74
Ni	13.84	15.60
Fe	4.98	5.34
S	37.55	23.12
TOTAL Wt.%		100.00

5.3.5 - Platinum-Group Minerals:

Twenty-six tiny grains, each containing one or more platinum-group minerals, were identified within two diamond drill core samples from the Kawene Intrusion and one surface sample from the Eva Lake Intrusion. Seventeen grains contain single mineral phases that were identified as six separate PGM. The remaining nine grains are complex intergrowths of two or more PGM and, occasionally, non-PGE-bearing minerals or native metals, making separate mineral identification difficult or impossible. There may be as many as nine different PGM, alloys, or native metals present within the intergrowths, which will be discussed separately following the single-phase mineral descriptions.

All grains observed were <20 μm and most were <2 μm in maximum dimensions. There are many grains <500 nm in diameter that were not examined nor included within the total grain count. The very small average grain-size makes accurate quantitative analyses very difficult; therefore, the EDS analyses presented are semi-quantitative in nature. The PGM observed occur in five ways:

1) generally euhedral grains completely enclosed by sulphides (Figure 5.3a);

2) subhedral to anhedral grains occurring along fractures within sulphides (Figure 5.3b);

3) euhedral to anhedral grains located along grain boundaries;

4) subhedral to anhedral grains occurring interstitial to, or along fractures within the silicate gangue (Figure 5.3c); and

5) subhedral to euhedral grains enclosed within silicate minerals.

Hollingworthite (RhAsS) is the most abundant PGM and occurs as six subhedral, prismatic to lath-shaped, single phase grains. These grains are usually <3 μm in diameter and are in contact with the margins of, or are slightly included within, pyrrhotite, nickeliferous cobaltite, or chalcopyrite. SQ-EDS analyses show that all grains contain some Pd, three contain Ir, and two contain Pt (Table 5.6); however, the very small grain-size and subsequent spectral interference from surrounding minerals, makes it difficult to accurately determine the content of these elements. It is also impossible to determine whether the presence of these elements is due to substitution, mineral zonation or intergrowth with separate mineral phases. Back-scattered electron imagery suggests that one 2 μm grain within DDH K-1-87, Sample 17, exhibits a hint of zonation. Pd- and Pt-rich hollingworthite, such as observed here, is apparently common within the Bushveld Complex, and Ir-rich hollingworthite is common at both Noril'sk and the Bushveld Complex (Cabri, 1981).
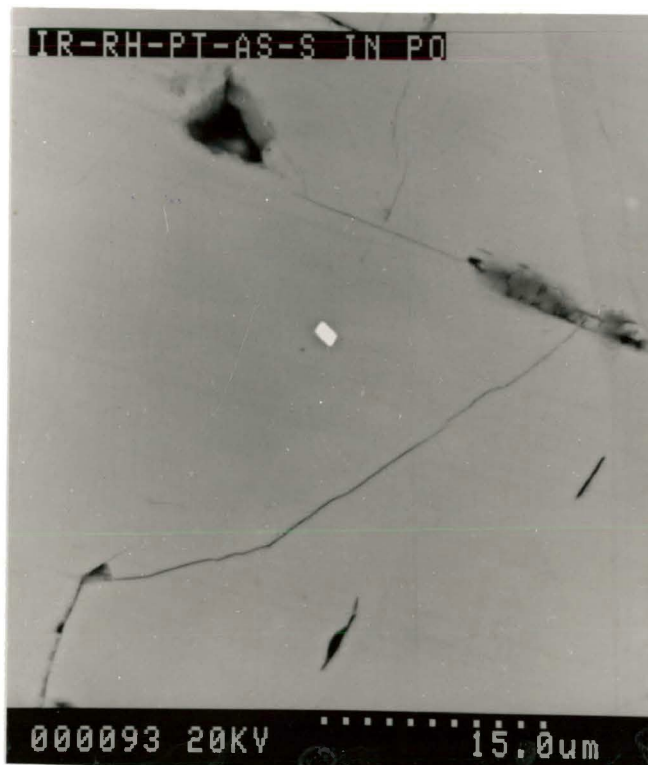
Figure 5.3a: Euhedral PGM, 1.5 μm in diameter, enclosed within pyrrhotite. Sample #15A, Drill Hole K-1-87.
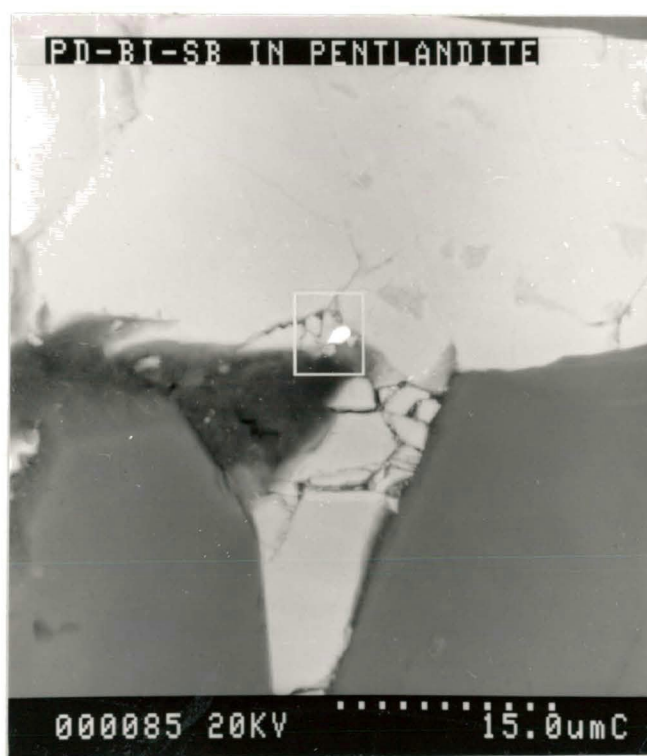
Figure 5.3b: Subhedral to anhedral PGM, 2.2 μm in diameter, occurring within fracture in pentlandite. Sample #15A, Drill Hole K-1-87.
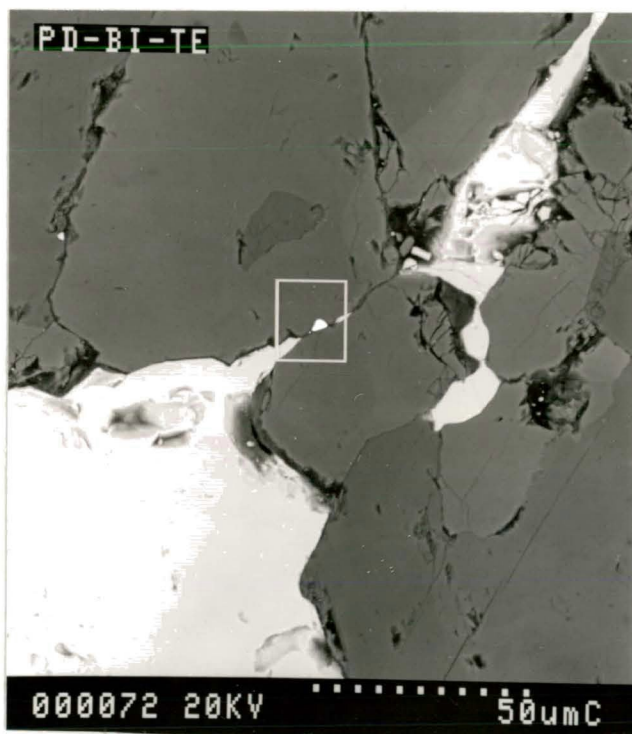
Figure 5.3c: Subhedral to anhedral PGM, about 4 μm in diameter, occurring interstitially to silicate gangue minerals near pyrrhotite. Sample #17, Drill Hole K-1-87.

Table 5.6

Representative Semi-quantitative EDS Analyses of Hollingworthite

Sample	K87-1 #17		K87-1 #17	
	At.%	Wt.%	At.%	Wt.%
Rh	14.51	25.96	21.22	33.37
Pd	2.14	3.96	2.15	3.49
Pt	N.D	N.D	0.73	2.17
Ir	N.D	N.D	1.01	2.96
Co	13.57	13.91	8.66	7.80
Fe	7.46	7.25	N.D	N.D
As	19.00	24.75	23.50	26.90
S	43.33	24.17	41.79	20.48
TOTAL Wt.%		100.00		100.00

NOTE: Sample #17(1) occurs within cobaltite.

Sample #17(2) occurs within pyrrhotite.

N.D = Not Detected

Michenerite (PdBiTe) occurs as five triangular to subround grains. These grains were classified by plotting the SQ-EDS analyses presented in Table 5.7 onto the Pd-Bi-Te ternary diagram presented in Figure 5.4. None of the minerals fall near end member compositions; however, they do tend to cluster near the michenerite end member.

Two grains occur along fractures within the gangue close to pentlandite or pyrrhotite (one is illustrated in Figure 5.3c). Two other grains occur at pyrrhotite grain margins. The fifth grain occurs at a chalcopyrite margin. Their size-range is 600 nm in diameter to 4.5 by 3 μm. SQ-EDS analyses indicate that the grains are relatively pure, but can contain small amounts of As and Fe. The Fe present within two grains (K-1-87, Sample 17) may be due to spectral contamination from adjacent pyrrhotite. Cabri (1981) states that michenerite is one of the principal Pd minerals within many Cu-Ni deposits such as those found at Sudbury, Ontario; Noril'sk, U.S.S.R; Kambalda, Western Australia; Hitura, Finland; and New Rambler, Wyoming. It has yet to be found within the Stillwater Complex, Montana and the Lac des Iles Complex, Ontario and is rare within the Merensky Reef of the Bushveld Complex, South Africa.

Four tiny grains consisting essentially of Pd and Bi were observed in Sample 17. SQ-EDS analyses of these Pd-Bi minerals (Table 5.8) were plotted on the Pd-Bi-Te ternary diagram (Figure 5.4). Two grains plot close to the froodite

Table 5.7

Representative Semi-quantitative EDS Analyses of Michenerite

Sample	K87-1 #15A		K87-1 #17		K87-1 #17	
	At.%	Wt.%	At.%	Wt.%	At.%	Wt.%
Pd	26.74	19.65	22.20	16.69	47.42	37.88
As	N.D	N.D	1.38	0.73	N.D	N.D
Bi	28.14	40.60	23.77	35.11	19.22	30.16
Fe	N.D	N.D	N.D	N.D	N.D	N.D
Te	45.12	39.75	52.64	47.47	33.36	31.96
TOTAL Wt.%		100.00		100.00		100.00

Sample	K87-1 #17		K87-1 #17	
	At.%	Wt.%	At.%	Wt.%
Pd	22.95	16.35	21.98	15.67
As	N.D	N.D	N.D	N.D
Bi	39.55	55.34	35.28	49.37
Fe	7.77	2.91	3.26	1.22
Te	29.73	25.40	39.48	33.74
TOTAL Wt.%		100.00		100.00

N.D = Not Detected

Table 5.8

Semi-quantitative EDS Analyses of Froodite, Sobolevskite, and Polarite

Mineral	Froodite		Froodite	
Sample	K87-1 #17		K87-1 #17	
	At.%	Wt.%	At.%	Wt.%
Pd	32.28	19.53	37.54	23.43
Bi	67.72	80.47	62.46	76.57
TOTAL Wt.%		100.00		100.00

Mineral	Sobolevskite		Polarite(?)	
Sample	K87-1 #17		K87-1 #17	
	At.%	Wt.%	At.%	Wt.%
Pd	47.29	31.36	15.40	15.40
Pb	N.D	N.D	24.33	47.38
S	N.D	N.D	48.82	14.77
Bi	52.71	68.64	11.45	22.50
TOTAL Wt.%		100.00		100.00

N.D = Not Detected

Pd-Bi-Te Ternary Diagram

Pd

Atomic %

● Pd-Bi-Te Minerals

○ Pd-Bi Minerals

(Sobolevskite) PdBi

Pd Te (Kotulskite)

(Froodite) PdBi$_2$

Pd Te$_2$ (Merenskyite)

X PdBiTe
(Michenerite)

Bi

Te
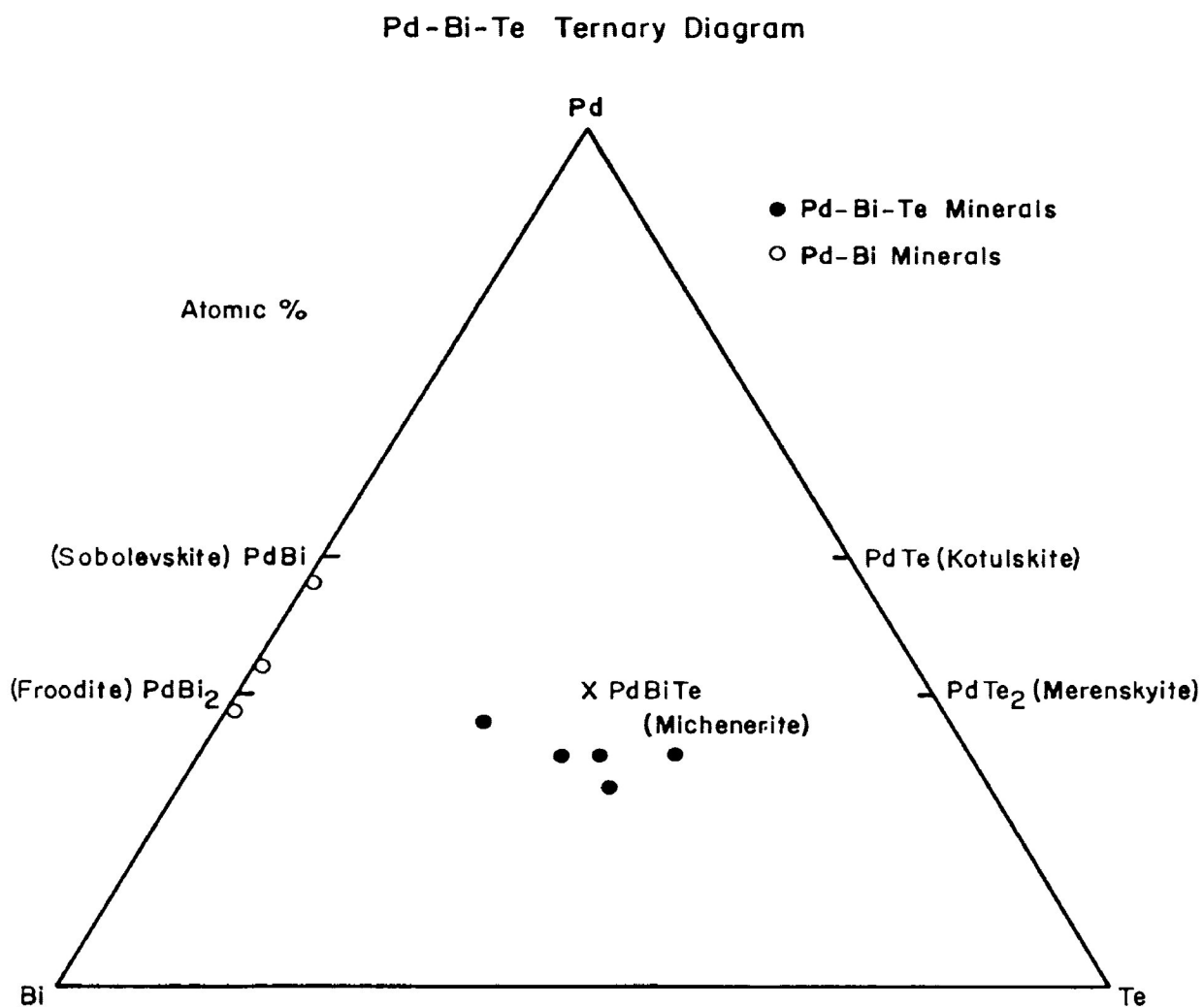
Figure 5.4: Pd-Bi-Te Ternary Diagram. All data (Atomic %) are from Tables 5.7 and 5.8. Five points cluster near the michenerite end member; 2 points very close to the froodite end member; one near the sobolevskite end member.

end member and another quite close to the sobolevskite end member. The fourth grain is very tiny and plots in the Pd-rich portion of the diagram well away from the sobolevskite end member. The accuracy of this last analysis is suspect, and it will not be discussed further.

The two froodite (PdBi$_2$) grains form inclusions within pyrrhotite about 300 nm from the grain margins. The smaller grain is indeterminant in shape and between 500 and 750 nm in diameter; however, the other grain is 1.4 μm in diameter and forms a euhedral, hexagonal grain. The two analyses seem to be relatively accurate, but spectral interference by an overlapping sulphur peak may have influenced the Bi analysis of the smaller grain. Froodite occurs as a minor PGM within numerous Cu-Ni deposits, particularly Sudbury, Ontario, and Noril'sk, U.S.S.R (Cabri, 1981).

The tentatively identified sobolevskite (PdBi) grain is <1 μm in diameter and occurs between grains of chalcopyrite and pentlandite. SQ-EDS analyses plot near the sobolevskite end-member within the Pd-Bi-Te system (Figure 5.4). A preliminary analysis, completed before data refinement, suggested the presence of considerable Pb; however, overlap with the Bi peak and spectral interference by the S peak of the hosting chalcopyrite and pentlandite, makes Pb discrimination difficult. If Pb is present this mineral might best be identified as polarite (Pd(Bi,Pb)).

Table 5.9

Semi-quantitative EDS Analysis of Pt-As Mineral (Sperrylite?)

Sample	K87-1 #17	
	At.%	Wt.%
Pt	45.49	68.77
Fe	12.66	5.48
Sb	4.01	3.78
As	37.84	21.97
TOTAL Wt.%		100.00

Sperrylite (PtAs₂) is the tentative identification of
the final single-phase grain that consists of essentially Pt
and As with subordinate Fe and Sb. This lath-shaped, 5-
sided, 5 by 3 μm grain forms an inclusion within pyrrhotite.
It is not associated with fracturing nor grain boundaries
suggesting that it formed before crystallization of the host
sulphide. SQ-EDS analyses (Table 5.9) show that there is
more Pt and less As than would be expected with a pure
sperrylite grain and it may be intergrown with one or all of
native Pt, a Pt-Fe alloy, or geversite (PtSb₂). Another
distinct possibility is that this is a non-stoichiometric
grain. Cabri (1981) states that sperrylite occurs within
every type of mineral deposit known to contain PGM.

5.3.6 - PGM Intergrowths:

Nine grains, composed of a variety of PGM, native
metals, alloys, and base metal sulphides were observed
within the three samples examined. They are usually larger
than the single-phase PGM, with a range of 800 nm to 10 μm
in diameter. One grain is 20 μm in length by 3 μm in width.
Representative SQ-EDS analyses are presented in Table 5.10.

Four intergrowths (DDH K-1-87, Sample 17) contain a
mixture of Rh-Pd-Ir-Co-As-S, and sometimes Fe, and range
from 800 nm to 10 μm in diameter. Three grains occur as
isolated inclusions within silicates, two within

Table 5.10

Semi-quantitative EDS Analyses of PGM Intergrowths

N.D = Not Detected

Sample	K87-1 #15A		K87-1 #17		K87-1 #17	
	At.%	Wt.%	At.%	Wt.%	At.%	Wt.%
Pd	38.67	30.45	2.25	3.38	1.58	2.41
Rh	N.D	N.D	21.09	30.59	25.48	37.47
Ir	N.D	N.D	7.08	19.18	5.87	16.14
Fe	N.D	N.D	N.D	N.D	4.48	3.58
Co	N.D	N.D	8.76	7.28	13.25	11.16
Ni	N.D	N.D	N.D	N.D	1.38	1.16
Bi	21.54	33.31	N.D	N.D	N.D	N.D
Te	9.11	8.60	N.D	N.D	N.D	N.D
Sb	30.68	27.64	N.D	N.D	N.D	N.D
As	N.D	N.D	20.04	21.16	37.96	17.39
S	N.D	N.D	40.77	18.42	37.96	17.39
TOTAL Wt.%		100.00		100.00		100.00

Sample	K87-1 #17		K87-1 #17		AKR-3-86	
	At.%	Wt.%	At.%	Wt.%	At.%	Wt.%
Pd	2.54	3.27	5.21	8.50	15.46	8.56
Rh	16.52	20.53	17.94	28.31	N.D	N.D
Ir	7.42	17.23	2.80	8.26	N.D	N.D
Pt	1.96	4.61	N.D	N.D	7.33	7.44
Fe	N.D	N.D	7.26	6.22	N.D	N.D
Co	N.D	N.D	24.38	22.04	N.D	N.D
Ni	N.D	N.D	3.24	2.92	N.D	N.D
Bi	N.D	N.D	N.D	N.D	77.21	84.00
As	18.77	16.98	6.83	7.85	N.D	N.D
S	44.18	17.11	32.34	15.91	N.D	N.D
TOTAL Wt.%		100.00		100.00		100.00

clinopyroxene, and one within titanite. The fourth grain occurs within the gangue but in direct contact with pyrrhotite. Grain shapes range from subhedral to euhedral. The dominant PGE is Rh, followed by Pd, and highly variable amounts of Ir. Cobalt appears to substitute directly within the PGM and does not occur as cobaltite inclusions. The dominant phases within the intergrowths appear to be sulphides and sulpharsenides, with the sulphides the most abundant.

A fifth intergrowth, similar to those just described, contains significant Pt, possibly as sperrylite. This subhedral to subround, four-sided grain is about 2 μm in diameter, and occurs between silicate minerals less than 5 μm from a pyrrhotite grain.

A complex Ir-Pt-Rh-As-S intergrowth occurs in Sample 15A as an isolated, euhedral, rhomb-shaped inclusion within pyrrhotite (Figure 5.3a). This 1.5 μm in diameter grain, does not occur near a grain margin, nor is not associated with any fractures suggesting formation before the crystallization of the host grain. SQ-EDS analyses detected considerable quantities of Ir, appreciable Pt and Rh, and subordinate As. The actual S-content is masked by spectral interference from the host pyrrhotite. There is much less As than would be expected if this grain were purely irarsite (IrAsS); however, some discrete irarsite may be present and intergrown with native iridium or platiniridium and,

possibly, hollingworthite.

A 1.5 μm diameter <u>Pd-Bi-Te-Sb</u> mixture occurs within pentlandite in Sample 15A. This teardrop-shaped grain occurs within a fracture adjacent to an altered portion of the pentlandite grain. It gave a relatively clean SQ-EDS analysis with a small amount of scatter from the host-mineral. Much of the grain may be sudburyite (PdSb), possibly intergrown with michenerite and froodite.

The final intergrowth, composed of <u>Pt-Pd-Bi</u>, occurs within serpentinized olivine (Sample AKR-3-86) closely associated with a cluster of nickel-rich, native bismuth grains. This 20 by 3 μm grain is sabre-shaped, completely surrounded by serpentine, and approximately 10 μm from a narrow magnetite veinlet (Figure 5.5). The constituents of this grain may be native Bi, froodite, and insizwaite ($PtBi_2$).

5.3.7 - Alloys and Native Metals:

Four alloys and three native metals were observed in the three PGM-bearing samples examined. One grain is contained within pentlandite; the other fourteen grains occur as isolated single grains or loose clusters within the gangue. Most of the grains occur in close association or in contact with secondary magnetite within serpentinized olivine or uralitized clinopyroxene. This strongly suggests that many of the grains, particularly the native metals,
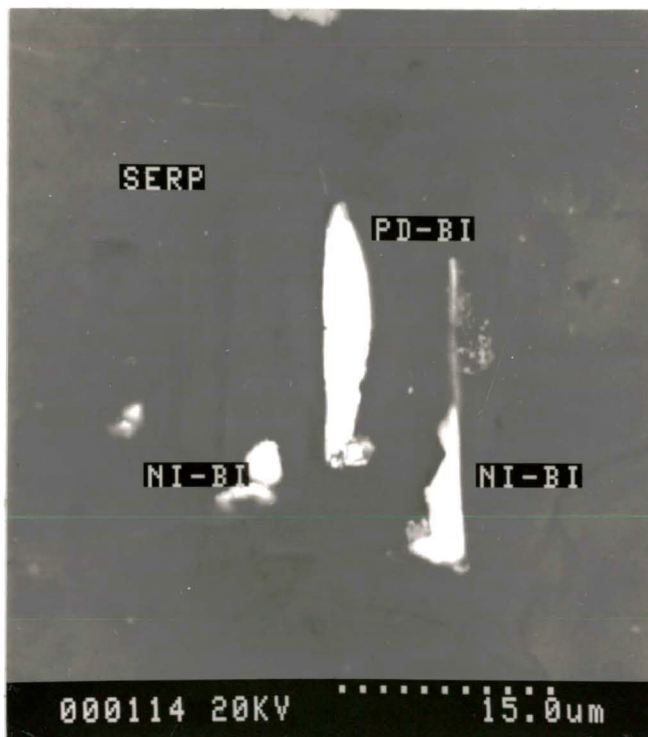
Figure 5.5: Pt-Pd-Bi mineral associated with a Ni-Bi alloy cluster within serpentine gangue; grain is labelled Pd-Bi in the photo. Sample AKR-3-86.
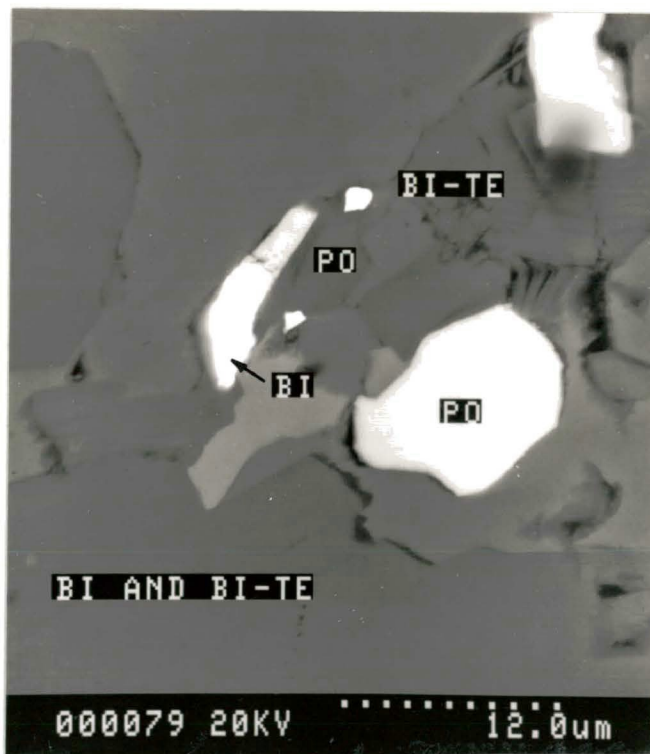
Figure 5.6: Native Bi and Bi-Te alloy grains within silicate gangue in close association with sulphides. Sample #15A, Drill Hole K-1-87.

were formed during the alteration process. Owing to the small size of many of the grains, it is unlikely that these analyses are accurate and can only be used as a guide to their actual composition. Representative SQ-EDS analyses are presented in Table 5.11.

The most common native metal is <u>bismuth</u> (Figure 5.6). Eight of the nine Bi grains observed occur within altered olivine or clinopyroxene. Many are roughly lath-shaped, between 1 and 7 μm in length, and contain small amounts of Pt and sometimes Pb. One grain (DDH K87-1, Sample 15A) occurs within pentlandite, appears to contain more Pt than usual, and may be intimately intergrown with insizwaite ($PtBi_2$). A Pb- and Fe-bearing <u>antimony</u> grain was observed within the gangue near a pyrrhotite grain, and a Pb-bearing <u>silver</u> grain occurs within an altered clinopyroxene in K87-1 Sample 15A.

The four alloys observed are all <5 μm in diameter and individually quite different. Two Bi-rich grains (Sample AKR-86-3) are in contact with magnetite within altered olivine. One is a mixture of Ag, Hg, Au, and Bi, while the other consists of S, Ni, and Bi. A third alloy (K87-1, Sample 17) is composed of Ag and Cd, occurs within altered clinopyroxene, and may contain a small amount of As and S. The fourth alloy is an Ir-bearing, Pd-rich, native Au grain within pyrrhotite.

Table 5.11

Semi-quantitative EDS Analyses of Alloys

Sample	K87-1 #17		AKR-3-86		AKR-3-86	
Alloy	Pd-Au		Ni-Bi(S)		Au-Ag-Bi	
	At.%	Wt.%	At.%	Wt.%	At.%	Wt.%
Pd	15.66	9.12	N.D	N.D	N.D	N.D
Ir	2.76	2.90	N.D	N.D	N.D	N.D
Au	81.58	87.97	N.D	N.D	44.79	47.08
Ag	N.D	N.D	0.79	0.93	16.05	9.24
Ni	N.D	N.D	54.70	35.09	N.D	N.D
Bi	N.D	N.D	25.03	57.15	39.16	43.68
S	N.D	N.D	19.48	6.83	N.D	N.D
TOTAL Wt.%		100.00		100.00		100.00

N.D = Not Detected

5.4: PGE and Base Metals Geochemistry - Mineralized Zones

This section will deal with the trace element geochemistry of base and precious metals present within the mineralized zones of the Quetico Intrusions and how they compare with other platinum-bearing intrusions. All samples were analyzed for Cu, Ni, Au, Co, Pt, and Pd. Selected Pt- and Pd-rich samples were also analyzed for the complete platinum-group. Analytical results of samples taken from the mineralized zones and their Pt:Pd, Cu:Cu+Ni, Pt:Pt+Pd, and Pd:Ir ratios (where applicable), are presented in Table 5.12. These data are expressed in ppm for the base metals and ppb for the precious metals. All ratios presented are calculated from the results presented in Table 5.12.

It has become common practice to recalculate Cu, Ni, Au, and PGE values to 100% sulphides (Hoffman et al., 1979; Naldrett, 1981); but Rowell (1984) postulated that this recalculation might prove to be meaningless in deposits where there is a hydrothermal component or a low overall sulphide content, since it would progressively inflate PGE- and Au-values as the sulphide content decreases. Barnes (1987) concurs and suggests that the assumptions involved in this calculation render it invalid for some rock types. To avoid these pitfalls some workers, including this author, prefer to use the base and precious metal concentrations present within the rock without the recalculation to 100% sulphides.

Table 5.12

Trace Element Geochemistry - Mineralized Zones

Sample Number	Cu ppm	Ni ppm	Co ppm	Pt ppb	Pd ppb	Rh ppb	Ru ppb	Ir ppb	Os ppb	Au ppb	Cu:Cu+Ni	Pt:Pt+Pd	Pd:Ir	Pt:Pd
AK-3-84	2060	2480	234	240	550	--	--	--	--	--	0.454	0.304	--	0.436
	--	--	--	190	570	55	BDL	23	3	14	--	0.25	24.8	0.333
AK-4-84	12600	1320	134	750	1100	--	--	--	--	--	0.905	0.405	--	0.682
	--	--	--	630	1200	17	BDL	7.7	3	34	--	0.344	155.8	0.525
AK-5-84	1650	490	68	460	280	--	--	--	--	--	0.771	0.623	--	1.643
	--	--	--	460	410	15	BDL	6.5	3	11	--	0.529	63.1	1.122
AK-6-84	1370	840	96	230	260	--	--	--	--	--	0.62	0.469	--	0.885
	--	--	--	270	280	5	BDL	2.4	BDL	18	--	0.491	116.7	0.964
AK-8-84	4500	2160	192	1100	1000	--	--	--	--	--	0.676	0.524	--	1.1
	--	--	--	1100	920	110	BDL	39	4	25	--	0.545	23.6	1.196
AK-9-84	2070	660	72	440	320	--	--	--	--	--	0.758	0.579	--	1.375
	--	--	--	380	430	10	23	4.7	BDL	460	--	0.469	91.4	0.884
AK-1-86	870	550	83	185	410	--	--	--	--	5	0.613	0.311	--	0.451
AK-2-86	2780	515	67	340	600	--	--	--	--	17	0.844	0.362	--	0.567
	--	--	--	410	730	15	BDL	6.9	BDL	8	--	0.36	105.8	0.562
AK-3-86	4300	1330	126	805	530	--	--	--	--	28	0.764	0.603	--	1.519
	--	--	--	610	550	4	BDL	2.1	BDL	11	--	0.523	261.9	1.109
AK-4-86	2700	1000	98	265	350	--	--	--	--	13	0.73	0.431	--	0.757
	--	--	--	270	380	14	BDL	6.8	BDL	8	--	0.415	55.9	0.711
AK-5-86	3020	315	43	465	360	--	--	--	--	190	0.906	0.564	--	1.292
	--	--	--	450	370	2	BDL	1.2	BDL	170	--	0.549	308.3	1.216
AK-6-86	1680	640	78	170	135	--	--	--	--	10	0.724	0.557	--	1.259
	--	--	--	210	160	5	BDL	2	BDL	6	--	0.568	80	1.313
AK-7-86	9300	1870	375	69	360	--	--	--	--	21	0.833	0.161	--	0.192
AK-8-86	10700	1960	410	63	260	--	--	--	--	18	0.845	0.195	--	0.242

Table 5.12

Table 5.12

Trace Element Geochemistry - Mineralized Zones

Sample Number	Cu ppm	Ni ppm	Co ppm	Pt ppb	Pd ppb	Rh ppb	Ru ppb	Ir ppb	Os ppb	Au ppb	Cu:Cu+Ni	Pt:Pt+Pd	Pd:Ir	Pt:Pd
AK-9-86	2660	980	88	315	340	--	--	--	--	7	0.731	0.481	--	0.926
	--	--	--	340	410	6	BDL	2.4	BDL	5	--	0.453	170.8	0.829
AK-10-86	3720	850	85	520	525	--	--	--	--	18	0.814	0.498	--	0.991
	--	--	--	290	620	7	BDL	4.1	BDL	11	--	0.319	151.2	0.468
AK-11-86	4720	605	85	600	525	--	--	--	--	33	0.886	0.533	--	1.143
	--	--	--	560	560	2	BDL	1	BDL	45	--	0.5	560	1
AK-12-86	355	245	46	165	78	--	--	--	--	38	0.592	0.679	--	2.115
AK-13-86	810	485	58	135	130	--	--	--	--	30	0.625	0.509	--	1.038
AK-16-86	300	382	76	50	55	--	--	--	--	12	0.44	0.476	--	0.909
AK-27-86	1600	570	84	395	325	--	--	--	--	84	0.737	0.549	--	1.215
AK-29-86	530	460	80	94	40	--	--	--	--	27	0.535	0.701	--	2.35
K86-1-12	702	123	15	41	83	--	--	--	--	28	0.851	0.331	--	0.494
K86-1-13	8460	1410	76	756	551	--	--	--	--	50	0.857	0.578	--	1.372
K86-1-15	7330	4450	258	905	2397	--	--	--	--	41	0.622	0.274	--	0.378
K86-1-16	13200	2710	139	666	1330	--	--	--	--	32	0.83	0.334	--	0.501
K86-1-17	5860	3610	193	649	1190	--	--	--	--	18	0.619	0.353	--	0.545
K86-1-18	716	137	14	26	86	--	--	--	--	5	0.839	0.232	--	0.302
K86-1-20	61	157	19	20	65	--	--	--	--	4	0.796	0.235	--	0.308
K86-1-20.5	2245	548	42	603	250	--	--	--	--	79	0.804	0.707	--	2.412
K86-1-22	1355	614	68	119	195	--	--	--	--	9	0.688	0.556	--	1.253
K86-1-23	1325	668	66	103	127	--	--	--	--	6	0.665	0.448	--	0.811
K86-1-24	791	352	38	38	33	--	--	--	--	1	0.692	0.535	--	1.152
K86-1-27	1845	958	79	603	250	--	--	--	--	79	0.658	0.707	--	2.412
K86-1-28	2820	1340	83	286	435	--	--	--	--	55	0.678	0.397	--	0.657
K86-1-29	1605	734	54	206	203	--	--	--	--	31	0.686	0.504	--	1.015
K86-1-30	681	337	43	52	50	--	--	--	--	18	0.669	0.51	--	1.04

Table 5.12 (Cont'd)

Table 5.12

Trace Element Geochemistry - Mineralized Zones

Sample Number	Cu ppm	Ni ppm	Co ppm	Pt ppb	Pd ppb	Rh ppb	Ru ppb	Ir ppb	Os ppb	Au ppb	Cu:Cu+Ni	Pt:Pt+Pd	Pd:Ir	Pt:Pd
K86-1-31	1780	543	38	205	126	--	--	--	--	11	0.766	0.619	--	1.627
K86-1-33	1820	690	53	159	207	--	--	--	--	20	0.725	0.434	--	0.768
K86-1-34	1100	460	45	89	117	--	--	--	--	8	0.705	0.432	--	0.761
K86-1-35	2185	836	69	151	163	--	--	--	--	58	0.723	0.481	--	0.926
AAb-6-84	6040	780	54	260	430	2	BDL	0.8	BDL	36	0.886	0.377	537.5	0.605
AAb-7-84	2700	580	48	720	310	3	BDL	1.9	BDL	45	0.823	0.699	163.2	2.322
AAb-8-84	2660	600	56	55	8	2	BDL	0.7	BDL	49	0.816	0.873	11.4	6.875
AAb-2-85	6200	1450	96	85	45	--	--	--	--	17	0.81	0.654	--	1.889
AAb-7-85	3350	785	44	90	830	--	--	--	--	20	0.81	0.098	--	0.108
	--	--	--	135	650	3	BDL	8.4	BDL	13	--	0.172	98.8	0.208
AAb-9-85	5700	640	50	90	500	--	--	--	--	--	0.899	0.153	--	0.18
	--	--	--	420	425	3	BDL	7.2	BDL	37	--	0.497	69.4	0.988
AAb-10-85	20400	700	46	180	530	--	--	--	--	70	0.967	0.253	--	0.339
	--	--	--	240	610	6	BDL	1.9	BDL	82	--	0.282	321.1	0.393
AAb-12-85	4850	2440	205	82	65	--	--	--	--	17	0.665	0.558	--	1.262
AAb-19-85	385	116	20	310	260	--	--	--	--	65	0.463	0.544	--	1.192
	--	--	--	285	210	1	BDL	1.4	BDL	57	--	0.576	185.7	1.357
AAb-24-85	4080	1150	92	240	320	--	--	--	--	23	0.78	0.429	--	0.75
	--	--	--	300	290	3	BDL	1.9	BDL	6	--	0.508	168.4	1.034
API-1-84	10900	2060	--	270	165	--	--	--	--	140	0.841	0.621	--	1.636
	--	--	--	250	140	1	BDL	0.6	3	86	--	0.641	23.3	1.786
API-2-84	15600	250	--	270	420	--	--	--	--	165	0.984	0.391	--	0.643
	--	--	--	300	540	1	17	0.8	BDL	92	--	0.357	67.5	0.556

Table 5.12 (Cont'd)

177

Table 5.12

Trace Element Geochemistry - Mineralized Zones

Sample Number	Cu ppm	Ni ppm	Co ppm	Pt ppb	Pd ppb	Rh ppb	Ru ppb	Ir ppb	Os ppb	Au ppb	Cu:Cu+Ni	Pt:Pt+Pd	Pd:Ir	Pt:Pd
AWS-1-85	6200	3160	--	230	100	--	--	--	--	90	0.662	0.697	--	2.3
	--	--	--	310	110	2	BDL	1.4	BDL	61	--	0.738	78.6	2.818
AWS-3-85	3100	220	--	290	70	--	--	--	--	50	0.934	0.806	--	4.14
	--	--	--	470	75	24	10	15.4	BDL	40	--	0.862	4.2	6.267
AWS-4-85	44000	730	--	185	125	--	--	--	--	250	0.984	0.597	--	1.48
	--	--	--	170	110	22	5	12.9	BDL	140	--	0.607	8.4	1.545
AWS-5-85	5120	2500	--	440	85	--	--	--	--	185	0.672	0.838	--	5.176
	--	--	--	160	90	2	BDL	1.3	BDL	160	--	0.64	69.2	1.778
ACP-1-86	6300	1580	100	1550	1020	--	--	--	--	530	0.799	0.603	--	1.52
	--	--	--	1200	1300	38	BDL	22.9	BDL	560	--	0.542	56.8	0.923
ACP-3-86	3920	1120	92	1020	1050	--	--	--	--	330	0.778	0.493	--	0.971
	--	--	--	1200	1300	33	BDL	19.1	BDL	360	--	0.486	67.9	0.923
ACP-5-86	745	445	82	130	90	--	--	--	--	40	0.626	0.591	--	1.444
	--	--	--	150	90	3	BDL	1.7	BDL	31	--	0.625	52.9	-1.667
AM-2-85	3700	920	80	33	60	--	--	--	--	8	0.801	0.355	--	0.55
AM-5-85	5800	320	60	30	17	--	--	--	--	7	0.948	0.638	--	1.765
AM-9-85	34500	690	--	95	115	--	--	--	--	--	0.98	0.452	--	0.826
AWM-1-86	17200	2020	--	65	50	--	--	--	--	--	0.895	0.565	--	1.3
	--	--	--	30	70	1	BDL	0.9	BDL	7	--	0.3	77.8	0.429
AWM-2-86	51200	2520	--	9	525	--	--	--	--	--	0.953	0.017	--	0.017
	--	--	--	21	400	2	BDL	3.5	BDL	13	--	0.031	114.3	0.053
AKR-3-86	12900	3940	210	630	760	--	--	--	--	730	0.766	0.453	--	0.829
AKR-4-86	8400	2620	152	225	840	--	--	--	--	430	0.762	0.211	--	0.268

Table 5.12 (Cont'd)

5.4.1 - Copper, Nickel, Platinum, and Palladium:

Copper is the most abundant base metal present within the mineralized zones and generally increases in abundance at a faster rate than Ni as the overall sulphide content increases. Cu:Cu+Ni ratios are almost always greater than 0.5 and usually greater than 0.6, with 81% of the samples falling between 0.6 and 0.9 (Table 5.12). Samples with ratios less than 0.6 tend to be the least mineralized, whereas those with greater than 0.9 usually contain the most sulphides.

Further evidence of the dominance of copper within the mineralized zones of the Quetico Intrusions is presented in Figure 5.7. This diagram clearly illustrates that Cu is the dominant component within the Cu-Ni-Co ternary system, and the ratios produce a markedly linear progression within the Cu-rich field.

The average Pt:Pd ratio of the mineralized zones of the Kawene, Abiwin, Chief Peter, and Plateau Intrusions is 1.53:1, with individual ratios of 0.96, 1.30, 1.37, and 2.50, respectively; and ranges of 0.11-2.41, 0.11-6.88, 0.92-2.17, and 0.59-6.26, respectively (Table 5.12; Figure 5.8). Pt:Pt+Pd ratios range from 0.096-0.913 with 64% of the samples falling between 0.3 and 0.6 (Table 5.12). There is a positive relationship between Pt and Pd, i.e. as the Pt content increases so does the Pd content.

Cu-Ni-Co Ternary diagram
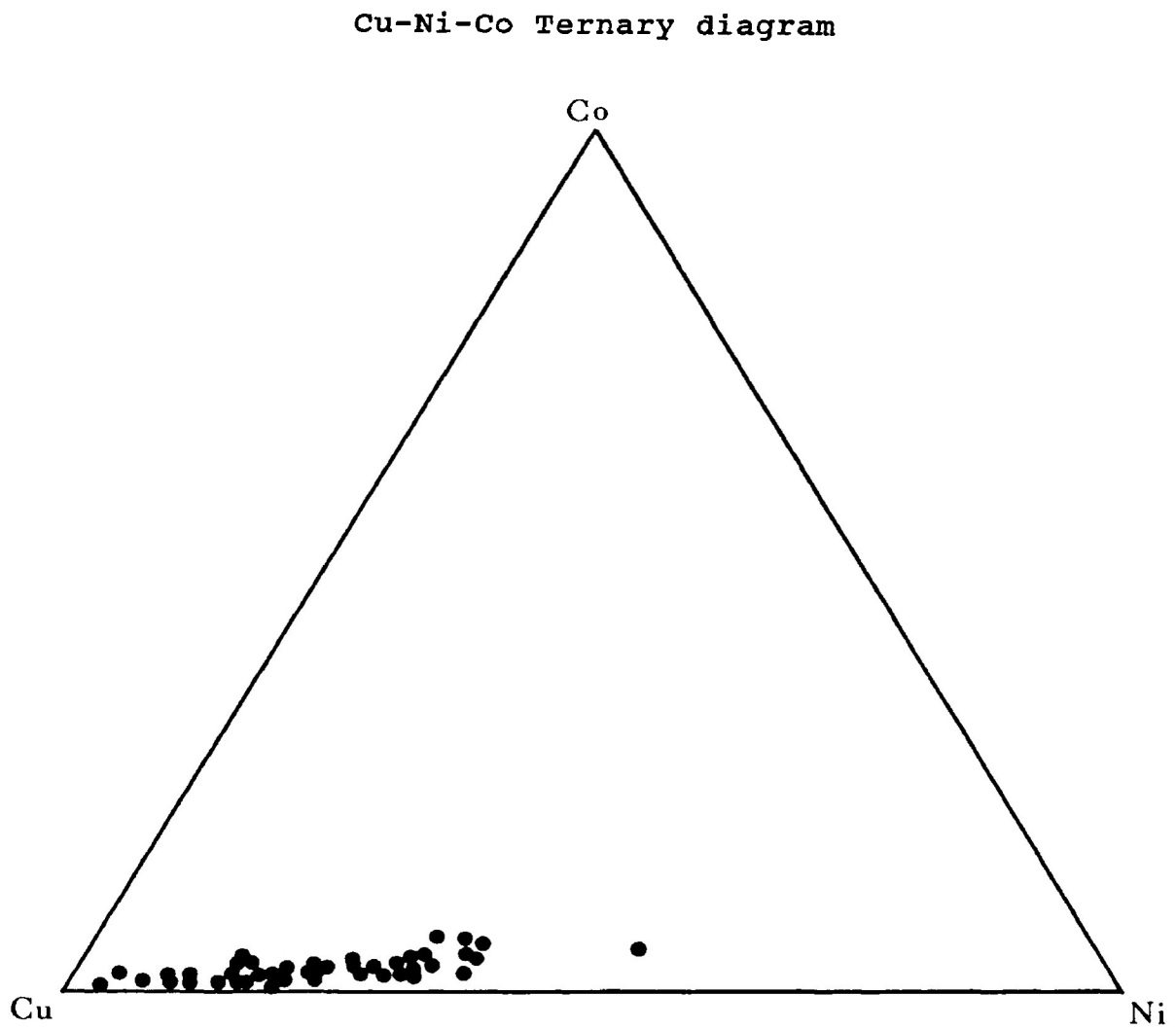
Figure 5.7: Cu-Ni-Co Ternary Diagram. Analytical data are all from Table 5.12 and illustrate the Cu-rich nature of the mineralized zones when compared to Ni and Co.

Plot of Pt/Pd Ratios for PGE-bearing Samples
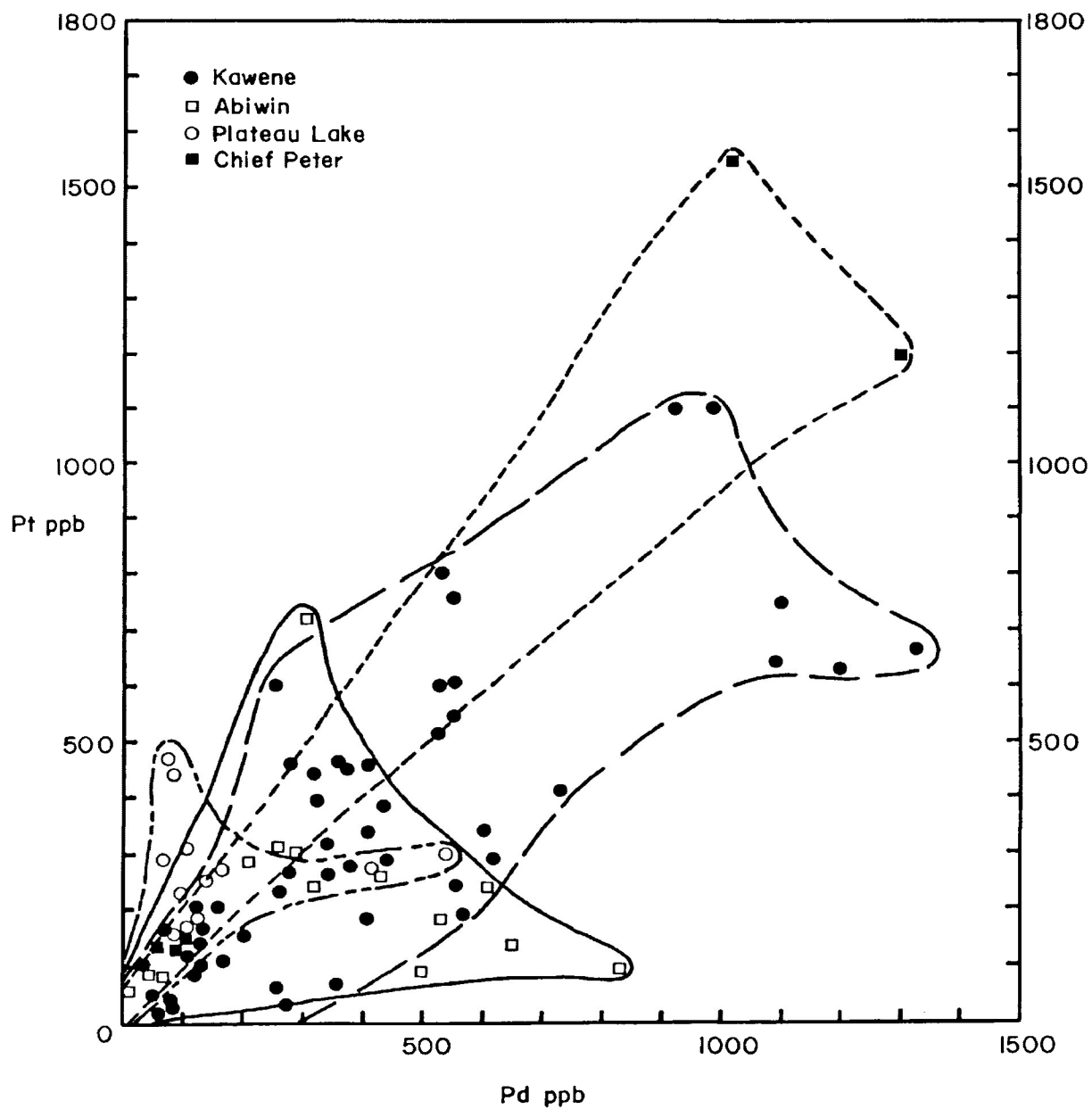
Figure 5.8: Plot of the ratio of Pt/Pd for PGE-bearing samples. Note the positive relationship between Pt and Pd and the considerable scatter evident within the Abiwin Intrusion data.

5.4.2 - Cu and Ni vs. Pt and Pd:

Plots of Pt/Cu, Pt/Ni, Pd/Cu, and Pd/Ni (Figures 5.9 and 5.10, respectively) are used to show the correlation between Cu, Ni, and the two PGE. There is a mainly positive correlation between Cu, Ni and Pt within the Kawene Intrusion and a similar, apparent correlation within the Chief Peter Intrusion. The Kawene Pt/Cu curve exhibits a steep positive slope that changes to a moderate negative slope at a Cu concentration of 0.6-0.7%. The Pt/Ni data are more scattered than the copper data, but they also exhibit a steep positive slope that eventually flattens at a concentration of 2200-2400 ppm. Similar relationships are present in the Pd/Cu and Pd/Ni data, but the flattening of the slope is either absent (Pd/Cu) or much less pronounced (Pd/Ni). The Kawene data are relatively well-defined but do exhibit some diffusion possibly due to deuteric and/or metamorphic alteration processes.

The data sets for the Abiwin Intrusion produce fields that partially overlap the Kawene fields, but the points are quite scattered. A hint of an original Kawene-like curve is present. It is probable that the injection of the lit-par-lit migmatites that envelop and disrupt the intrusion may have modified any original pattern.

Data from the Mud Lake Intrusion exhibit only marginally anomalous Pt and Pd concentrations that are too widely scattered to be useful. Data from the Eva Lake and
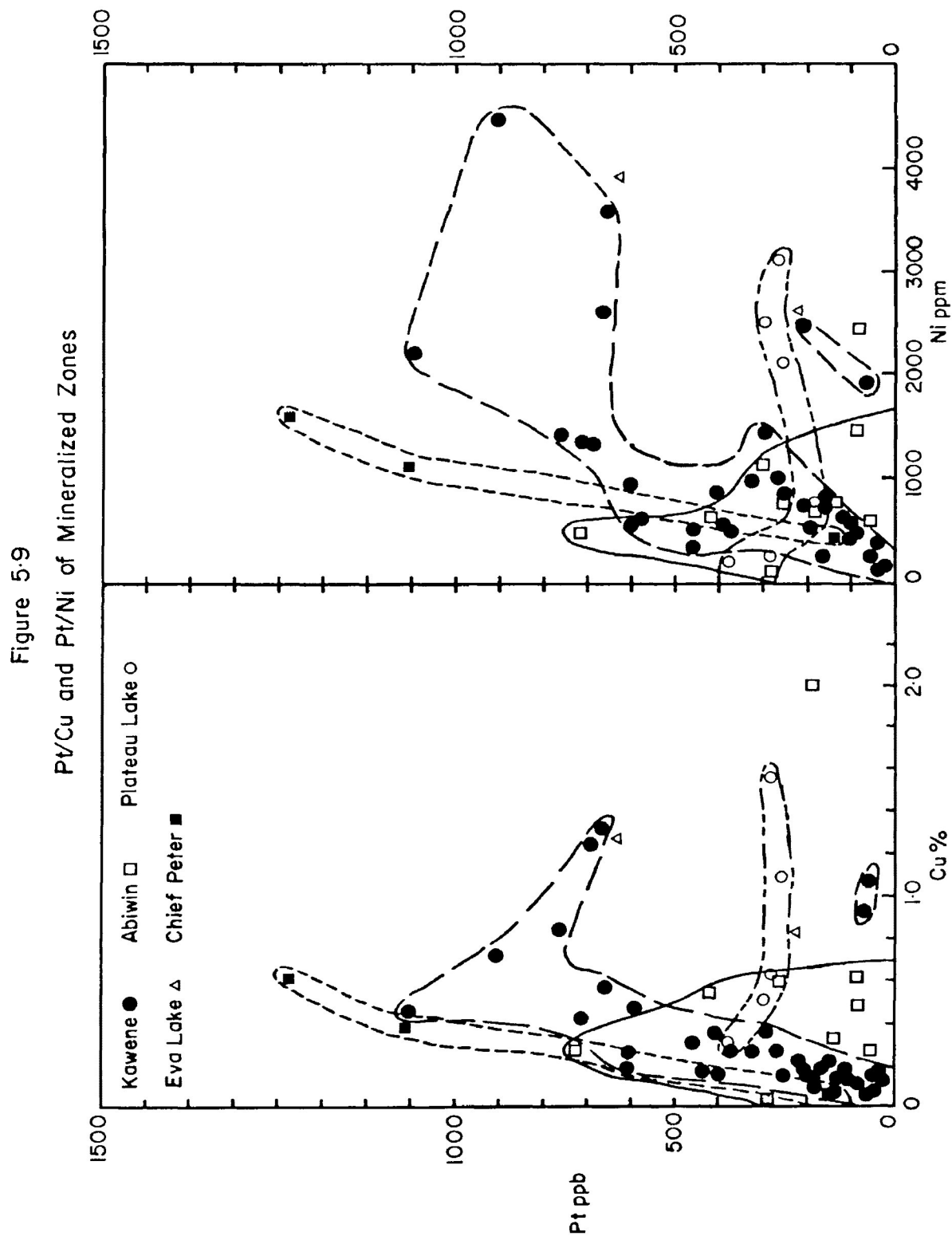
Figure 5.9: Plot of the Pt/Cu and Pt/Ni ratios of the mineralized zones. Positive relationship is evident for most of the fields.

Figure 5·10

Pd/Cu and Pd/Ni of Mineralized Zones

● Kawene
□ Abiwin
○ Plateau Lake
△ Eva Lake
■ Chief Peter
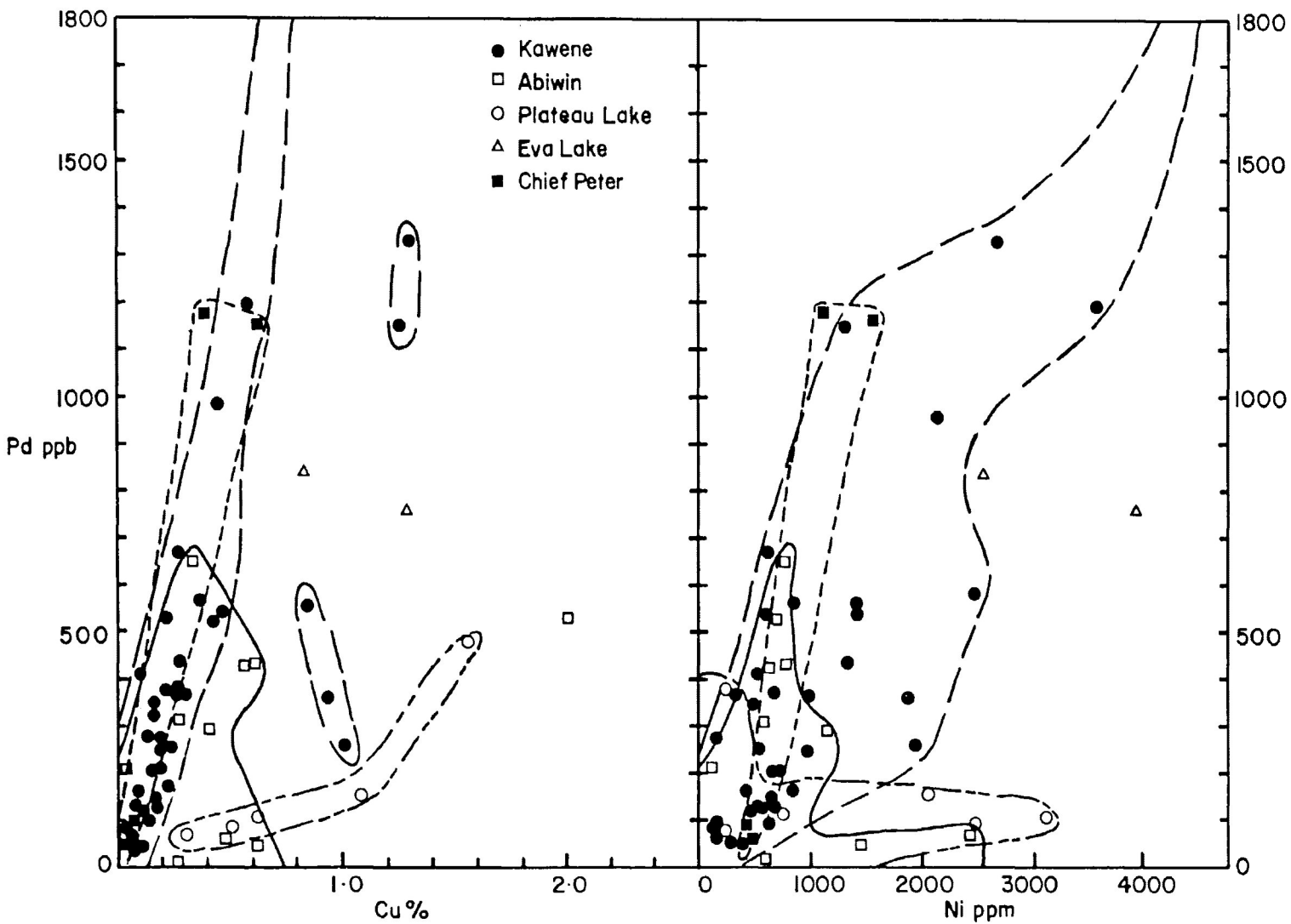
Figure 5.10: Plot of the Pd/Cu and Pd/Ni ratios of the mineralized zones. Note the positive and linear nature of most of the fields.

184

Plateau Lake Intrusions, while highly anomalous in base and precious metals, contain too few data points to allow meaningful interpretations.

5.4.3 - Pt:Pt+Pd vs. Cu:Cu+Ni:

The use of Pt:Pt+Pd/Cu:Cu+Ni ratios has become an important tool in classifying PGE deposits (Naldrett et al., 1980) when the data is compared to other deposits.

Figure 5.11 shows a large amount of scatter in the Quetico data, but it also shows that much of the data, particularly that from the Kawene Intrusion, cluster in the region between the tholeiitic and the Rathbun Lake fields. All deposits that plot within the tholeiitic field are thought to be of magmatic origin. The Rathbun Lake Deposit is hosted by a tholeiitic intrusion, but its ratios plot well away from the tholeiitic field. Rowell (1984) believes that this may reflect a genetic difference due to a postulated hydrothermal, rather than magmatic, origin of the Rathbun Lake Deposit. There is no evidence that the Quetico PGE distributions are due to hydrothermal processes; however, the data may reflect the suspected calc-alkaline nature of the intrusions possibly modified by the effects of late stage deuteric alteration and regional metamorphism. There are few data of this nature from PGE-bearing alkaline or calc-alkaline intrusions that can be used as comparison with the Quetico data.
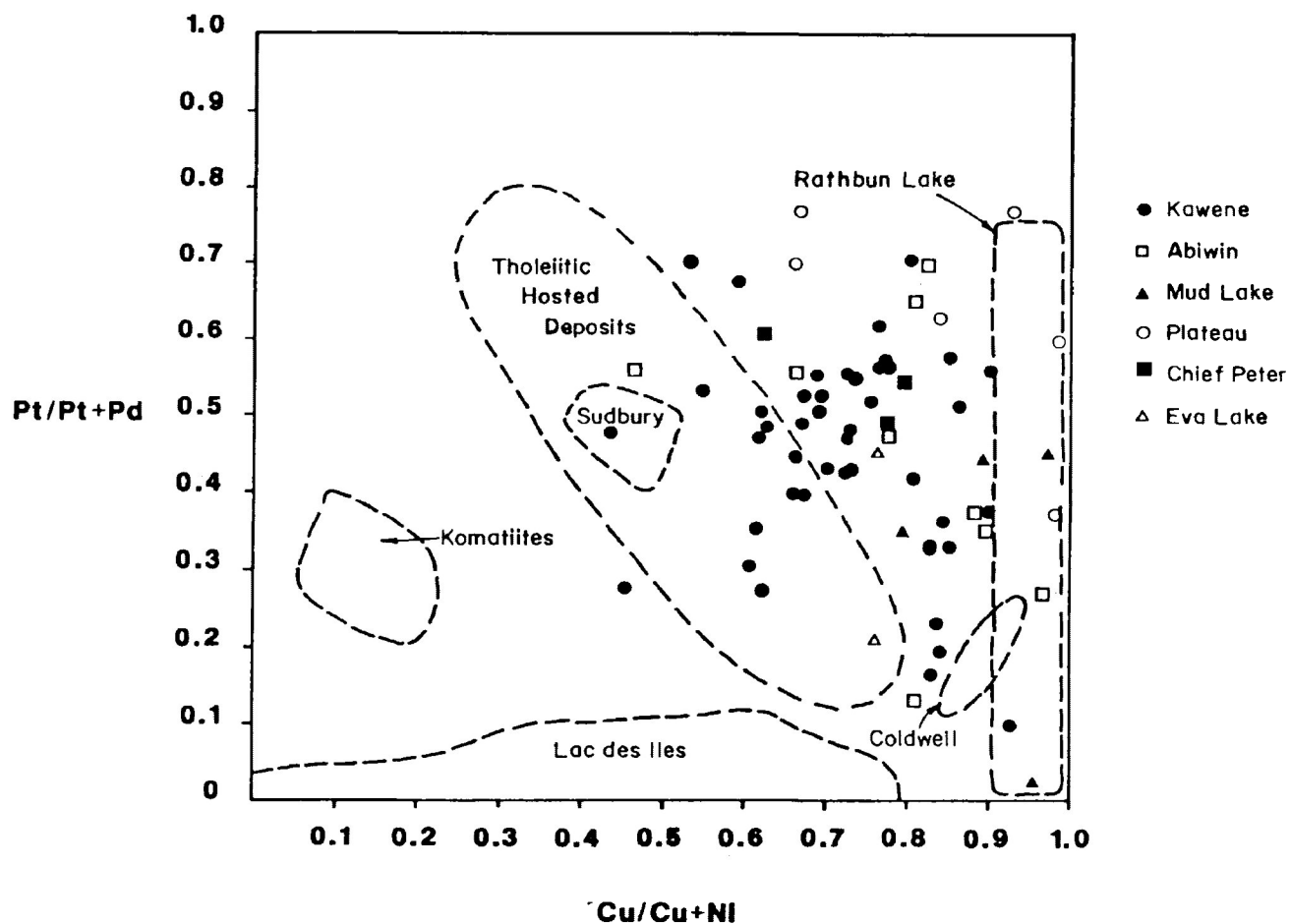
Figure 5.11: Plot of Pt/(Pt+Pd) vs Cu/(Cu+Ni). There is a large amount of scatter in the Quetico data; however, much of the data does appear to cluster between the tholeiitic and Rathbun Lake Fields. Data points are taken from Table 5.12. Field boundaries are from Naldrett et al. (1980, Rowell (1984), Talkington and Watkinson (1984), Sutcliffe et al. (1989); Watkinson et al. (1983).

5.4.4 - Pd/Ir Ratios:

Keays et al. (1982) state that the ratio of palladium to iridium is a function of the degree of fractionation. Barnes et al. (1985) generalized that primitive rock types exhibit lower Pd/Ir ratios than do the more fractionated rock types, and work by Barnes and Naldrett (1986) on PGE concentrations within the Alexo Mine komatiite showed that Pd/Ir ratios may be useful in classifying metamorphosed mafic and ultramafic rocks so long as the ratio has not been subsequently modified.

Pd/Ir ratios from the Quetico Intrusions exhibit an extremely wide range of 4.2 to 560.0 (Table 5.12), an overall average of 132.12, and a mean of 80.0. Figure 5.12 shows that most of the values form a positive, but fairly diffuse trend, suggesting an original magmatic trend that has been modified by later deuteric and/or metamorphic processes. Keays et al. (1982) state that, in a magmatic environment, Ir and Pd increase in a more or less linear manner with increasing Ni content. This may be illustrated in the Pd:Ni diagram (Figure 5.10) for the Quetico Intrusions. The somewhat erratic nature of some of the Quetico Pd/Ir data may be explained by Keays et al. (1981), who stated that the fairly erratic metal contents within many magmatically-derived deposits can be accounted for in terms of sulphide-melt fractionation of the metals during initial cooling and subsequent metamorphism and deformation.

Pd/Ir of Mineralized Samples
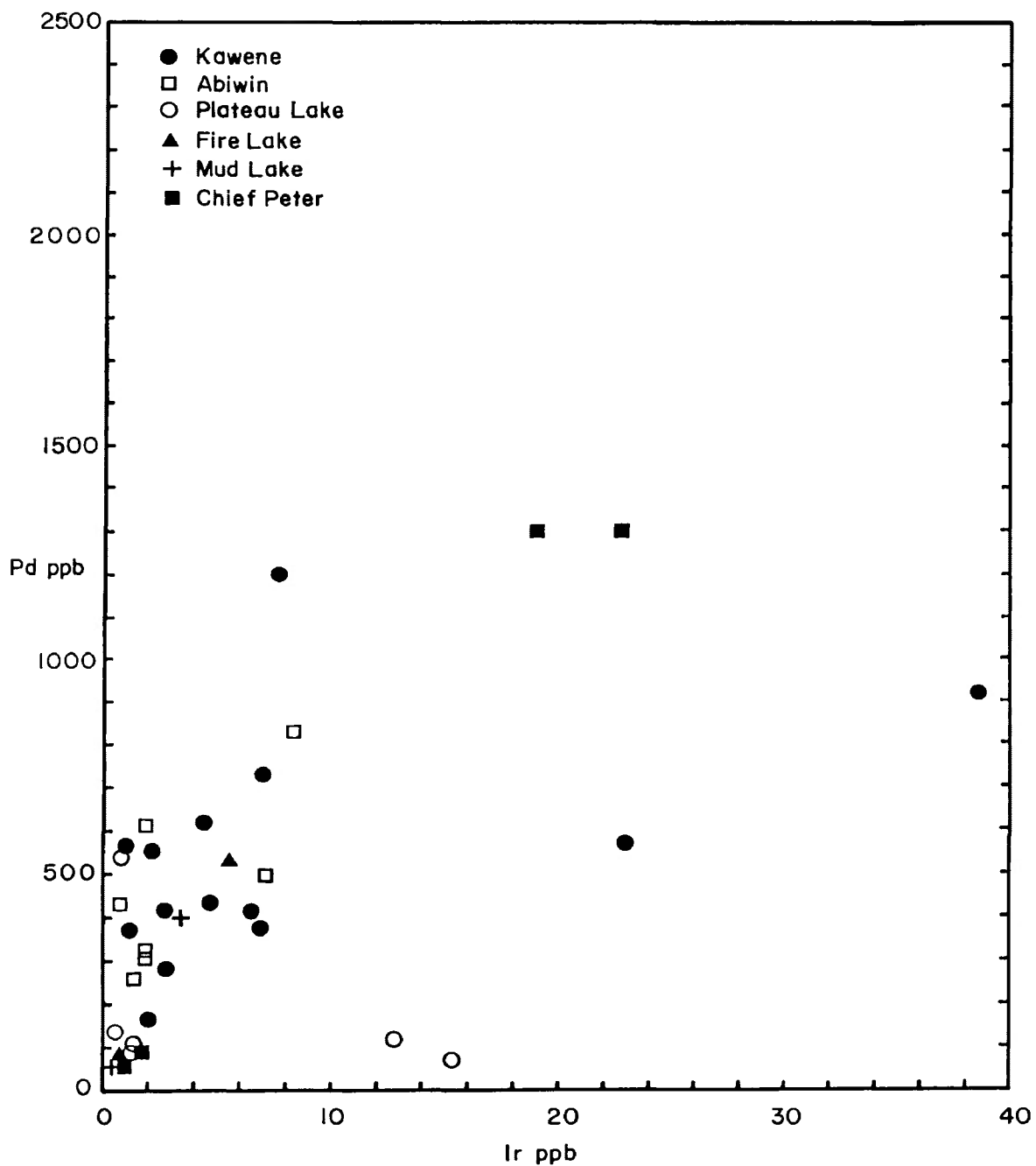
Figure 5.12: Plot of Pd/Ir ratios of PGE-bearing samples. The ratios have a very wide range and generally form a positive, but diffuse trend. Data are from Table 5.12.

The average Pd/Ir ratios for five of the Quetico Intrusions span a range of 41.87 to 220.58. The Plateau Lake, Chief Peter, Mud Lake, and Kawene Intrusions exhibit ratios of 41.87, 59.4, 96.05, and 144.95, respectively, that may be due to successively advancing levels of fractionation. The Plateau Lake and Chief Peter Intrusions are very olivine-rich, plagioclase-poor, poorly zoned, and lack any layering, suggesting that they formed from a more primitive melt than the other PGE-bearing intrusions. Both the Mud Lake and Kawene Intrusions exhibit modal layering and locally contain considerable plagioclase, and the Kawene Intrusion contains much less olivine than the Plateau and Chief Peter Intrusions, suggesting formation from a more evolved melt. The extremely high Pd/Ir ratio of 220.58 exhibited by the Abiwin Intrusion may be due to remobilization during high-grade regional metamorphism and deformation; however, there is presently no evidence other than field relationships to support this supposition.

5.4.5 - C1-Chondrite Normalized PGE+Au Ratios:

PGE+Au data from four of the Quetico Intrusions were normalized against the PGE content of C1-chondrites. The chondrite values used are from Naldrett et al. (1980) and comprise 1020 ppb Pt, 545 ppb Pd, 200 ppb Rh, 690 ppb Ru, 514 ppb Ir, 540 ppb Os, and 152 ppb Au. The averaged data (Figure 5.13) show that Pd, Pt, Au and Rh are depleted, but

still come close to approximating chondrite values, whereas Ir, Os and Ru are very depleted. The Kawene Intrusion tends to be more enriched in Ir than the other intrusions. Os and Ru are usually at or below detection limits.

When compared to other PGE-bearing intrusions (Figure 5.14), the Quetico data show a positively sloped profile that compares closely to the Rathbun Lake curve in shape, if not in magnitude, with Pt, Pd, Rh, and Au considerably enriched with respect to Os, Ir, and Ru. There are also some similarities to the Lac des Iles curve, but the relative enrichment of Pd over Au and Pt is considerably less. Since the mineralization at both Rathbun Lake and Lac des Iles is thought to have formed due to hydrothermal (Rowell, 1984) and late magmatic volatile activity (Talkington and Watkinson, 1984; Sutcliffe et al., 1989), respectively, it may be possible to hypothesize that there is evidence of some mechanism of remobilization at work, albeit at much less intense levels, within the Quetico Intrusions. The mechanisms responsible may be remobilization during metamorphism, reconcentration by deuteric processes, or some combination of the two. The deuteric hypothesis may be supported by the commonly observed concentration of alteration and volatile-rich phases in contact with, or adjacent to, Cu-Ni sulphides; and the presence of PGM along fractures, interstitial to gangue minerals and, rarely, within the silicate gangue minerals.

Cl-Chondrite Normalized PGE+Au Plot - Quetico Intrusions
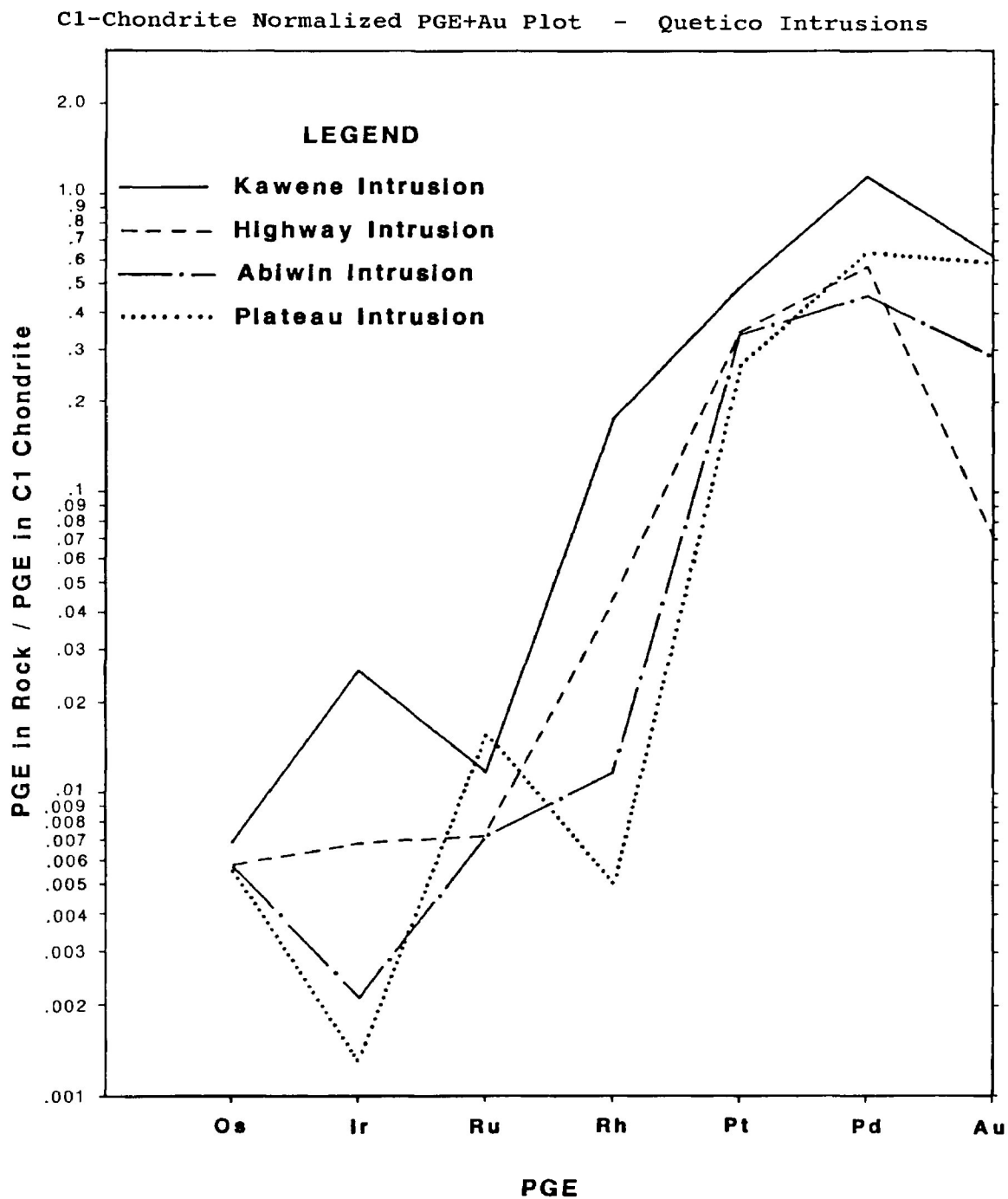
Figure 5.13: Cl-Chondrite normalized PGE+Au plot for four of the Quetico Intrusions. Pd, Pt, Au and Rh are depleted, but come close to approximating chondrite concentrations, whereas Ir, Os, and Ru are very depleted. Data are from Table 5.12. The Highway Intrusion is the largest of the Fire Lake Dykes.
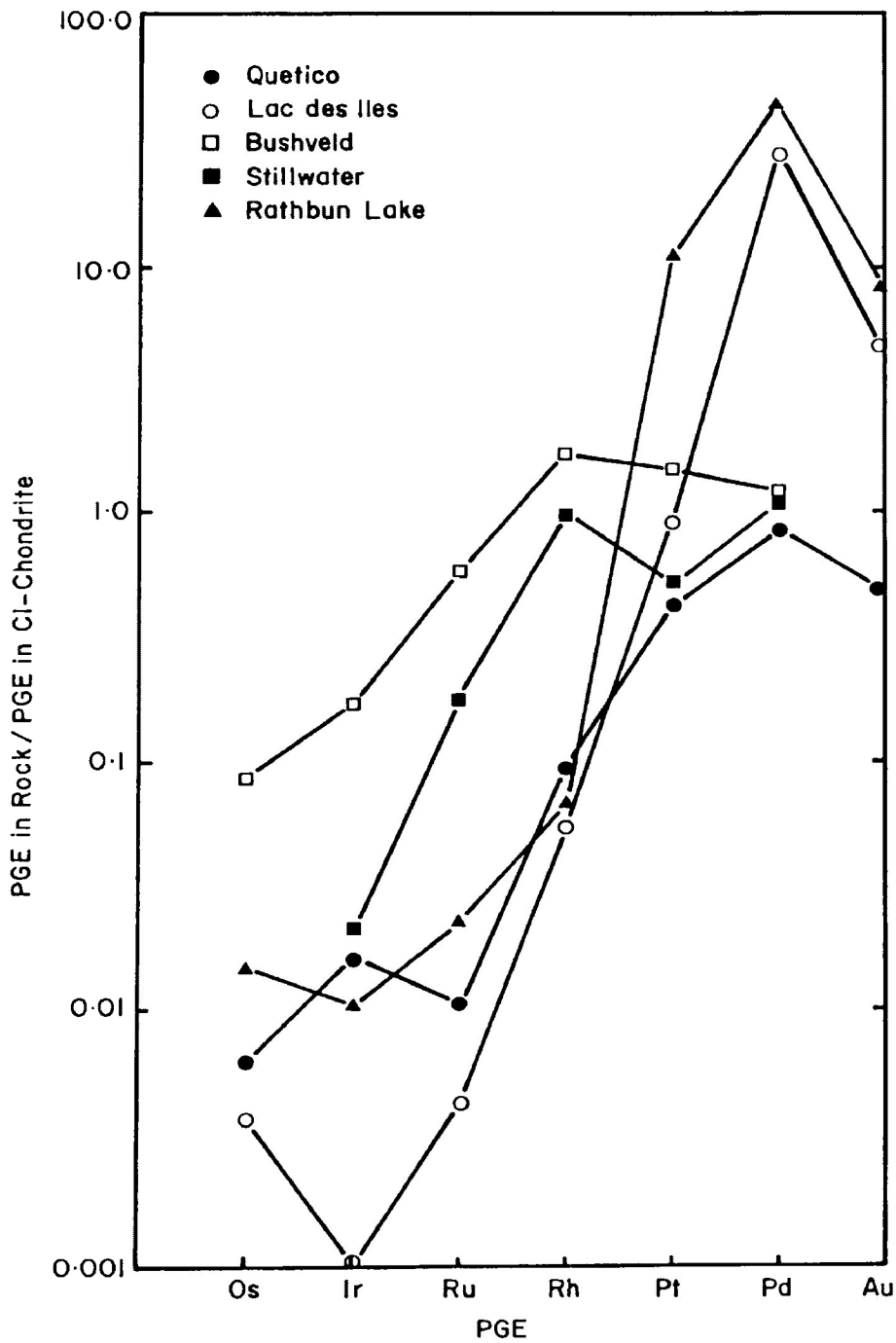
Figure 5.14: C-1 Chondrite Normalized PGE+Au - Comparison. The Quetico Intrusions exhibit a profile similar to the Rathbun Intrusion and the Lac des Iles Complex. Data are from Rowell (1984), Page and Talkington (1984), Page et al. (1982), Sutcliffe et al. (1989), Talkington and Watkinson (1984). C1-chondrite values are from Naldrett et al. (1980)

CHAPTER 6

DISCUSSION, CONCLUSIONS, AND RECOMMENDATIONS

6.1: Discussion

6.1.1 - Comparisons With Other Intrusions:

The distinctive characteristics of the Quetico Intrusions distinguish them from many other intrusive types and help categorize them within the mafic/ultramafic rock spectrum. In particular: are they Archean equivalents of the appinite suite or the Alaskan-type ultramafic complexes?

The Quetico Intrusions form a widespread group of small, hornblende-rich, geochemically primitive, mafic to ultramafic bodies closely associated with the margins of the Quetico Batholithic Complex. Most occur within, or near, a narrow, clastic metasedimentary belt sandwiched between the northern margins of the batholith and the Quetico Fault Zone; however, a few occur in the Redhorse Lake area near the western margins of the complex considerably south of the Quetico Fault Zone (Resident Geologist's Assessment Files, Ministry of Northern Development and Mines, Thunder Bay, Ontario). Field evidence suggests that the Quetico Intrusions may have formed over a period of time spanning the emplacement of much of the batholithic complex.

The setting of the Quetico Intrusions is very similar to that of the appinite suite rocks of the British Isles, Italy, Spain, and elsewhere, which form loose clusters

closely associated with granitoid plutons and batholiths of Caledonian age, approximately 400 Ma (Bailey and Maufe, 1916; Read, 1961; Roach, 1964; French, 1966; Hall, 1967; Pitcher and Berger, 1972; Kennan, 1979; Palicova, 1982; Sutherland, 1982; Galan and Suarez, 1989).

The Alaskan-type Complexes of Alaska, British Columbia, the Urals Mountains, and Venezuela occur in a distinctly different setting as groups of intrusions within long, linear, orogenic belts parallel to major regional structures and often adjacent to roughly parallel belts of alpine-type ultramafic bodies (Murray, 1972; Taylor and Noble,1969; Berg, 1972; Irvine, 1974; Irvine, 1976). There is a close spatial association with contemporaneous volcanism and the complexes usually intrude gabbroic rocks (Taylor, 1967; Taylor and Noble, 1969; Findlay, 1969; Irvine, 1974), often exhibiting a different chemical affinity.

The Quetico, Alaskan, and appinite suite bodies are all relatively small when compared with other mafic/ultramafic intrusive varieties, i.e. the Bushveld Complex; however, the Alaskan-type complexes, with an average area of 42 km^2 (Ruckmick and Noble, 1959; Borisenko, 1967; Taylor, 1967; Murray, 1972; Irvine, 1974; Clarke, 1979), are about two orders of magnitude larger than the Quetico Intrusions and the appinite suite, which average less than 0.3 km^2, and 0.5 km^2 (French, 1966; Pitcher and Berger, 1972), respectively.

The Alaskan-type complexes often exhibit a diffuse,

locally well-developed, roughly concentric zonation of rock types with the least evolved rocks occupying the central portions of an intrusion. A very diffuse, often asymmetric zonation is present within the Kawene and Chief Peter Intrusions and occasionally within some of the appinite suite bodies (Pitcher and Berger, 1972); however, it is not common enough to be a characteristic feature.

The three types of intrusions under discussion are all composed of hornblende-rich lithologies with quite distinctive textures. The appinite suite exhibit a slightly wider range of lithologies than the Quetico Intrusions, but the observed rock types and textural features are practically identical. The suite, as classified by French (1966), is initially characterized by two generally coarse-grained to pegmatitic textural series that range from granodiorite to feldspathic hornblendite before becoming texturally indistinguishable. The ultramafic rock types range from hornblendite to hornblende peridotite and are sometimes split into pyroxene-rich and pyroxene-poor varieties (French, 1966; Pitcher and Berger, 1972). The Quetico Intrusions commonly exhibit good examples of both textural series, but the pyroxene-rich and pyroxene-poor ultramafic rock varieties are often not distinguishable due to the effects of metamorphism, i.e. the Chief Peter and Eva Lake Intrusions. The rocks of the Alaskan-type bodies range in composition from hornblendite to hornblende-poor dunite

and tend to intrude older, often geochemically different gabbros (Ruckmick and Noble, 1959; Andreyeva, 1959; Borisenko, 1967; Taylor, 1967; Taylor and Noble, 1969; Taylor, 1969; Findlay, 1969, Irvine, 1974; Clark, 1980). Dunites do not occur within the Quetico or appinite suite bodies (Taylor, 1967; Taylor and Noble, 1969; Berg, 1972; Clark, 1980; Yefimov and Tavrin, 1978). Contacts within each intrusive type are generally diffuse and gradational.

Chromite is ubiquitous within olivine-rich Alaskan-type complexes (Clark, 1979; Irvine, 1974), but is absent within olivine-rich rocks of the Quetico Intrusions and is a minor accessory within the some of the appinite suite bodies (Sutherland,1982). Orthopyroxene does not occur within Alaskan-type rocks, except as a minor component (<2%) within the Urals Mountains varieties (Ruckmick and Noble, 1959, Taylor, 1967; Borisenko, 1967), but it is locally common within the Quetico Intrusions (this study; Watkinson and Irvine, 1964; Legault, 1976) and the appinite suite (Sutherland, 1982). Magnetite is common within all three intrusive types; however, it is most abundant, often up to 15-20%, within a characteristic magnetite-hornblende clinopyroxenite common to Alaskan-type complexes (Taylor, 1967; Irvine, 1974; Clark, 1979).

There are distinct similarities in major oxide distributions between the Quetico Intrusions and the appinite suite, both of which are essentially dissimilar to

the Alaskan-type complexes. All three are initially very rich in MgO and CaO; however, differences become evident with the continued enrichment in $FeO+Fe_2O_3$ and CaO within the Alaskan-type complexes (Ruckmick and Noble, 1959; Taylor, 1967; Findlay, 1969; Irvine, 1974; Clark, 1980), whereas the Quetico and appinite suite intrusions show a slight decrease in CaO, no discernible enrichment in FeO, and an eventual enrichment in the alkalis (Bowes et al., 1964; Hall, 1967; Jennings and Sutherland, 1969; Haslam, 1970; Bowes and McArthur, 1976; Key, 1977; French, 1978; Wright and Bowes, 1979; Brooks et al. 1981; Stephens and Halliday, 1984).

The Quetico olivines are rich in MgO and are characterized by a very narrow range in forsterite content of $Fo_{77.55-80.89}$. The olivines of the Alaskan-type complexes are often richer in MgO and exhibit a much wider forsterite range of Fo_{77-93} (Findlay, 1969; Irvine, 1974; Cawthorn, 1975). There are no data available on the compositions of the olivines of the appinite suite.

The Quetico clinopyroxenes are mainly diopsidic in composition with $Wo_{44.60-50.53}$, $En_{39.03-49.02}$, and $Fs_{5.35-11.31}$. This range is quite similar to that of Alaskan-type (Ruckmick and Noble, 1959; Findlay, 1969; Irvine, 1974; Clark, 1980; Himmelberg et al., 1986) and appinite suite clinopyroxenes (Haslam, 1970; Bishop and Key, 1983; Galan and Suarez, 1989). Al_2O_3, TiO_2, Cr_2O_3, and Al^{iv} contents have narrow

ranges and are quite low within Quetico and appinite suite
clinopyroxenes and quite high, with wider ranges, within the
Alaskan-type complexes. Further comparisons of SiO_2/Al_2O_3
and Alz/TiO_2 enhance the differences by showing that the
clinopyroxenes of the Alaskan-type complexes exhibit a
pronounced trend toward alkaline affinities, whereas the
similar Quetico and appinite suite clinopyroxenes have
compositional ranges with a sub-alkaline affinity.

The above data comparison clearly shows the similarity
of the Quetico Intrusions with the appinite suite and their
dissimilarity to the Alaskan-type complexes.

6.1.2 - Theories of Origin:

The similarity between the appinite suite and the
Quetico Intrusions implies that they should also share a
similar origin. Theories on the origins of the appinite
suite have been evolving since early in this century. There
is still considerable controversy on the source and
composition of the parent magma, the amount of crustal
contamination, the source of the water so evident in the
final mineralogy, and the timing and methods of emplacement.

Read (1931), Deer (1935), and Read (1961) championed a
theory proposing the production of a hybrid magma from the
mixing of granitic with ultrabasic magma or solid ultrabasic
rock. Later versions of this hybridization theory
postulated that the appinite suite was derived from an acid

magma by differential separation of ultrabasic or basic
material, followed by hybridization of the resulting magma
(Bailey, 1958; Joplin, 1959).

Bowes et al. (1964) examined rhythmic amphibole
overgrowths, similar to those observed in some of the
Quetico Intrusions and suggested that the overgrowths were
the result of pressure variations within a basic magma under
high P_{H2O}. The high volatile content was supported by the
very coarse-grained nature of most of the amphiboles present
within relatively small intrusions and the abundance of
other hydrous minerals and apatite. These observations also
apply to the Quetico Intrusions. Work by Hall (1967),
Pitcher and Berger (1972), Bowes and McArthur (1976), and
Kennan (1979) supports the basic premise of Bowes et al.
(1964) with the resultant hypothesis that most of the
appinite suite are cumulates formed from a mantle-derived,
basaltic magma that incorporated water from the lower crust
and differentiated at a high P_{H2O}, possibly in the order of
5-10 kb. The presence of a high water vapour pressure would
increase the width of the amphibole stability field (Yoder
and Tilley, 1962) at the expense of olivine and pyroxene
(Pitcher and Berger, 1972) producing an interconnected suite
of amphibole-rich rock types over a wide compositional
range.

Wright and Bowes (1979) theorize that the appinites are
a suite of subvolcanic intrusions, with a predominantly

mantle source, that exhibit geochemical characteristics indicative of normal differentiation of a volatile-, potassium-, and trace element-rich basaltic magma. Hall (1967) advanced the notion that the volatile-rich appinite suite intrusions, upon reaching a near-surface environment, form an explosive gas phase that produces an explosion breccia often observed in subvolcanic pipes throughout Great Britain. Pankhurst and Sutherland (1982) state that many of the rocks of the suite exhibit affinities with lamprophyres. They also state that chemistry and mineralogy suggest that the appinite suite are cumulates formed from a basaltic or andesitic magma, unusually enriched in water, that may be subsurface expressions of Devonian-age volcanism.

Watkinson and Irvine (1964) examined the Quetico Intrusions, east of the present study area and proposed that they formed by fractional crystallization of a tholeiitic olivine basalt liquid, at a P_{H2O} of at least 2.5 kb. They also noted that the order of crystallization was olivine; olivine + clinopyroxene; clinopyroxene (possibly) + hornblende, giving way to hornblende alone; then hornblende + plagioclase and, eventually, titanite.

6.2: Summary and Conclusions

The Quetico Intrusions are a group of small, sometimes asymmetrically zoned, syntectonic dykes, plugs, and stocks closely associated with the margins of the Quetico

Batholithic Complex. They are composed of hornblende-rich lithologies that range from hornblende wehrlite, and locally hornblende peridotite, to quartz diorite. The order of crystallization is similar to that observed by Watkinson and Irvine (1964), ie. olivine, olivine + clinopyroxene, clinopyroxene (locally orthopyroxene), clinopyroxene + hornblende, hornblende, hornblende + plagioclase. Biotite, apatite, and titanite are present within most rock types, but the latter two are most abundant within the later, more evolved plagioclase-rich lithologies, particularly the appinites. Most of the rocks, excluding the appinites, are cumulates and weak to well-developed igneous layering is present locally. Hornblende is present in quantity throughout the most of the crystallization history of the intrusions, and petrographic evidence shows that it often formed at the expense of pre-existing clinopyroxene. Textures characteristic of the Caledonian-age appinite suite are present as pods, patches, and veins within all rock types. A complete unit composed of appinitic diorite is present within the Mud Lake Intrusion.

Due to the variable effects of metamorphism and the cumulus nature of the intrusions the whole rock and trace element data are unclear as to their magmatic affinity, but clinopyroxene mineral chemistry may hint at a calc-alkaline parent magma. Additional support for a calc-alkaline affinity may be the presence of myrmekitic intergrowths of

magnetite within clinopyroxene which suggests that the f_{O2} was high enough to allow the presence of a stable oxide phase during magmatic conditions. The intrusions were initially very rich in MgO and CaO. MgO decreased quickly and generally reflects the presence of olivine. CaO content remained high and decreased only slightly with differentiation. FeO content is relatively constant and exhibits little enrichment with apparent fractionation. An elevated potassium-content in many rock types is evidence of the localized presence of considerable primary biotite. There is a subtle, systematic increase in the incompatible trace element concentrations with increasing SiO_2.

Most lithological, textural, and chemical data show that the Quetico Intrusions are very similar to the appinite suite, and are quite dissimilar to the Alaskan-type complexes. It is the conclusion of this author that the Quetico Intrusions represent Archean equivalents of the appinite suite. They are cumulates that may have crystallized from a sub-alkaline, possibly calc-alkaline, olivine basalt liquid, in the presence of considerable water at a relatively high P_{H2O} and possibly P_{O2}. The intrusions must have crystallized under a relatively high P_{H2O} in order for hornblende to remain stable over such a wide range of magmatic conditions. Significant numbers of variably assimilated metasedimentary xenoliths within the marginal rocks of the larger intrusions suggests that modification of

the original magma may have occurred due to the incorporation of wall-rock material. The distinctive appinite units and veins may have formed from the intrusion of late-stage volatile- and incompatible element-enriched differentiates, or deuteric fluids concentrated by filter pressing. Isolated appinite patches and pods may have formed from small, trapped concentrations of late-stage deuteric fluids. There are no data to support a subvolcanic origin for the Quetico Intrusions, as was proposed for the appinite suite by Wright and Bowes (1979) and Pankhurst and Sutherland (1982).

The Cu-Ni-PGE mineralization present within many of the intrusions is associated with contacts with surrounding clastic metasedimentary country rocks and occasionally with internal contacts. Sulphide and oxide mineralization within these zones appears relatively simple, consisting primarily of chalcopyrite, pyrrhotite, pentlandite, and magnetite. Pyrite is rare. Minor accessory phases include nickeliferous cobaltite, altaite, empressite, cubanite, breithauptite, violarite, covellite, and various alloys and native metals. The PGM are tiny, usually <2 μm in diameter and are dominated by palladium minerals such as michenerite, froodite, and sobolevskite. The rhodium mineral, hollingworthite, is also common and the iridium mineral, irarsite, is present locally. Sperrylite is rare and the only platinum mineral found. Complex intergrowths including

the above PGM are common. The only alloy containing PGE was palladian gold.

The PGM exhibit conflicting parageneses and occur in five ways: completely enclosed within pyrrhotite, or Cu-Ni sulphides; along sulphide grain margins; along fractures within sulphides; interstitially to silicate minerals in close proximity to sulphides; and within silicate minerals. The first example implies crystallization of the PGM before the sulphides, the second two suggest crystallization contemporaneous with the sulphides, whereas the latter two suggest that some form of remobilization was important in their formation. Evidence that late deuteric fluids may have been responsible for some minor remobilization are: PGM occurring interstitial to silicates and the presence of a complex PGM intergrowth entirely contained within a late-stage titanite grain. Another possible remobilization mechanism may be metamorphism; however, there is no direct evidence to support this hypothesis.

Cu-Ni sulphide parageneses suggest that most sulphide minerals crystallized from a PGM-bearing, nickeliferous and cupriferous, monosulphide phase (mss) trapped interstitially to most of the higher temperature silicate phases. Some sulphides occur as inclusions within silicates, particularly clinopyroxene and occasionally hornblende, suggesting that a mss phase may have exsolved from the melt before clinopyroxene and cumulus hornblende crystallization was

complete. The presently observed sulphide textures are mainly due to subsolidus reequilibration and the formation of lower temperature phases as the intrusions slowly cooled. There has been some remobilization into stringers and veinlets during regional deformation and metamorphism. Metamorphic effects such as annealing textures and recrystallization are not observed within the Kawene and Mud Lake Intrusions. Some recrystallization is apparent within the Abiwin, Chief Peter, and Eva Lake Intrusions.

There are a number of processes that may have been responsible for the formation and eventual emplacement of the sulphide zones observed within the Quetico Intrusions:

1) Exsolution of an mss phase at magmatic temperatures after S-saturation during normal fractional crystallization of the melt. The denser sulphides were collected and concentrated by settling through a less dense silicate crystal mush or by later injection along favourable pathways. The internal, contact-related sulphide zones present at the Chief Peter and Plateau Intrusions may have formed in this manner.

2) Exsolution of an mss phase at magmatic temperatures after S-saturation was triggered by the assimilation of the silica-rich, clastic metasedimentary wall-rocks. This is supported by the presence of partially assimilated xenoliths within the marginal regions of many of the intrusions and an irregular, plagioclase-

rich, reaction rim at the contact between the Kawene
Intrusion and surrounding country rocks.

3) Remobilization, concentration, and deposition of
magmatically-derived Cu-Ni-PGE mineralization by late-
stage, deuteric fluids. This may have produced some
minor remobilization, but the lack of intense deuteric
alteration within the mineralized zones precludes this
as the main mineralization process.

4) Deposition from volatile-enriched hydrothermal
fluids after the emplacement of an intrusion. As was
mentioned in number 3, above, there is no evidence of
the intense alteration that would be expected if large
quantities of mineralizing fluids had moved through the
host-rocks. Hydrothermal alteration, unlike deuteric
alteration, would probably not be completely confined
to the host intrusion and would have had some visible
effect on surrounding country rocks.

5) Emplacement along fractures, faults, and shear zones
in response to regional deformation. The Abiwin
Intrusion, and to a much lesser extent the Kawene
Intrusion, do exhibit the effects of regional strain
and there has been some minor remobilization of PGE-
rich Cu-Ni sulphides. However, in both cases the
observed shearing is characterized by narrow, discrete
zones that have remobilized existing mineralization
into narrow, discontinuous stringers and veinlets.

6.3:   Recommendations

Possible future research projects that could be directed at the Quetico Intrusions are:

1) A detailed examination of the platinum-group mineralization present within the Kawene, Eva Lake, and Chief Peter Intrusions. This study would fully describe the PGM present and the processes that lead to their formation.

2) A detailed examination of the mineral chemistry of hornblende and biotite. This study might better define the progression of fractionation and the original magmatic affinity of the intrusions.

3) An examination of oxygen isotope chemistry of the intrusions, the surrounding metasediments, and the nearby Quetico Batholithic Complex, in an effort to define whether any crustal contamination or hybridization has taken place.

4) A sulphur isotope study to identify the source of the sulphur within the mineralized zones, and possibly provide additional data on the processes leading to mineralization.

5) A series of detailed examinations of the North Elbow Lake Stock, the surrounding contact metamorphic aureole, and nearby clastic metasediments. The purpose would be to better define mechanisms responsible for emplacement of the intrusion, and to describe its petrology, whole rock lithogeochemistry, and mineral chemistry.

REFERENCES

Andreyeva, Ye.D.
   1959:   Gabbroic Pegmatite in Sinyana Mountain Pyroxenite,
   the Middle Urals; Isvest. Akad. Nauk SSSR. Ser. Geol.
   (English Trans.) No. 9, p.29-40.

Atkins, F.B.
   1969:   Pyroxenes of the Bushveld Intrusion; Journal of
   Petrology, Vol. 10, Part 2, p.222-249.

Bailey, E.B
   1958:   Some Chemical Aspects of South-west Highland Devonian
   Igneous Rocks; Geological Survey of Great Britain, Bulletin,
   xv, p.1-20.

Bailey, E.B., and Maufe, H.B.
   1916:   The Geology of Ben Nevis and Glen Coe; Geological
   Survey of Great Britain, Memoir liii, p.150-186.

Barker, Daniel S.
   1978:   Magmatic Trends on Alkali-Iron-Magnesium Diagrams;
   American Mineralogist, Vol. 63, p.531-534.

Barnes, Sarah-Jane
   1987:   Unusual Nickel and Copper to Noble Metal Ratios From
   the Rana Layered Intrusion, Northern Norway; Norsk Geologisk
   Tidsskrift, Vol. 67, p.215-231.

Barnes, Sarah-Jane, and Naldrett, A.J.
   1986:   Variations in Platinum-Group Element Concentrations
   in the Alexo Mine Komatiite, Abitibi Greenstone Belt,
   Northern Ontario; Geological Magazine 123, Part 5, p.515-
   524.

Barnes, Stephen J., and Naldrett, Anthony J.
   1986:   Geochemistry of the J-M Reef of the Stillwater
   Complex, Minneapolis Adit Area II.   Silicate Mineral
   Chemistry and Petrogenesis; Journal of Petrology, Vol. 27,
   Part 4, p.791-825.

Barnes, S.-J., Naldrett, A.J., and Gorton, M.P.
   1985:   The Origin of the Fractionation of Platinum-Group
   Elements in Terrestrial Magmas; Chemical Geology, Vol. 53,
   p.303-323.

Berg, Henry C.
   1972:   Thrust Faults, Annette-Gravina Area, Southeastern
   Alaska; U.S.G.S. Professional Paper 800-C, p.C79-83.

Bishop, A.C. and Key, C.H.
1983: Nature and Origin of Layering in the Diorites of SE Jersey, Channel Islands; Journal of the Geological Society of London, Vol. 140, p.921-937.

Blackburn, C.E., Bond, W.D., Breaks, F.W., Davis, D.W., Edwards, G.R., Poulsen, K.H., Trowell, N.F., and Wood, J.
1985: Evolution of Archean Volcanic Sedimentary Sequences of the Western Wabigoon Subprovince and its Margins: A Review; In Evolution of Archean Supracrustal Sequences, Edited by L.D. Ayers, P.C. Thurston, K.D. Card, and W. Weber, Geological Association of Canada Special Paper 28, p.89-116.

Blackburn, C.E., and Mackasey, W.O.
1977: Nature of the Quetico-Wabigoon Boundary in the DeCourcey-Smiley Lakes Area, Northwestern Ontario: Discussion; Canadian Journal of Earth Sciences, Vol. 14, p.1959-1961.

Borisenko, L.F.
1967: Trace elements in Pyroxenes and Amphiboles from Ultramafic Rocks of the Urals; Mineralogical Magazine, Vol. 36, p.403-410.

Bowes, D.R., Kinlock, E.D., and Wright, A.E.
1964: Rhythmic amphibole overgrowths in appinites associated with explosion breccias in Argyll; Mineralogical Magazine, Vol. 33, p.963-973.

Bowes, D.R., and McArthur, A.C.
1976: Nature and Genesis of the Appinite Suite; Krystalinikum 12, p.31-46.

Brindley, J.C., Gupta, N., and Kennan, P.S.
1976: Explosion breccias and related features in the Leinster Caledonian Massif, southeast Ireland; Proceedings of the Royal Irish Academy, Vol. 76, Sect. B, p. 337-348.

Brooks, C.K., Fawcett, J.J., Gittins, J., and Rucklidge, J.C.
1981: The Batbjerg Complex, East Greenland: A Unique Ultrapotassic Caledonian Intrusion; Canadian Journal of Earth Science, Vol. 18, p.274-285.

Cabri, L.J. (Ed.)
1981: Platinum-Group Elements: Mineralogy, Geology, Recovery; CIM Special Volume 23, 267p.

Card, K.D., and Ciesielski, Andre
1986: Subdivisions of the Superior Province of the Canadian Shield; Geoscience Canada, Vol. 13, Number 1, p.5-13.

Cawthorn, Grant R.
     1975:   The Amphibole Peridotite-Metagabbro Complex, Finero,
     Northern Italy; Journal of Geology, Vol. 83, p.437-454.

Clark, Thomas
     1979:   Oxide Minerals in the Turnagain Ultramafic Complex,
     Northwestern, B.C.; Canadian Journal of Earth Science, Vol.
     15, p.1893-1903.

Clark, Thomas
     1980:   Petrology of the Turnagain Ultramafic Complex,
     Northwestern British Columbia; Canadian Journal of Earth
     Sciences, Vol. 17, p.747-757.

Czamanske, Gerald K., and Zientek, Michael L. (Technical Editors)
     1985:   The Stillwater Complex, Montana: Geology and Guide;
     Montana Bureau of Mines and Geology, Special Publication 92,
     396p.

Davies, J.C., and Pryslak, A.P.
     1967:   Kenora-Fort Frances Sheet, Geological Compilation
     Series; Ontario Department of Mines, Map 2115, scale 1 inch
     to 4 miles.

Deer, W.A.
     1935:   The Cairnsmore of Carphairn Igneous Complex;
     Quarterly Journal of the Geological Society, xci, p.47-76.

Deer, W.A., Howie, R.A., and Zussman, J.
     1978:   Rock Forming Minerals, Vol. 2A, Second Edition,
     Single Chain Silicates.   John Wiley, New York.

Droop, G.T.R.
     1987:   A General Equation for Estimating Fe^{3+} Concentrations
     in Ferromagnesian Silicates and Oxides From Microprobe
     analyses, Using Stoichiometric Criteria; Mineralogical
     Magazine, Vol. 51, p.431-435.

Fenwick, K.R.
     1976:   Geology of the Finlayson Lake Area, District of Rainy
     River; Ontario Division of Mines, Geological Report 145,
     86p.

Findlay, D.C.
     1969:   Origin of the Tulameen Ultramafic-gabbro Complex,
     Southern British Columbia; Canadian Journal of Earth
     Sciences, Vol. 6, p.399-425.

French, W.J.
     1966:   Appinitic Intrusions Clustered Around the Ardara
     Pluton, County Donegal; Proceedings of the Royal Irish
     Academy, Vol. 64, Sect. B, p.303-322.

French, W.J.
    1976:   The Origin of Leucodiorites Associated With the
    Appinitic Intrusions of County Donegal; Proceedings of the
    Yorkshire Geological Society, V. 41, Pt. 1, No. 10, p.107-
    126.

French, W.J.
    1977:   Breccia-pipes Associated With the Ardara Pluton,
    County Donegal; Proceedings of the Irish Academy, Sect. B,
    Vol. 77, No. 4, p.101-117.

French, W.J.
    1978:   Lamprophyric Dykes Associated with the Appinitic
    Intrusions of County Donegal; Scientific Proceedings, Royal
    Dublin Society, Series A, Vol. 6, p.97-107.

Fumerton, S.L.
    1982:   Redefinition of the Quetico Fault Near Atikokan,
    Ontario; Canadian Journal of Earth Sciences, Vol. 19,
    p.222-224.

Galan, G. and Suarez, O.
    1989:   Cortlanditic Enclaves Associated With Calc-Alkaline
    Granites From Tapia-Asturias (Hercynian Belt, Northwestern
    Spain); Lithos, Vol. 23, p.233-245.

Garuti, G., and Rinaldi, R.
    1986:   Mineralogy of the Melonite-Group and Other Tellurides
    From the Ivrea-Verbano Basic Complex, Western Italian Alps;
    Economic Geology, Volume 81, No. 5, p.1213-1217.

Gibb, Fergus G.F.
    1973:   The Zoned Clinopyroxenes of the Shiant Isles Sill,
    Scotland; Journal of Petrology, Vol. 14, Part 2, p.203-230.

Gronlie, Arne
    1988:   Platinum-group Minerals in the Lillefjellklumpen
    Nickel-copper Deposit, Nord-Trondelag, Norway; Norsk
    Geologisk Tidsskrift, Vol. 68, p.65-72.

Hall, A.
    1967:   The Chemistry of Appinitic Rocks Associated With the
    Ardara Pluton, Donegal, Ireland; Contributions to Mineralogy
    and Petrology, Vol. 16, p.156-171.

Harney, Dirk M.W. and Merkle, Roland K.W.
    1990:   Pt-Pd Minerals from the Upper Zone of the Eastern
    Bushveld Complex, South Africa; Canadian Mineralogist,
    Volume 28, p.619-628.

Haslam, H.W.
    1970:   Appinite Xenoliths and Associated Rocks From the Ban
    Nevis Igneous Complex; Geological Magazine, Vol. 107, No. 4,
    p.341-356.

Hawley, J.E.
    1929:   Geology of the Sapawe Lake Area, With Notes on Some
    Iron and Gold Deposits of Rainy River District; Ontario
    Department of Mines Annual Report, Vol. 38, part 6, p. 1-58.
    Accompanied by Map No. 38e, scale 1 inch to 3/4 mile.

Hess, H.H.
    1960:   Stillwater Igneous Complex, Montana - A Quantitative
    Mineralogical Study; Geological Society of America Memoir
    80, 230p.

Himmelberg. Glen R., Loney, Robert A., and Craig, John T.
    1986:   Petrogenesis of the Ultramafic Complex at the Blashke
    Islands, Southeastern Alaska; U.S. Geological Survey
    Bulletin 1662, 14p.

Hoffman, E.L., Naldrett, A.J., Alcock, R.A., and Hancock, R.G.
    1979:   The Noble Metal Content of Ore in the Levack West and
    Little Stobie Mines, Ontario; Canadian Mineralogist, V. 17,
    p.437-452.

Irvine, T.N.
    1963:   Western Lac des Mille Lacs Area; Ontario Department
    of Mines, Geological Report No. 12, 24p.

Irvine, T.N.
    1973:   Bridget Cove Volcanics, Juneau Area, Alaska:
    Possible Parental Magma of Alaskan-type Ultramafic
    Complexes; Carnegie Institution of Washington Yearbook 72,
    p.478-491.

Irvine, T.N.
    1974:   Petrology of the Duke Island Ultramafic Complex,
    Southeastern Alaska; Geological Society of America Memoir
    138, 240p.

Irvine, T.N.
    1976:   Studies of Cordilleran Gabbroic and Ultramafic
    Intrusions, B.C.; Part 2:   Alaskan-type Ultramafic-gabbroic
    Bodies in the Aiken Lake, McConnell Creek, and Toodoggone
    Map-areas; Geological Survey of Canada Paper 76-1A, p.76-81.

James, Odette B.
    1971:   Origin and Emplacement of the Ultramafic Rocks of the
    Emigrant Gap Area, California; Journal of Petrology, Vol.
    12, Part 3, p.530-560.

Jennings, D.J. and Sutherland, F.L.
     1969: Geology of the Cape Portland Area With Special
     Reference to the Mesozoic(?) Appinitic Rocks; Tasmania
     Department of Mines Technical Reports, No. 13, p.45-82.

Joplin, Germain A.
     1959: On the Origin and Occurrence of Basic Bodies
     Associated With Discordant Bathyliths; Geological Magazine,
     V. 96, No. 5, p.361-373.

Keays, R.R., Ross, J.R., and Woolrick, P.W.
     1981: Precious Metals in Volcanic Peridotite-associated
     Nickel Sulphide Deposits in Western Australia. II.
     Distribution Within the Ores and Host Rocks at Kambalda;
     Economic Geology, Vol. 76, p.1629-1644.

Keays, R.R., Nickel, E.H., Groves, D.I., and McGoldrick, P.J.
     1982: Iridium and Palladium as Discriminants of Volcanic
     Exhalative, Hydrothermal, and Magmatic Nickel Sulphide
     Mineralization; Economic Geology Vol. 77, p.1535-1547.

Kehlenbeck, Manfred M.
     1976: Nature of the Quetico-Wabigoon Boundary in the
     DeCourcey-Smiley Lakes Area, Northwestern Ontario; Canadian
     Journal of Earth Sciences, Vol. 13, p.737-748.

Kennan, Padhraig S.
     1979: Plutonic Rocks in the Irish Caledonides; In The
     Caledonides of the British Isles - Reviewed, Geological
     Society of London, Special Publication No. 8, A.L. Harris,
     C.H. Holland and B.E. Leake, Editors, p.705-711.

Kennedy, M.C.
     1984: The Quetico Fault in the Superior Province of the
     Southern Canadian Shield; Unpublished M.Sc. Thesis, Lakehead
     University, Thunder Bay, Ontario.

Key, C.H.
     1987: Geochemistry of Diorites and Associated Plutonic
     Rocks of S.E. Jersey, Channel Islands; Mineralogical
     Magazine, Vol. 51, p.217-229.

Key, Colin H.
     1977: Origin of Appinitic Pockets in Diorites of Jersey,
     Channel Islands; Mineralogical Magazine, Vol. 41, p.183-192.

Kushiro, I.
     1960: Si-Al Relations in Clinopyroxenes From Igneous Rocks;
     American Journal of Science, Vol. 258, p.548-554.

214

Kushiro, Ikuo
    1979: Fractional Crystallization of Basaltic Magma; **In** The
    Evolution of the Igneous Rocks: Fiftieth Anniversary
    Perspectives, H,S.Yoder, Jr., Editor, Princeton University
    Press, p.171-203.

Larsen, Chris Robert
    1974: The Silicate and Sulphide Petrology of the Kawene
    Lake Intrusion; unpublished H. B.Sc. Thesis, Lakehead
    University, Thunder Bay, Ontario, 93p.

LeBas, M.J.
    1962: The Role of Aluminium in Igneous Clinopyroxenes with
    Relation to Their Parentage; American Journal of Science,
    Vol. 260, p.267-288.

Legault, Mary
    1976: A Petrographic Study of the Elbow Lake Mafic
    Intrusion; Unpublished Bachelor of Science Thesis,
    University of Ottawa, Ottawa, Ont., 19p.

Leterrier, Jacques, Maury, Rene C., Thonon, Pierre, Girard,
    Danielle, and Marchal, Michele
    1982: Clinopyroxene Composition as a Method of
    Identification of the Magmatic Affinities of Paleo-Volcanic
    Series; Earth and Planetary Science Letters, Vol. 59, p.139-
    154.

MacTavish, A.D., and Dutka, R.
    1988: PGE Prospective Areas in Ontario; Archean Mafic
    Ultramafic Suites: Quetico Sub-province; **In** The Platinum
    Group Elements of Ontario, Ontario Geological Survey, Open
    File Report 5681, p.90-98.

McIlwaine, W.H. and Chorlton, L.B.
    1973: East Half of Sapawe Lake Area, District of Rainy
    River; p.71-74. **In** Summary of Field Work, 1973, by the
    Geological Branch, edited by V.G. Milne, D.F. Hewitt and
    W.J. Wolfe, Ontario Division of Mines, MP56, 202p.

McIlwaine, W.H., and Hillary, E.M.
    1974: East Half of Sapawe Lake Area, District of Rainy
    River; p.65-69, **In** Summary of Field Work, 1974, by the
    Geological Branch, Edited by V.G. Milne, D.F. Hewitt, and
    K.D. Card, Ontario Division of Mines, MP59, 206p.

McIlwaine, W.H. and Larsen, C.R.
    1981: Sapawe Lake Area, West Part, Rainy River District;
    Ontario Geological Survey Preliminary Map P.2389 (Revised),
    Geological Series, scale 1:15840 or 1 inch to 1/4 mile.
    Geology 1973, 1974.

McIlwaine, W.H. and Larsen, C.R.
    1981:   Sapawe Lake Area, East Part, Rainy River District;
    Ontario Geological Survey Preliminary Map P.2388 (Revised),
    Geological Series, scale 1:15840 or 1 inch to 1/4 mile.
    Geology, 1973, 1974.

Moore, E.S.
    1939:   Geology and Ore Deposits of the Atikokan Area;
    Ontario Department of Mines, Vol. 48, part 2, p.1-34.
    Accompanied by Map No. 48a, scale 1:63360 (1 inch to 1
    mile). Geology in 1937.

Morimoto, Nobuo
    1989:   Nomenclature of Pyroxenes; Sub-committee on
    Pyroxenes, Nobuo Morimoto, Chairman; Canadian Mineralogist,
    Vol. 27, p.143-156.

Murray, C.G.
    1972:   Zoned Ultramafic Complexes of the Alaskan-type:
    Feeder Pipes of Andesitic Volcanoes; Geological Society of
    America Memoir 132, p.313-335.

Naldrett, A.J.
    1981:   Platinum-Group Element Deposits; Canadian Institute
    of Mining and Metallurgy, Special Volume 23, p.197-232.

Naldrett, A.J., Innes, D.G., and Sowa, J.M.
    1980:   Platinum-Group Element Concentration in Some Magmatic
    Ores in Ontario; Ontario Geological Survey Miscellaneous
    Paper 93, p.171-178.

Ontario Department of Mines
    1961:   Pickerel Lake Map Sheet, Airborne Magnetic Survey,
    Geophysics Paper 1122G, scale: 1" = 1 mile.

Osborn, E.F
    1959:   Role of Oxygen Pressure in the Crystallization and
    Differentiation of Basaltic Magma; American Journal of
    Science, Vol. 257, p.609-647.

Page, Norman J. and Talkington, Raymond W.
    1984:   Palladium, Platinum, Rhodium, Ruthenium and Iridium
    in Peridotites from Ophiolite Complexes in Newfoundland;
    Canadian Mineralogist, Vol. 22, p.137-149.

Page, Norman J., Von Gruenewaldt, Gerhard, Haffty, Joseph,
    Aruscavage, Philip J.
    1982:   Comparison of Platinum, Palladium and Rhodium
    Distributions in Some Layered Intrusions, with Special
    Reference to the Late Differentiates (Upper Zone) of the
    Bushveld Complex, South Africa; Economic Geology, Vol. 77,
    No. 6, p.1405-1418.

Palicova, Marie
    1982:   Petrogenetic Significance of Textural Development of
    Basic Rocks in the Southern Adamello Massif (Mte. Mattoni,
    Mte. Cadino), Italy; Transformists' Petrology, Theophrastus,
    Athens, Greece, p.149-179.

Pankhurst, R.J. and Sutherland, D.S.
    1982:   Caledonian Granites and Diorites of Scotland and
    Ireland; **In** <u>Igneous Rocks of the British Isles</u>. D. S.
    Sutherland, Editor, Wiley Interscience Publication, John
    Wiley and Sons, p.149-190.

Percival, J.A. and Stern, R.A.
    1984:   Geological Synthesis in the Western Superior
    Province, Ontario; **In** <u>Current Research</u>, Part A, Geological
    Survey of Canada, Paper 84-1A, p.397-408.

Percival, John A.
    1989:   A Regional Perspective of the Quetico Metasedimentary
    Belt, Superior Province, Canada; Canadian Journal of Earth
    Sciences, Vol. 26, p.677-693.

Percival, John A., Stern, Richard A., and Digel, Mark R.
    1985:   Regional Geological Synthesis of Western Superior
    Province, Ontario; **In** <u>Current Research</u>, Part A, Geological
    Survey of Canada, Paper 85-1A, p.385-397.

Percival, John A., and Williams, Howard R.
    1989:   Late Archean Quetico Accretionary Complex, Superior
    Province, Canada; Geology, Vol. 17, p.23-25.

Pirie, J. and Mackasey, W.O.
    1978:   Preliminary Examination of Regional Metamorphism in
    Parts of Quetico Metasedimentary Belt, Superior Province,
    Ontario; **In** <u>Metamorphism in the Canadian Shield</u>, ed. J.A.
    Fraser and W.W. Heywood, Geological Survey of Canada, Paper
    78-10, p.37-48.

Pirie, James
    1978:   Geology of the Crooked Pine Lake Area, District of
    Rainy River; Ontario Geological Survey Geology Report 179,
    73p.

Pitcher, Wallace S., and Berger, Anthony R.
    1972:   The Appinite Suite: The Basic Rocks Genetically
    Associated with Granite; **In** <u>The Geology of Donegal: A Study</u>
    <u>of Granite Emplacement and Unroofing</u>; Wiley Interscience,
    Regional Geology Series, John Wiley and Sons, Inc.; Chapter
    7, p.143-168.

Pye, E.G., and Fenwick, K.G.
     1965:   Atikokan-Lakehead Sheet, Districts of Kenora, Rainy
     River and Thunder Bay; Ontario Department of Mines,
     Geological Map 2065, Geological Compilation Series, Scale 1
     inch to 4 miles.

Read, H.H
     1931:   The Geology of Central Sutherland; Memoir of the
     Geological Survey, Vol. 165.

Read, H.H.
     1961:   Aspects of Caledonian Magmatism in Britain;
     Proceedings of the Liverpool and Manchester Geological
     Society, Vol. 2, p.653-683.

Roach, Robert A.
     1964:   Mineral banding and Appinites in the Bon Repos
     Meladiorite, Guernsey;, Channel Islands; Geologists'
     Association. Proceedings, Vol. 75, part 2, p.185-198.

Rowell, William Frank
     1984:   Platinum-group Elements and Gold in the Wanapitei
     Nipissing-type Intrusions, Northeastern Ontario; Unpublished
     M.Sc. Thesis, University of Western Ontario, London,
     Ontario, 87p.

Ruckmick, John C. and Noble, James A.
     1959:   Origin of the Ultramafic Complex at Union Bay, S.E.
     Alaska; G.S.A. Bulletin Vol. 70, Part II, p.981-1018.

Schwerdtner, W.M., Morgan, J., and Stott, G.M.
     1985:   Contacts Between Greenstone Belts and Gneiss
     Complexes Within the Wabigoon Subprovince, Northwestern
     Ontario; In Evolution of Archean Supracrustal Sequences,
     edited by L.D. Ayers, P.C. Thurston, K.D. Card, and W.
     Weber, Geological Association of Canada Special Paper 28,
     p.117-123.

Scoon, Roger N., and DeKlerk, William J.
     1987:   The Relationship of Olivine Cumulates and
     Mineralization to Cyclic Units in Part of the Upper Critical
     Zone of the Western Bushveld Complex; Canadian Mineralogist,
     Vol. 25, p.51-77.

Snoke, Arthur W., Quick, James E., and Bowman, Harry R.
     1981:   Bear Mountain Igneous Complex, Klamath Mountains,
     California: An Ultrabasic to Silicic Calc-Alkaline Suite;
     Journal of Petrology, Vol. 22, Part 4, p.501-552.

Stephens, W.E. and Halliday, A.N.
    1984:   Geochemical Contrasts Between Late Caledonian
    Granitoid Plutons of Northern, Central and Southern
    Scotland; Transactions of the Royal Society of Edinburgh:
    Earth Sciences, Vol. 75, p.259-273.

Stockwell, C.H., McGlynn, J.C., Emslie, R.F., Sanford, B.V.,
    Norris, A.W., Donaldson, J.A., Fahrig, W.F., and
    Currie, K.L.
    1970:   Geology of the Canadian Shield; **In** Geological Survey
    of Canada, Economic Geology Report No. 1, R.J.W. Douglas,
    Scientific Editor, p.44-150.

Streckeisen, A.
    1976:   To Each Plutonic Rock Its Proper Name; Earth Science
    Reviews, 12, p.1-33.

Sutcliffe, R.H., Sweeny, J.M., and Edgar, A.D.
    1989:   The Lac des Iles Complex, Ontario: Petrology and
    Platinum-Group-Elements Mineralization in an Archean Mafic
    Intrusion; Canadian Journal of Earth Science, Vol. 26,
    p.1408-1427.

Talkington, Raymond W. and Watkinson, David H.
    1984:   Trends in the Distribution of the Precious Metals in
    the Lac-des-Iles Complex, Northwestern Ontario; Canadian
    Mineralogist, Vol. 22, p.125-136.

Tanton, T.L.
    1940:   Quetico (West Half); Map 534A, Department of Mines
    and Resources, Canada, Geological Survey, scale 1:253,440 (1
    inch to 4 miles). Geology, 1937.

Taylor, H.P. Jr.
    1967:   The Zoned Ultramafic Intrusions of Southeastern
    Alaska; **In** Ultramafic and Related Rocks, ed. P.J. Wylie:
    John Wiley, N.Y., p.97-121.

Taylor, Hugh P. Jr., and Noble, James A.
    1969:   Origin of Magnetite in the Zoned Ultramafic Complexes
    of S.E. Alaska; **In** Magmatic Ore Deposits, Economic Geology
    Monograph 4, H.B.D. Wilson, Editor, p.209-230.

Tracy, Robert J., Robinson, Peter, and Wolff, Robert A.
    1984:   Metamorphosed Ultramafic Rocks in the Bronson Hill
    Anticlinorium, Central Massachusetts; American Journal of
    Science, Vol. 284, p.530-558.

Watkinson, D.H. and Irvine, T.N.
    1964:   Peridotitic Intrusions Near Quetico and Shebandowan,
    Northwestern Ontario: A Contribution to the Petrology and
    Geochemistry of Ultramafic Rocks; Canadian Journal of Earth
    Sciences, Vol. 1, p.63-98.

Watkinson, D.H, Whittaker, P.J, and Jones, P.L
    1983:   Platinum Group Elements in the Eastern Gabbro,
    Coldwell Complex, Northwestern Ontario; Grant 107, p.183-
    191; **in** Geoscience Research Grant Program, Summary of
    Research 1982-1983, Edited by E.G. Pye, Ontario Geological
    Survey, Miscellaneous Paper 113, 199p.

Wilkinson, J.F.G.
    1956:   Clinopyroxenes of Alkali Olivine Basalt Magma;
    American Mineralogist, Vol. 41, p.724-743.

William, H., Turner, F.J., and Gilbert, C.M.
    1982:   Petrography: An Introduction to the Study of Rocks
    in Thin Sections; Freeman and Co., New York; 606p.

Williams, H.R.
    1990:   Subprovince Accretion Tectonics in the South-central
    Superior Province; Canadian Journal of Earth Sciences, V.
    27, p.570-581.

Williams, H.R.
    1991:   Quetico Subprovince; **In** Geology of Ontario, Ontario
    Geological Survey, Special Volume 4, Part 1, p.383-403.

Winkler, Helmut G.F.
    1974:   Petrogenesis of Metamorphic Rocks, Third Edition;
    Springer Verlag, New York Inc., 320p.

Wright, A.E. and Bowes. D.R.
    1979:   Geochemistry of the Appinite Suite; **In** The
    Caledonides of the British Isles, Geological Society of
    London, Special Publication No. 8, A.L. Harris, C.H. Holland
    and B.E. Leake, Editors, p.699-704.

Yefimov, A.A. and Tavrin, I.F.
    1978:   Common Origin of the Platinum-bearing Dunites of the
    Urals and the Aldan Shield; Doklady Academii Nauk SSSR, Vol.
    243, No. 4, p.991-994.

Yoder, H.S.Jr. and Tilley, C.E.
    1962:   Origin of Basalt Magmas: An Experimental Study of
    Natural and Synthetic Rock Systems; Journal of Petrology.
    Vol. 3, p.342-532.

APPENDIX I

Mineral Chemistry Analyses

All mineral chemistry analyses were completed by the author using the Energy Dispersive X-ray Spectrometer (EDS) attachment of the Hitachi 750 Scanning Electron Microscope (SEM) located at Lakehead University.

Quantitative analyses of olivine and clinopyroxene were completed under the following operating conditions: an accelerating voltage of 20 kV, an 18° take-off angle, a working distance of 28, a beam current of 0.38 Na, and a spot size of approximately 2 μm. Counting time averaged 120 seconds. All spectra obtained were analyzed using Tracor Northern ZAF computer programs. All standards were acquired on a daily basis by Al McKenzie of the Lakehead Instrument Laboratory.

Semi-quantitative analyses of sulphides, tellurides, antimonides, and PGM were completed under the following conditions: an accelerating voltage of 20 Kv, a take-off angle of 15°, a working distance of 25, a beam current of 0.38 Na and a spot size of approximately 2 μm. All spectra obtained were analyzed using Tracor Northern ZAF computer programs and the SQ internal standards program.

APPENDIX II

WHOLE ROCK, TRACE ELEMENTS,

BASE AND PRECIOUS METALS ANALYSES

A: Whole Rock and Trace Element Analyses

The whole rock analyses were completed in two batches at outside laboratories. The first batch of 19 samples was analyzed by the Ontario Geological Survey (OGS) Geoscience Laboratory and the second batch of 13 samples was analyzed by Chemex Labs Ltd. All trace element analyses were completed by Chemex Labs Ltd. H_2O determinations for the batch of 13 samples was completed by Keith Prignitz, of the Lakehead University Instrument Laboratory, by CHN elemental analyzer.

The OGS Geoscience Laboratory determined most of the major oxides by XRF. FeO was determined by titration; CO_2 by the Leco Infrared Absorption Detector; and H_2O by the Beckman Infrared absorption analyzer. The detection limits for H_2O+, CO_2, FeO, and S, by the above methods, are 0.2%, 0.01%, 0.10%, and 0.01%, respectively.

Chemex Labs Ltd. determined most of the major oxides by Inductively Coupled Plasma-Atomic Emission Spectrometry (ICP-AES). FeO was determined by titration, CO_2 by Leco-Gasimetric, and S by Leco Infrared Absorption. The detection limit for the major oxides, CO_2, FeO, and S are 0.01%, 0.2%, 0.01%, and 0.001%, respectively.

In all cases ferric iron was calculated from chemically determined FeO and Total Iron and then expressed as Fe_2O_3.

Trace elements were determined by ICP-AES, except for Nb, Y, and Zr, which were determined by XRF, and Rb by Atomic Absorption Spectrometry. Detection limits are as follows:

1 ppm	Co, Cr, Cu, Ni, Sc, Sr, Rb, V
2 ppm	Pb, Zn
5 ppm	Zr, Nb, Y
10 ppm	Ba, La

B: Base and Precious Metals Analyses

Mineralized surface sample analyses were completed by the OGS Geoscience Laboratory; similar analyses of diamond drill core samples were completed by Bondar Clegg and Company and made available to the author by Fleck Resources Ltd. Analyses for the platinum-group were completed by X-Ray Assay Laboratories and made available to the author by the Ontario Geological Survey. All samples, except those from the Eva Lake Intrusion, were collected by the author.

Au, Pt, and Pd determinations by the OGS Geoscience Laboratory were completed by flameless atomic absorption spectrophotometry, with detection limits of 2 ppb for Au, and 1 ppb for Pt and Pd. Cu, Ni, Co, and Cr were determined by flame atomic absorption spectroscopy, with detection limits of 5 ppm.

Bondar Clegg and Company analyzed the Fleck Resources drill core samples by using flame atomic absorption spectroscopy for Cu, Ni, and a fire assay preconcentration with a DC Plasma finish for Pt, Pd, and Au. Detection limits are as follows:

1 ppm	Cu, Co
2 ppm	Ni
1 ppb	Au
2 ppb	Pd
15 ppb	Pt

The complete platinum-group and Au analyses completed by X-Ray Assay Laboratories Limited were determined by fire assay preconcentration with a neutron activation finish. Detection limits are:

0.10 ppb	Ir
1.00 ppb	Au, Rh
3.00 ppb	Os
5.00 ppb	Pt, Pd, Ru

APPENDIX III

Log for Diamond Drill Hole K-1-87

Fleck Resources Cross-section for

Drill Holes K-1-87 and K-2-87

Kawene Intrusion

Diamond Drill Hole K-1-87

Collar: L20+00E, 0+26N   **Started:** August 20, 1987

Azimuth: 180°   **Finished:** August 28, 1987

Dip: 45°   **Length:** 122.83 m

Core Size: NQ   **Logged By:** A.D. MacTavish

FROM	TO	DESCRIPTION
0.00	1.70	CASING – OVERBURDEN
1.70	2.34	BIOTITE-QUARTZ FELS – fine-grained, weakly schistose, contact metamorphosed sedimentary rock; greyish in colour, locally hematite stained; occasionally very narrow, highly deformed quartz stringers exhibiting 1-3 mm thick alteration haloes.
2.34	3.95	FELDSPAR PORPHYRY DYKE – slightly sheared and biotitic; white to buff coloured subhedral to locally euhedral plagioclase phenocrysts, up to 5 mm in diameter; groundmass composed of fine-grained plagioclase, biotite and quartz. – <1% cp and minor py and po; very finely disseminated. – 2.34 – sharp, not noticeably chilled contact at approximately 40 deg. core axis angle (CAA). – 3.95 – contact identical with that at 2.34 m at approximately 68 deg. CAA.
3.95	12.26	BIOTITE-QUARTZ FELS – similar to 1.70 to 2.34. – 3.95 to 5.00 – slight schistosity @ 70 deg. to CAA. – narrow quartz-filled fractures at 4.40, 4.50, 5.72 to 5.80, 6.02 to 6.38.

- 9.66 to 9.82 - Feldspar porphyry dyke - sharp
  contacts.

12.26	12.56	**FELDSPAR PORPHYRY DYKE**

- the same as 2.34 to 3.95.
- minor alignment of biotite; minor blebby
  chalcopyrite at 12.50.

12.56	12.70	**QUARTZ-BIOTITE SCHIST**

- sheared, weakly metamorphosed sedimentary rock,
  probably once at turbiditic greywacke.
- schistosity at 62 deg. CAA.

12.70	12.90	**FELDSPAR PORPHYRY DYKE**

- similar to 2.34 to 3.95.
- <5% very finely disseminated cp and minor py and po.
- 12.80 to 12.90 - feldspar content increases while
  that of biotite decreases.

12.90	13.98	**OLIVINE HORNBLENDITE - MINERALIZED**

- fine- to coarse-grained, altered, green to dark
  green rock composed mainly of dark-green hornblende
  partially altered to a lighter green actinolite with
  3 to 7% granular, light-green olivine grains.
- 4 to 6% coarse, blebby chalcopyrite and pyrrhotite;
  cp commonly rims po; remobilized cp also occurs
  along numerous hair thin fractures.
- 13.00 to 13.98 - grain size gradually increases from
  fine-grained to coarse-grained and oikocrystic; some
  clinopyroxene is observed.
- 13.50 - cp and po concentrated near a fracture.
- 13.77 to 13.82 - divided feldspar porphyry vein -
  sheared at 13.77, with an irregular, but sharp
  contact at 13.82.

13.98	15.45	**FELDSPAR PORPHYRY DYKE**

- similar to 2.34 to 3.95.
- <1% very finely disseminated cp with minor py, po.
- 13.98 - irregular, sheared contact.
- 13.98 to 14.08 - sheared and biotitic.
- 15.45 - slightly irregular and sheared, sharp

contact at 50 deg. CAA.

15.45	16.22	OLIVINE HORNBLENDITE - HIGHLY MINERALIZED

- similar to 12.90 to 13.98.
- 10 to 20% disseminated, blebby, locally net-textured po and cp; locally po approaches semi-massive (30 to 60%) while associated cp drops to less than 3%.
- 15.76 to 15.81 - silicates are highly altered and sheared.
- 16.22 - sharp, slightly irregular and sheared contact at approximately 35 deg. CAA.

16.22	16.57	FELDSPAR PORPHYRY DYKE

- similar to 2.34 to 3.95.
- contains 5 to 7% po and cp throughout.
- 16.22 to 16.24 - 10 to 15% cp, with minor po, near slightly sheared contact with olivine hornblendite.
- biotite commonly altered throughout.

16.57	17.80	OLIVINE HORNBLENDITE - WELL MINERALIZED

- 16.57 to 17.00 - similar to 15.45 to 16.22.
  - after 17.00 there is a gradual increase in clinopyroxene and a gradual decrease in olivine until the rock becomes a hornblende pyroxenite or a pyroxene hornblendite.
- hornblende extensively altered to actinolite.
- 5 to 8 mm oikocrysts of hornblende common.
- 6 to 14% disseminated, blebby, locally net-textured po and cp; local discontinuous po and po-cp stringers up to 10 mm in width due to remobilization.
- 16.57 - sharp contact at 35 deg. CAA; 2-4 mm chill margin.
- 17.80 - sharp, slightly irregular contact at 50 deg. CAA.

17.80	20.50	FELDSPAR PORPHYRY DYKE

- similar to 16.22 to 16.57.
- up to 12% slightly aligned biotite nearly parallel to contacts; biotite commonly alters to chlorite; <0.5% to 4% very finely disseminated cp and po and

content decreases with depth.
- 0.5 to 1 cm thick alteration halos, due to silicification, commonly observed around fractures.
- 17.93 to 17.97 - mineralized ultramafic xenolith containing 8-10% blebby cp and po.
- 19.33 to 19.37 - silicified shear.
- 19.85 - silicified shear.
- 20.50 - sharp contact @ 77 deg. CAA; very slightly sheared; shearing has produced deformed feldspar phenocrysts exhibiting pressure shadows.

20.50   21.12   OLIVINE HORNBLENDE PYROXENITE(?) - MINERALIZED
- green to dark green, fine- to coarse-grained, with 5 to 8% biotite as subhedral to anhedral grains (1 to 3 mm in diameter); darker green, possibly hornblende phenocrysts (2 to 4 mm in diameter), that have been altered to actinolite; numerous, small, dark green to black, clinopyroxene (possibly hornblende) grains.
- mineralization decreases very quickly away from sheared upper contact @ 20.50 m; 3 to 4% blebby cp and po; some remobilized cp along shears and fractures near upper contact; cp and po content drops to trace very finely disseminated grains near lower contact @ 21.12.
- 20.55 to 20.57 - mineralized shear; 15 to 20% cp and po smeared along shear folia.
- 20.57 to 20.68 - narrow Feldspar Porphyry Dyke.
- 20.68 to 20.98 - a 2 to 3 mm quartz-carbonate stringer at a low CAA ; 5 to 10% blebs and stingers po, cp.

21.12   27.02   HORNBLENDE PERIDOTITE(?)
- dark green to dark greyish-green, variably fine- to medium-grained, locally coarse-grained.
- hornblende is usually altered to actinolite; olivine is granular and serpentinized; clinopyroxene is present in small, dull-black grains that are difficult to see.
- rock becomes increasingly biotitic with depth to about 15% anhedral to subhedral grains and some

large poikiloblasts (?) up to 1 cm in diameter.
- mineralization consists of 1 to 6% disseminated to
  finely disseminated po and cp; blebby sulphides
  occur where silicates are coarser-grained and along
  narrow fractures.
- locally feldspathic, containing 1 to 5% plagioclase.
- irregular, patchy, very altered zones occur locally.
- 23.40 to 23.66 - silicified zone, composed of an
  irregular mixture of highly altered hornblende
  peridotite and a quartzo-feldspathic material which
  exhibits a pronounced silicified alteration halo.
- 25.00 to 25.06 - 2 to 5% plagioclase.
- 25.20 to 25.25 - 3 to 4% disseminated po.
- 25.31 to 25.42 - irregular silicified blebs composed
  of K-spar, plagioclase and minor quartz associated
  with a narrow shear.
- 25.73 - 3 cm thick biotitic, chloritic, calcareous
  shear.
- 25.84 - 1 cm thick biotitic, chloritic, calcareous
  shear.
- 26.75 to 26.90 - 2 to 4% disseminated to blebby
  po and cp.
- 26.90 to 27.02 - lamprophyre dyke; slightly
  foliated, porphyritic, dark green; 2 to 3 mm biotite
  phenocrysts and 2 to 5 mm amphibole phenocrysts;
  plagioclase-rich groundmass.

27.02   37.98   HORNBLENDE PYROXENITE
- variably fine- to coarse-grained, layered(?) rock.
- alternating units of fine- to medium-grained, grey-
  green to dark green, variably altered, locally
  slightly porphyritic rock and a mottled, medium to
  coarse-grained, light grey to greenish-grey rock
  containing a large number of oikocrysts of
  hornblende (5 to 10 mm in diameter amphiboles).
- 27.02 to 36.35 - non-mottled hornblende pyroxenite.
  - variably altered with hornblende readily
    altering to actinolite and calcite; clinopyroxene
    is usually very dark green to black in colour and
    almost always fine-grained.
  - well mineralized containing <1 to 15% disseminated

                              to blebby cp and po (composite grains).
                          - 27.40 to 28.40 - 3 to 10% disseminated, to blebby
                            to stringered cp, po.
                          - 28.70 to 29.55 - 3 to 6% cp and po.
                          - 33.15 to 34.06 - 3 to 10% cp and po.
                          - 35.23 to 35.31 - lamprophyre dyke.
                          - 35.31 to 35.78 - 3 to 10% cp and po.
                          - 35.78 to 36.05 - lamprophyre dyke @ 70 deg. CAA.
                          - 36.05 to 36.35 - non-mottled hornblende
                            pyroxenite.
                      - 36.35 to 40.37 - mottled hornblende pyroxenite.
                          - clinopyroxene is readily visible as dull, dark
                            green to black, anhedral to subhedral grains.
                          - the mottled appearance is very distinctive due to
                            the presence of oikocrysts of hornblende and
                            higher clinopyroxene content.
                          - 36.39 to 36.66 - 3 to 5% blebby cp and po.

37.98   40.37   FELDSPAR PORPHYRY DYKE
                      - quite biotitic, grey in colour, slightly foliated.
                      - feldspar phenocrysts are smaller than those
                        observed in other similar rocks described above
                        (usually <4 mm in diameter).
                      - biotite occurs as interstitial masses; 5 to 7% of
                        rock.
                      - <1 to 3% very finely to finely disseminated po and
                        occasionally cp and py; pyrite commonly smeared
                        along fracture surfaces.
                      - 37.98 - upper contact @ 77 deg. CAA.
                      - 40.37 - lower contact @ 64 deg. CAA.

40.37   62.55   HORNBLENDE PYROXENITE
                      - similar to 27.02 to 37.98 with alternating units
                        of mottled and non-mottled hornblende clino-
                        pyroxenites.
                      - 40.37 to 42.23 - non-mottled hornblende pyroxenite.
                          - locally mineralized.
                          - 40.83 to 41.00 - 1 to 3% finely disseminated
                            cp, po.
                          - 41.00 to 41.18 - 5 to 8% small to large blebs and
                            stringers of po with some cp.

- 41.61 to 42.00 - 1 to 3% finely disseminated po
  with some cp.
  - 40.62 to 40.74 - biotitic Feldspar Porphyry Dyke.
  - 41.18 - 4 cm thick chloritic, pyritic and carbon-
    itized shear.
- 42.23 to 43.69 - mottled hornblende pyroxenite.
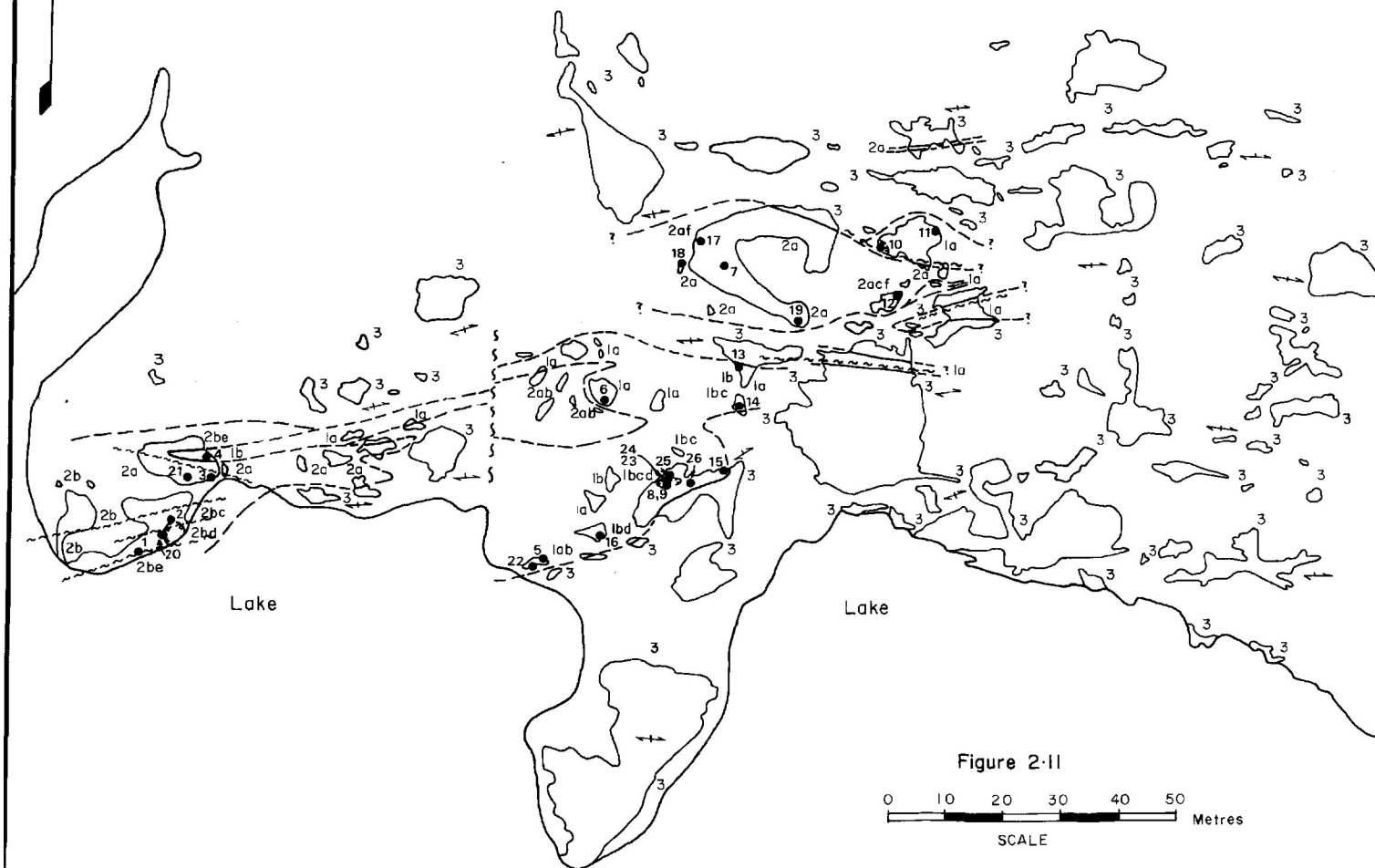 - 1 to 4% disseminated to blebby po and cp.
- 43.69 to 45.22 - hornblende pyroxenite; contains
  usually <1 to 2% finely disseminated cp and po.
  - 44.19 to 44.25 - 6 to 10% blebby cp and po.
  - 45.00 - very narrow, chloritic, carbonitized
    shear at low CAA.
- 45.22 to 46.14 - mottled hornblende pyroxenite.
  - 1 to 5% disseminated to blebby po and minor cp.
- 46.14 to 46.80 - non-mottled hornblende pyroxenite.
  - <1 to 2% po, minor cp.
- 46.80 to 49.32 - mottled hornblende pyroxenite.
  - 1 to 2% disseminated po,cp.
- 49.32 to 49.52 - hornblendite dyke; fine- to
  medium-grained, dark green and composed entirely
  of hornblende and actinolite.
  - 1 to 2% blebby cp and po.
  - upper contact is sharp @ 50 deg. CAA.
  - lower contact is sharp @ 70 deg. CAA.
- 49.52 - 53.00 - mottled hornblende pyroxenite.
  - 49.82 - 11 cm thick, highly calcareous, fine-
    grained lamprophyre dyke containing 20 to 30% po.
  - <1% to 1% disseminated po and minor cp in
    pyroxenite.
- 53.00 to 53.46 - non-mottled hornblende pyroxenite.
  - trace very finely disseminated po.
- 53.46 to 55.83 - mottled hornblende pyroxenite.
  - <1% disseminated po, minor cp.
- 55.83 to 59.40 - non-mottled hornblende pyroxenite.
  - very altered, large percentage of actinolite,
    moderately calcareous.
  - <1% finely disseminated po, minor cp.
  - 56.45 to 58.00 - many, thin, chloritic shears @
    many orientations.
- 59.40 to 62.55 - mottled hornblende pyroxenite.
  - trace to 1% very finely disseminated po, minor

cp, and few composite cp/po blebs occur locally.

62.55   63.95   FELDSPATHIC HORNBLENDE PYROXENITE
- similar to 40.37 to 62.55 except for the presence
  of 1 to 3% interstitial plagioclase.
- slightly more altered; contains 3% biotite grains.
- locally slightly to moderately hornblende
  porphyritic.
- <1 to 5% disseminated, locally blebby cp, po.

63.95   71.80   PYROXENE HORNBLENDITE
- green to dark green, fine to medium-grained and
  contains oikocrysts of hornblende; clinopyroxenes
  occur interstitially to amphiboles and as small
  black chadacrysts within oikocrysts of hornblende.
- some minor olivine observed (<5%) at top of unit.
- locally some minor plagioclase observed.
- localized, 1 to 5%, interstitial biotite over short
  intervals.
- 63.95 to 64.35 - trace to 2% po, and cp.
- 64.35 to 65.80 - <1 to 3% po, and cp.
- 65.80 to 67.00 - <1% po, and cp.
- 67.00 to 67.35 - 1 to 3% po, and cp.
- 68.00 to 71.80 - 1 to 10% po, and cp.
- 71.80 - lower contact sheared @ 40 deg. CAA.

71.80   122.83   BIOTITE - QUARTZ FELS
- contact metamorphosed turbiditic metasediments
  of greywacke composition; very fine- to fine-
  grained.
- buff to grey brown in colour, massive to locally
  schistose; schistosity increases gradually with
  depth away from the contact with the intrusion.
- local narrow quartz stringers throughout @ 40 deg.
  to 45 deg. CAA.
- numerous narrow shears @ CAA of 40 deg. to 45 deg.
- biotitic throughout.
- <1% very finely disseminated po throughout.

122.83   END OF HOLE.
- casing left in; not cemented.

S

N

.012 oz/t Pt
.013 oz/t Pd
.32 % Cu
over 9 metres

.012 oz/t Pt
.018 oz/t Pd
.20 % Cu
over 6 metres

.019 oz/t Pt
.041 oz/t Pd
.82 % Cu
over 2.5 metres

.006 oz/t Pt
.009 oz/t Pd
.23 % Cu
over 14.5 metres

Metasediments

Metasediments

Kawene
mafic/ultramafic
Intrusion

DHK 87-1

DHK 87-2

SCALE |—5m—|

Kawene Intrusion – Vertical Cross-section

Fleck Resources Ltd.

14
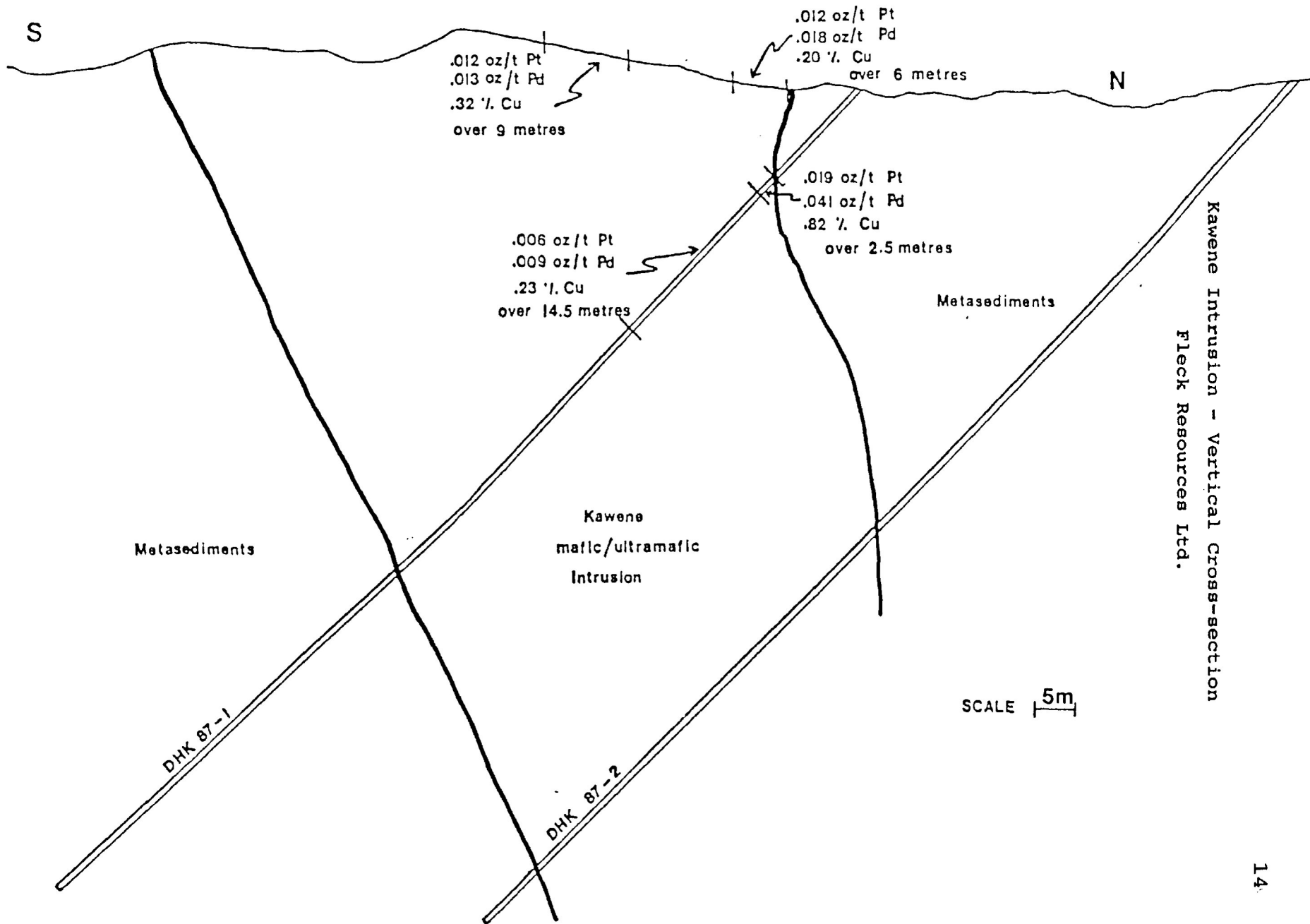
GEOLOGY OF THE ABIWIN INTRUSION

Figure 2·11

LEGEND

1a	Hornblendite, locally sheared
b	Feldspathic hornblendite
c	Clinopyroxene-bearing
d	Mineralized
2a	Hornblende gabbro
b	Hornblende melagabbro
c	Clinopyroxene-bearing
d	Mineralized
e	Biotitic
f	Foliated
3	Metasedimentary Migmatite

Symbols

⬯	Outcrop
⟍	Contact (observed, inferred)
⟋	Fault/shearing
⟍	Schistosity (vertical, inclined)
◌	Trench/pit
•3	Sample location, sample number

Sample Index

1	AAb-1-85	14	AAb-19-85
2	-2-85	15	-23-85
3	-3-85	16	-24-85
4	-4-85	17	-25-85
5	-5-85	18	-26-85
6	-6-85	19	-1-84
7	-8-85	20	-2-84
8	-9-85	21	-3-84
9	-10-85	22	-4-84
10	-12-85	23	-5-84
11	-13-85	24	-6-84
12	-15-85	25	-7-84
13	-18-85	26	-8-84

GEOLOGY OF THE KAWENE INTRUSION

N

LEGEND

6 Hornblende Wehrlite

5a Hornblende Clinopyroxenite
b Olivine-hornblende Clinopyroxenite
c Biotitic

4a Hornblendite
b Olivine-clinopyroxene Hornblendite
c Clinopyroxene Hornblendite
d Feldspathic
e Porphyritic
f Biotitic
g Appinite

3a Hornblende Melagabbro
b Biotitic
c Appinitic

2 Metasedimentary Migmatite

1 Turbiditic Wacke

Chalcopyrite
Pyrrhotite

SYMBOLS

◯ Outcrop
✕ Small Outcrop
⌔ Trench/Pit
● Drill Hole
Contact, observed, assumed
Foliation, vertical, inclined
Fault/Shearing
Contact, gradational
● Sample Location
Mineralization Limit

SAMPLE INDEX

1	AK-1-86	21	AK-21-86	40	AK-43-86
2	-2-86	22	-22-86	41	-44-86
3	-3-86	23	-23-86	42	-45-86
4	-4-86	24	-24-86	43	-46-86
5	-5-86	25	-25-86	44	-47-86
6	-6-86	26	-26-86	45	-48-86
7	-7-86	27	-27-86	46	-49-86
8	-8-86	28	-28-86	47	-50-86
9	-9-86	29	-29-86	48	-51-86
10	-10-86	30	-30-86	49	-52-86
11	-11-86	31	-31-86	50	-53-86
12	-12-86	32	-32-86	51	-2-84
13	-13-86	33	-33-86	52	-3-84
14	-14-86	34	-34-86	53	-4-84
15	-15-86	35	-37-86	54	-5-84
16	-16-86	36	-39-86	55	-6-84
17	-17-86	37	-40-86	56	-7-84
18	-18-86	38	-41-86	57	-8-84
19	-19-86	39	-42-86	58	-9-84
20	-20-86				
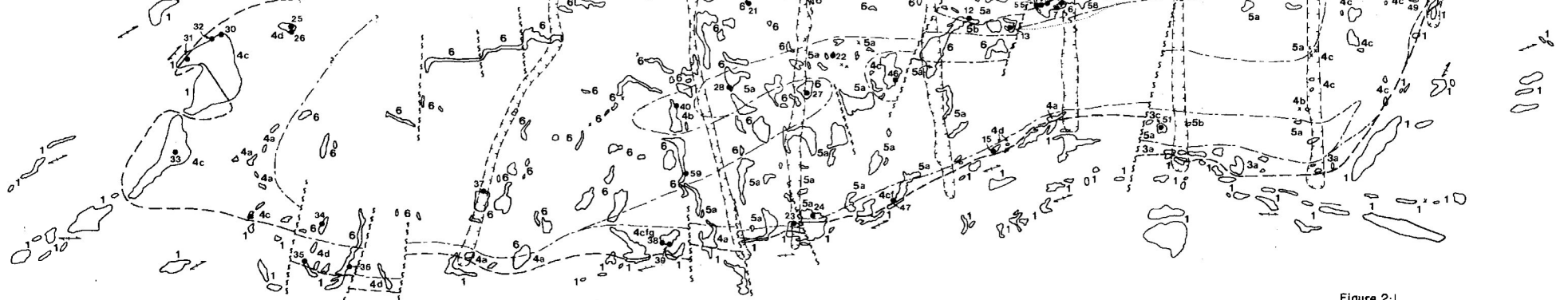
NOTE- Subcrop exposed during overburden trenching was not included on this map to prevent clutter; however, the rock-types, contacts, structures, and mineralization observed have been included in the maps' interpretation.

Figure 2-1
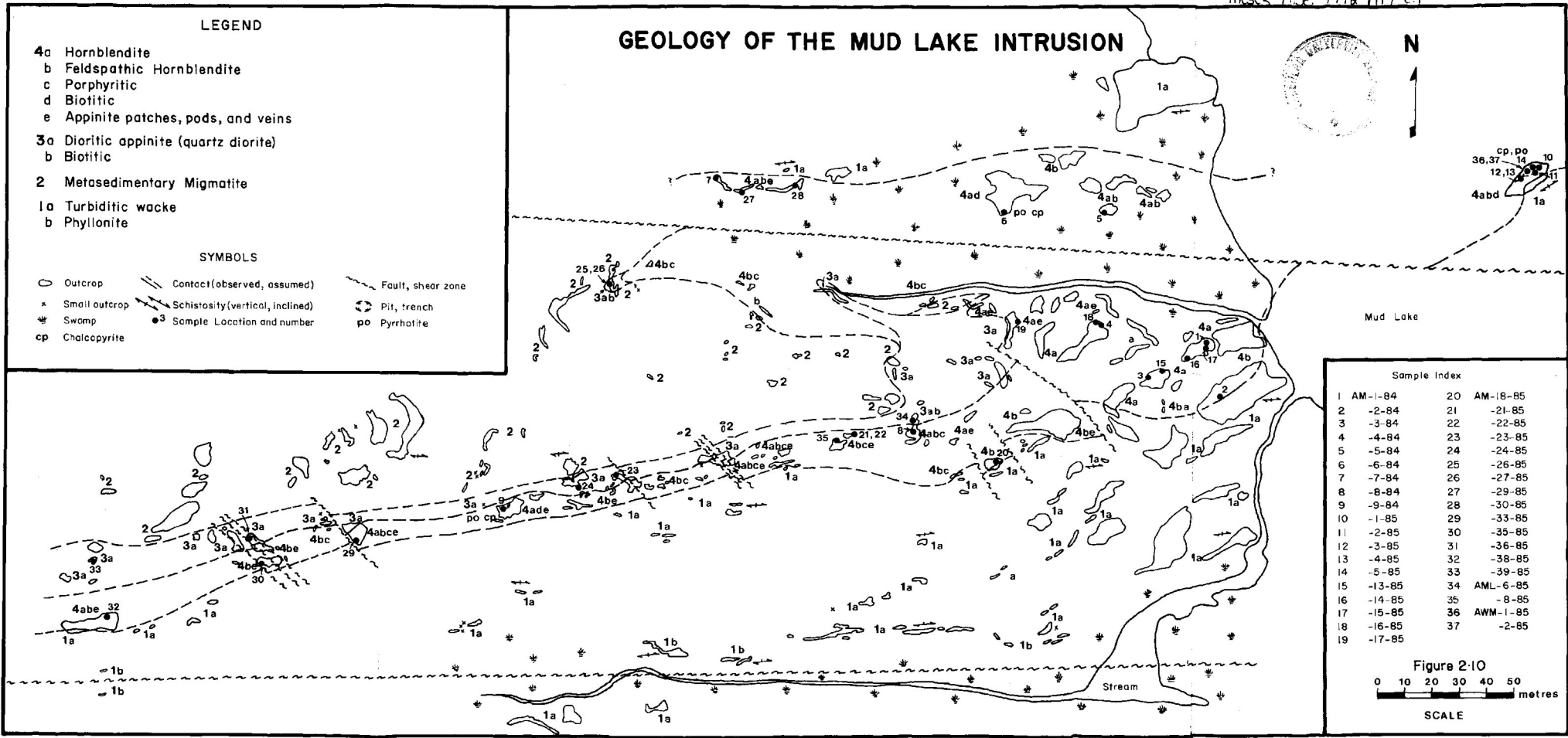
0 10 20 30 40 50 metres

SCALE

GEOLOGY OF THE MUD LAKE INTRUSION

N

LEGEND

4a Hornblendite
  b Feldspathic Hornblendite
  c Porphyritic
  d Biotitic
  e Appinite patches, pods, and veins

3a Dioritic appinite (quartz diorite)
  b Biotitic

2 Metasedimentary Migmatite

1a Turbiditic wacke
  b Phyllonite

SYMBOLS

⌒ Outcrop	Contact (observed, assumed)
× Small outcrop	Schistosity (vertical, inclined)
✹ Swamp	⟨⟩ Pit, trench
cp Chalcopyrite	● Sample Location and number
	po Pyrrhotite

Fault, shear zone

Mud Lake

Stream

Sample Index

1	AM-1-84	20	AM-18-85
2	-2-84	21	-21-85
3	-3-84	22	-22-85
4	-4-84	23	-23-85
5	-5-84	24	-24-85
6	-6-84	25	-26-85
7	-7-84	26	-27-85
8	-8-84	27	-29-85
9	-9-84	28	-30-85
10	-1-85	29	-33-85
11	-2-85	30	-35-85
12	-3-85	31	-36-85
13	-4-85	32	-38-85
14	-5-85	33	-39-85
15	-13-85	34	AML-6-85
16	-14-85	35	-8-85
17	-15-85	36	AWM-1-85
18	-16-85	37	-2-85
19	-17-85		

Figure 2·10

0 10 20 30 40 50 metres

SCALE